

Some pages of this thesis may have been removed for copyright restrictions.

If you have discovered material in AURA which is unlawful e.g. breaches copyright, (either yours or that of a third party) or any other law, including but not limited to those relating to patent, trademark, confidentiality, data protection, obscenity, defamation, libel, then please read our [Takedown Policy](#) and [contact the service](#) immediately

**NOVEL BIODEGRADABLE FIBRES FOR
APPLICATIONS IN TISSUE ENGINEERING AND DRUG
DELIVERY**

MATTHEW RICHARD WILLIAMSON

Doctor of Philosophy

May 2003

**ASTON PHARMACY SCHOOL
ASTON UNIVERSITY
BIRMINGHAM, U.K.**

Supervisor

Dr A.G.A. Coombes

Associate Supervisors

Dr E.F. Adams

Dr H.R. Griffiths

This copy of the thesis has been supplied on condition that anyone who consults it is understood to recognize that its copyright rests with its author and that no quotation from the thesis and no information derived from it may be published without proper acknowledgement.

DEDICATION

I would like to dedicate this thesis to my family and thank them for their love and support. I would also like to dedicate this to 'The Family' for their continual friendship.

I would like to thank my supervisor,

for his support and advice throughout

the project.

I would like to take this opportunity to thank my

family for their support and advice in many aspects of my PhD.

I would like to thank my friends

for their support and advice throughout the project.

I would like to thank my

supervisor for his support and advice throughout the project.

I would like to thank my

family for their support and advice throughout the project.

ACKNOWLEDGEMENTS

I wish to thank my supervisor, Dr. Allan Coombes, for his support, advice and encouragement.

I would also like to thank my associated supervisors, Dr. Eric Adams and Dr. Helen Griffiths for their support and advice throughout my PhD.

I would like to take this opportunity to thank my colleague, Kevin Woollard for his continual help, support and advice in many aspects of my PhD.

Thanks to Chris Bache, the chief technician for technical support.

Thanks to James Duggins for technical support on SEM examination.

Lastly, I would like to thank my parents, sister and all my friends and colleagues for their support and encouragement.

THESIS SUMMARY

The preparation and characterisation of novel biodegradable polymer fibres for application in tissue engineering and drug delivery are reported. Poly(ϵ -caprolactone) (PCL) fibres were produced by wet spinning from solutions in acetone under low shear (gravity flow) conditions. The tensile strength and stiffness of as-spun fibres were highly dependent on the concentration of the spinning solution. Use of a 6% w/v solution resulted in fibres having strength and stiffness of 1.8 MPa and 0.01 GPa respectively, whereas these values increased to 9.9 MPa and 0.1 GPa when fibres were produced from 20% w/v solutions. Cold drawing to an extension of 500% resulted in further increases in fibre strength (up to 50 MPa) and stiffness (0.3 GPa). Hot drawing to 500% further increased the fibre strength (up to 81 MPa) and stiffness (0.5 GPa). The surface morphology of as-spun fibres was modified, to yield a directional grooved pattern by drying in contact with a mandrel having a machined topography characterised by a peak-peak separation of 91 μm and a peak height of 30 μm . Differential scanning calorimetry (DSC) analysis of as-spun fibres revealed the characteristic melting point of PCL at around 58°C and a % crystallinity of approximately 60%. The biocompatibility of as-spun fibres was assessed using cell culture.

The number of attached 3T3 Swiss mouse fibroblasts, C2C12 mouse myoblasts and human umbilical vein endothelial cells (HUVECs) on as-spun, 500% cold drawn, and gelatin coated PCL fibres were observed. The results showed that the fibres promoted cell proliferation for 9 days in cell culture and was slightly lower than on tissue culture plastic. The morphology of all cell lines was assessed on the various PCL fibres using scanning electron microscopy. The cell function of HUVECs growing on the as-spun PCL fibres was evaluated. The ability HUVECs to induce an immune response when stimulated with lipopolysaccharide (LPS) and thereby to increase the amount of cell surface receptors was assessed by flow cytometry and reverse transcription-polymerase chain reaction (RT-PCR). The results showed that PCL fibres did not inhibit this function compared to TCP.

As-spun PCL fibres were loaded with 1% ovine albumin (OVA) powder, 1% OVA nanoparticles and 5% OVA nanoparticles by weight and the protein release was assessed in vitro. PCL fibres loaded with 1% OVA powder released 70%, 1% OVA nanoparticle released 60% and the 5% OVA nanoparticle released 25% of their protein content over 28 days. These release figures did not alter when the fibres were subjected to lipase enzymatic degradation. The OVA released was examined for structural integrity by SDS-PAGE. This showed that the protein molecular weight was not altered after incorporation into the fibres.

The bioactivity of progesterone was assessed following incorporation into PCL fibres. Results showed that the progesterone released had a pronounced effect on MCF-7 breast epithelial cells, inhibiting their proliferation.

The PCL fibres display high fibre compliance, a potential for controlling the fibre surface architecture to promote contact guidance effects, favorable proliferation rate of fibroblasts, myoblasts and HUVECs and the ability to release pharmaceuticals. These properties recommended their use for 3-D scaffold production in soft tissue engineering and the fibres could also be exploited for controlled presentation and release of biopharmaceuticals such as growth factors.

LIST OF CONTENTS

TITLE PAGE	1
THESIS SUMMARY	2
DEDICATION	3
ACKNOWLEDGEMENTS	4
LIST OF CONTENTS	5
LIST OF TABLES	10
LIST OF FIGURES	13
CHAPTER 1 ~ INTRODUCTION	19
1.1 Tissue Engineering	19
1.2 Biomaterials	21
1.3 Natural Polymers	24
1.4 Synthetic Polymers	28
1.5 Polycaprolactone	30
1.6 Scaffold Production Techniques	30
1.7 Fibre Spinning Techniques	32
1.8 Cell Interaction with Tissue Engineering Scaffolds	36
1.9 Cell Adhesion	37
1.10 Cell Proliferation	41
1.11 Cell Differentiation	42
1.12 Tissue Development	43
1.13 Tissue Engineering of Blood Vessels	44
1.14 Tissue Engineering of Skeletal Muscle	46
1.15 Scaffold Design	47
1.16 Bioactive Scaffolds	48
1.17 Aims and Objectives	50
CHAPTER 2 ~ MATERIALS AND METHODS	51
2.1 Materials	51

2.2 Methods	52
2.2.1 Development of Discontinuous Fibres Spinning Technique	52
2.2.2 Continuous Fibre Production	53
2.2.3 Modification of Spinneret Diameter on Fibre Production	53
2.2.4 Measurements of Discontinuous Fibre Spinning Rate	53
2.2.5 Measurements of Continuous Fibre Spinning Rate	54
2.2.6 Scanning Electron Microscopy	54
2.2.7 Modification of Fibre Surface Topography	55
2.2.8 Mechanical Properties of As-spun PCL Fibres	55
2.2.9 Retraction of PCL Fibres	58
2.2.10 Mechanical Properties of Drawn PCL Fibres	58
2.2.11 Mechanical Properties of Hot Drawn PCL Fibres	58
2.2.12 Mechanical Properties of PCL Fibres Extended at Various Crosshead Speeds	58
2.2.13 Mechanical Properties of PCL Fibres After Incubation at 37°C	59
2.2.14 Thermal Analysis	59
2.2.15 Cell Preparation	60
2.2.16 Assay of Cell Proliferation on Fibres	60
2.2.17 Optimisation of Cell Proliferation on Fibres	61
2.2.18 Cell Interaction with 500% Cold Drawn PCL Fibres	62
2.2.19 Cell Interaction with Gelatin Coated PCL Fibres	62
2.2.20 Cell Proliferation on 1) As-spun, 2) Gelatin Coated, 3) 500% Cold Drawn PCL Fibres and 4) Dacron Monofilament	63
2.2.21 The Initial Interaction of Human Umbilical Vein Endothelial Cells (HUVEC) with PCL Fibres	64
2.2.22 Optimised Interaction of HUVEC with PCL Fibres	64
2.2.23 Assay for Maintained Cell Function	65
2.2.23.1 mRNA Extraction and RT-PCR of ICAM-1 Expression	65
2.2.23.2 Polymerase Chain Reaction (PCR)	67
2.2.23.3 Agarose Gel Electrophoresis of PCR Products	67
2.2.23.4 Flow Cytometry Analysis of ICAM-1 Expression	68
2.2.24 Scanning Electron Microscopy Analysis of Cell-Fibre Interactions	69
2.2.25 Protein Microparticles Loading of PCL Fibres	70

2.2.26 Protein Nanoparticles Loading of PCL Fibres	71
2.2.27 Modification of Fibre Surface with Protein	72
2.2.28 Measurement of Surface Protein Loading of PCL Fibres	72
2.2.29 Measurement of Protein Release from Gelatin-Coated PCL Fibres	72
2.2.30 Measurement of Surface Protein Loading	73
2.2.31 Protein Release from PCL Fibres	73
2.2.32 Protein Release from PCL Fibres Loaded with Protein Nanoparticles	74
2.2.33 The Effect of Lipase on Protein Release from PCL Fibres	74
2.2.34 SDS-PAGE Analysis of OVA Release from PCL Fibres	75
2.2.35 Activity of Bioactive Compounds Following Incorporation in PCL Fibres	75
2.2.36 Statistical Analysis	76
CHAPTER 3 ~ FIBRE PRODUCTION AND PROPERTIES	77
3.1 Introduction	77
3.2 Development of Continuous Fibre Spinning Technique for PCL Fibres	77
3.3 Continuous PCL Fibre Production Using the Gravity Spinning Technique	83
3.4 Measurements of Fibre Spinning Rate	84
3.5 Measurements of Continuous Fibre Spinning Rate	85
3.6 The Effect of Spinneret Diameter on PCL Fibre Production	85
3.7 Scanning Electron Microscopy	85
3.8 Modification of Fibre Surface Topography	88
3.9 Mechanical Properties of PCL Fibres	89
3.10 Mechanical Properties of PCL Fibres Tested at Various Speeds	92
3.11 Mechanical Properties of PCL Fibres After Incubation in PBS at 37°C	93
3.12 PCL Fibre Extension and Retraction	93
3.13 Cold Drawing PCL Fibres	94
3.14 Hot Drawing of PCL Fibres	100
3.15 Thermal Analysis	102
3.16 Discussion	104

CHAPTER 4 ~ CELL INTERACTIONS WITH PCL FIBRES	110
4.1 Introduction	110
4.2 Cell Proliferation Experiments	110
4.3 Cell Interactions with 1) As-spun PCL Fibres 2) Gelatin Coated As-spun PCL Fibres and 3) Dacron Monofilament	118
4.4 Cell Interactions with 1) As-spun PCL Fibres 2) 500% Cold Drawn PCL Fibres and 3) Dacron Monofilament	118
4.5 Fibroblast Cell Attachment to As-spun PCL Fibres and 500% Cold Drawn PCL Fibres	123
4.6 Fibroblast Cell Attachment to As-spun PCL Fibres and Gelatin Coated As-spun PCL Fibres	123
4.7 SEM Study of Cell-Fibre Interaction and Morphology	126
4.8 Discussion	146
CHAPTER 5 ~ PRIMARY CELL INTERACTIONS WITH PCL FIBRES	152
5.1 Introduction	152
5.2 Initial HUVECs Proliferation Experiment	153
5.3 HUVECs Proliferation Experiments	153
5.4 Cell-Fibre Morphology	158
5.5 Retention of HUVECs Function	170
5.6 Discussion	174
CHAPTER 6 ~ BIOACTIVE FIBRES	180
6.1 Introduction	180
6.2 Protein Loading of PCL Fibres	180
6.3 Mechanical Properties	182
6.4 Thermal Properties	183
6.5 Fibre Surface Modification by Incorporated Protein	184
6.6 Fibre Surface Modification by Gelatin Coating	185
6.7 SEM Examination of Modified PCL Fibres Surface Topography	188
6.8 Release of Protein from OVA-Loaded PCL Fibres	192

6.9 <i>The Effect of Lipase in the PBS Release Medium on Protein Release from OVA-Loaded PCL Fibres</i>	201
6.10 <i>SDS-PAGE Analysis of Protein Release from PCL Fibres</i>	203
6.11 <i>Release of Progesterone from PCL Fibres</i>	204
6.12 <i>Discussion</i>	206
CHAPTER 7 ~ SUMMARY AND GENERAL DISCUSSION	211
REFERENCES	215
ABBREVIATIONS	233
PUBLICATIONS	235

LIST OF TABLES

Table 1.1	Types of collagen and their location within the body	25
Table 1.2	The melting points $T_{(m)}$ and degradation times of PLG, PLA and PGA	29
Table 3.1	The effect of methanol:water combination as the non-solvent on discontinuous PCL fibre production using the gravity spinning technique.	81
Table 3.2	The effect of PCL solution concentration on discontinuous fibre formation using the gravity spinning technique	82
Table 3.3	Spinning rates and characteristics of PCL fibres under discontinuous production conditions	84
Table 3.4	The effect of PCL solution concentration on the spinning rate of continuous PCL fibres	85
Table 3.5	The tensile properties of as-spun PCL fibres 1 Day after production	89
Table 3.6	The tensile properties of as-spun PCL fibres 2 Days after production	90
Table 3.7	The tensile properties of as-spun PCL fibres 7 Days after production	90
Table 3.8	The tensile properties of as-spun PCL fibres 14 Days after production	90
Table 3.9	The tensile properties of as-spun PCL fibres 28 Days after production	91
Table 3.10	The tensile properties of as-spun 10% PCL fibres at various test speeds	92
Table 3.11	The tensile properties of as-spun 10% PCL fibres after incubation at in PBS at 37°C for various time periods	93
Table 3.12	The % retraction and diameter of 6% and 10% PCL fibre following extension at room temperature	94
Table 3.13	The % retraction and diameter of 15% and 20% PCL fibre following extension at room temperature	94

Table 3.14	The tensile properties of cold drawn PCL fibres produced for 6% and 10% polymer solutions	95
Table 3.15	The tensile properties of cold drawn PCL fibres produced for 6% and 10% polymer solutions	96
Table 3.16	The tensile properties of 10% PCL fibres after hot drawing at 37°C and testing once cooled at room temperature.	100
Table 3.17	The thermal properties of PCL fibres 1–28 days after production	103
Table 3.18	The thermal properties of as-spun and cold drawn PCL fibres	104
Table 3.19	Tensile properties of synthetic biodegradable fibres	107
Table 4.1	Summarised cell proliferation of Swiss 3T3 mouse fibroblasts on various substrates over time.	146
Table 4.2	Summarised cell proliferation of C2C12 mouse myoblasts on various substrates over time.	147
Table 6.1	Observations on spinning of PCL fibres from 10% w/v solution in acetone containing OVA powder.	181
Table 6.2	Spinning rate and diameters of PCL fibres produced from different concentration of PCL solutions containing 0.1% w/v OVA powder	182
Table 6.3	Spinning rate and diameter of PCL fibre produced from a 10% PCL solution containing different concentrations of OVA nanoparticles.	182
Table 6.4	The tensile properties of 10% PCL fibres spun from solutions containing 0.1% w/v OVA powder, 0.1% w/v and 0.5% w/v nanoparticles	183
Table 6.5	The thermal properties 10% PCL fibres spun from solutions containing 0.1% w/v OVA powder, 0.1% w/v and 0.5% w/v nanoparticles	183
Table 6.6	The amount of OVA measured on the surface of a 10% PCL fibre after incubation in PBS at 37°C	184
Table 6.7	The amount of gelatin measured on the surface of a 10% as-spun PCL fibre coated using various concentrations of gelatin solution	185

Table 6.8 The amount of protein released from the OVA-loaded PCL modified fibre into 2ml of PBS

192

Sample	Protein released (µg)
Control	25
...	27
...	28
...	29
...	30

Sample	Protein released (µg)
...	39
...	40
...	41
...	42
...	43

LIST OF FIGURES

Figure 1.1	Evolution of biomaterial science and technology	22
Figure 1.2	The structure of a collagen fibril	25
Figure 1.3	The structure of hyaluronic acid	26
Figure 1.4	The structure of alginate	27
Figure 1.5	The structure of (A) chitin and (B) chitosan	28
Figure 1.6	Chemical structure of poly(ϵ -caprolactone)	30
Figure 1.7	Schematic of melt spinning technique	33
Figure 1.8	Schematic of dry spinning technique	34
Figure 1.9	Schematic of solution/wet spinning technique	36
Figure 1.10	Schematic of electrospinning technique	33
Figure 1.11	A schematic of the tissue engineering approach involving cell seeding on scaffolds	37
Figure 1.12	Structural features of integrin cell surface receptors	38
Figure 1.13	Schematic diagram of integrin clustering to form a focal contact and the intracellular binding of proteins from the integrins to the actin cytoskeleton	39
Figure 1.14	Syndecan-4 acts as an organizing center for transmembrane receptors and is anchored to the actin cytoskeleton	40
Figure 1.15	Anchorage regulation of the cell cycle	43
Figure 1.16	Schematic of the structure of an artery	45
Figure 1.17	Schematic of the structure of a vein	46
Figure 1.18	Schematic diagram of the organisation of a muscle	47
Figure 2.1	Picture of a Hounsfield H10KS tensile testing machine	57
Figure 2.2	Picture of Hounsfield tensile testing machine with a fibre clamped with a 5N load-cell	58
Figure 2.3	Force-extension curve of a PCL fibre	58
Figure 2.4	Equations used to determined mechanical properties	59
Figure 2.5	Schematic diagram of Polymerase Chain Reaction (PCR)	69
Figure 3.1	Continuous PCL fibre formations by the gravity spinning method using a 10% w/v polymer solution	85

Figure 3.2	Original U-tube apparatus used to produce discontinuous PCL fibres by gravity spinning	86
Figure 3.3	Gravity spinning apparatus based on a 250 ml measuring cylinder as the non-solvent bath	87
Figure 3.4	Experimental systems used for continuous production of PCL fibres by gravity spinning	90
Figure 3.5	SEM of the surface topography of as-spun PCL fibre produced from a 10% w/v polymer solution	93
Figure 3.6	SEM of the surface topography of as-spun PCL fibre Produced from a 10% w/v polymer solution	94
Figure 3.7	SEM of the modified fibre surface topography formed by drying as-spun PCL fibres produced from a 10% w/v polymer solution, in contact with a mandrel	95
Figure 3.8	Force-extension curve of an as-spun PCL fibre produced using 10% w/v solution	98
Figure 3.9	Force-extension curve of a 10% w/v 'as-spun' fibre extended at 1000 mm/min	100
Figure 3.10	Force-extension curve of a 10% w/v fibre cold drawn to 100% extension	104
Figure 3.11	The morphology of a 10% PCL fibre after 50% extension	105
Figure 3.12	SEM of 10% PCL fibre after 500% extension	106
Figure 3.13	Force-extension curve of a 10% w/v fibre cold drawn to 200% extension	107
Figure 3.14	Force-extension curve of a 10% w/v fibre cold drawn to 500% extension	107
Figure 3.15	Force-extension curve of a 10% w/v fibre hot drawn at 37°C to 100% extension and tested once cooled at room temperature	109
Figure 3.16	Force-extension curve of a 10% w/v fibre hot drawn at 37°C to 200% extension and tested once cooled at room temperature	109
Figure 3.17	Force-extension curve of a 10% w/v fibre hot drawn at 37°C to 500% extension and tested once cooled at room temperature	110
Figure 3.18	A typical thermal trace of as-spun 10% PCL fibre	112
Figure 3.19	Schematic of the morphology of a polyester fibre	117

Figure 4.1	Initial Swiss 3T3 fibroblasts attachment and proliferation rate on 10% as-spun PCL fibres and TCP substrates over 3 days	112
Figure 4.2	C2C12 mouse myoblasts attachment and proliferation rate on 10% as-spun PCL fibres and TCP substrates over 8 days	113
Figure 4.3	Swiss 3T3 fibroblasts attachment and proliferation rate on 10% as-spun PCL fibres and TCP substrates over 8 days	114
Figure 4.4	Swiss 3T3 fibroblasts attachment and proliferation rate on 10% as-spun PCL fibres and TCP substrates over 9 days	116
Figure 4.5	C2C12 mouse myoblasts attachment and proliferation rate on 10% as-spun PCL fibres and TCP substrates over 9 days	117
Figure 4.6	Swiss 3T3 fibroblasts attachment and proliferation rate after on 10% as-spun PCL fibres, 10% PCL fibres coated with a 5% gelatin solution, Dacron monofilament and TCP substrates over 9 days	119
Figure 4.7	C2C12 mouse myoblasts attachment and proliferation rate after on 10% as-spun PCL fibres, 10% PCL fibres coated with a 5% gelatin solution, Dacron monofilament TCP substrates over 9 days	120
Figure 4.8	Swiss 3T3 fibroblasts attachment and proliferation rate on 10% as-spun PCL fibres, 500% cold drawn (10%) PCL fibres, Dacron monofilament and TCP substrates over 9 days	121
Figure 4.9	C2C12 mouse myoblasts attachment and proliferation rate after on 10% as-spun PCL fibres, 500% cold drawn (10%) PCL fibres, Dacron monofilament and TCP substrates over 9 days	122
Figure 4.10	Swiss 3T3 fibroblasts attachment rate on 10% as-spun PCL fibres and 10% PCL fibre cold drawn to 500% and tissue culture plastic substrates over 8 hours	124
Figure 4.11	Swiss 3T3 fibroblasts attachment rate on 10% as-spun PCL fibres and 10% as-spun PCL fibre coated with a 5% w/v gelatin solution and tissue culture plastic substrates over 8 hours	125
Figure 4.12	SEM of Swiss 3T3 mouse fibroblasts on an as-spun PCL fibre coated with a 5% gelatin solution	127
Figure 4.13	SEM of C2C12 mouse myoblasts on an as-spun PCL fibre coated with a 5% gelatin solution	128

Figure 4.14A	SEM of Swiss 3T3 mouse fibroblasts on as-spun PCL fibre	130
Figure 4.14B	SEM of Swiss 3T3 mouse fibroblasts on as-spun PCL fibre	131
Figure 4.15A	SEM of C2C12 mouse myoblasts on as-spun PCL fibre	132
Figure 4.15B	SEM of C2C12 mouse myoblasts on as-spun PCL fibre	133
Figure 4.16	SEM of Swiss 3T3 mouse fibroblasts on an as-spun PCL fibre coated with gelatin	134
Figure 4.17	SEM of C2C12 mouse myoblasts on an as-spun PCL fibre coated with gelatin	135
Figure 4.18A	SEM of Swiss 3T3 mouse fibroblasts on 500% cold drawn PCL fibre	136
Figure 4.18B	SEM of Swiss 3T3 mouse fibroblasts on 500% cold drawn PCL fibre	137
Figure 4.19	SEM of C2C12 mouse myoblasts on 500% cold drawn PCL fibre	138
Figure 4.20	SEM of Swiss 3T3 mouse fibroblasts on an as-spun PCL fibre	139
Figure 4.21	SEM of Swiss 3T3 mouse fibroblasts on an as-spun PCL fibre coated with gelatin	140
Figure 4.22	SEM of Swiss 3T3 mouse fibroblasts on 500% cold drawn PCL fibre coated with gelatin	141
Figure 4.23	SEM of C2C12 mouse myoblasts on an as-spun PCL fibre	142
Figure 4.24	SEM of C2C12 mouse myoblasts on an as-spun PCL fibre coated with gelatin	143
Figure 4.25	SEM of C2C12 mouse myoblasts on 500% cold drawn PCL fibre	144
Figure 4.26	SEM of C2C12 mouse myoblasts on 500% cold drawn PCL fibre	145
Figure 4.27	Schematic diagrams of the structures of (A) Fibronectin, (B) Laminin and (C) Vitronectin	148
Figure 4.28	A diagram of the chemical structure gelatin	150
Figure 5.1	HUVECs attachment and proliferation rate on 10% as-spun PCL fibres and tissue culture plastic substrates over 9 days	155
Figure 5.2	HUVECs attachment and proliferation rate on 10% as-spun PCL fibres, 10% PCL fibres coated with a 5% gelatin solution, Dacron monofilament and TCP substrates over 9 days	156

Figure 5.3	HUVECs attachment and proliferation rate on 10% as-spun PCL fibres, 500% cold drawn (10%) PCL fibres, Dacron monofilament and TCP substrates over 9 days	157
Figure 5.4	SEM of HUVECs on an as-spun 10% PCL fibre	159
Figure 5.5	SEM of HUVECs on an as-spun PCL fibre coated with a 5% gelatin solution	160
Figure 5.6	SEM of HUVECs on 500% cold drawn PCL fibre	161
Figure 5.7	SEM of HUVECs on an as-spun 10% PCL fibre	163
Figure 5.8A	SEM of HUVECs on an as-spun PCL fibre coated with gelatin	164
Figure 5.8B	SEM of HUVECs on an as-spun PCL fibre coated with gelatin	165
Figure 5.9	SEM of HUVECs on an as-spun 10% PCL fibre	166
Figure 5.10	SEM of HUVECs on an as-spun PCL fibre	167
Figure 5.11	SEM of HUVECs on an as-spun PCL fibre coated with gelatin	168
Figure 5.12	SEM of HUVECs on a 500% cold drawn PCL fibre	169
Figure 5.13	The change in percentage positive HUVECs expressing ICAM-1	171
Figure 5.14	Histograms of FL-1 fluorescence labelled ICAM-1 on HUVECS grown on (A) TCP, control and (B) as-spun PCL fibre	172
Figure 5.15	Photograph of UV-illuminated gel electrophoresis of (1) GADPH specific mRNA and (2) ICAM-1 specific mRNA	173
Figure 5.16	Optical density levels of ICAM-1 after normalisation to GADPH as internal standard	174
Figure 6.1	OVA expression on the surface of 10% as-spun PCL fibres spun from a 0.1% OVA powder suspension	184
Figure 6.2	The amount of gelatin measured on the surface of a 10% as-spun PCL fibre coated using a 5% w/v gelatin solution	186
Figure 6.3	Release of gelatin from an as-spun PCL fibre coated with a 5% w/v gelatin solution	187
Figure 6.4	SEM of the surface topography of an as-spun PCL fibre spun from a 0.1% OVA powder suspension	189
Figure 6.5	SEM of the surface topography of an as-spun PCL fibre spun from a 0.5% w/v OVA nanoparticles suspension	190
Figure 6.6	SEM of the surface topography of an as-spun PCL fibre coated with a 5% w/v gelatin solution	191

Figure 6.7	Release of OVA from a 1% OVA loaded PCL fibre	193
Figure 6.8	Cumulative release (%) of OVA from a 1% OVA loaded PCL fibre	194
Figure 6.9	Cumulative release of OVA from PCL fibres with a 1 % OVA powder, 1% OVA nanoparticles and 5% OVA nanoparticles loadings	196
Figure 6.10	Cumulative release (%) of OVA from PCL fibres with a 1% OVA powder, 1% OVA nanoparticles and 5% OVA nanoparticles loadings	197
Figure 6.11	Cumulative release of OVA from PCL fibres with a 1% OVA powder, 1% OVA nanoparticles and 5% OVA nanoparticles loadings	198
Figure 6.12	Cumulative release (%) of OVA from PCL fibres with a 1% OVA powder, 1% OVA nanoparticles and 5% OVA nanoparticles loadings	199
Figure 6.13	Cumulative release of OVA from PCL fibres with a 1% OVA powder, 1% OVA nanoparticles and 5% OVA nanoparticles loadings	201
Figure 6.14	Cumulative release (%) of OVA from PCL fibres with a 1% OVA powder, 1% OVA nanoparticles and 5% OVA nanoparticles loadings	202
Figure 6.15	Photograph of the a SDS-PAGE gel to analyse protein release from as-spun PCL fibres with a 1% OVA powder or 5% OVA nanoparticles loading and incubated at 37°C for 2 and 7 days	203
Figure 6.16	Activity of progesterone released from a PCL fibre over 4 days	205
Figure 6.17	Schematic diagram of steroid receptor and how it acts to bring about a physiological change to its target cells	210

CHAPTER 1

INTRODUCTION

1.1 Tissue Engineering

Tissue engineering is a broad term describing work at the interface of the biomedical and engineering sciences that uses living cells or attraction of endogenous cells to develop biological substitutes to restore, maintain, or improve tissue function and thereby produce therapeutic or diagnostic benefit (Rabkin et al. 2002). Sometimes also called reparative and regenerative medicine, tissue engineering is an emerging interdisciplinary area of science and technology that has the potential to revolutionize methods of health care treatment and dramatically improve the quality of life for millions of people throughout the world.

Tissue engineering as defined in this thesis is “the application of principles and methods of engineering and life sciences to obtain a fundamental understanding of structure-function relationships in tissues and the development of biological substitutes to restore, maintain, or improve tissue function” (Skalak et al. 1988). The term “tissue engineering” was established in 1987 many definitions exist; Langer et al (1993) defined tissue engineering as “an interdisciplinary field that applies the principles of engineering and the life sciences toward the development of biological substitutes that restore, maintain or improve tissue function.” Gallettie et al. (1995) defined tissue engineering as “the basic science and development of biological substitutes for implantation into the body or the fostering of tissue remodeling for the purpose of replacing, repairing, regenerating, reconstructing, or enhancing function.” These definitions are essentially the same as the one that has been used in this thesis. Recently two other terms that have been used, *regenerative medicine* and *reparative biology*, have considerable, sometimes total, overlap with the aims and goals of tissue engineering.

Tissue engineering continues to provide a focus for interdisciplinary research worldwide because of the potential for obtaining ‘living’ tissue replacements and thereby reducing the reliance on donor tissue and organs (Nerem, 1991). Worldwide

organ replacement therapies utilizing standard, organometallic devices consume 8 percent of medical spending, or approximately \$350 billion per year. This is the scope of the problem that tissue engineering could address (Lysaght et al. 2000). The synthetic implants although being continuously improved, in terms of function and reliability cannot perform as effectively as a natural body part. In recent times, organ transplantation has become a procedure of choice. There are however several major factors that limit progress in this area: the lack of donor organs, immune rejection and the possibility of transferring viruses to the recipient. Xenotransplantation (transplantation of organs from one species to another) is limited by rapid immune rejection of the animal organ by the human recipient. This has led to the routine use of immunosuppressive drugs (drugs that either suppress or interfere with the immune system's attack on the transplanted organ). Another approach preventing immune attack is the use of transgenic animals, which contain specific genes that have been artificially introduced. These genes allow the body to recognise the organ as "self" and thus reduce the immunological response. A major concern with the above approach however is that a new infectious agent will be introduced into the human population.

Until very recently, most scientists and clinicians believed that damaged or diseased some human tissue could only be replaced by donor transplants or with totally artificial parts. Tissue engineering promises an alternative approach in which organs or tissues can be repaired, replaced, or regenerated. This approach also responds to clinical needs that cannot be met by organ donation alone.

Tissue engineering has already led to a broad range of potential products involving repair and replacement of human tissues or organs and the combination of selected or expanded human or other mammalian cells (e.g., stem/progenitor cells, genetic, and somatic cellular therapies), with or without biomaterials. Some products, which are in different stages of development, include both structural/mechanical substitutes and metabolic substitutes. Structural/mechanical substitutes include artificial skin constructs; expanded cells for cartilage regeneration; engineered ligament and tendon; bone graft substitutes/bone repair systems; products for nerve regeneration; engineered cornea and lenses; and products for periodontal tissue repair. Metabolic

substitutes include implanted, encapsulated pancreatic islet cells; engineered products for cardiovascular repair/regeneration; blood substitutes; and encapsulated cells for restoration of tissue/organ function, other than encapsulated islet cells used as implants or encapsulated hepatocytes used as *ex vivo* metabolic support systems (Hellman et al. 1998; Hellman et al. 2000; Bonasser et al. 1998). To date, the FDA has approved only a few of these products while many are under either preclinical investigation or regulatory evaluation (Hellman et al. 1998, Hellman et al. 2000).

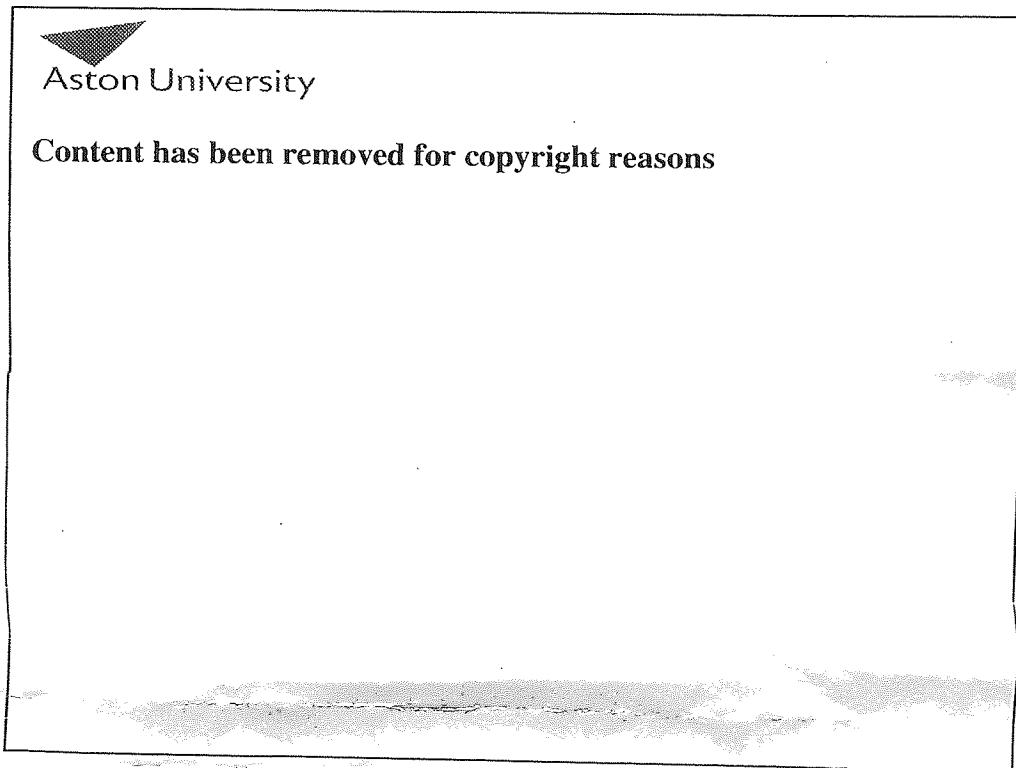
Cell-based tissue-engineered systems may also be utilized as exceptionally sensitive biosensors. Applications could include detection of infrared signals over large distances and development of predictive models for toxicity assessment. The combination of cells and silicone based technology also holds great promise for development of *in vitro* neural networks and novel computational device development. As research tools, these systems could also be employed as correlates of *in vitro* and *in vivo* biological activity.

1.2 Biomaterials

The term 'biomaterials' has alternately been used to describe materials derived from biological sources or to describe materials used for implantation in the human body. The main applications for biomaterials in tissue engineering are as scaffolds to guide the organization, growth and differentiation of cells in the process of forming functional tissue and to provide both physical and chemical stimuli. The use of polymers in this role in medicine dates back almost to the birth of polymer science (Rabkin et al. 2002). The development of biomaterials for surgical implants has evolved through three stages, overlapping over time, yet each with a distinctly different objective (Figure 1.1) (Hench et al. 2002). The goal of early biomaterials was to achieve a suitable combination of functional properties to adequately match those of the replaced tissue without deleterious response by the host. The first generation of biomaterials (1950's and 1960's) used largely off the shelf, widely available, industrial materials that were not developed specifically for their intended medical use. They were selected because of the desirable combination of physical properties specific to the clinical use, and they were intended to be bioinert (elicit

minimal response from the host tissue). This principle underlying the bulk of biomaterial development was to reduce minimize the immune response to the foreign body, and this is still valid 22 years later (Hench et al. 2002).

Figure 1.1 Evolution of biomaterial science and technology. Three overlapping generations of biomaterials for surgical implants have evolved over time: from inert (with minimal tissue interaction), to biologically interactive (with incorporated bioactive components to elicit a controlled reaction in the tissues) and, finally, to biointeractive, able to regenerate functional tissue. (Adapted from Rabkin et al. 2002)



metabolism, or other means. Thus, a long term interface between the implant site and the host tissue could be eliminated, because the foreign material would ultimately be degraded by the host and replaced by tissues. Degradability is one of the most important properties of a biomaterial (Griffith, 2000). Although some tissues, particularly bone, can tolerate very slowly degrading or permanent materials of specific compositions, permanent implants almost always elicit a chronic inflammation called a foreign body response (Anderson, 1988, Babensee et al. 1998, Anderson et al. 1999). This response is characterized by formation of a poorly vascularized fibrous layer analogous to a scar at the material-tissue interface (Griffith, 2000). The degradation products resulting from implantation of a material must be nontoxic and non-immunogenic. Other aspects of biocompatibility are typically context-dependent. Many groups continue to search for biodegradable polymers with the combination of strength, flexibility and a chemical composition conducive to tissue development (Freed et al. 1994, Hubbell, 1995, Langer, 1999, Griffith, 2000). Biodegradable sutures such as 'Vicryl' composed of polylactic acid (PLA) and polyglycolic (PLGA) acids have been used since the 1970s. However the acidic breakdown products produced by degradation of commonly-used degradable polyesters have been associated with adverse tissue reactions when used as fixation devices in bony sites (Böstman, 1990, Hirvensalo et al. 1990; Suganama, 1992, Alexander et al. 1992), due to the increased amounts of degradation products produced by relatively large devices.

Most degradable materials used in tissue engineering today were adapted from other surgical applications but now new degradable materials with improved mechanical properties, degradation properties, cell-interaction properties, and processability polymers are being specifically designed for tissue engineering. The mechanical properties requirement of biomaterials and devices vary with application. Constraints may range from in vivo performance needs (for example, matching tissue compliance) to practical issues of ease of handling in a laboratory or during surgery, where brittle or flexible devices may increase the chances of error or failure rates. Attaining the specific range of mechanical properties is of great importance in connective tissue applications such as bone, cartilage, and blood vessel replacement.

The biomaterial will be made into a device and the mechanical properties of this device are governed both by materials composition and by materials processing. For example, poly (lactide-co-glycolide) [PLGA] polymers can be made into flexible fabrics (Vicryl mesh used for Dermagraf) as well as a rigid solid or a porous block. In most tissue engineering applications the mechanical properties of the device are not constant due to the fact that biological processes are degrading the device as the tissue grows. Degradation properties can be affected by the composition and structure of the material and by the loading on the device at the site of the implant site. As more animal and clinical data emerge relating device performance to structure and composition, investigations into designing the time-dependent aspects of mechanical properties will increase. In addition to the role of bulk mechanical properties on device performance, local cell-molecular-level mechanics may also govern tissue response through modulation of cell behavior (Griffiths, 2000).

1.3 Natural Polymers

Biomaterials used in tissue engineering can be broadly divided into categories of synthetic or naturally derived. Natural polymers include both extracellular matrix (ECM) proteins and derivatives (e.g., collagen) and materials derived from plants.

Collagen is the single most abundant protein found in mammalian tissue (Table 1.1) (it accounts for approximately 30% of these proteins (Williams, 1998)) and is the most widely used in tissue engineering. Collagens form a family of proteins, Type I collagen is the main structural protein in ECM and mixtures of Type I collagen and other matrix components have been successfully used in several tissue-engineering applications (Badylak et al. 1999).

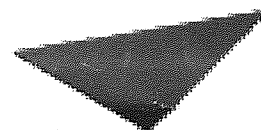
Collagen is comprised of three different polypeptide chains with a triple helical structure (Figure 1.2). Each of the polypeptide chains has a sequence of [-glycine-X-Y-] where X is any amino acid other than glycine typically proline and Y is also another amino acid usually hydroxyproline. Collagen does not appear to exist as isolated molecules in the extracellular tissue but forms aggregates known as fibrils.

Table 1.1 Types of collagen and their location within the body

Collagen Type	Distribution
I	cornea, skin, arteries, muscle, bone
II	arteries, muscle, cartilage
III	skin, arteries, muscle
IV	arteries, muscle
V	cornea, skin
VI	nerves, arteries
VII	skin

A collagen fibril can be as small as 50 nm and as large as 300 nm in diameter, with varying length. The fibrils can form sheets that provide tensile strength. Collagen has been used as a natural-tissue analogue in several types of medical device (artificial skin, Integra Life Sciences). Some of these are reliant on mechanical properties (artery reconstruction (Badylak et al. 1999)), others on the biological characteristics (skin substitutes) and some on the gel forming ability (skin reconstruction Organogenesis) of collagen (Williams, 1998). In early applications collagen-rich tissues were used in surgical procedures, like catgut due to its strength and biodegradability.

Figure 1.2 The structure of a collagen fibril. (www.rcsb.org/pdb/molecules)

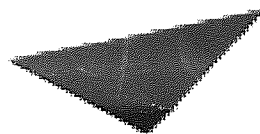


Aston University

Illustration removed for copyright restrictions

Hyaluronic acid (HA) or hyaluronate (Figure 1.3) has been used extensively as a biomaterial for tissue engineering (Campoccia et al. 1998, Galassi et al. 2000, Lisignoli et al. 2001). HA is a naturally occurring polysaccharide of the extracellular matrix and a main glycosaminoglycan, which is widely distributed in the connective tissue and synovial fluids of mammals (Lloyd et al. 1998). It plays a multi-task role, having structural, rheological, physiological and biological functions in the body (Campoccia et al. 1998). It also interacts with a wide range of biomolecules including tissue components, proteins, proteoglycans and growth factors. In a wound environment it acts as a scavenger for free radicals and so modulates inflammation (Presti et al. 1994, Abatangelo et al. 1995). HA is also recognised by specific cell receptors such as CD14, regulating the adhesion, growth, differentiation, locomotion and activity of specific cell types. However there are severe limitations on the use of hyaluronic acid as scaffolds because of its solubility in water, rapid resorption and short residence time in tissue. Attempts are being made to chemically reduce its solubility by cross-linking but the cross-linking agents themselves could be toxic.

Figure 1.3 The structure of hyaluronic acid. (www.bssv01.lancs.ac.uk)



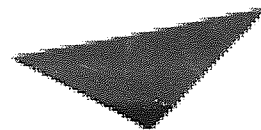
Aston University

Illustration removed for copyright restriction.

Alginate is an algal polysaccharide obtained from the cell walls of brown algae such as seaweeds (Lloyd et al. 1998) that has been widely used in wound healing (Leor et al. 2000, Marijnissen et al. 2002, Eiselt et al. 2000). Alginate (Figure 1.4) can be made into gels and sponges by cross-linking calcium ions with two guluronic acid residues which occurs in the presence of divalent cations. These are thermally stable and have also been reported to deodorize wounds and absorb pain-stimulating compounds. Numerous types of wound have been successfully treated with alginate

preparations but after a period of time the dressing becomes partially liquid as the sodium present in the wound exudate is gradually exchanged for calcium. An increase in calcium effects many cellular activities including adhesion, differentiation and proliferation.

Figure 1.4 The structure of alginate. (www.sbu.ac.uk)



Aston University

Illustration removed for copyright restrictions

Chitin is a naturally occurring polysaccharide found in the outer shell of crustaceans (Figure 1.5 (A)). Chitosan (Figure 1.5 (B)) is the name given to the partially deacetylated form of chitin. Chitosan is biocompatible and has been evaluated in a number of medical applications including wound dressings. The properties of chitosan depend heavily upon its cationic nature. It has one positive charge per glucosamine (one of its building blocks) residue and so will interact with negatively charged molecules including proteins, anionic polysaccharides and nucleic acids. For these reason many investigators have examined chitosan as a scaffold material (Ma et al. 2001, Madihally et al. 1999, Zhang et al. 2001, Kast et al.).

Scaffolds for tissue engineering have also been produced by extraction or partial purification of whole tissue to leave the 3D matrix structure intact. Demineralized bone matrices are used clinically in bone wound healing and may be considered a form of tissue engineering matrix (Burg et al. 2000). The partially purified small intestinal submucosal matrix (Badylak et al. 1999) has been shown to induce regeneration of a variety of tissues.

Figure 1.5 The structure of (A) chitin and (B) chitosan. (www.food-insects.com)



1.4 Synthetic Polymers

There are numerous examples of synthetic, permanent implant materials such as acrylic polymer, silicone elastomer and porous PTFE-carbon fibre composite (Coombes et al. 1994). However there is a tendency to replace these materials wherever possible as the implants can elicit a chronic inflammation leading to clinical complications (Griffith, 2000). Synthetic degradable polyesters were adopted in surgery 30 years ago as materials for sutures and bone fixation devices and include polyglycolic acid (PGA), poly (DL lactide co-glycolide) [PLG] and poly(L-lactide) [PLA]. These poly(α -hydroxy acids) or synthetic α -polyesters are synthesised from α -hydroxy acids such as glycolic acid and lactic acid (Coombes et al.1994). Lactide is a chiral molecule, existing in L and D isomers (the L isomer is the biological metabolite) and thus poly (lactide) actually refers to a family of polymers made from the different forms of pure PLA. Poly (DL lactide) is a mixture of D and L isomers and is amorphous whereas PLA is produced from only one isomer and is a crystalline

material. PGA is synthesised from glycolide derived from glycolic acid. PLG refers to a family of copolymers prepared from various ratios of lactide and glycolide monomers. Dexon (PLG) and Vicryl (polyglactin 910) are fast degrading materials and the resulting sutures are only designed to maintain wound closure for short times. This makes them highly suitable for applications in soft tissue repair but their high shrinkage (Coombes et al. 1994) during resorption could relieve anchorage-dependent cells of a stable substrate for laying down extra-cellular matrix of optimal quantity and orientation when the repair process is extended. PLA is a slow-resorbing polymer and is characterised by resorption times in excess of one year. This extends the design options for 3-D scaffolds in tissue engineering giving extra scope for matching tissue growth characteristics. PLA suffers from low compliance; a tendency to degrade during melt processing and the starting polymer is expensive.

Table 1.2 The melting points $T_{(m)}$ and degradation times of PLG, PLA and PGA (Coombes et al. 1994)

Aston University

Illustration removed for copyright restrictions

The lactide and glycolide monomers are insoluble in water but degrade by undergoing extensive random chain scission to form small soluble oligomers or monomers by hydrolytic attack of the ester bond. The degradation properties are affected by crystallinity, molecular weight, glass transition temperature and hydrophobicity. The difference in degradation rates of the different polymers has been attributed to accessibility of water to the ester bond.

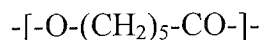
Other resorbable polymers that have interest for tissue engineering include poly(orthoesters) [POE] and polyanhydrides. POEs are hydrophobic biodegradable polymers, which may be prepared by transesterification using a diethyl orthoester and a diol (Coombes et al. 1994). POE is amorphous, the polymer is more hydrophobic

than PLA and is similarly extremely resistant to degradation. Polyamides contain linkages, which are more hydrolytically unstable than polyorthoesters and polyesters and tend to give matrices, which erode heterogeneously at the surface (Coombes et al. 1994).

1.5 Polycaprolactone

PCL is noted for its biocompatibility (Pachence et al. 2000) and like PLA, is a slowly degrading poly(ϵ -hydroxy acid) characterised by resorption times in excess of one year, due to its semi-crystalline nature and hydrophobicity (Figure 1.6). The long resorption time extends the design options for 3-D scaffolds in tissue engineering giving extra scope for matching tissue growth characteristics. PCL (in moulded form) exhibits lower tensile modulus (0.3 GPa) and strength (19 MPa) than PLA (4 GPa, 70MPa) but higher extensibility, which presents opportunities for adjusting the compliance of soft tissue substitutes such as cardiovascular implants. The rubbery characteristic of PCL due to the low T_g of -60°C dramatically increases its permeability relative to PLA and this has been exploited for diffusion controlled delivery of low molecular weight drugs such as steroids (Coombes et al. 1994). PCL films have been shown to provide a favourable substrate for growth of bone cells (Ali et al. 1993) and the polymer has been applied as the matrix component in composites intended for bone repair (Marra et al. 1999).

Figure 1.6 Chemical structure of poly(ϵ -caprolactone)



1.6 Scaffold Production Techniques

A variety of techniques have been used to produce the scaffold component for cell seeding in tissue engineering;

Solvent casting is a widely used and simple technique for producing polymer scaffolds, mainly in the form of thin films. The polymer is dissolved in a solvent, which is then allowed to evaporate leaving the polymer cast in the desired shape. Residual solvent can cause toxicity and another problem is the low solubility of some polymers in solvents.

Gel casting, makes use of a polymer-solvent system in which the polymer forms a three dimensional stable network in the solvent. The formation of gels depends on several factors such as solution concentration, degree of regularity of the chemical structure of the polymer, the form of the macromolecule, interaction between polymer and solvent, molecular weight and chain flexibility. Gel casting of a microporous scaffold basically involves polymer dissolution in a solvent, casting in a mould, gel formation in situ, solvent extraction and drying to obtain relatively thick section materials (Coombes et al. 1994).

Solid Freeform Fabrication involves use of droplets of a polymer melt, which are dropped on to a mould and solidify on impact forming beads. Overlapping of adjacent beads forms a line and overlapping of adjacent lines creates a layer. Other layers are added to build up the desired shape. The mould is removed often by immersing in ethanol. The creation of these scaffolds is controlled by CAD software so precise shapes can be produced (Sacholos et al. 2003).

Freeze drying is widely used to produce collagen-based matrices. Solutions are mixed and then frozen to form a continuous interpenetrating network of ice and precipitate. The reduction in the chamber pressure causes the ice to sublime, leaving a highly porous solid (Freyman et al. 2001).

Foaming can create a porous scaffold. Carbon dioxide gas is dissolved in a polymer under high pressure and then expanded to form bubbles by releasing the pressure (Mooney et al. 1996).

Salt leaching gives a microstructure similar to a foam. Sieved NaCl particles are combined with PLA or PLG powder in a solution of chloroform or methylene

chloride. The solvent is evaporated and the remaining solid is heated to above the melting point of the polymer to consolidate it more uniformly. After cooling, the material is immersed in water to leach out the salt, leaving a porous structure (Freyman et al. 2001).

Supercritical fluid processing has recently been applied for production of porous polymer scaffold. The CO₂ becomes supercritical by raising the temperature and pressure above its critical point (72 bar and 31.1°C). Under these conditions, CO₂ has enhanced solvent properties and can plasticise the polymer. On depressurisation, nucleation of the gas bubbles occurs as gas attempts to escape from the polymer and forms a foamed structure (Whitaker et al. 2001).

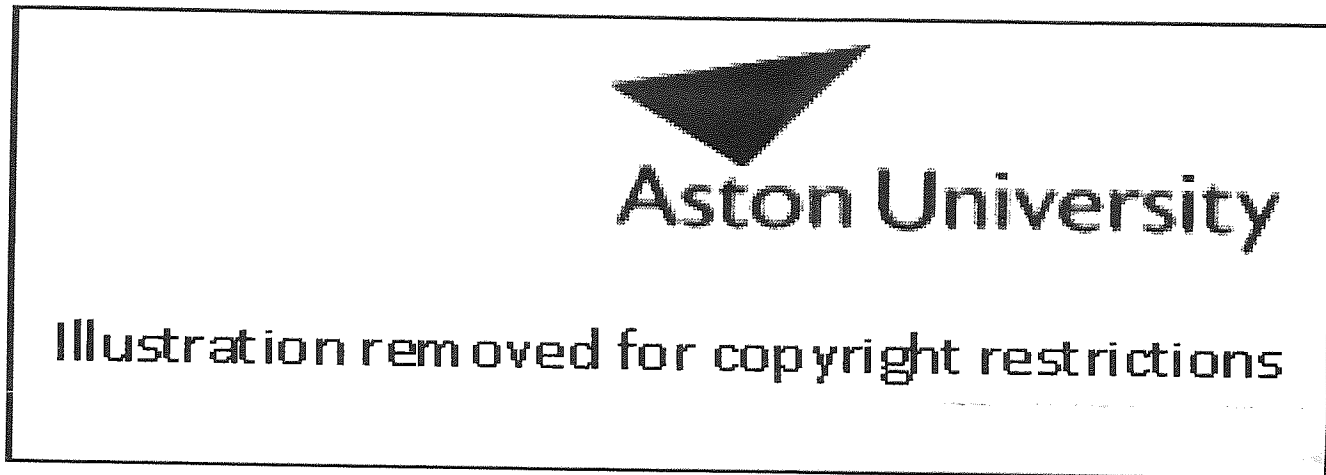
1.7 Fibre Spinning Techniques

Fibres are used in biomedical applications for several reasons; the surface to volume ratio is very large which is important in surface dominated applications such as separation technology. Inherently porous, fibre constructs of various designs based on woven, knitted and non-woven technologies, such as fused deposition modelling (Zein et al. 2002), have been widely investigated for improving cell attachment and tissue infiltration of the scaffold (Wintermantel, 1996). The design and production advantages associated with polymer fibres have already led to the use of both natural and synthetic fibres for a wide range of tissue repair applications involving bone and cartilage, skin substitutes, nerve regeneration (Marler, 1998) and blood vessels (Hanson. 1998). Indeed the early observations of favourable cell growth on silk fibres stimulated much of the research into biomaterials-cell interaction. Fibrous mats or meshes of synthetic resorbable polymers such as PGA or PLG are being investigated extensively as scaffold materials for seeded cells in tissue engineering (Freed et al. 1998, Hubbell, 1995, Marler, 1998. One production technique entails heating of a wad of PGA fibres in a mould to produce point welding between the individual fibres (Mikos et al. 1993). On cooling the mesh retains the shape of the mould and is used as a template to support cell adhesion and tissue infiltration.

Fibre spinning may be broadly divided into three main categories, melt spinning dry spinning and solution spinning.

Melt spinning, the polymer melt is forced through a spinneret under pressure. The molten polymer is first fed through filters that remove large solid or gel particles, which could block the spinneret. The polymer is first converted into a rod by the melting process then extruded, threads are collected continuously on exiting the spinneret. Cool filtered air is blown across the molten threads to encourage uniform cooling to form solid threads. The polymer threads are subjected to a drawing procedure to control chain orientation and fibre tensile properties.

Figure 1.7 Schematic of melt spinning technique. (www.pct.edu)



Dry spinning, a polymer solution is extruded from a spinneret through a zone in which solvent is rapidly evaporated. The fibre is continuously collected and drawn to control final properties. Dry spinning of the poly(α -hydroxy acids) such as PLA normally requires high solution viscosities to enable extrusion of a filament, prior to drawing.

Figure 1.8 Schematic of dry spinning technique. (www.polymerprocessing.com)



Solution spinning is the slowest production method of the three and is based upon extrusion under pressure of concentrated polymer solutions into a non-solvent. The spinnerets are immersed in a non-solvent bath and are normally positioned in the horizontal or vertical position with the extruded polymer thread being collected upwards. This process is based on precipitation only rather than chemical regeneration used for production of cellulose fibres (rayon). The solvent diffuses out of the extruded filament into the bath and the non-solvent diffuses from the bath into the extruded. The polymer filament initially precipitates as a gel at the extruded materials coagulant interface and the rate of coagulation is dependant upon the characteristics of gel structure.

High strength polyethylene (PE) fibres have been spun from solutions undergoing shear flow in a Couette flow apparatus rather than by extrusion through an orifice. Investigations demonstrated the marked influence of spinning temperature on fibre strength and stiffness occasioned by the improvement in polymer chain alignment and

reduction of the chain folded element ('kebab structure') in the fibrous 'shishkebab' structures, which made up the fibre (Goglewski et al. 1983).

Figure 1.9 Schematic of solution/wet spinning technique. (www.psrc.usm.edu)



Electrospinning, this can be achieved by using polymer, such as poly(ethylene-co-vinyl alcohol) and PCL solutions by dissolving in solvents (chloroform). Applying a charge to the liquid, typically 5-30kV, produces the fibres, with respect to a ground voltage a short distance away. As the jet accelerates towards the ground collector, the solvent evaporates giving rise to a continuous fibre of 20 nm to 8 μm (Kenawy et al. 2003, Yoshimoto et al. 2003). The fibres that are spun have application in tissue engineering.

Figure 1.10 Schematic of electrospinning technique. (www.che.vt.edu)

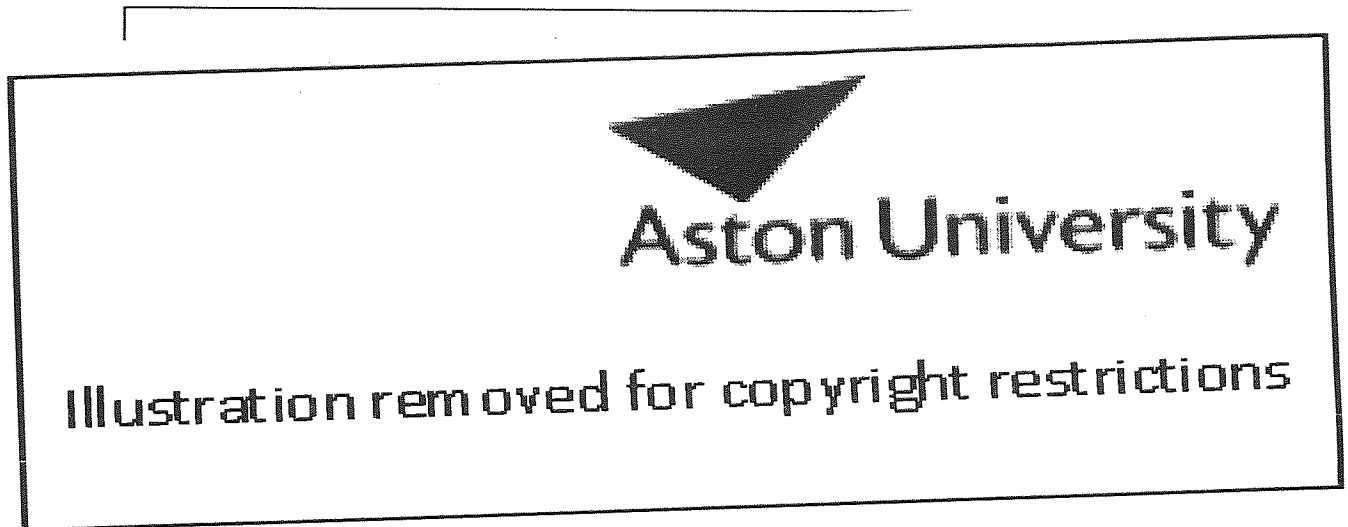


1.8 Cell Interaction with Tissue Engineering Scaffolds

One tissue engineering approach involves biodegradable scaffolds or matrices being seeded with cells that are then implanted for subsequent development of new integrated tissue (Figures 1.11). Most cells from solid tissues grow as adherent monolayers. Unless cells have transformed and become anchorage independent following tissue disaggregation or subculture they will need to attach and spread out on a substrate before proliferation will occur.

The surface chemistry (eg hydrophobicity, surface charge), morphology and microtopography of the scaffold exert profound effects on cell adhesion, distribution, morphology, alignment and importantly cell proliferation and differentiation (Freed et al. 1998, Hubbell, 1995, Marler, 1998).

Figure 1.11 A schematic of the tissue engineering approach involving cell seeding on scaffolds. (www.camd.unsw.edu.au)

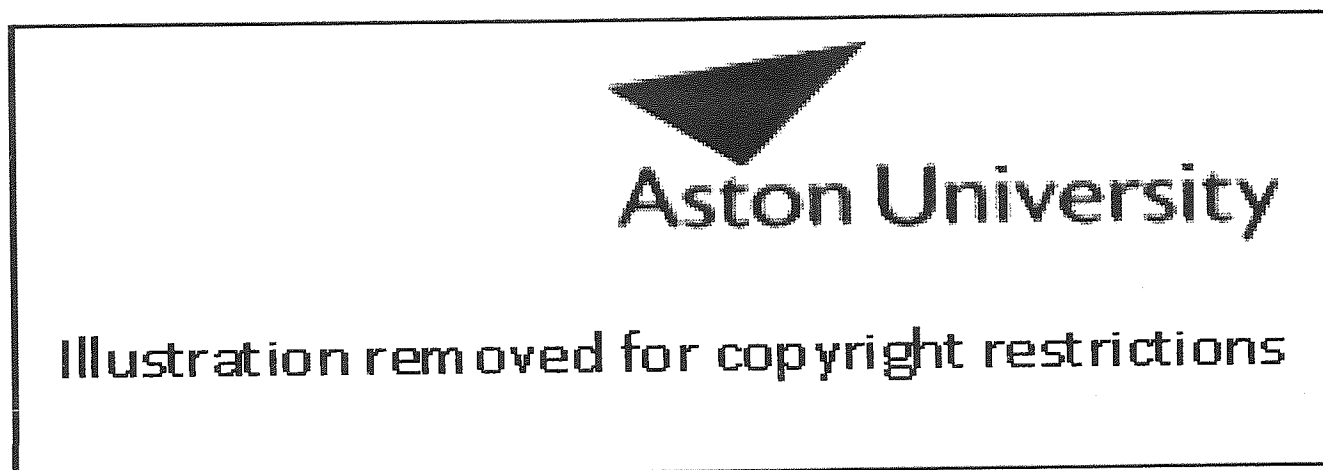


1.9 Cell Adhesion

Cells adhere to a material via glycoproteins and extracellular proteins, such as fibronectin, vitronectin and laminin (Hubbell, 1995, Boyan et al. 1996, Fabrizio-Homan et al. 1991, Grinnell et al. 1982, Nikolovski et al. 2000, Steele et al. 1996, Underwood et al. 1989), which are absorbed onto the material surface from serum in the cell culture media or body fluids *in vivo* (Yamada, 1983, Hubbell, 1999). The interactions between these adhesion molecules and the cell are mediated primarily by integrins, which are cell surface receptors that bind to a specific motif, usually containing the arginine-glycine-aspartic acid (RGD) sequence, found in many ECM proteins. All integrins are $\alpha\beta$ heterodimers. The α subunits vary in size between 120 and 180 kD and are each non-covalently associated with β subunit (90-110kD), each subunit has a large extracellular domain and a short cytoplasmic domain (Figure 1.12). Most integrins are expressed on a variety of cells, and most cells express several integrins (Hynes, 1992). Although 8 β subunits and 16 α subunits are known which could in theory associate to give more than 100 integrin heterodimers, the

actual number is limited to about 22. Many α subunits can associate with only a single β subunit. This has led to sub-families with shared β subunits, however several α subunits can associate with more than one β subunit.

Figure 1.12 Structural features of integrin cell surface receptors. (a) The overall shape, as deduced from electron microscopy. The shaded area represents the ligand-binding region. (b) Schematic arrangement of the polypeptide chains. (Hynes, 1992)



Focal contacts are specialized sites where cells attach to the ECM. At focal adhesions, clusters of integrins bind to the ECM proteins and internally specialized cytoplasmic proteins bind to the integrins that then bind to actin filaments. Focal contacts are dynamic structures that change size as the cell process progresses (Aplin et al. 1998). As the focal contact matures, the actin filaments extend and bundle to form prominent structures called stress fibres (Figure 1.13).

The cytoplasmic structural proteins involved in the focal contact including talin and α -actinin directly bind to the β subunit of the integrin. These in turn bind to other structural proteins including paxillin, vinculin and tensin (which both bind directly to the actin filament), ultimately leading to the recruitment of actin filaments (Figure 1.13). Integrin-mediated phosphorylation of several cytoskeletal proteins has a role in

the organization of stress fibres at focal adhesions, the main one of these being focal adhesion kinase (FAK).

Integrins do not just function as receptors for cell adhesion, but also elicit signal transduction. FAK associates with the focal adhesion via the β subunit, which results in the autophosphorylation of a tyrosine. This creates a binding site for the Src homology region 2 (SH2) domain of Src (a protein tyrosine kinase) that then binds and phosphorylates several tyrosines on FAK, which allows growth factor receptor binding protein 2 (GRB2) to bind. GRB2 then complexes with SOS (a Ras guanine nucleotide exchange factor), this complex catalyses the exchange of guanosine 5'-diphosphate (GDP) for guanosine 5'-triphosphate (GTP) on Ras (a membrane-bound guanine nucleotide-binding protein), which in turn activates Raf (a serine/threonine kinase). Raf then activates MAPK-ERK kinase (MEK) by phosphorylation. This active form of MEK causes the phosphorylation and activation of mitogen-activated protein kinase (MAPK) so that it can translocate into the nucleus and cause the activation downstream of various genes that lead to cell spreading or motility (Aplin et al. 1998). The actual pathway is not known but the system described above is favored.

Figure 1.13 Schematic diagram of integrin clustering to form a focal contact and the intracellular binding of proteins from the integrins to the actin cytoskeleton. (www.pingu.salk.edu)



Aston University

Illustration removed for copyright restrictions

A second group of cell adhesion molecules transmembrane proteoglycans, also interact with ECM molecules such as collagen or proteoglycans but not via the RGD sequence. The main proteoglycan involved is syndecan-4 and it has been suggested that focal contacts cannot be formed without them present (Crouchman et al. 1999). Integrins appear to be the primary receptors, whose binding must precede that of signaling through syndecan-4 (Woods et al. 2000). Syndecans are transmembrane proteoglycans that normally bear heparan sulfate glycosaminoglycan chains covalently attached to their core proteins and they bind to the HepII heparin-binding domain of fibronectin (Woods et al. 2001). Syndecan-4 is localized to the focal contact and also aligns with the actin stress fibres (Figure 1.14). Clustering of syndecan-4 stimulates the rearrangement of the actin cytoskeleton into ordered stress fibres (Bass et al. 2002). Syndecan-4 signals via Rho-family GTPases that are activated by protein kinase C α (PKC α). The activation of Rho leads to the activation of several downstream molecules and gene activation.

Figure 1.14 Syndecan-4 acts as an organizing center for transmembrane receptors and is anchored to the actin cytoskeleton. (Woods et al. 2001)



1.10 Cell Proliferation

Cell proliferation involves five phases of the cell cycle (Figure 1.15). G₀ is the phase where the cell is at rest. In the G₁ phase, the cell either progresses towards DNA synthesis or irreversibly commits to differentiation. G₁ is followed by the S phase (DNA synthesis) in which the DNA replicates. S is in turn followed by the G₂ (Gap 2) phase in which the cell prepares for entry into mitosis. There are several check points, one at the beginning of DNA synthesis and in G₂ to determine the integrity of the DNA. These will halt the cell cycle to allow DNA repair or entry into apoptosis if repair is not possible. Entry of a cell into the cell cycle is regulated by signals from the environment. Low cell density leaves the cells with free edges, which renders them capable of spreading and permits their entry into the cycle in the presence of growth factors, such as epidermal growth factor (EGF), fibroblast growth factor (FGF). High cell density however inhibits proliferation, due to cell-to-cell contact and a lack of spreading. Cell binding to the ECM activates the G₀ to G₁ transition via integrin binding and then promotes G₁ to S phase progression through mechanisms related to cell spreading (Hansen et al. 1994). The adhesion of integrins and their clustering without cell spreading can cause the progression of G₀ to G₁ (Ingber et al. 1995). The stress imposed upon the cytoskeleton by the cell and the subsequent change in nuclear shape by spreading or expansion has a major effect on progression through the cell cycle.

As well as adhesion to a substrate, cyclins are needed to progress cell proliferation. These are either environmental or can be produced via downstream signalling after adhesion (Assoian et al. 1997). Other factors required for cell proliferation include, mitogens, growth factors and survival factors (Alberts, 1994). Mitogens stimulate cell division primarily by relieving intracellular negative controls that otherwise block progress through the cell cycle. There are about 50 proteins that are known to be mitogens, including platelet-derived growth factor and epidermal growth factor. Growth factors stimulate cell growth by promoting the synthesis of proteins and macromolecules and by inhibiting degradation. These growth factors include vascular endothelial growth factor (VEGF), nerve growth factor (NGF) etc and bind with receptors on the surface of the cell activating intracellular pathways that increase

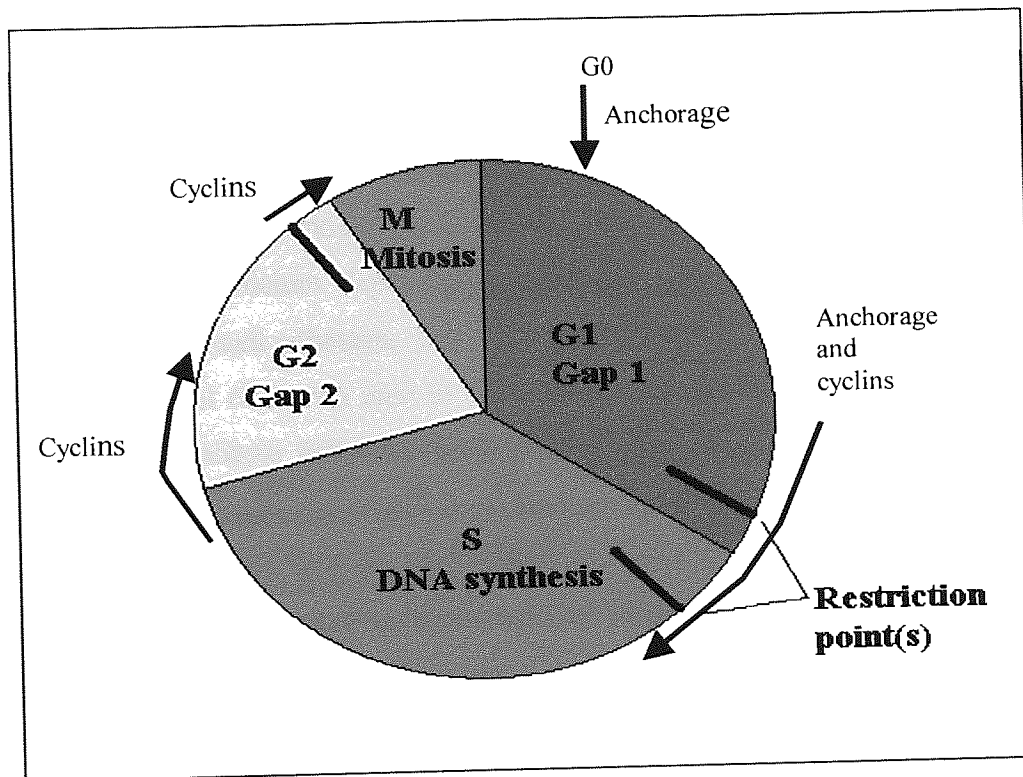
synthesis of proteins and macromolecules. Finally survival factors (signals from other cells) also bind to surface receptors that then activate a signaling pathway (Alberts, 1994).

1.11 Cell Differentiation

Cell differentiation is the process leading to the expression of phenotypic properties characteristic of the functionally mature cell. As differentiation progresses, cell division is reduced and eventually lost. There are four main controls of differentiation; i) soluble inducers, ii) cell interactions, iii) cell-matrix interactions and iv) shape and polarity. Soluble inducers are physiological and nonphysiological. The physiological inducers include hormones, paracrine factors, IL-6, interferons, vitamins and inorganic ions such as calcium. Non-physiological inducers, include chemicals, such as dimethyl sulfoxide and benzodiazepines. The action of these compounds is unclear, but may be mediated by changes in membrane fluidity.

Cell interactions that cause differentiation are also divided into two subsets, homologous and heterologous. Homologous cell interactions occur at high cell density and probably involve gap junction communication where metabolites, second messengers (such as cyclic AMP, calcium or electrical charge) transfer between cells. Cell-cell molecules like cell adhesion molecules (CAMs) or cadherins provide another means, by which cells communicate with each other. Following interaction of extracellular domains, the intracellular domain will become phosphorylated and start a signal cascade causing downstream activation. Heterologous cell interactions, where one cell type interacts with another cell type to provide a stimulus are also responsible for differentiation. The mechanism is unclear but is thought to involve transmission of paracrine factors.

Figure 1.15 Anchorage regulation of the cell cycle. Key regulators of the cell cycle include cyclins



A complex mixture of glycoproteins and proteoglycans surrounds most cells, which is known as the extracellular matrix and is specific for each tissue. The cell binds to the ECM this via integrins and proteoglycans, which then causes a signal cascade, inducing differentiation. Polarity and shape also play a vital role in differentiation as they do in proliferation. The cells need to be spread and the nucleus needs to be positioned at the base of the cell.

1.12 Tissue Development

Tissue is formed from precursor cells, which are localised by attachment to the extracellular matrix, to other cells or both. These cells do not remain passively adhered. Instead the tissue architecture is generated and actively maintained by selective adhesions that are continuously adjusting (Alberts, 1994). The selective adhesions are more important in tissues with more complicated origins. In these tissues one population of cells invades another population and then binds with it. This

cell motility and adhesion are controlled by a mechanism for directing cells into their final destination. The probable mechanisms are chemotaxis (which is the secretion of soluble chemicals that attracts or repels migrating cells) and pathway guidance. This involves the laying down of adhesive or repellent molecules in the extracellular matrix or on the surface of cells to guide the migrating cells. The cell must then recognise the cells that it should bind to form a tissue. Cells adhere to each other through cell adhesion molecules (CAMs), which can be calcium dependent or independent. The calcium dependant CAMs seem to be primarily responsible for tissue specific cell-cell adhesion. There are three different types of cadherin and three different ways that cadherins bind to each other. Homophilic, heterophilic and binding through an extracellular linker molecule. This is how the cells sort themselves into the desired tissue structure, cells will only bind to cells with the same cadherin or the same affinity cadherin and so both qualitative and quantitative differences in the expression of cadherins play an important role in the organisation of tissues (Alberts 1994) and ultimately organ development.

1.13 Tissue Engineering of Blood Vessels

The development of tissue engineered blood vessels is of great interest as atherosclerotic vascular disease, in the form of coronary artery and peripheral vascular disease, is one of the largest cause of mortality (Niklason et al. 1999).

Artery Structure. The inner layer of an artery (Figure 1.16) consists of squamous (flat, smooth) endothelial cells and is known as the endothelium. At the base of the epithelial layer is a thin layer of spongy connective tissue that secretes a layer of elastic collagen. This 'stretchy' layer forms the "basement membrane" for the endothelium. These two layers together are known as the tunica intima, or inner sheath. In larger arteries, which must stretch considerably, the tunica media is often highly folded when the artery is relaxed.

The surrounding layer of smooth muscle is quite thick in arteries, and can stretch to accommodate passing blood, or contract to restrict blood flow. It (like other smooth muscles) is under involuntary control. The muscle layer is also underlain by a spongy

layer of connective tissues that produces elastic collagen fibres. The loss of elasticity in these fibres is one of the causes of cardiovascular diseases, such as high blood pressure, in older people and in diabetics. Surrounding the tunica media is a layer of connective tissues that produces both elastic collagen fibres and more rigid collagen fibres. This layer the tunica externa will stretch, but only to a limit. This tougher fibrous layer prevents the ballooning of the blood vessel walls that could take place when systolic pressure is high.

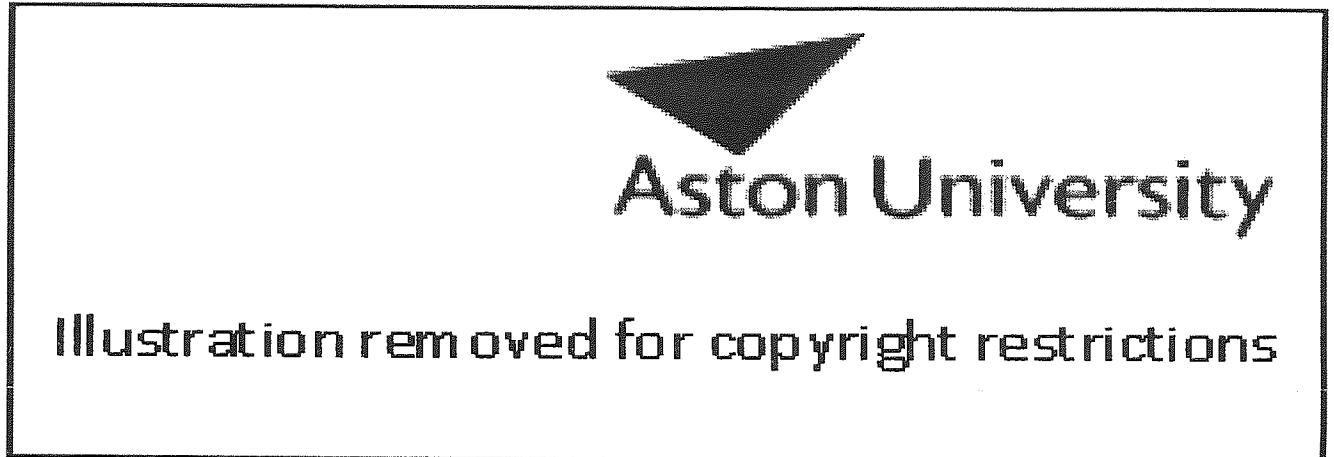
Figure 1.16 Schematic of the structure of an artery. (www.sonofsun.sdsu.edu)



Vein Structure. The walls of veins have the same three layers as the arteries (Figure 1.17). Although all the layers are present, there is less smooth muscle and connective tissue. This makes the walls of veins thinner than those of arteries, which is related to the fact that blood in the veins has less pressure than in the arteries. Because the walls of the veins are thinner and less rigid than arteries, veins can hold more blood. Almost

70 percent of the total blood volume is in the veins at any given time. Medium and large veins have venous valves, similar to the semilunar valves associated with the heart that help keep the blood flowing toward the heart.

Figure 1.17 Schematic of the structure of a vein. (www.sonofsun.sdsu.edu)



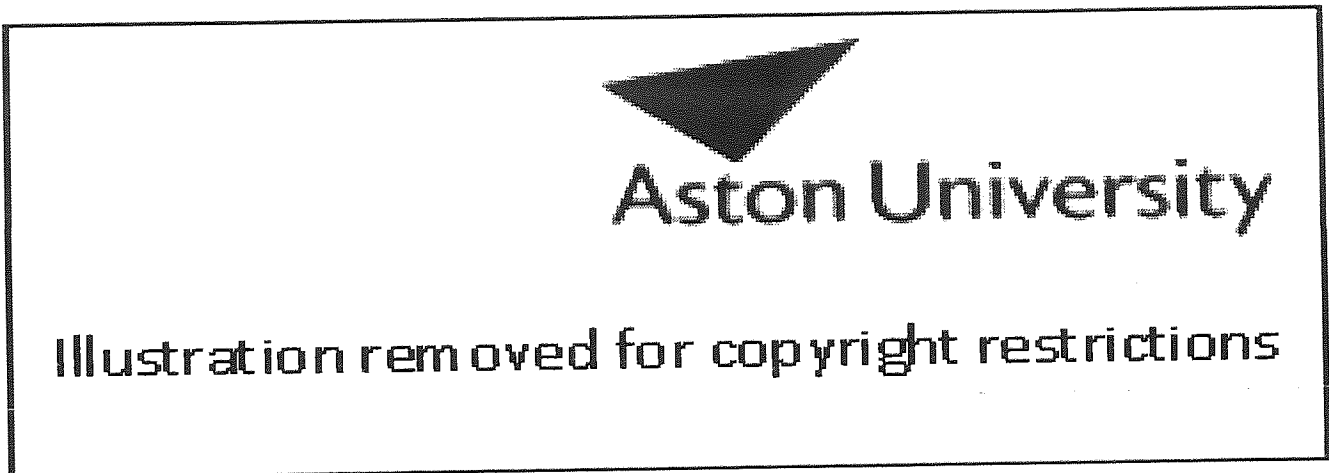
1.14 Tissue Engineering of Skeletal Muscle

Tissue engineering of skeletal muscle is in the interest for rebuilding muscle mass lost during muscular dystrophy or following trauma or surgery. A single skeletal muscle cell, known as a muscle fibre is relatively large, elongated and cylinder-shaped, measuring from 10 to 100 μm in diameter and 750,000 μm or 2.5 feet in length. An individual skeletal muscle may be made up of hundreds, or even thousands, of muscle fibers bundled together and wrapped in a connective tissue covering sheath called the epimysium. Fascia (connective tissue outside the epimysium) surrounds and separates the muscles. Portions of the epimysium project inward to divide the muscle into

compartments. Each compartment contains a bundle of muscle fibers called a fasciculus. Within the fasciculus, each individual muscle cell is surrounded by connective tissue called the endomysium.

Skeletal muscle cells (fibres), like other body cells, are soft and fragile. The connective tissue covering furnishes support and protection for the delicate cells and allow them to withstand the forces of contraction. The coverings also provide pathways for the passage of blood vessels and nerves.

Figure 1.18 Schematic diagram of the organisation of a muscle.
(www.training.seer.cancer.gov)



1.15 Scaffold Design

As tissue engineering moves closer to the regeneration of organs the scaffold design will become more sophisticated. The scaffold related factors that can influence cell growth and differentiation are; spatial cell arrangement (2D vs 3D cultivation), cell morphology following attachment, and cell density (Freed et al. 1998). Most cells especially ones involved in tissue engineering are anchorage dependant and their growth is affected by interaction with the substrate. Some materials promote cell proliferation but suppress differentiation and others do the opposite (Ingber et al.

1997). The basic function of the scaffold is to provide structural integrity and to define space for the tissue; to guide restructuring that occurs through proliferation of cells and ingrowth of the host tissue (Marler et al. 1998). Cell culture has to be taken into account as cultivation in 2D monolayers causes dedifferentiation in several cell types and does not allow complete differentiation in others (Freed et al. 1998). The use of 3D scaffolds for culturing can avoid these problems. Ideally the scaffold should be: 1) a 3-D shape, 2) highly porous so that it can a) permit uniform cell distribution during seeding, b) minimise diffusional constraints for gas and nutrients, c) allow in growth of vasculature from the host, 3) controllable in terms of chemical, structural and mechanical properties, 4) able to minimise the time in suspension for anchorage-dependent cells, so that it promotes cell spreading and proliferation and allow the transmission of biochemical and mechanical signals and 5) biodegradable and biocompatible (Freed et al. 1998).

Several investigations have focussed on the surface morphology of the scaffold to influence the behaviour of cells. It is well known that surface texture affects cell shape, alignment and cellular response and that attachment of many cell types is improved on rougher surfaces (Boyan et al. 1996). Cells use the morphology/topography of the substrate for orientation and migration. Epithelial cells and fibroblasts align along specifically machined or replicated grooves on culture surfaces through contact guidance effects (Boyan et al. 1996). This behaviour suggests that scaffolds might benefit from grooves and ridges sized in the order of micrometers for regulation of cell behaviour. Such structures could organise the cells into tissue by deciding the degree and direction of cell movement (Dalby et al. 2003, Walboomers et al. 1998, Ito, 1999). Improved tendon repair has been reported using a grooved topography implant as a cell guide (Wojciak et al. 1995).

1.16 Bioactive Scaffolds

Engineered surface, which are mentioned above, is part of the third generation of biomaterials but the main transition of the advance from second to third is with drug delivery. The key factors, which have stimulated the emergence of the field, are the rise of proteins and nucleic acids as potential pharmaceuticals, such as

biopharmaceuticals. Controlled drug delivery now enables a wide range of drugs to be administered on a one time or sustained basis with regulated dosage. The demonstration that sustained release of therapeutic proteins is possible has stimulated the development of new implantable polymers and devices for controlled delivery of growth factors, DNA and vaccines (LaVan et al. 2002). Tissue engineering is set to benefit from advances in drug delivery due to the fact that successful tissue growth may need spatial and temporal control over delivery of growth factors. Biomaterials have been developed for delivery of growth factors to induce vascularisation and wound healing (Rabkin et al. 2002). For example, the molecule vascular endothelial cell growth factor (VEGF) is a cell secreted protein that induces the local formation of blood vessels (angiogenesis) (Griffith, 2000). The possible clinical uses of VEGF include stimulation of blood vessel growth in patients with poor peripheral circulation and the stimulation of new vessel growth to bypass blocked heart arteries (Griffith, 2000). Biodegradable polymer scaffolds have been produced which release plasmid DNA encoding for growth factors over extended time periods (Mooney et al. 1999). The surrounding cells take up the DNA and produce growth factors. However the inserted DNA is free-floating rather than incorporated into the cell's own DNA and is eventually degraded.

A constraint on growth factor incorporation in tissue engineering is provided by the potential for adverse drug-polymer interactions, especially with protein-based drugs. Water penetration into devices following implantation hydrates the drug contained within the matrix, potentially enabling chemical reactions between the protein molecules or protein and polymer leading to inactivation (Costantino et al. 1998, Fu et al. 1999).

An alternative approach to the production of bioactive scaffolds uses surface coatings to achieve or block a biological response. There has been much work on immobilising biologically active ligands on materials, which can mediate cell adhesive interactions with the material (Hubbell, 1995). Such biologically active ligands include RGD, YIGSR, REDV and other sequences, which are often affixed to biomaterial scaffolds or natural tissues to selectively promote attachment of relatively specific cell types. Interestingly cell attachment and cell migration may both vary in relation to the

relative density of the adhesion peptide/receptor interactions and either cell attachment or migration may be selectively promoted by modulating these interactions.

Novel PCL fibres have been developed for production of 3-D scaffolds in tissue engineering using a wet spinning technique under low shear (gravity flow) conditions. The work described in this thesis describes the development of the fibre spinning technique and the mechanical, thermal and morphological properties of the resultant fibres. The interaction of fibroblasts, muscle cells and endothelial cells with the PCL fibres *in vitro* was investigated to assess potential applications in soft tissue engineering. The thesis also describes bioactive incorporation into the fibres for potential use in controlled drug delivery and tissue engineering.

1.17 Aims and Objectives

The aims of this thesis were to develop the crude spinning technique of the PCL fibres to a more advanced stage that included a continuous spinning technique. Assess the physio-chemical properties of the PCL fibres using mechanical testing and thermal analysis. Investigate the interaction of cells with the PCL fibres and their potential for drug release.

CHAPTER 2

MATERIALS AND METHODS

2.1 Materials

All gases, solvents, non-solvents and glassware were acquired from Fisher Scientific Ltd, Loughborough, UK and all plasticware was obtained from Appleton Woods, Birmingham, UK. Poly (ϵ -caprolactone) (PCL, MW 115,000) was obtained from Solvay Interlox, Warrington, UK. 2',7'-bis(Carboxyethyl)-5'(6')-carboxylfluorescein/acetoxyethyl ester (BCECF/AM), Phosphate buffered saline (PBS), Bicinchoninic acid solution (BCA), copper (II) sulfate, Dimethyl Sulfoxide (DMSO), Lipopolysaccharide from *E. coli* strain 026:B6 (LPS), Glutaraldehyde 25%, sodium cacodylate buffer, Hexamethyl-disilazane (HMDS), Chicken egg albumin powder grade V (OVA), gelatin (type B bovine skin, bloom 225), Lactic acid, Polyvinyl-pyrrolidone (PVP), Lipase from *Rhizopus arrhizus*, Progesterone, Agarose, Ethidium bromide solution, TEMED, SDS, 30% Acrylamide were obtained from Sigma Chemicals Company, Poole, UK. GibcoBRL (Invitrogen Ltd), Paisley, UK supplied Minimum Essential Medium Eagle (10x) with Hanks' salts without L-glutamine and NaHCO_3 , Dulbecco's Minimal Essential Medium (1x) containing Earles' salts (DMEM), HEPES, Hanks buffered saline solution (HBSS), Fetal Bovine Serum, 7.5% sodium bicarbonate, EDTA disodium salt, MEM (100x) Non-Essential Amino Acids, Trypsin-EDTA solution (10x), Penicillin-Streptomycin (10,000 units/ml penicillin G sodium, 10000ug/ml streptomycin sulfate in 0.85% saline,) and Trypan blue. Isoton II (Azide-free balanced electrolyte solution) and Zaponin was bought from Beckman Coulter Ltd. The cryopreserved adult Human umbilical vein endothelial cells (HUVEC) (single donor) and the HUVEC Growth Medium Bulletkit (EBM BulletKit) containing a 500 ml bottle of Endothelial Basal Medium (EBM), at a 0.15 mM calcium concentration and Bovine Brain Extract (BBE) (2.0 ml), human recombinant Epidermal Growth Factor (hEGF) (0.5 ml), hydrocortisone (0.5 ml), and GA-1000-Gentamicin/ Amphotericin-B and Fetal bovine serum (FBS) were bought from BioWhittaker, Inc Oxford, UK. Anti-human ICAM-1 antibodies and anti-human IgG antibodies were acquired from Serotec, Oxford, UK. All reagents for RT-PCR came from Promega Ltd, Southampton, UK.

2.2 Methods

2.2.1 Development of Discontinuous Fibres Spinning Technique

Fibres were produced from Poly (ϵ -caprolactone) (PCL) having a weight average molecular weight (M_w) of 115KDa. PCL pellets were dissolved in acetone with gentle heating to produce a solution of 10% (w/v). 2 ml of the solution was transferred to a spinneret (1mm internal diameter), which was a glass pasteur pipette. This was positioned so that the free end was immersed just below the level of the methanol contained in a glass U-tube (shown in Figure 3.2). The polymer solution was then allowed to flow under gravity through the spinneret into the methanol bath to form a discontinuous fibre of approximately 100mm in length. This was then collected from the bottom of the U-tube using a length of wire.

The glass U-tube was subsequently replaced by a 250ml glass measuring cylinder containing 300 ml of non-solvent for easier collection of the fibre. This method produced discontinuous fibres of approximately 300-1000mm in length.

The effect of composition of the non-solvent on the fibre production was investigated using the 250ml non-solvent bath. The non-solvent bath was tested using a methanol:water mixture. Three different ratios of methanol:water were examined namely 90:10, 94:6 and 95:5 to determine the effect on spinning rate and properties of the fibres.

The effect of concentration of the polymer solution on fibre production rate and properties was ascertained using concentrations of 5, 6, 7, 8, 9, 10, 15, 20, 25, 30, 35, 40, 50, 75 and 100% (w/v).

Fibre production was also examined under conditions where slight pressure was applied to cause flow of the PCL solution. A 10% polymer solution was transferred into a 10 ml syringe and a 21-gauge needle was attached. The end of the needle was submerged in methanol and the polymer solution was injected in a continuous stream by hand compression of the syringe plunger.

2.2.2 Continuous Fibre Production

PCL pellets were dissolved in acetone to produce solutions of concentrations ranging from 6 – 20% w/v. The solution was then transferred to the glass spinneret and the free end of the spinneret was positioned in a 1000 ml glass beaker containing 1000 ml of methanol. The polymer solution was allowed to flow under gravity through the spinneret into the non-solvent forming a fibre. The ‘as-spun’ fibre was collected using a length of wire and the fibre was attached to a variable speed PTFE take-up drum powered by a Eurostar P7 overhead stirrer (IKA, Staufen, Germany) positioned horizontally above the beaker. The take-up speed was determined using the digital output of the stirrer and the circumference of the take-up drum. The amount of fibre spun depends on the concentration of the polymer solution, 2 ml of a 10% w/v polymer solution would produce 5 m of fibre where 2 ml of a 20% w/v solution would spin 10 m.

2.2.3 Modification of Spinneret Diameter on Fibre Production

A glass spinneret was heated and drawn out to a lower diameter and the internal diameter was measured using a light microscope (Nikon TMS, Nikon, Japan) and calibrated eyepiece graticule. The diameters of the fibres were measured using a light microscope (Nikon TMS, Nikon, Japan) and calibrated eyepiece graticule.

2.2.4 Measurements of Discontinuous Fibre Spinning Rate

PCL fibres were spun from solutions of various concentration (6, 10, 15 and 20% w/v) and the production rate of m/min was measured using the time taken to produce approximately 200 mm length timed over a distance of approximately 200mm to provide a measurement in terms of m/min. The diameters of the fibres were measured using a light microscope (Nikon TMS, Nikon, Japan) and calibrated eyepiece graticule.

2.2.5 Measurements of Continuous Fibre Spinning Rate

PCL fibres were spun at various solution concentrations (6, 10, 15 and 20% w/v). The spun fibre was taken up on a PTFE mandrel attached to a variable speed overhead stirrer (Figure 3.4). The circumference of the mandrel and rotation speed in rpm were used to calculate the fibre production rate in m/min. The diameters of the fibres were measured using a light microscope (Nikon TMS, Nikon, Japan) and calibrated eyepiece graticule.

2.2.6 Scanning Electron Microscopy

Scanning electron microscopy (SEM) uses an electron gun which is housed on the top of the column and which generates the beam of electrons that rushes towards the sample housed in the specimen chamber. Electrons are very small and easily deflected by gas molecules in the air. Therefore, to allow the electrons to reach the sample, the column is under a vacuum. When the electron beam hits the sample, the interaction of the beam electrons from the filament and the sample atoms generates a variety of signals. Depending on the sample, these can include secondary electrons (electrons from the sample itself), backscattered electrons (beam electrons from the filament that bounce off nuclei of atoms in the sample), X-rays, light, heat, and even transmitted electrons (beam electrons that pass through the sample). Two detectors pick up the electrons; a secondary electron detector that detects the secondary electrons and a backscattered electron detector that is located above the sample that detects backscattered electrons. The secondary electron micrograph is virtually a direct image of the real surface structure. The attainable resolution of the technique is limited by the minimum spot size that can be obtained with the electron beam, and ultimately by the scattering of this beam as it interacts with the substrate.

The morphology and surface topography of as-spun and cold drawn PCL fibres were examined using a Cambridge Stereoscan 90 scanning electron microscope (SEM). Fibre samples were attached to SEM stubs (Argar Scientific, Stanstead, UK) using carbon tabs (Argar Scientific) and sputter coated with gold using an Emscope SC500 prior to examination in the SEM.

2.2.7 Modification of Fibre Surface Topography

Modification of fibre surface topography was achieved by wrapping wet, as-spun PCL fibres around a 40 mm diameter mandrel submerged in the non-solvent bath prior to fibre drying. Wrapping of fibres around the mandrel after they have been removed from the methanol did not produce the desired effect. The mandrel surface exhibited a machined topography characterised by a peak-to-peak separation of 91 μ m and a peak height of 30 μ m that was measured by a Talysurf 4 (Taylor Hobson, Leicester, UK). A Talysurf measures the roughness of a surface, roughness is produced by the action of the cutting tool or machine upon the surface. The Talysurf machine has an arm with a diamond tipped stylus that moves across 10 mm of the desired surface and measures the amplitude (vertical distance between peaks and troughs), spacing (horizontal distance between peaks and troughs) and slope (sharpness of individual peaks and troughs).

2.2.8 Mechanical Properties of As-spun PCL Fibres

The mechanical properties of PCL fibres (prepared using 6, 10, 15, 20% polymer solution concentrations) were measured at room temperature using a Hounsfield H10KS tensile testing machine (Hounsfield, Cambridge, UK) (Figure 2.1), at a crosshead speed of 15mm/min. Specimens with a gauge length of 25 mm were attached to 5 N load cell using the bulldog grips (Figure 2.2). Fibres were tested on 1, 2, 7, 14 and 28 days following production to determine whether there was an effect due to solvent retention in the fibres. Fibre tensile modulus [or Young modulus (E)], yield stress, tensile strength and % failure extension were determined for as-spun fibres using the corresponding values of force taken from the force extension curve (Figure 2.3) and the fibre cross-section area as indicated in Figure 2.4A. The fibre extension was obtained from the crosshead movement.

Figure 2.1 Picture of a Hounsfield H10KS tensile testing machine

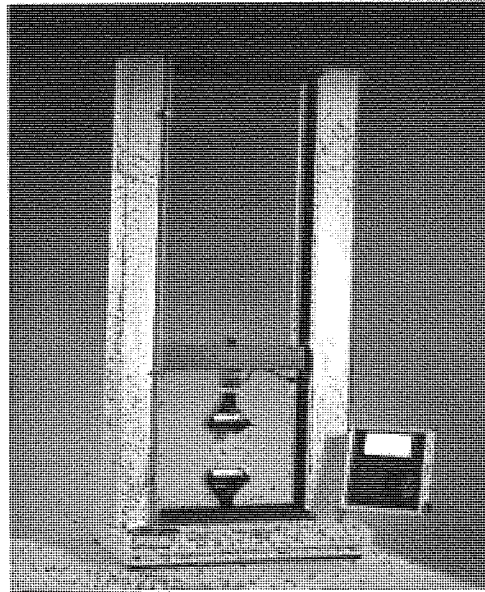


Figure 2.2 Picture of Hounsfield tensile testing machine with a fibre clamped with a 5N load-cell.

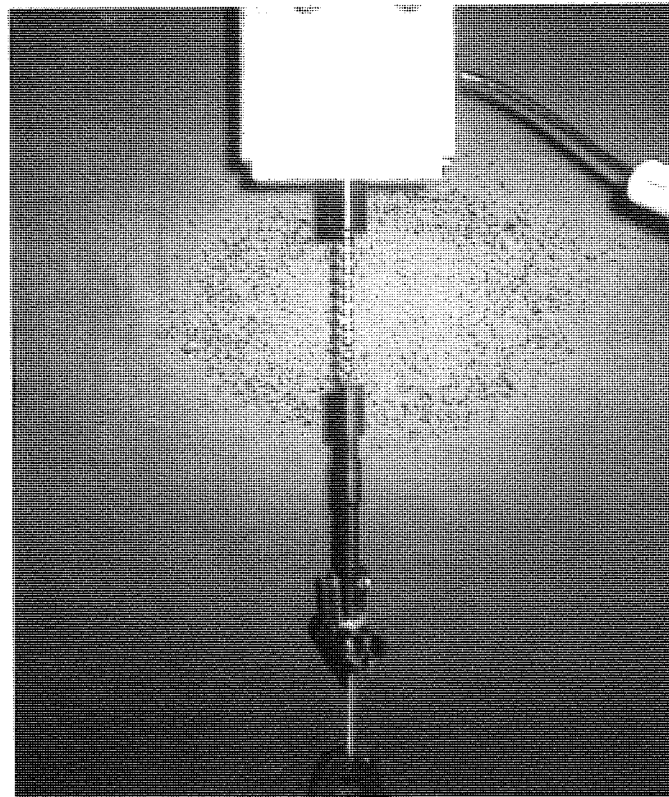


Figure 2.3 Force-extension curve of a PCL fibre. (A) force at break (B) extension at break (C) force at yield and (D) extension at yield.

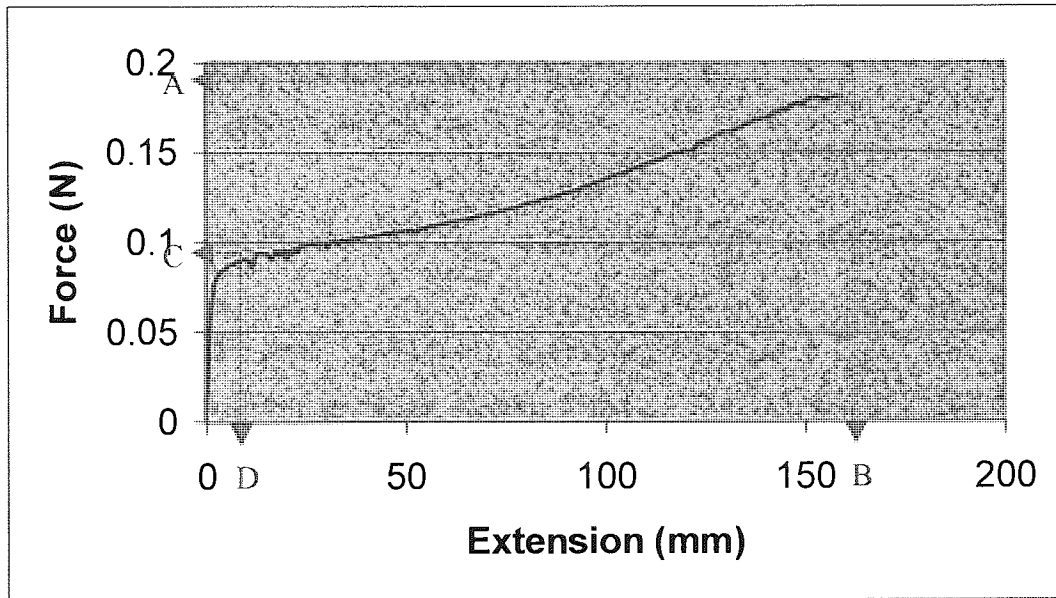


Figure 2.4 Equations used to determined mechanical properties. (A) Fibres cross-section area (B) Tensile modulus (C) Tensile strength (D) % Failure extension (E) Yield stress and (F) % extension at yield.

(A) Cross-section area = $\frac{\pi (\text{Diameter} \times 10^{-6})^2}{4}$

(B) *E (Tensile modulus or Young's modulus) = $\frac{\delta (\text{stress} = \text{Force}/\text{Area})}{\epsilon (\text{strain} = \text{Change in sample length}/\text{Sample length})}$

(C) Tensile strength = $\frac{\text{Force at break}}{\text{Area}}$

(D) % Failure extension = $\frac{\text{Fibre extension at break}}{\text{Initial sample length}}$

(E) Yield stress = $\frac{\text{Force at yield}}{\text{Area}}$

(F) % Extension at yield = $\frac{\text{Fibre extension at yield}}{\text{Initial sample length}}$

* Tensile modulus is measured over the first 1% of the stress-strain curve.

2.2.9 Retraction of PCL Fibres

The retraction of as-spun fibres was measured after drawing at room temperature to produce an increasing fibre elongation between 50 and 500%. The diameters of the drawn fibres were measured using a calibrated eyepiece graticule and light microscope (Nikon TMS, Nikon, Japan).

2.2.10 Mechanical Properties of Drawn PCL Fibres

The diameters of as-spun and drawn fibres were measured using a light microscope and calibrated eyepiece graticule. Drawn fibres of 50, 100, 200 and 500% were re-tested to determine fibre tensile modulus [or Young modulus (E)], yield stress, tensile strength and % failure extension.

2.2.11 Mechanical Properties of Hot Drawn PCL Fibres

As-spun fibres produced from a 10% w/v solution were hot drawn and then re-tested to fibre tensile modulus [or Young modulus (E)], yield stress, tensile strength and % failure extension. In the absence of a heating chamber the fibres had to be crudely hot drawn. 150mm of fibre was placed in 1.5ml eppendorfs tubes these were then placed into a water-bath at 37°C for 1 hour. The fibres were removed and immediately drawn to 50, 100, 200 and 500%, by hand. They were then allowed to cool for 15 minutes and then tested to obtain the tensile properties.

2.2.12 Mechanical Properties of PCL Fibres Extended at Various Crosshead Speeds

As-spun 10% fibres were used to examine the effect of extension rates on the fibres' mechanical properties. The Hounsfield H10KS tensile tester was used for these experiments with crosshead speeds of 50, 100, 200, 500 and 1000 mm/min.

2.2.13 Mechanical Properties of PCL Fibres After Incubation at 37°C

The mechanical properties of fibres were tested after incubation in PBS at 37°C. As-spun fibres (150 mm) produced from 10% w/v solution were placed into six 1.5ml eppendorffs and 1ml of PBS was added. The fibres were retained in a water bath for 1, 2, 7, 14, 21 and 28 days, before removing from the solution and air drying for 1 hour. The tensile properties of the fibres were determined using the Hounsfield tensile testing machine fibres were tested at a crosshead speed of 15 mm/min.

2.2.14 Thermal Analysis

Differential scanning calorimetry (DSC) was performed on as-spun PCL fibres produced from 6, 10, 15 and 20% w/v solutions at 1, 2, 7, 14, 21 and 28 days following production to determine whether there was an effect due to solvent retention in the fibres. A Perkin-Elmer System 4 calorimeter was employed for these measurements. A scan speed of 10°C/min was used and the sample weight was typically between 6.2 and 6.8mg. The melting point, heat of fusion and % crystallinity were determined, the latter property being estimated from the area under the curve measurements using a value of 139.5 J/g for the heat of fusion of fully crystalline PCL (Pitt et al. 1981).

The glass to rubber transition (T_g) of the PCL fibres was determined using a Perkin Elmer Pyris Diamond DSC fitted with a CCA 7 liquid nitrogen cooling system (Nottingham University, UK). T_g data were generated for as-spun PCL fibres produced from 6, 10, 15 and 20% solution concentration respectively and cold drawn fibres (50, 100, 200 and 500% extension), produced from 10% w/v solution. Duplicate samples were cooled from 20°C to -90°C at a rate of 100°C/min and held at -90°C for 5 minutes before heating at a rate of 10°C/min to 100°C.

2.2.15 Cell Preparation

The medium used for culturing 3T3 fibroblasts (BioWhittaker) and C2C12 myoblasts (BioWhittaker) was Eagle's Minimal Essential Medium containing Hanks' salts (MEM). Hanks' salts were selected for biomaterial/cell investigations because the cultures were placed into airtight tubes so equilibrium can be achieved and pH maintained. To produce the medium, 400 ml of distilled H₂O was first autoclaved in a 500 ml glass bottle. On cooling, the following reagents were added under sterile conditions: 50 ml MEM, 50 ml FCS, 5 ml NEAA, 5 ml 2 mM HEPES and 5 ml of 10mM NaHCO₃. The mixture was incubated at 37°C for 2 days and the sterility was checked prior to storage at 4°C. Before use 5ml penicillin/streptomycin solution, 5 ml of 200 mM glutamine was added to the medium, to give a concentration of 100 µl/ml of streptomycin, 100 µl/ml of penicillin and of 2 mM glutamine.

Cells were subsequently cultured in Dulbecco's Minimal Essential Medium (to enable experiments to be cultured in 5% CO₂, which is similar to *in vivo*) containing Earles' salts (DMEM) containing 50 ml FCS, 5 ml penicillin/streptomycin solution and 5 ml of 200mmol glutamine was added to the medium, to give a concentration of 100 µl of streptomycin, 100 µl of penicillin and of 2mmol glutamine.

Swiss 3T3 fibroblasts and C2C12 myoblasts were grown in MEM containing 10% FCS and antibiotics, as described above. The dividing time of 3T3 fibroblasts is 24 hours and they grow to 90% confluence. Myoblast dividing time is approximately 18hrs and cells are only allowed to grow to 80% confluence to avoid differentiation. When the cells reach confluence they start to detach from the flask and die and therefore it is necessary to passage the cells at least once a week. Cells were grown in T75 culture flasks with closed lids.

2.2.16 Assay of Cell Proliferation on Fibres

In initial experiments three 15 mm lengths of PCL fibres were held in the base of a 24 well plate by silicon O-rings (RS components, UK) and tissue culture plastic (TCP) was used as a control. The samples were sterilised by immersion in 70% ethanol and

were placed under UV light for 30 minutes. Swiss 3T3 mouse fibroblasts and C2C12 mouse myoblasts were grown to 80% confluence, the medium was removed and the cells were washed with 5 ml of sterile HBSS. The HBSS was removed, 3 ml 0.25% trypsin solution was added and the samples were incubated at 37°C for 5 minutes to detach the cells. 10ml of medium was added to the flasks to inactivate the trypsin and the suspension is transferred into a centrifuge tube and centrifuged at 1200 rpm for 5 minutes. The supernatant was removed and the pellet was resuspended in 5 ml of culture medium. The cells were counted using a haemocytometer (Imp. Neubauer, Weber Scientific Int. Ltd, Appleton Woods, Birmingham, UK). The required number of cells (20,000 cells/ml per substrate) were removed from the suspension and made up to the required volume. The cell suspension was then dispensed onto the substrates of PCL fibres and TCP, each substrate was seeded in triplicate for each time point. The cells were allowed to attach and grow for 2, 3, 4, 7 and 8 days. The medium was removed and the substrates with attached cells were washed with PBS. The adhered cells were subsequently treated with 0.25% trypsin for 5 minutes to detach the cells and the cell number was counted using a haemocytometer. Cell attachment was subsequently quantified in terms of cell number/fibre surface area, the fibre contact area being estimated using 50% of the fibre circumference due to the fact that the cells only have 50% of the fibre area to colonise. The other 50% would not be exposed to the cells, as it would be covered by the surface of the well. The cell viability was examined by adding a 1:1 dilution of cell suspension:trypan blue.

The following method was used to investigate an alternative cell counting approach. Adhered cells were lysed with Zaponin, which breaks down the cell walls and the nuclei were counted using a Z1 Cell and Particle Beckman Coulter counter (Beckman Coulter, Miami, Florida, USA).

2.2.17 Optimisation of Cell Proliferation on Fibres

Cell-fibre interaction and proliferation rates of fibroblasts and myoblasts on as-spun PCL fibres were investigated using cell culture methods to assess the biocompatibility of PCL fibres and their potential as scaffold materials for soft tissue engineering. Swiss 3T3 mouse fibroblasts and mouse C2C12 myoblasts were seeded at a density of

25,000/ml and 2 ml were added to PCL fibres wrapped around 22 mm x 22 mm glass coverslips and tissue culture plastic (TCP) used as a control into 6-well plates. The PCL fibres wrapped around the coverslips and the TCP of the 6 well plate were sterilised by immersing in 70% ethanol followed by washing twice with sterile HBSS and then 30 minutes of exposure to UV light. The number of attached cells was counted at 1, 2, 4, 7 and 9 days. At each time point, all substrates were washed with HBSS to remove non-adherent cells and then the fibres were placed into a separate container prior to each detachment so as to measure only the cells that had attached to the fibre and not the glass coverslip. PCL fibre samples and TCP with attached cells were subsequently treated with trypsin for 5 minutes to detach the cells and the cell number was counted using a haemocytometer. Cell attachment was subsequently quantified in terms of cell number/fibre surface area, the fibre contact area being estimated using 50% of the fibre circumference.

2.2.18 Cell Interaction with 500% Cold Drawn PCL Fibres

PCL fibres were cold drawn to 500% extension at room temperature using a Hounsfield H10KS tensile testing machine, at a crosshead speed of 15mm/min. PCL fibres were wrapped around 22mm x 22mm glass coverslips contained in 6-well plates, sterilisation of the substrate was the same as in section 2.2.17. Swiss 3T3 mouse fibroblasts were seeded at a density of 50,000/ml and 2 ml was added onto the drawn PCL fibres, as-spun PCL fibres and TCP as a control. A higher cell seeding density was used so that adequate cell numbers could attach and be counted with a haemocytometer. The number of attached cells was counted (as described in section 2.2.17) at 0.5, 1, 2, 4 and 8 hours and cell attachment was subsequently quantified in terms of cell number/fibre surface area, the fibre contact area being estimated using 50% of the fibre circumference.

2.2.19 Cell Interaction with Gelatin Coated PCL Fibres

Gelatin powder (1 g) was dissolved in 20 ml of distilled water under gentle heat to create a 5% w/v solution. The solution was then decanted into a petri dish where the as-spun PCL fibres were coated by being pulled through the solution and then dried

for 24 hours. PCL fibres were wrapped around 22 mm x 22 mm glass coverslips contained in 6-well plates. Swiss 3T3 mouse fibroblasts were seeded at a density of 50,000/ml and 2 ml was added to each of the substrates gelatin coated as-spun PCL fibres, as-spun PCL fibres and TCP as a control. All of the substrates were sterilised as described in section 2.2.17. The number of attached cells was counted (as described in section 2.2.17) at 0.5, 1, 2, 4 and 8 hours and cell attachment was subsequently quantified in terms of cell number/fibre surface area, the fibre contact area being estimated using 50% of the fibre circumference.

2.2.20 Cell Proliferation on 1) As-spun, 2) Gelatin Coated, 3) 500% Cold Drawn PCL Fibres and 4) Dacron Monofilament.

Cell interaction and proliferation of fibroblasts and myoblasts with as-spun PCL fibres, as-spun gelatin coated PCL fibres, 500% cold drawn PCL fibres and Dacron monofilament (SulzerVascutek, UK) were investigated. All the substrates were sterilized with 70% ethanol and then washed with sterile HBSS, as described in section 2.2.17. The gelatin coated fibres (as described in section 2.2.19) were washed in HBSS for 48 hours to remove excess gelatin. Swiss 3T3 mouse fibroblasts and mouse C2C12 myoblasts were seeded at a density of 25,000/ml and 2 ml were added to each substrate. The as-spun PCL fibres, as-spun gelatin coated PCL fibres, 500% cold drawn PCL fibres and Dacron monofilament were all wrapped around glass coverslips contained in 6-well plates and TCP was used as a control. The number of attached cells was counted at 1, 2, 5, 7 and 9 days. At each time point, non-adherent cells were removed by washing the samples in HBSS. All substrates were washed and then all the fibres were placed into a separate container prior to each detachment so as to measure only these cells that had attached to the fibre and not the glass coverslip. All the substrates with attached cells were subsequently treated with trypsin for 5 minutes to detach the cells and the cell number was counted using a haemocytometer as described in section 2.2.17. Cell attachment was subsequently quantified in terms of cell number/fibre surface area, the fibre contact area being estimated using 50% of the fibre circumference.

2.2.21 The initial interaction of human umbilical vein endothelial cells (HUVEC) with PCL fibres

Human umbilical vein endothelial cells (HUVECs) at passage 4 (BioWhittaker) were plated out at a concentration of 3×10^4 into 24 well plates, which contained as-spun PCL fibres. The fibres were secured by a silicone O-rings and the TCP were used as a control. Both the control surfaces and the fibres were sterilised by addition of 70% ethanol and then removing and washing twice with HBSS. Samples were then placed under UV-light. The attached cells were counted on days 1, 2, 4, 5 and 6. The fibres were washed and then placed into a separate container prior to each detachment so as to measure only these cells that had attached to the fibre and not the TCP well. The cell numbers were counted using an intracellular fluorescence dye 2',7'-bis(Carboxyethyl)-5'(6')-carboxylfluorescein/acetoxymethyl ester (BCECF/AM) as an alternative to the coulter counter. The dye is actively up taken via carbohydrate receptors into the cell. The BCECF/AM had to be diluted prior to use. This is achieved by adding 0.2 ml of DMSO to dissolve the solid and then adding 0.8ml of HBSS. A calibration curve was obtained by plating 0.005×10^5 , 0.01×10^5 , 0.02×10^5 , 0.05×10^5 , 0.1×10^5 , 0.5×10^5 , 1.0×10^5 , 2.0×10^5 and 5.0×10^5 HUVEC cells (passage 4), into a 24-well plate. The cells were allowed to attach to the plate over 2 hours. The EBM medium was removed and the cells were washed twice with HBSS. 0.5 ml of medium was added to each well followed by 10 μ l of BCECF/AM dye. Plates were then placed in the dark at room temperature for 30 minutes to allow for the uptake of the dye. Following this stage the medium was removed and 1ml of Triton X (a lysing agent) was added and the plates were placed in the dark at room temperature for a further 15 minutes. 0.1 ml samples were removed from all cell samples and placed into a well of a 96-well plate. The cell number was quantified using a fluorescence plate reader (Wallac Spectrofluorimeter) at a wavelength of 500 nm.

2.2.22 Optimised Interaction of HUVEC with PCL Fibres

The cell interaction assay technique was the same as that employed to optimise the cell proliferation for the fibroblasts and myoblasts cell lines (section 2.2.17). The same experiments were subsequently carried out for HUVECs namely cell

proliferation on as-spun PCL fibres, 500% cold drawn fibres, gelatin coated as-spun fibres and Dacron monofilament.

2.2.23 Assay for Maintained Cell Function

2.2.23.1 mRNA Extraction and RT-PCR of ICAM-1 Expression

RT-PCR is a sensitive method for the detection and analysis of rare mRNA transcripts or other RNAs present in low abundance. RNA cannot serve as a template for PCR, so it must first be isolated and then reverse transcribed into cDNA [e.g. with reverse transcriptase from Moloney murine leukemia virus (M-MuLV) or avian myeloblastosis virus (AMV)]. A combined technique (now commonly known as RT-PCR) couples reverse transcription (RT) with PCR amplification of the resulting cDNA.

Figure 2.5 Schematic diagram of Polymerase Chain Reaction (PCR). (Roche Diagnostics)



The PCR reaction uses two oligonucleotide primers that hybridize opposite strands and flank the target DNA sequence that is to be amplified. The elongation of the primers is catalyzed by a heat-stable DNA polymerase (such as Taq DNA Polymerase). A repetitive series of cycles involving template denaturation, primer annealing, and extension of the annealed primers by polymerase results in exponential accumulation of a specific DNA fragment. The ends of the fragment are defined by the 5' ends of the primers. The primer extension products synthesized in a given cycle can serve as a template in the next cycle, thus the number of target DNA copies approximately doubles every cycle; so that, 20 cycles of PCR yield about a million copies of the target DNA (Figure 2.5).

The PCL fibres wrapped around 22 mm x 22 mm glass coverslips and the 6 well plates were sterilised by immersing in 70% ethanol washing twice with sterile HBSS followed by exposure to UV light for 30 minutes. HUVECs were seeded at a density of 50,000/ml (a higher cell density was used to ensure confluence) on the PCL fibres and TCP was used as a control. The cells were allowed to grow to confluence, which typically occurred in 4 days. At this point 1µg/ml of lipopolysaccharide (LPS) was added to the cell culture and incubation was continued for 24 hrs. The samples were washed with HBSS, the fibres were removed from the cover slips and placed into 1.5 ml eppendorfs. The adherent cells were detached from the substrates by treating with 0.5 ml trypsin for 5 minutes. The reaction was quenched by adding 1ml of cell culture medium. The cells from TCP were transferred to eppendorfs after detaching with trypsin. The cell suspensions were spun in a microcentrifuge at 7,000 rpm for 5 minutes. The supernatant was carefully removed and cells were washed once more with HBSS and centrifuged.

The mRNA extraction was carried out using Dynal mRNA direct kit (Dynal, Oslo, Denmark). Cell pellets were resuspended in 1 ml of lysis buffer (100mM Tris-HCL, pH7.5, 500µM LiCl, 10mM EDTA, pH8.0, 1% LiDS and 5mM DTT) for 15 minutes. The solution was then aspirated 5x using sterile 21 gauge needles and repeated using 25 gauge needles, in order to shear the DNA. Oligo (dT)₂₅ beads (80 µl) were washed with 80 µl lysis buffer and 20 µl of the Oligo (dT)₂₅ beads were added to 200 µl the DNA solution. Samples were incubated and mixed for 5mins at 25°C. The solution

was magnetized (DynaL MPC-E) and the supernatant was removed. The pellet was resuspended twice in Buffer A (200µl; 10mM Tris-HCL, pH7.5, 0.15M LiCl, 1mM EDTA and 0.1% LiDS) and the solution was magnetized. The pellet was washed three times in Buffer B (200µl; 10mM Tris-HCL, pH7.5, 0.15M LiCl and 1mM EDTA) and finally the beads were resuspended in 20µl DEPC treated H₂O. For reverse transcription, mRNA beads were incubated at 37 °C for 1 hour in Expand RT buffer (10mM DTT, 1mM dNTP's, 25U RNAsin, 1U RQ1 Rnase-free DNase). DNase was heat inactivated at 70 °C for 10 minutes, the samples were incubated with or without 1µl of Expand RT AMV (50U) and incubated at 42 °C for 1 hour. cDNA samples were then analysed by PCR or stored at -20 °C prior to analysis.

2.2.23.2 Polymerase Chain Reaction (PCR)

Glyceraldehyde-3-phosphate dehydrogenase (GADPH) primers were used in order to standardize transcription (GibcoBRL); Forward: 5'-AGAACATCATCCCTGCCTC-3' and reverse: 5'-GCCAAATTCGTTGTCATACC-3'. PCR conditions for GADPH are detailed in Hall et al. 1998, which consist of; 1 cycle of 98 °C for 3 minutes, 57 °C for 2 minutes, 72 °C for 2 minutes; 26 cycles of 94 °C for 30 seconds, 57 °C for 30 seconds and 72 °C for 30 seconds; 1 cycle of 94 °C for 30 seconds, 57 °C for 30 seconds and 72 °C for 4 minutes. I-CAM-1 transcripts were detected by using primers from R&D Systems, Abingdon, UK and using the PCR conditions detailed in the manufacturers instructions, 1 cycle of 94°C for 4 minutes; 35 cycles of 94 °C for 45 seconds, 55 °C for 45 seconds and 72 °C for 45 seconds; 1 cycle of 72 °C for 10 minutes. PCR reactions were performed in PCR buffer Biomix Red (Bioline Ltd, London, UK) containing DEPC H₂O, 2mM dNTP's, 10pmol of each primer, 32mM (NH₄)₂SO₄, 125mM Tris-HCL, 0.02% Tween 20, 1.25U Taq DNA polymerase.

2.2.23.3 Agarose Gel Electrophoresis of PCR Products

PCR products were analyzed by gel electrophoresis. A 123bp DNA ladder was mixed with gel loading solution (2.5 µl; 0.05% w/v bromophenol blue, 40% w/v sucrose, 0.1M EDTA pH8.0) and the PCR products (15 µl) were separated on a 1.5% agarose

gel made up in 1xTBE (89mM Tris, 89mM boric acid and 2.5mM EDTA pH 8), containing ethidium bromide (10 µg/ml) at 115 V for 1 hrs. PCR products were photographed on a UV Syngene transilluminator at 312nm and imaging software (Syngene, Synoptics Group, Cambridge, UK). Expression levels were quantified using Scion Image Beta 3b (Scion Corp, Frederick, MD, USA) and normalised to GADPH expression levels.

2.2.23.4 Flow Cytometry Analysis of ICAM-1 Expression

Flow cytometry involves the analysis of the fluorescence and light scattering properties of single particles (e.g. cells, nuclei, chromosomes) during their passage within a narrow, precisely defined liquid stream. The suspension of a single particle emerges from the sample needle into a surrounding liquid that is moving with a greater velocity. The resulting acceleration at the orifice forces the particles to travel one by one in the central portion of the fluid jet that emerges from the flow chamber, a process called hydrodynamic focusing. Typical orifice diameters are in the range 50 - 100 µm, resulting in jet velocities between 1-10 m/s. The particles within the stream then traverse the focus of an intense beam of light at rates in the range 100 -1000 particles.

A typical flow cytometer consists of several basic components: a light source, a flow chamber and optical assembly, photodetectors and processors to convert light signals into analog electrical impulses, analog-to-digital converters, and a computer system for analysis and storage of digitised data.

The particles in the flow stream scatter the illuminating light. Simultaneously, if particles have previously been stained with a fluorescent dye capable of absorbing the illuminating light, fluorescence emission will occur. Some particles may contain natural fluorochromes (e.g. chlorophyll), which upon excitation also fluoresce. Scattered light and emitted fluorescence is collected by lenses behind which optical filters may be located. These are used to exclude the excitation wavelength for fluorescence measurement and, if needed, to divide the fluorescence emission for

simultaneous measurement of two or more fluorescent dyes. Detectors (mostly photomultiplier tubes) convert light pulses to electric current pulses, which are then amplified by a linear or logarithmic amplifier. After amplification, the electronic signal is digitized for further computer processing and storage. The results of analysis are usually displayed in the form of a histogram of fluorescence intensity among the particles in the sample.

The samples were prepared as described in section 2.2.23.1. The cells were allowed to achieve confluence, which typically occurred in 4 days. At this point 1µg/ml of lipopolysaccharide (LPS) was added to the cell culture and incubation was continued for 24 hrs. The samples were washed with HBSS, the fibres were removed from the cover slips and placed into 1.5 ml eppendorfs. The adherent cells were detached from the substrates by treating with 0.5 ml trypsin for 5 minutes. The reaction was quenched by adding 1ml of cell culture medium. The cells from TCP were transferred to eppendorfs after detaching with trypsin and the fibres were removed from the eppendorfs then the cell suspensions were spun in a microcentrifuge at 7,000 rpm for 5 minutes. The supernatant was carefully removed and cells were washed once more with HBSS and centrifuged. The cells were suspended in 100 µl of HBSS and 10 µl of monoclonal anti-human mouse ICAM-1 antibody conjugated to FITC (Serotec, Oxford, UK) was added and incubated at room temperature in the dark for 30 minutes (Woollard et al. 2002). Optilyse 250 µl, (Beckman Coulter, Miami, Florida, USA) was added to lyse the HUVECs, and then incubated at room temperature in the dark for 10 minutes. The percentage activation of ICAM-1 was measured by a flow cytometry (Beckman Coulter, Miami, USA) following excitation by an argon laser at 488nm. The samples were negatively controlled by using anti-IgG antibody (Serotec, Oxford, UK) to correct background fluorescence.

2.2.24 Scanning Electron Microscopy Analysis of Cell-Fibre Interactions

Cell morphology and interaction with as-spun, as-spun gelatin coated and 500% cold drawn PCL fibre were examined using a Cambridge Stereoscan 90 scanning electron microscope (SEM). The as-spun PCL fibres, as-spun gelatin coated PCL fibres and

500% cold drawn PCL fibres were all wrapped around glass coverslips contained in 6-well plates. All the substrates were sterilized with 70% ethanol and then washed with sterile HBSS, as described in section 2.2.17. The gelatin coated fibres (as described in section 2.2.19) were washed in HBSS for 48 hours to remove excess gelatin. All cell types (3T3 fibroblasts, C2C12 myoblasts and HUVECs) were seeded at a density of 50,000/ml and 2 ml were added to each substrate and were cultured for 8 hours, 1 day and 3 days. At each time points the medium was removed and the fibre samples with attached cells were rinsed briefly with PBS. Glutaraldehyde 25% was diluted with 0.1M sodium cacodylate buffer to a concentration of 2.5% and 1 ml was added to the samples for 30 minutes to fix the cells and then removed. The samples were washed with 0.1M sodium cacodylate buffer and the cells were then dehydrated in a series of ethanol dilutions (20, 30, 40, 60, 70, 90 and 100%) for 10 minutes per dilution. The cells were dried overnight in hexamethyl-disilazane (HMDS). Following drying the fibre samples which were still wrapped around the glass cover slips had to be very carefully cut with a scalpel from the underside of the cover slip with special care not to allow the fibres to spring up whilst being cut. The individual fibres were then placed with forceps carefully on to SEM stubs using carbon tabs and sputter coated with gold prior to examination in the SEM as described in section 2.2.6.

2.2.25 Protein Microparticles Loading of PCL Fibres

Two types of protein (Ovalbumin and gelatin (denatured collagen) were incorporated in PCL fibres to investigate the potential for loading of biopharmaceuticals such as growth factors. Ovalbumin (OVA) (ground in a pestle and mortar) and gelatin (type B bovine skin, Bloom 225) were added to 10% w/v PCL solutions in acetone to give protein concentrations of 0.05, 0.1, 0.5, 1, 2, 3, 4 and 5% (w/v). PCL fibres were spun as described in section 2.2.2 and observations were recorded of flow behaviour and fibre properties. Optimal protein loading of the starting PCL solution was achieved by homogenisation using a Silverton L4RT homogeniser (Silverion Machines, Chesham, UK) at a speed of 800 rpm.

2.2.26 Protein Nanoparticles Loading of PCL Fibres

In a second approach nanoparticles of OVA were added to the PCL solution prior to fibre spinning. The nanoparticles were produced from a 2% (w/v) solution of OVA in distilled water using the technique described by Chen et al. 1994. The pH of the solution was adjusted to 4.3 (measured by a MP230 pH meter from Mettler Toledo Ltd) using lactic acid and acetone was added in droplets to achieved a 1:3 ratio of OVA solution to acetone whilst the solution was being magnetically stirred. The suspension of nanoparticles obtained at this point was halved and to one volume 0.1% w/v PVP was added to aid resuspension following freeze drying (Edwards Freezedryer, Crawley UK). The acetone was allowed to evaporate over night. Following solvent evaporation the solutions were transferred to plastic 30 ml universals and frozen at -20°C in a freezer. Once the samples were frozen they were placed in a freeze drier for 24hrs. The particle sizing of the resulting powders were analysed for particulate size using a Brookhaven ZetaPlus Particle Sizer (Brookhaven Instruments Corp., New York, USA). Approximately 20mg powder was resuspended in 2 ml of distilled water and was transferred to a measuring cuvette this was then placed into the ZetaPlus Particle Sizer for determination of size. The Brookhaven ZetaPlus Particle Sizer measures particle size based on the principles of Dynamic Light Scattering (DLS).

The nanoparticle powders with and without PVP respectively were incorporated into a 10% PCL solution in acetone at concentrations of 0.1, 0.5, 0.75 and 1% w/v. The solutions were then homogenised and gravity spun as described in section 2.2.2 and observations of flow behaviour and fibre properties were recorded.

The mechanical and thermal properties of protein-loaded PCL fibres prepared using 0.1% w/v crude OVA and 0.1 and 0.5% w/v suspensions of OVA nanoparticles were determined using the methods described in sections 2.2.8 and 2.2.14.

2.2.27 Modification of Fibre Surface with Protein

PCL fibres were surface modified with gelatin (type B bovine skin, Bloom 225) by immersing and dragging the fibres (30mg) through gelatin solutions of concentration 5%, 10% and 20% respectively. The fibres were removed and allowed to dry overnight at room temperature. The gelatin-treated fibres were sterilized by washing with 2 ml of 70% ethanol for about approximately 1 minute and were then washed with PBS.

2.2.28 Measurement of Surface Protein Loading of PCL Fibres

The surface protein associated with PCL fibres was measured using the BCA total protein assay. The gelatin-coated fibres (30 mg) prepared using a concentration of 5% gelatin solution as described in section 2.2.27) and uncoated fibres (30 mg) were used as a control. Fibres were placed in 5mls of PBS to determine the amount of residual protein associated with the fibres over time. The fibres were placed in a 96 well plate at each time point (1, 2, 7, 14, 21 and 28 days) and 200 μ l of BCA reagent (bicinchoninic acid solution and copper II sulphate 4% w/v at a ratio of 50:1) solution was added. The test and calibration fibres were placed in an oven at 60°C for 15 minutes. The plate was removed and a plate reader (Dynex Technologies MRX) was used to obtain the absorbance at 562nm. The control absorbance was subtracted from all results.

2.2.29 Measurement of Protein Release from Gelatin-Coated PCL Fibres

PCL fibres (produced from a 10% PCL solution) were coated using a 5% w/v gelatin solution. The fibres were allowed to dry for 24 hrs and were washed with 70% ethanol and PBS. Fibres (30 mg) were placed in 5 mls of PBS to determine the amount of gelatin release over time. A sample of the release medium (20 μ l) was tested for protein content and was placed in a 96 well plate and 200 μ l of BCA reagent solution was added at time points of 1, 2, 7, 14, 21 and 28 days. The test and calibration samples were placed in an oven at 60°C for 15 minutes. The plate was removed and a

plate reader (Dynex Technologies MRX) was used to obtain the absorbance at 562nm. The control absorbance was subtracted from all results. It should be noted that the release medium was not completely removed at during the release study.

2.2.30 Measurement of Surface Protein Loading

Crude Ovalbumin powder was incorporated into the PCL spinning solution at a concentration of 0.1% w/v before producing the fibre. The degree of protein modification of the surface of the resulting fibres was tested using the BCA assay as described in 2.2.27. Fibre samples, including unloaded PCL fibres as a control (30 mg) were immersed in 2ml of PBS at 37°C for 1, 2 and 7days. The fibre samples were removed from the PBS medium at each time point and placed in a 96 well plate and 200 µl of BCA reagent solution was added at the time points. The test and calibration samples were placed in an oven at 60°C for 15 minutes. The plate was removed and a plate reader (Dynex Technologies MRX) was used to obtain the absorbance at 562nm. The control absorbance was subtracted from all results. It should be noted that the release medium was not changed at each sampling point.

A similar experiment was subsequently performed to analyse the surface loading of the protein on the fibres at time points of 1, 2, 7, 14, 21 and 28 days. The control absorbance was subtracted from all results. It should be noted that the release medium was not removed at each sampling point.

2.2.31 Protein Release from PCL Fibres

Crude Ovalbumin powder was incorporated into a 10% w/v PCL spinning solution to give a protein loading of 0.1% w/v. Samples of protein loaded PCL fibres and as-spun fibres (30 mg) were immersed in 2 ml of PBS at 37°C for 1, 2 and 7 days. Samples (n=6) of 20 µl of the PBS release medium were removed at each time period and placed in a 96 well plate for protein content determination using the BCA assay. BCA reagent solution (200 µl) was added at time points of 1, 2 and 7 days. The test and calibration samples were placed in an oven at 60°C for 15 minutes. The plate was

removed and a plate reader (Dynex Technologies MRX) was used to obtain the absorbance at 562nm. The control absorbance was subtracted from all results. It should be noted that the PBS release medium was not completely removed during the release study.

The above experiment was repeated to determine protein release from PCL fibres at time points of 1, 2, 7, 14, 21 and 28 days. The control absorbance was subtracted from all results. It should be noted that the PBS release medium was not completely removed during the release study.

2.2.32 Protein Release from PCL Fibres Loaded with Protein Nanoparticles

Release of protein was also examined from PCL fibres spun from a solution containing 0.1, 0.5% w/v nanoparticles with and without the presence of PVP suspending agent. As-spun PCL fibres produced from solutions containing 0.1% w/v crude OVA powder and unloaded PCL fibres were used as controls. Fibres (30 mg) were immersed in 5mls of PBS and samples of the release media were taken every 3 days for this assay of released protein. The release medium was replaced at each sampling point to avoid protein being reabsorbed onto the fibre. The remaining stages of the release experiment are described in section 2.2.30.

2.2.33 The Effect of Lipase on Protein Release from PCL Fibres

Protein release from PCL fibres spun from solutions containing 0.1, 0.5% w/v nanoparticles (with and without PVP) a 0.1% crude OVA powder and as-spun fibres was determined in the presence of lipase in 5mls of PBS. The lipase was added as 1000 units/ml. Samples of release media were taken every 3 days and the release medium was replaced completely at each sampling interval to avoid protein being reabsorbed onto the fibre and fresh lipase was added. The amount of protein released was assessed using the BCA assay described in section 2.2.30. The control plus lipase absorbance readings were subtracted from test sample absorbance.

2.2.34 SDS-PAGE Analysis of OVA Release from PCL Fibres

30 mg PCL fibres prepared from 10% PCL solution in acetone containing 0.5% w/v OVA nanoparticles or 0.1% w/v crude OVA powder respectively were placed into a 1.5 ml eppendorfs and 1 ml of PBS was added. The protein loaded fibres and a 1 mg/ml OVA solution were placed into a water bath at 37°C for 48 hours and 7 days. At these time points the release medium was removed completely and stored at -20°C until tested. A 20 µl aliquot of the release medium was mixed with SDS sample buffer (187.5mM Tris-HCL (pH 6.8), 6% w/v SDS, 30% glycerol, 150mM DTT and 0.03% w/v bromophenol blue). The samples and rainbow M.W. markers (7.5-199 kDa) were loaded into a 5% stacking gel (DDI H₂O, 10% w/v SDS, 10% w/v APS, 30% degassed acrylamide, 0.5M Tris-HCL (pH 6.8) and TEMED), set up on a 10% resolving gel (DDI H₂O, 10% w/v SDS, 10% w/v APS, 30% degassed acrylamide, 1.5M Tris-HCL (pH 8.8) and TEMED) The different molecular weight markers (7.5-199 kDa) and the samples were separated by SDS-PAGE using a with running buffer (25mM Tris, 192mM Glycine and 0.1% w/v SDS, pH8.3). The resulting protein bands were stained using comassie blue stain (0.1%) and the excess stain was removed with destain. The product bands were then photographed using Syngene transilluminator with white light and imaging software (Syngene, Synoptics Group, Cambridge, UK).

2.2.35 Activity of Bioactive Compounds Following Incorporation in PCL Fibres

PCL fibres (30 mg) were spun from a 12.5% w/v solution containing 5% w/v progesterone by Xhin-I Chang and incubated in 5ml of DMEM at 37°C for 3 days to obtain sufficient release of progesterone for testing of drug activity.

The concentration of released progesterone in DMEM was measured as 15 µg/ml. MCF-7 mouse breast epithelial cells (BioWhittaker) were cultured in DMEM and seeded into 24-well plate at a density of 20,000 cells/ml. After 24 hrs the medium was removed and 1ml of the DMEM release medium that contained progesterone loaded fibre and as-spun fibre respectively were added to the cells. The cell number was counted at 1, 2 and 3 days after addition of the media. The cells were detached by

incubating with trypsin at 37°C and counted using a haemocytometer. Cell viability was ascertained using a 1:1 dilution of trypan blue stain.

2.2.36 Statistical Analysis

Data was analysed using unpaired T-test and one-way anova with a Newman-Keuls post-test. The result is statistically significant when the P value is less than 0.05 (* P<0.05, ** P<0.01, *** P<0.001). The data are shown as mean \pm SD (SD: standard deviation) when sample numbers (n) are not less than three.

CHAPTER 3

FIBRE PRODUCTION AND PROPERTIES

3.1 Introduction

The biodegradable fibres generally used for scaffold production in tissue engineering are produced from poly (lactide-co-glycolide) (Eling et al. 1982, Gogolewski et al. 1983, Schmack et al. 2001). Fibres were developed in the main for resorbable sutures (eg Vicryl) and meshes for skin and soft tissue repair. The fibres were therefore required to retain mechanical properties for fairly short timescales of 2-4 weeks and are resorbed in 6-8 weeks.

The slow-resorbing polymers, such as poly (lactide) (PLA) or poly (ϵ -caprolactone) (PCL) are characterised by resorption times in excess of one year. These extend the design options for 3-D scaffolds in tissue engineering giving extra scope for matching tissue growth characteristics, such as bone mineralisation and angiogenesis. PLA fibres suffer from low compliance; a tendency to degrade during melt processing and the starting polymer is expensive. PCL fibres provide a lower cost alternative for scaffold production. In addition PCL is more compliant than PLA (Modulus of 0.01 – 0.5 GPa compared to 6 – 15 GPa respectively), which may present advantages for regeneration of slower healing wounds in soft tissue, such as hernia repair.

Novel PCL fibres have been developed for production of 3-D scaffolds in tissue engineering based on a discontinuous spinning method. This chapter describes the development of a continuous spinning technique for PCL fibres, the mechanical and the thermal properties of the resulting fibres.

3.2 Development of Continuous Fibre Spinning Technique for PCL Fibres

The PCL fibres are produced from processed pellets dissolved in acetone. This solution is subsequently allowed to flow under gravitational conditions through a glass spinneret into a methanol bath. Figure 3.1 shows the polymer solution flowing as a stream into the non-solvent bath. The acetone in the polymer solution is extracted into the methanol solvent via diffusion causing precipitation of the polymer as a thread, which gradually hardens to produce the finished fibre.

Figure 3.2 shows the original apparatus used to produce discontinuous PCL fibres from a 10% (w/v) polymer solution. As the figure shows the U-tube used does not provide an angle that allows the fibre to be continuously drawn off. In this system when the fibre is grabbed by a length of wire and subsequently drawn off in attempts to create a continuous spinning system the fibre tends to attach to the upper section of the U-tube bend and fracture when pulled upon. This behaviour only allowed fibre lengths of approximately 100 mm to be produced. The idea behind this initial system was to guide the fibre around the U-tube, thereby extending the time in the methanol bath to extract solvent (acetone) and increase the extent of fibre hardening before exit from the non-solvent.

The fibre spinning technique which developed from the U-tube method used a 250 ml glass measuring cylinder to allow the thread of polymer solution from the spinneret to flow a greater distance in the methanol and for easier extraction of the fibre from the non-solvent bath. This system allowed production of greater lengths of fibre, in the range of 300-1000mm. Attempts to scale up this system for continuous production proved unsuccessful as the opening of the cylinder was too small to allow a fibre to be spun and collected disrupting polymer flow from the spinneret.

Figure 3.1 Continuous PCL fibre formation by the gravity spinning method using a 10% w/v polymer solution. (A) Spinneret orifice submerged in the methanol bath. (B) Transparent stream of polymer solution flowing into the methanol bath. (C) Acetone extracted from the thread of polymer solution, causing hardening of the fibre. (The graduation are on the surface of the beaker used as the non-solvent bath).

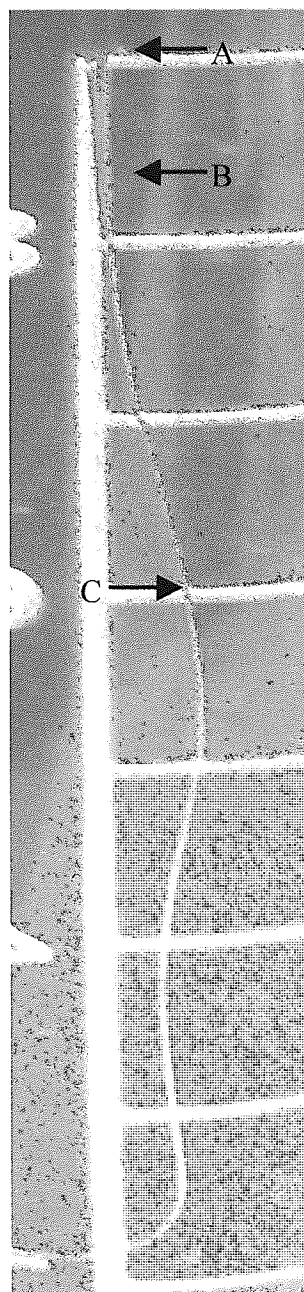
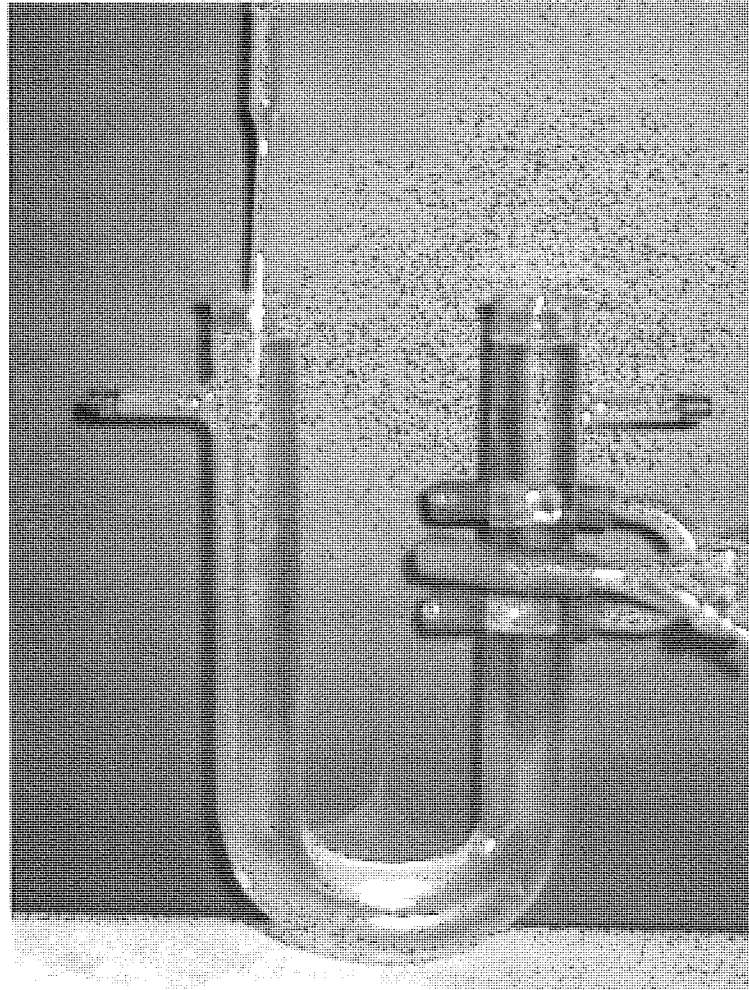


Figure 3.2 Original U-tube apparatus used to produce discontinuous PCL fibres by gravity spinning



The measuring cylinder system was however advantageous for assessing fibre production under various processing conditions such as using a methanol:water combination as the non-solvent. The key observations are shown in Table 3.1. The methanol:water (v/v) ratio was found to be crucial for fibre production. PCL fibres were formed using a 95:5 methanol:water ratio but with a higher water content the formation of the polymer fibre was not formed. The behaviour was due to the density of the polymer solution being too low to fall through the non-solvent mixture under gravity. Once the polymer solution had floated to the surface of the non-solvent mixture the acetone was extracted and globules of polymer solution formed.

Figure 3.3 Gravity spinning apparatus based on a 250 ml measuring cylinder as the non-solvent bath

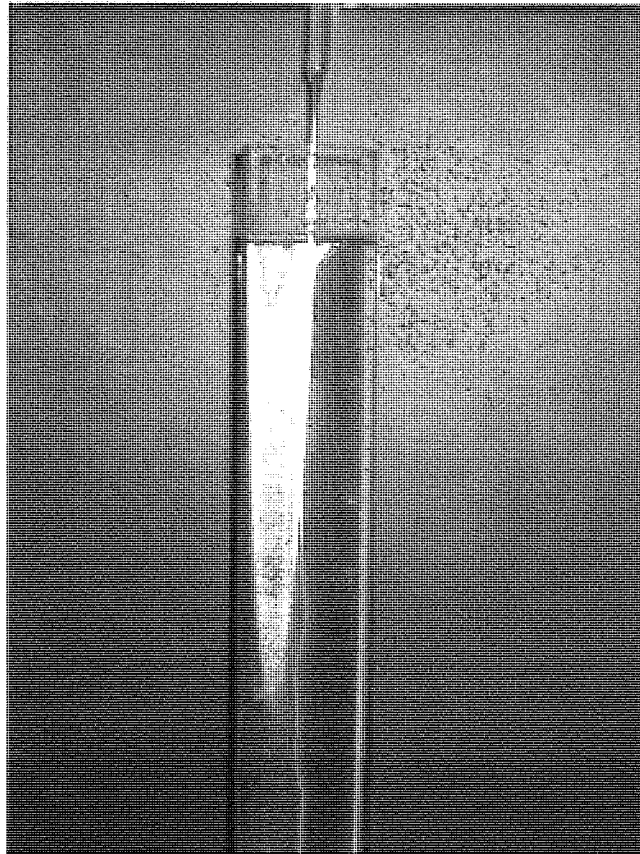


Table 3.1 The effect of methanol:water combination as the non-solvent on discontinuous PCL fibre production using the gravity spinning technique.

Methanol:Water ratio	Observations
100:0	Fibre formed
95:5	Fibre formed
94:6	Fibre not formed. Polymer solution floated.
90:10	Fibre not formed. Polymer solution floated.

The measuring cylinder system was also used to examine the effect of polymer solution concentration on the production of PCL fibres. The results are shown in Table 3.2. Concentrations of 25% w/v and above produced a gel rather than a solution. A polymer solution of 5% w/v did not result in a fibre. The thread of polymer solution leaving the spinneret did not retain integrity and so formed very short strands of uneven diameter. PCL fibres were spun successfully from a 6% solution w/v, but the fibres were not uniform in diameter and fibre hardening in methanol occurs at a slower rate. Fibres are produced from the concentrations above this point and hardening of the fibres decreases as the concentration increases.

Table 3.2 The effect of PCL solution concentration on discontinuous fibre formation using the gravity spinning technique.

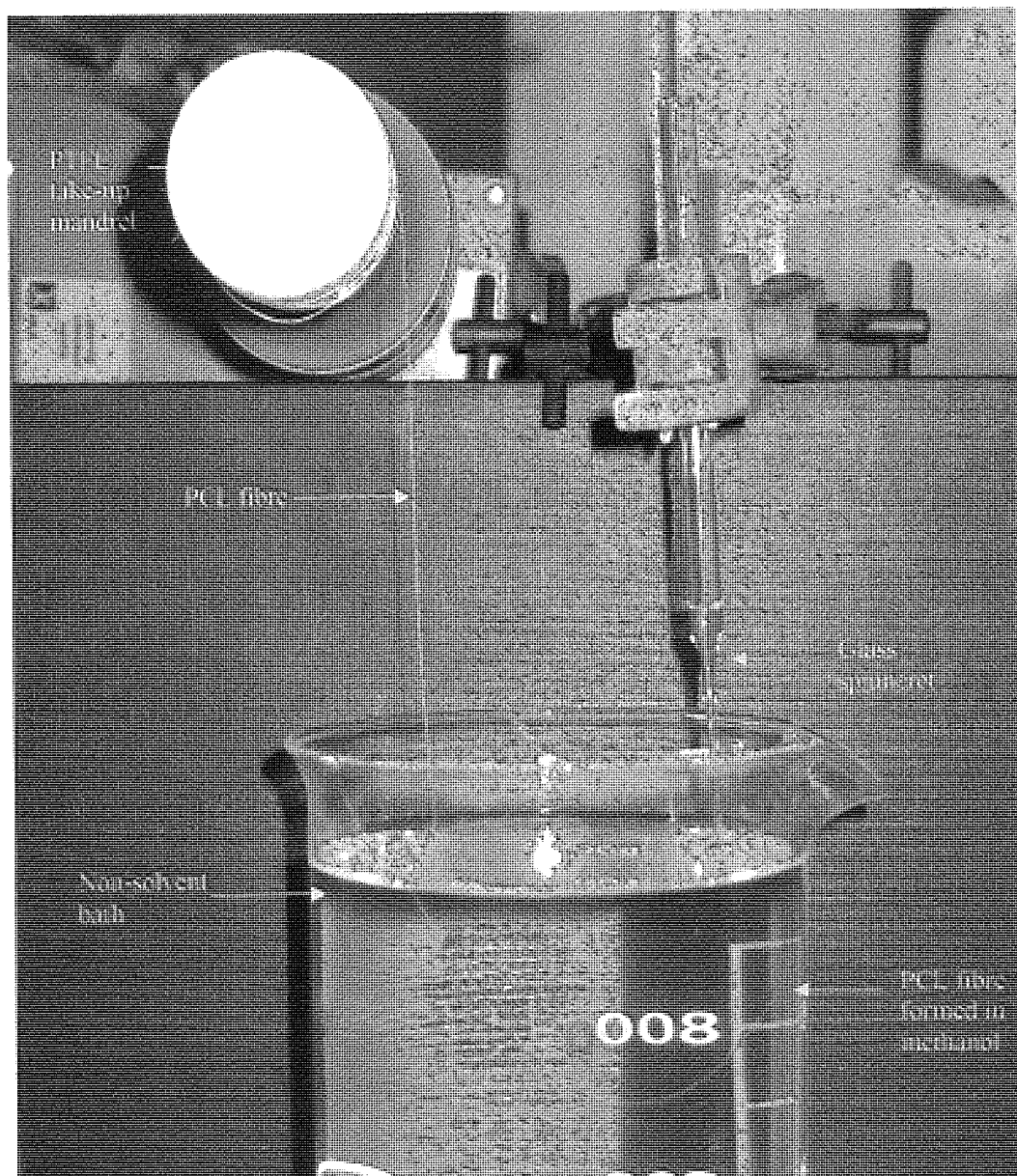
PCL concentration % (w/v)	Observations
5	Fibre not formation not generated
6 - 20	Fibre formation
> 25	Complete polymer dissolution not obtained

PCL fibre production under pressure, using a syringe loaded with polymer solution and compressed by hand as an alternative to the glass spinneret, was examined as an alternative to the gravity flow system. Fibres were produced having diameter approximately the same as the fibres produced using the gravity spinning system. The fibre in the pressurised system were extended through a 21 gauge needle which has a decreased orifice diameter (0.5 mm) compared with the glass spinneret used for gravity spinning. This means that a bioactive protein added to the PCL solution could be exposed to high shear stress, which may result in denaturation.

3.3 Continuous PCL Fibre Production Using the Gravity Spinning Technique

The optimal system determined in these studies for continuous fibre production by gravity spinning is shown in Figure 3.4. Use of a 1000 ml glass beaker for the non-solvent bath allowed greater access for fibre collection and also allowed sufficient contact time of the fibre with the methanol to allow fibre hardening. The fibre was taken-up on a PTFE mandrel attached to a variable speed take-up drive which allowed matching of the fibre spinning rate.

Figure 3.4 Experimental system used for continuous production of PCL fibres by gravity spinning



3.4 Measurements of Fibre Spinning Rate

The fibre spinning rate was calculated for discontinuous fibre production over a length of 200 mm. PCL fibres were produced at speeds ranging from 0.5 to 1.7 m/minute (Table 3.3). The maximum rate of fibre production was found to be influenced by the concentration of the spinning solution. The data in Table 3.3 show that the use of lower concentration polymer solutions resulted in fibre production at a higher rate due to the lower viscosity of the solution that passes through the spinneret under gravity. The rate of fibre production using a 6% w/v PCL solution is 3.5 times greater than that obtained using the 20% solution. The table also shows the diameters of the as-spun fibres. Use of a low solution concentrations resulted in fibres having larger diameters, which were not as consistent in diameter as fibres produced from higher concentration solution.

Table 3.3 Spinning rates and characteristics of PCL fibres under discontinuous production conditions

PCL concentration % w/v	Time of fibre production over 200mm (secs)	Speed m/min	Diameter of fibre (μm)
6	7.0 ± 1.6	1.7	190.0 ± 52.2
7	7.6 ± 1.1	1.6	166.7 ± 28.9
8	10.6 ± 1.1	1.1	155.0 ± 4.1
9	12.6 ± 1.1	1	153.3 ± 2.4
10	15.4 ± 1.7	0.8	153.3 ± 4.7
15	17.4 ± 2.3	0.7	151.7 ± 6.2
20	23.8 ± 7.6	0.5	147.6 ± 4.7

3.5 Measurements of Continuous Fibre Spinning Rate

The continuous fibre spinning rate was measured under steady state conditions. As with discontinuous fibre spinning (Table 3.3) the use of lower concentration solutions gave rise to the highest rate of fibre production (Table 4). Use of the 6% w/v PCL solution results in a spinning rate almost 3 times greater than that obtained using a 20% solution.

Table 3.4 The effect of PCL solution concentration on the spinning rate of continuous PCL fibres.

PCL Concentration % w/v	Production Rate m/min	Diameter of fibre (μm)
6	2.5 \pm 1.0	190.0 \pm 8.2
10	2.1 \pm 0.6	153.3 \pm 4.7
15	1.9 \pm 0.6	150.0 \pm 8.2
20	0.9 \pm 0	150.3 \pm 7.1

3.6 The Effect of Spinneret Diameter on PCL Fibre Production

Alteration of the orifice diameter of the glass spinneret had a direct effect on the diameter of the fibre. Halving the diameter of the spinneret from 0.5 mm (measured by a light microscope with a calibrated eyepiece graticle) resulted in the diameter of the fibre being halved from 150 to 75 μm .

3.7 Scanning Electron Microscopy

As-spun PCL fibres are circular in cross-section and exhibit a rough, porous surface (Figures 3.5 and 3.6). This is in contrast to the smooth surface normally exhibited by melt-spun fibres (Zein et al. 2002).

Figure 3.5 SEM of the surface topography of as-spun PCL fibre produced from a 10% w/v polymer solution

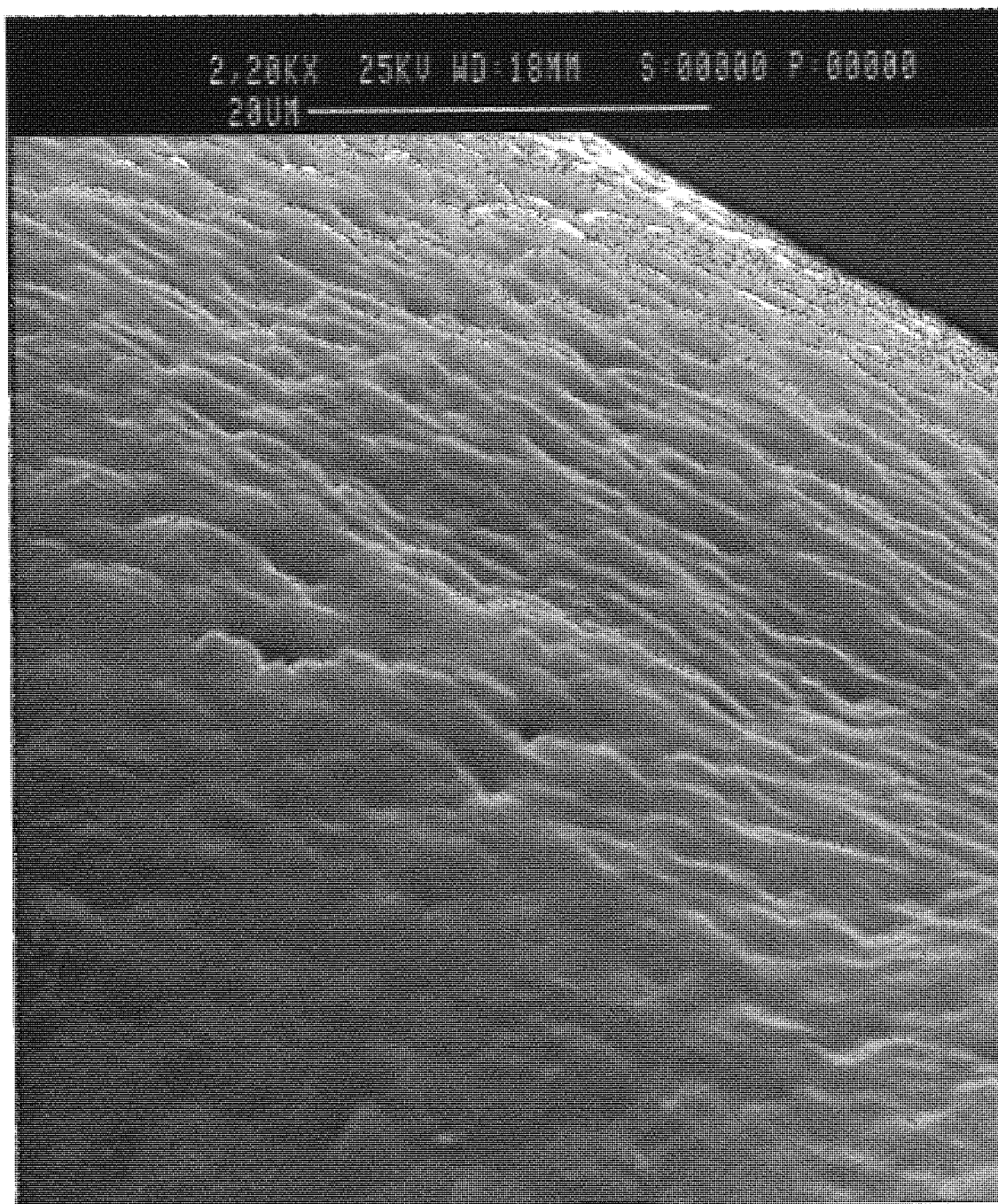
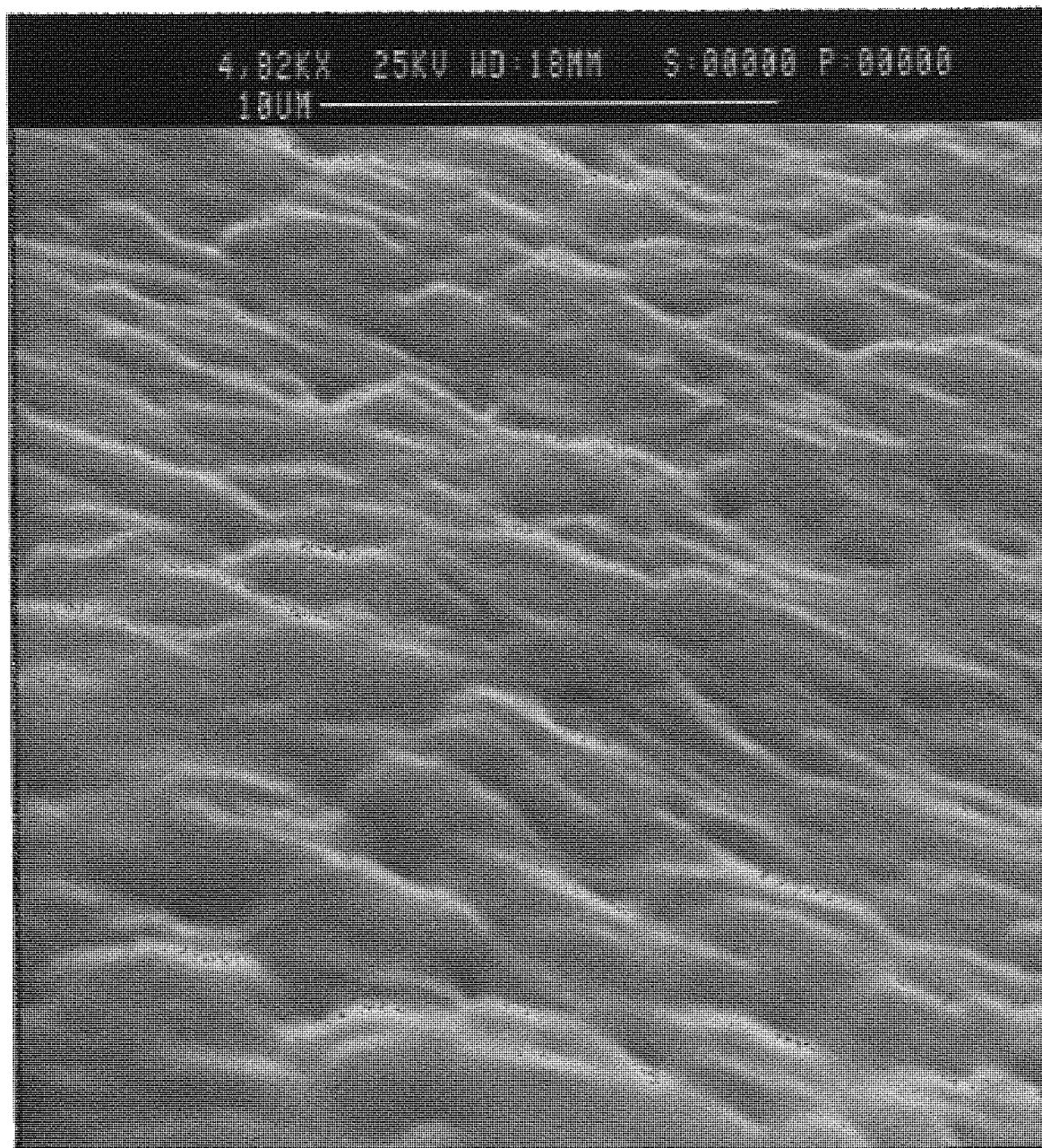


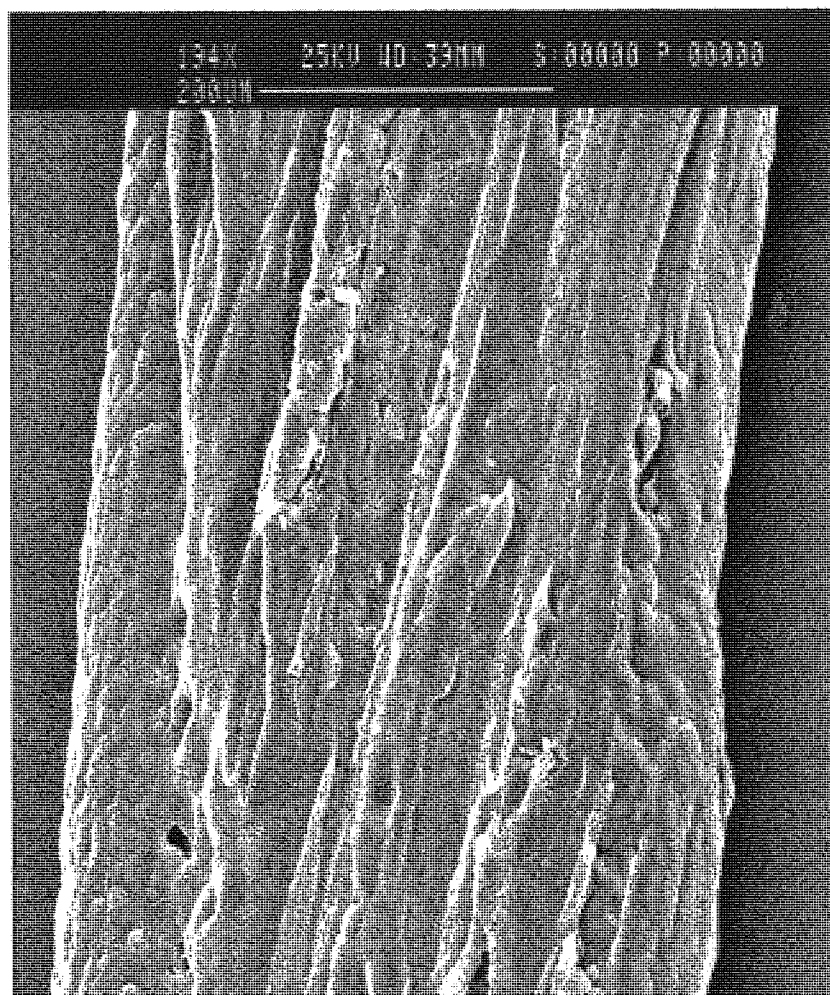
Figure 3.6 SEM of the surface topography of as-spun PCL fibre produced from a 10% w/v polymer solution



3.8 Modification of Fibre Surface Topography

Fibre surface topography is important in cell attachment and cell guidance. In this study fibre's topography was modified for potential of nerve axon regeneration. Earlier experiments showed that once the PCL fibres were withdrawn from the methanol bath they could not be wound around the mandrel tightly enough to alter the surface topography. This appeared to be a result of the rapid drying of the fibre surface. Changes in the fibre surface topography (Figure 3.7) were achieved by winding wet, as-spun fibres around a mandrel in the non-solvent bath and subsequent drying. Production of a textured fibre surface is apparent resulting from moulding of the solvent swollen fibre to the surface contours of the mandrel.

Figure 3.7 SEM of the modified fibre surface topography formed by drying as-spun PCL fibres produced from a 10% w/v polymer solution, in contact with a mandrel.



3.9 Mechanical Properties of PCL Fibres

Tables 3.5-3.9 show the tensile properties of PCL fibres produced from different concentration polymer solutions (6%, 10%, 15% and 20%) over time periods ranging from 1 to 28 days. These experiments were performed to determine whether solvent retention was a factor influencing tensile properties. The greatest effect of solvent retention was on the fibre % failure extension, which was generally higher on at Day 1 than at later times. Comparing the effect of solution concentrations spun from 6% solution (6% PCL fibre) displayed consistently decreased tensile properties compared with the other PCL fibres. The 6% fibres exhibited the lowest tensile modulus of 0.01 – 0.02 GPa, tensile strength of 1.8 – 3.0 MPa and elongation at break of 150 - 250%. Comparing this to PCL fibres produced from 20% w/v solutions were found to exhibit a tensile modulus (E) of around 0.1 GPa, tensile strength of 8 - 10 MPa and elongation at break of approximately 500 - 650%. The PCL fibres produced from 10 and 20% polymer solutions gave the highest tensile properties with the 10% fibre often displaying a slight increase in values of the 20% fibre. Force-extension curves for as-spun fibres typically displayed a yield point at around 10% extension followed by a gradual increase of force until sample failure (Figure 3.8).

Table 3.5 The tensile properties of as-spun PCL fibres 1 Day after production

Soln Concentration %	6	10	15	20
Tensile modulus GPa	0.01±0.001	0.059±0.04	0.031±0.007	0.084±0.01
Failure stress MPa	1.9±0.42	7.9±1.6	6.1±0.62	9.3±0.21
% Failure extension	269.2±38	684±157	749.4±84.8	665.7±72.1
Yield stress MPa	1.0±0.33	3.8±0.78	2.4±0.33	5.1±0.46
% Extension at yield	21.9±5.1	12.1±1.5	19.9±4.4	20.2±1.3

Table 3.6 The tensile properties of as-spun PCL fibres 2 Days after production

Soln Concentration %	6	10	15	20
Tensile modulus GPa	0.02±0.0085	0.08±0.02	0.03±0.01	0.064±0.01
Failure stress MPa	2.8±1.1	9.2±2.0	5.0±0.62	7.9±0.0012
% Failure extension	155±64.5	589.9±31.8	437.2±123.8	520±124.3
Yield stress MPa	1.6±0.49	4.2±0.65	2.1±0.41	3.5±0.4
% Extension at yield	16.3±5.1	13.3±3.8	18.8±4.4	14.2±3.63

Table 3.7 The tensile properties of as-spun PCL fibres 7 Days after production

PCL Concentration %	6	10	15	20
Tensile modulus GPa	0.02±0.008	0.09±0.018	0.09±0.02	0.05±0.008
Failure stress MPa	2.9±0.29	11.7±0.47	8.6±0.59	8.3±1.7
% Failure extension	248.6±25.4	751.9±52.4	404.1±38.9	496.5±153.5
Yield stress MPa	1.5±0.16	5.7±0.51	4.2±0.52	3.9±0.52
% Extension at yield	16.2±5.6	18±1.9	9.6±0.94	14.3±1.75

Table 3.8 The tensile properties of as-spun PCL fibres 14 Days after production

Soln Concentration %	6	10	15	20
Tensile modulus GPa	0.024±0.005	0.07±0.016	0.039±0.0075	0.071±0.028
Failure stress MPa	3.2±0.16	9.3±0.17	6.1±0.29	7.9±1.2
% Failure extension	180±55.1	651±75.8	531.6±57.3	590.1±40.8
Yield stress MPa	1.8±0.25	5.0±0.21	3.1±0.41	4.2±1.3
% Extension at yield	11.8±3.2	11.5±0.66	17±5.6	14.3±1.7

Figure 3.8 Force-extension curve of an as-spun PCL fibre produced using 10% w/v solution. (10% PCL fibre)

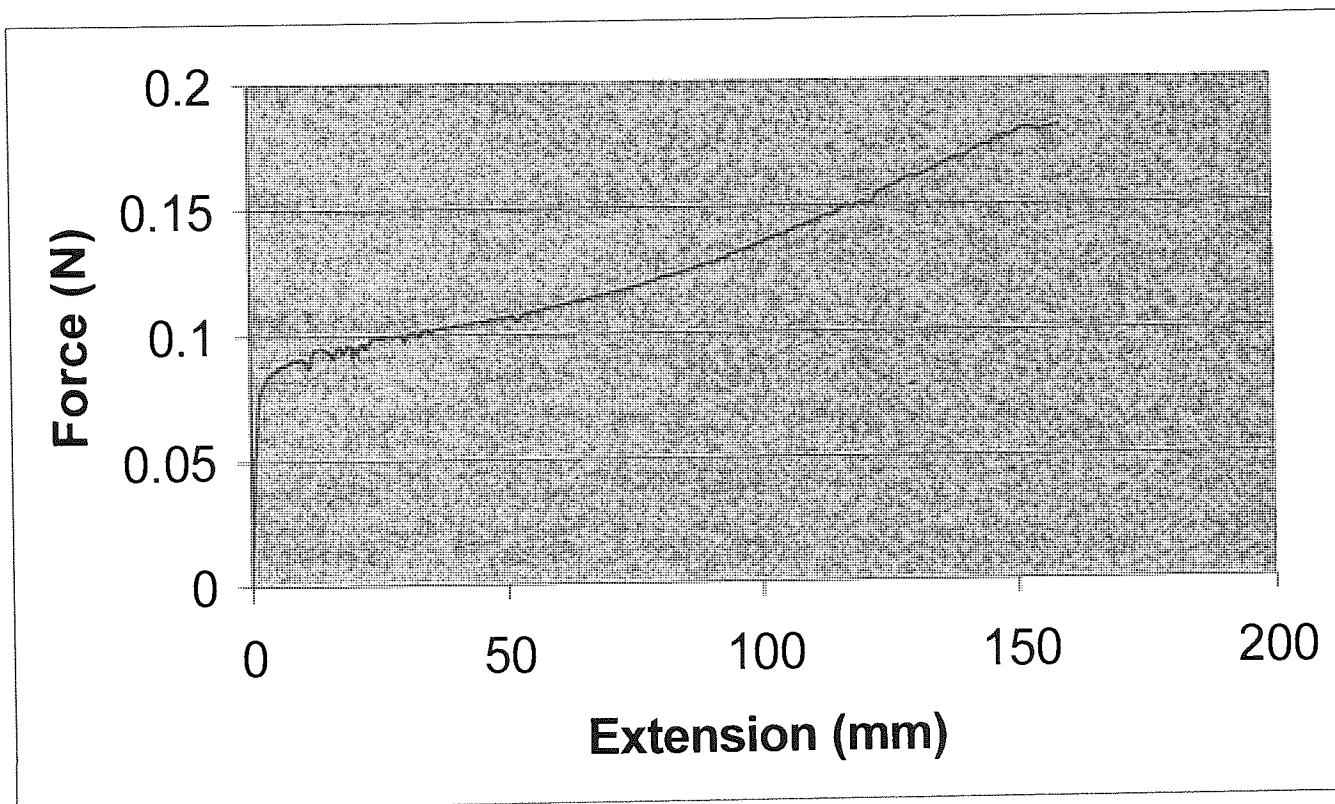


Table 3.9 The tensile properties of as-spun PCL fibres 28 Days after production

Soln Concentration %	6	10	15	20
Tensile modulus GPa	0.01±0.003	0.08±0.01	0.04±0.06	0.1±0.04
Failure stress MPa	1.8±0.72	7.9±2.0	6.1±0.12	9.9±0.76
% Failure extension	175.4±38.8	514.9±257.3	429±63.6	596.1±117.5
Yield stress MPa	1.0±0.34	3.8±0.51	2.9±0.29	5.0±0.39
% Extension at yield	17.1±1.1	10.8±6	15.9±1.5	8.7±1.7

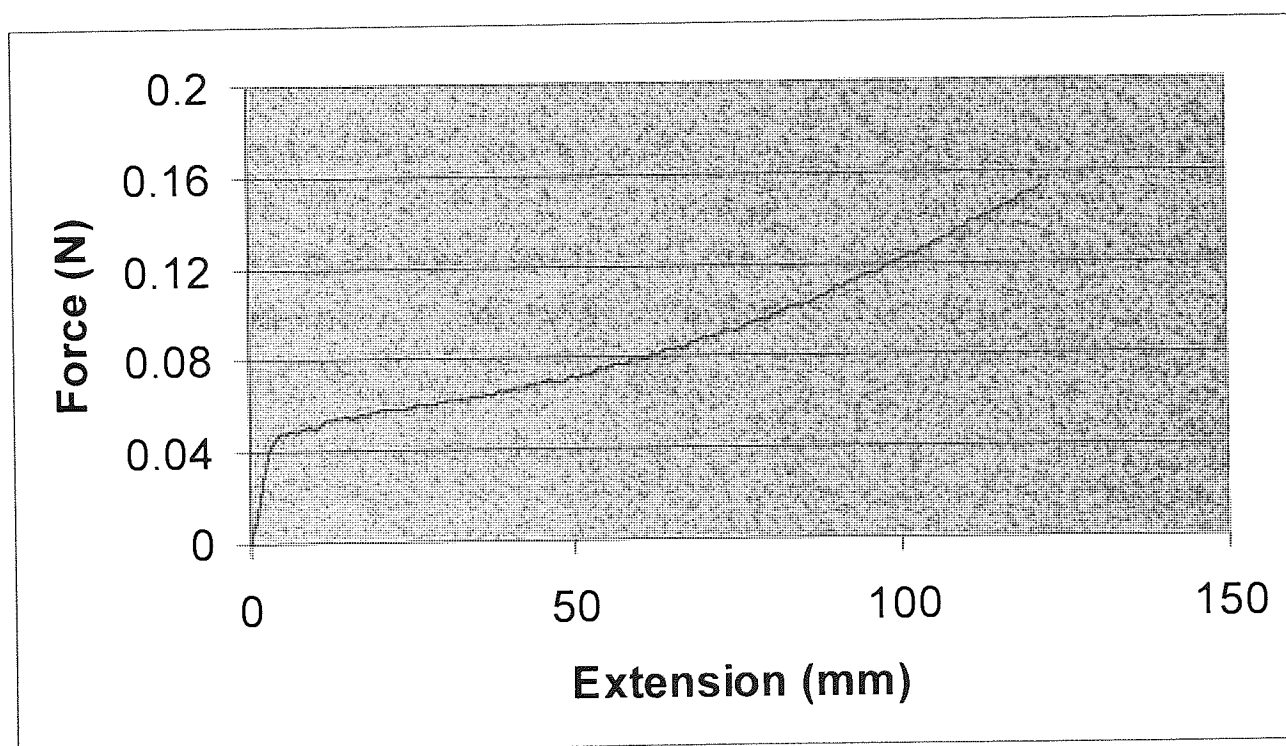
3.10 Mechanical Properties of PCL Fibres Tested at Various Speeds

Table 3.10 shows that the mechanical properties of a PCL fibre produced from a 10% w/v polymer solution do not alter when the fibre is tested at different cross-head speeds. Compared to Tables 3.5 – 3.9 where the speed of testing was 10 mm/min.

Table 3.10 The tensile properties of as-spun 10% PCL fibres at various test speeds

Cross-head speed m/min	50	100	200	500	1000
Yield stress MPa	2.9±0.3	3.2±0.6	2.9±0.4	3.6±0.5	2.9±0.4
% extension at yield	9.9±1.1	9.0±1.1	8.1±1.4	12.9±0.7	19.5±1.6
Failure stress MPa	8.9±0.3	7.9±0.3	9.1±3.8	9.0±1.1	8.8±0.9
Failure % extension	434.0±48.6	463.0±25.9	364.0±28.3	502.5±44.2	482.0±24.4
E-modulus GPa	0.03±0.01	0.03±0.0004	0.04±0.005	0.03±0.008	0.021±0.02

Figure 3.9 Force-extension curve of a 10% w/v ‘as-spun’ fibre extended at 1000 mm/min



3.11 Mechanical Properties of PCL Fibres After Incubation in PBS at 37°C

The results in Table 11 shows that the mechanical properties of as-spun PCL fibre do not alter when the fibres have been incubated in PBS at 37°C for one month. This experiment was carried out to gain an indication of the change of fibre mechanical properties *in vivo* compared to Tables 3.5 – 3.9.

Table 3.11 The tensile properties of as-spun 10% PCL fibres after incubation at in PBS at 37°C for various time periods.

Days	1	2	7	14	21	28
Tensile modulus GPa	0.04±0.004	0.05±0.003	0.06±0.008	0.07±0.02	0.06±0.05	0.07±0.05
Failure stress MPa	8.4±0.2	8.2±0.8	12.0±1.5	11.0±0.5	9.0±1.0	10.0±0.5
% Failure extension	357.0±65.3	366.0±45.6	423.0±22.2	433.0±19.5	449.0±11.9	480.4±83.9
Yield stress MPa	3.3±0.2	3.2±0.05	5.3±0.8	4.9±0.5	3.9±0.9	4.8±0.2
% Extension at yield	11.6±1.6	10.7±4.6	13.2±2.9	12.5±2.3	11.5±2.9	10.1±1.1

3.12 PCL Fibre Extension and Retraction

The results in Tables 3.12-3.13 show the % retraction of PCL fibres after drawing at room temperature. Fibres produced from all the solution concentrations investigated showed the same trends. As the extension of the fibres increased so did the % retraction. The diameters of the fibres all decreased with increasing fibre extension.

Table 3.12 The % retraction and diameter of 6% and 10% PCL fibre following extension at room temperature

6% PCL fibres			10% PCL fibres	
Extension of Fibre	Retraction	Diameter	Retraction	Diameter
%	%	μm	%	μm
0		190.0 \pm 52.2		153.3 \pm 4.7
50	1.4 \pm 0	130 \pm 0	3.2 \pm 2.5	113 \pm 4.7
100	8 \pm 2.8	116 \pm 4.7	15.3 \pm 4.7	93 \pm 4.7
200	10.5 \pm 3.9	93 \pm 4.7	10.7 \pm 1.9	80 \pm 0
500			13.2 \pm 0.33	67 \pm 4.7

Table 3.13 The % retraction and diameter of 15% and 20% PCL fibre following extension at room temperature

15% PCL fibres			20% PCL fibres	
Extension of Fibre	Retraction	Diameter	Retraction	Diameter
%	%	μm	%	μm
0		151.7 \pm 6.2		147.6 \pm 4.7
50	3.2 \pm 2.5	123 \pm 4.7	2.3 \pm 1.2	123 \pm 4.7
100	3.3 \pm 0.94	93 \pm 4.7	9.3 \pm 0.94	103 \pm 4.7
200	8 \pm 1.1	77 \pm 4.7	12 \pm 1.1	87 \pm 4.7
500	9.4 \pm 1.9	63 \pm 4.7	15 \pm 3.2	70 \pm 8.2

3.13 Cold Drawing PCL Fibres

Table 3.14 and 3.15 show the effect of cold drawing on the tensile properties of drawn PCL fibres prepared from various solution concentrations. The general trend is an increase in tensile strength and stiffness and a decrease in failure extension with increasing draw ratio (Figure 3.10). However the drawability of PCL fibres produced from 6% solutions was less than 500% resulting in a limitation of fibre tensile strength and stiffness to around 20 MPa and 0.1 GPa respectively. PCL fibres

produced from the highest concentration solution (20% w/v) tended to develop higher strength and stiffness at a lower draw ratio (Table 3.14). The maximum fibre tensile strength of 47 MNm⁻² and stiffness (0.3 GPa) was obtained following 500% extension of as-spun fibres prepared from 15% and 20% PCL solutions respectively.

The cold drawn fibres were examined with SEM. Signs of surface cracking were sometimes observed after drawing as seen in Figure. 3.11. At 100% extension and above the fibres' surface topography showed distinct changes, forming an oriented, fibrillar texture (Figure 3.12) was generated on extension of as-spun PCL fibres indicative of a high degree of structural re-organisation and alignment induced by the process of cold drawing. After cold drawing to 200% and above the fibres exhibited a pronounced yield drop on mechanical testing indicative of neck formation (Figures 3.13 and 3.14), however this could also be due to slippage of the fibre within the grips.

Table 3.14 The tensile properties of cold drawn PCL fibres produced for 6% and 10% polymer solutions

Spun from 6% Solution

% fibre extension	50	100	200	500
Tensile modulus GPa	0.06±0.01	0.09±0.01	0.1±0.03	N/A
Failure stress MPa	12.3±0.47	13.7±1.2	20.0±2.9	N/A
% Failure extension	260.1±15.7	188.2±16.2	107.6±37.3	N/A
Yield stress MPa	6.5±0.41	8.4±0.29	15.0±0	N/A
% Extension at yield	19.3±1	16.4±0.87	21.8±4.1	N/A

Spun from 10% Solution

Tensile modulus GPa	0.04±0.003	0.05±0.016	0.12±0.01	0.31±0.03
Failure stress MPa	10.0±2.6	15.3±3.1	29.0±5.0	42.7±3.3
% Failure extension	330±120.5	266.9±23.6	369.2±153.8	140.5±117
Yield stress MPa	5.7±0.9	8.1±1.8	17.0±3.7	31.7±4.0
% Extension at yield	26.1±7.8	29.9±13.2	22.4±6.3	14.2±3.1

Table 3.15 The tensile properties of cold drawn PCL fibres produced for 6% and 10% polymer solutions

Spun from 15% Solution

Tensile modulus GPa	0.05±0.02	0.11±0.06	0.11±0.02	0.24±0.003
Failure stress MPa	8.2±1.3	16.3±4.5	21.7±2.9	47.3±3.3
% Failure extension	213.5±18.6	260.3±36.4	302.8±34.6	148.2±46
Yield stress MPa	5.2±0.31	8.8±3.2	14.3±2.5	32.7±5.2
% Extension at yield	20±4.2	20.4±3.4	26.2±3.5	23±7.4

Spun from 20% Solution

Tensile modulus GPa	0.09±0.03	0.16±0.08	0.24±0.09	0.32±0.03
Failure stress MPa	16.7±1.7	23.0±2.4	37.0±7.1	39.0±10.0
% Failure extension	607.6±171.1	338.4±59.2	338.7±87.9	136.3±51.2
Yield stress MPa	8.0±0.76	13.0±2.2	22.3±4.8	29.3±3.9
% Extension at yield	17.2±4.9	13.6±4.2	18±1.9	10.4±1.5

Figure 3.10 Force-extension curve of a 10% w/v fibre cold drawn to 100% extension.

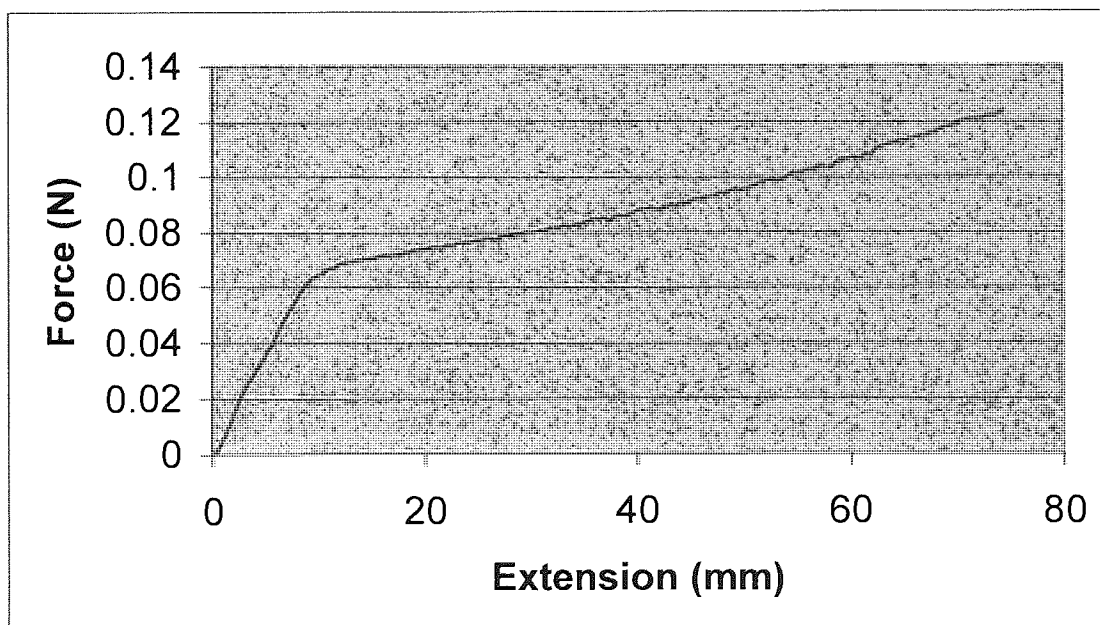


Figure 3.11 The morphology of a 10% PCL fibre after 50% extension.

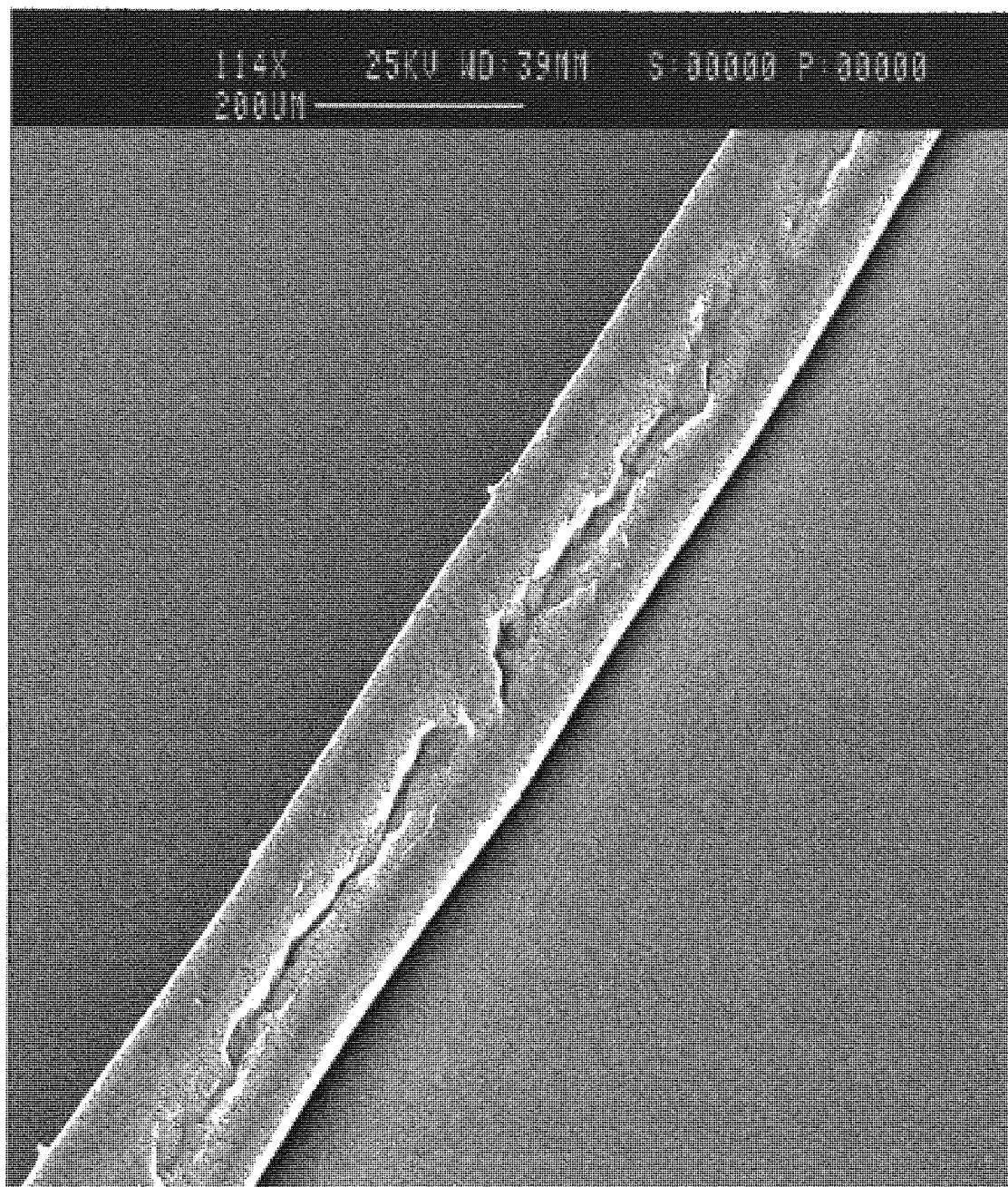


Figure 3.12 SEM of 10% PCL fibre after 500% extension.

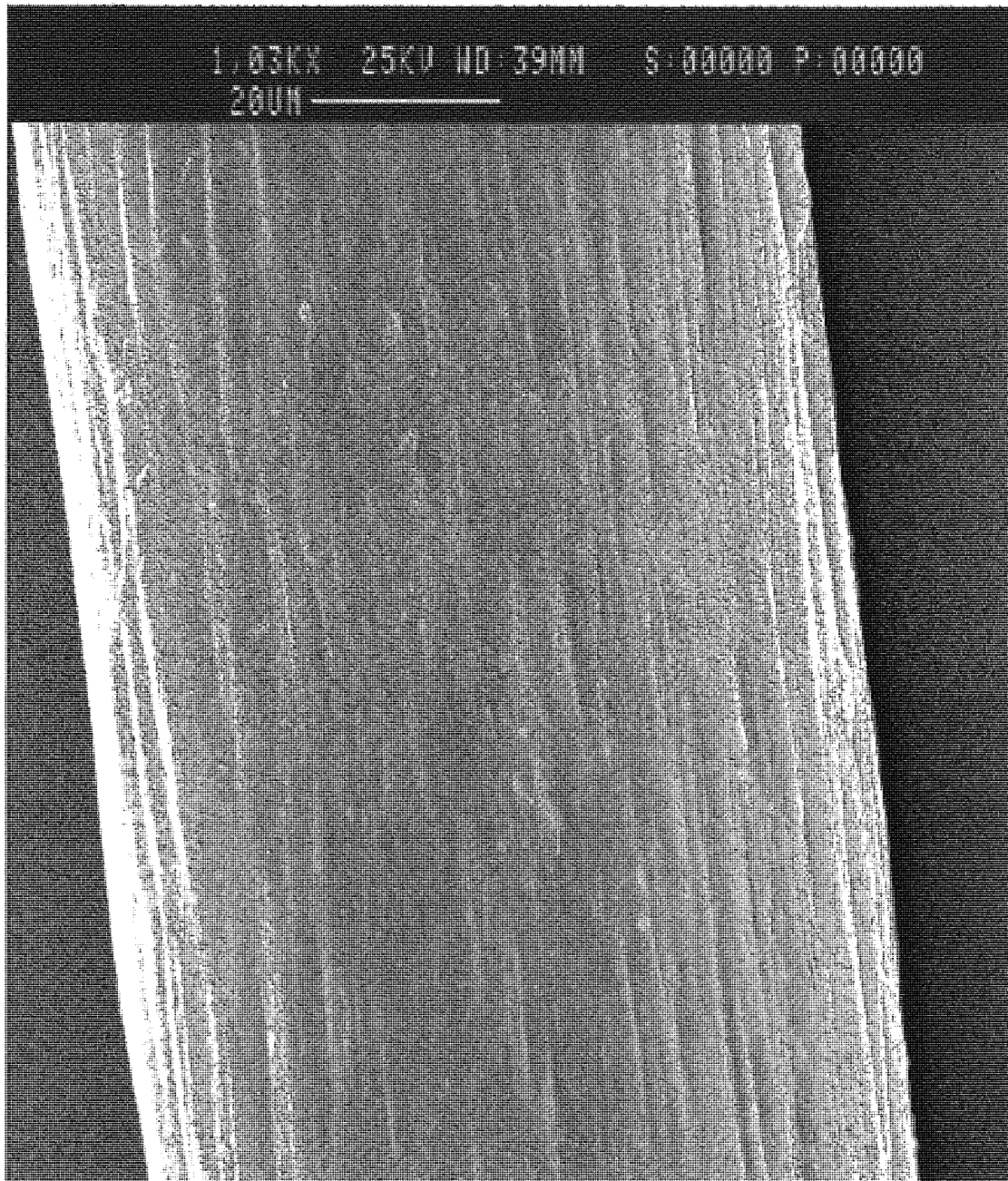


Figure 3.13 Force-extension curve of a 10% w/v fibre cold drawn to 200% extension.

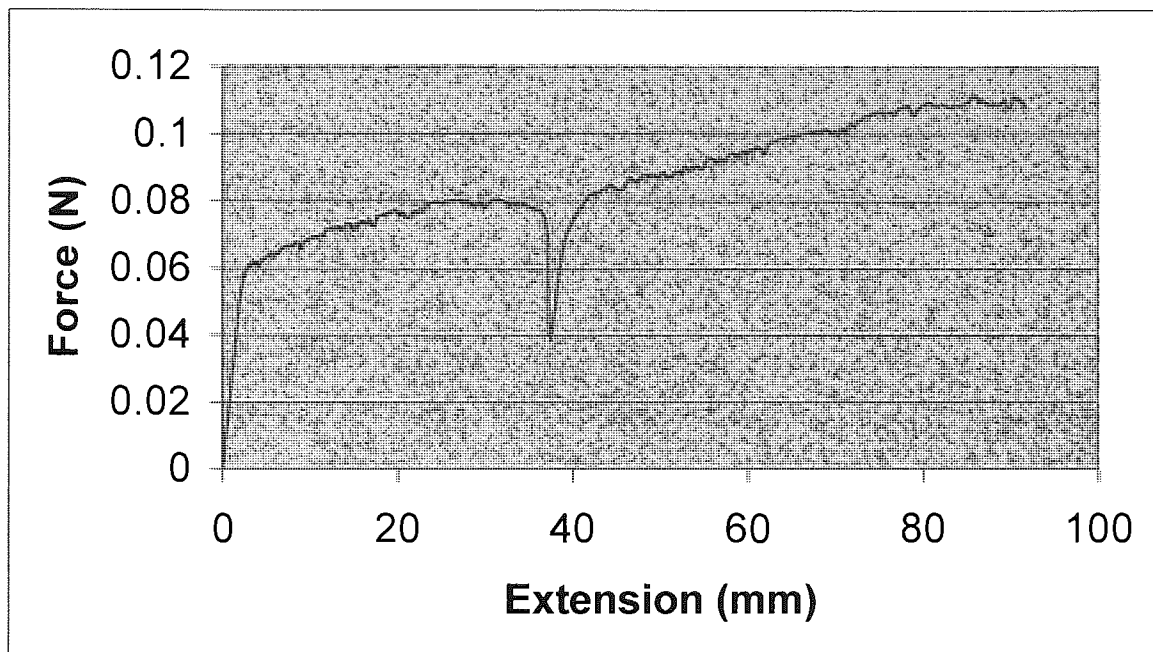
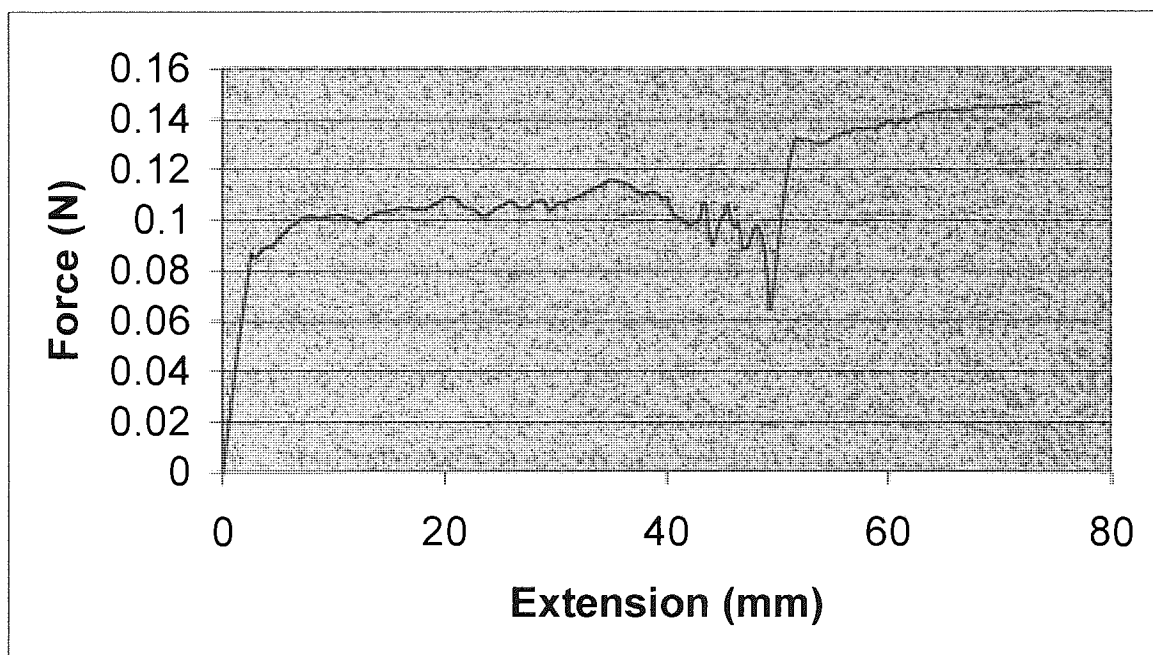


Figure 3.14 Force-extension curve of a 10% w/v fibre cold drawn to 500% extension.



3.14 Hot Drawing of PCL Fibres

The mechanical properties of hot drawn 10% w/v PCL fibres are shown in Table 3.16. The general trend is an increase in tensile strength and stiffness and a decrease in failure extension with increasing draw ratio. The failure stress at 50% fibre extension is 12.0 MPa compared with 81 MPa at 500% extension. Large increases are also observed in the yield stress and fibre tensile modulus. When the results are compared with those of cold drawn 10% w/v fibre (Table 3.14), there is similarly and only an increase in extension 500% with yield stress and failure stress. However the failure stress and yield stress of hot drawn 500% extension fibres are approximately double that of the cold drawn 10% w/v fibres. The tensile modulus of the hot drawn PCL fibres was around 1.5 times higher than cold drawn fibres.

Table 3.16 The tensile properties of 10% PCL fibres after hot drawing at 37°C and testing once cooled at room temperature.

% Fibre extension	50	100	200	500
Tensile modulus GPa	0.04±0.005	0.055±0.003	0.15±0.03	0.47±0.03
Failure stress MPa	12.0±0.5	16.0±0.9	32.0±2.2	81.0±3.7
% Failure extension	291.0±32.4	231.0±77.0	242.0±108.6	109.7±16.5
Yield stress MPa	4.8±0.2	6.7±0.3	16.0±0.9	60.0±7.0
% Extension at yield	16.0±0.7	15.9±0.6	15.4±4.3	19.2±0.6

Figure 3.15 Force-extension curve of a 10% w/v fibre hot drawn at 37°C to 100% extension and tested once cooled at room temperature

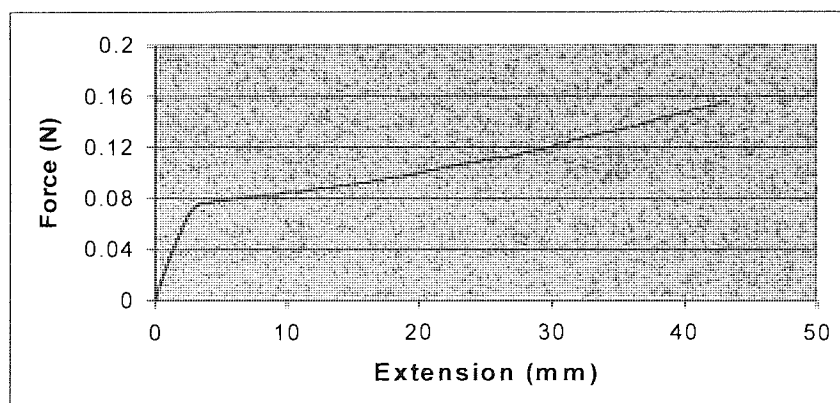


Figure 3.16 Force-extension curve of a 10% w/v fibre hot drawn at 37°C to 200% extension and tested once cooled at room temperature

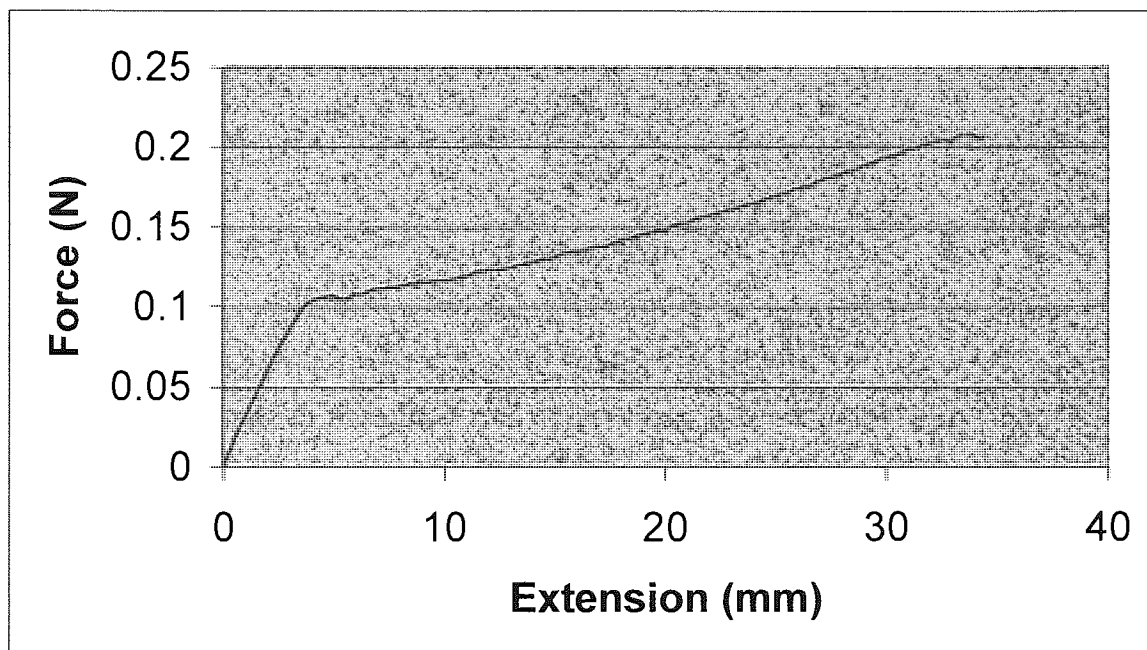
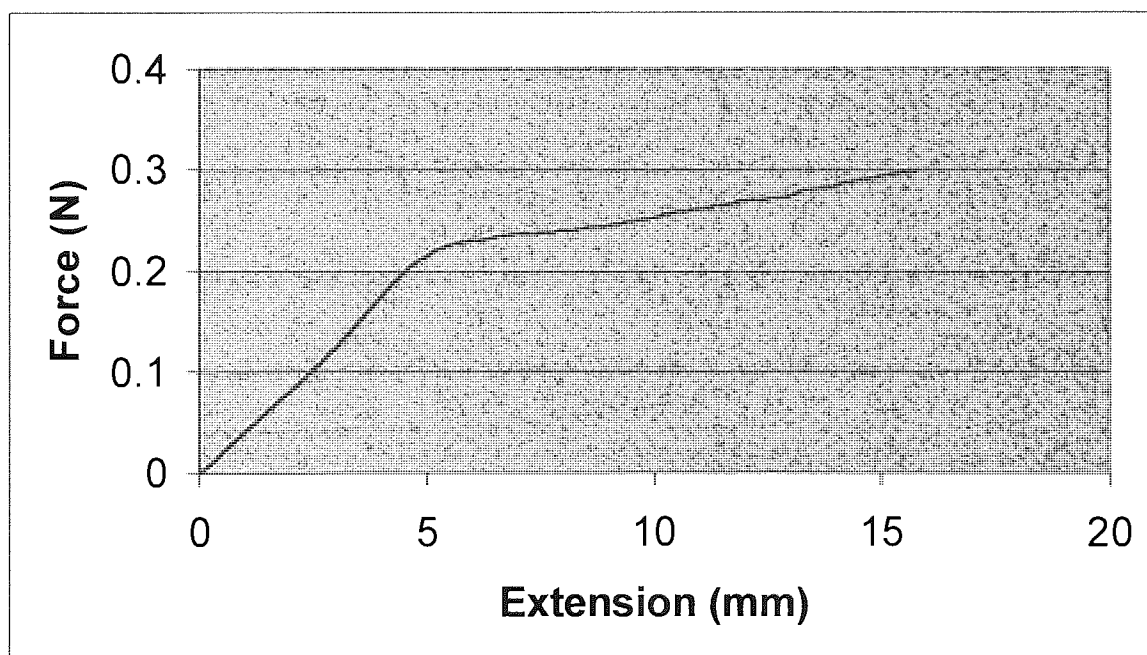


Figure 3.17 Force-extension curve of a 10% w/v fibre hot drawn at 37°C to 500% extension and tested once cooled at room temperature



3.15 Thermal Analysis

Table 3.17 present the thermal properties over time of as-spun PCL fibres prepared from solutions of various concentrations. The melting point of the fibres does not vary significantly with the solution concentration used to prepare the fibre or over times up to 28 days. The melting point (T_m) of the fibres is consistently around 56°C , the Heat of Fusion (ΔH_m) is approximately 91 J/g^{-1} . The % crystallinity of PCL fibres varied between 52 and 69% but was typically around 61%.

The thermal characteristics of as-spun and cold drawn PCL fibres are shown in Table 3.18. The T_g of as-spun fibres and cold drawn fibres was generally in the region of -60°C , comparable with the normally quoted value for PCL. The reduction in T_g of as-spun PCL fibres produced using 6% solutions suggests a lower constraint on chain mobility in the amorphous phase. The T_m and % crystallinity of as-spun and cold-drawn fibres remained fairly constant in line with a process of physical breakdown of the original crystal structure rather than one of melting and recrystallisation, which occurs during hot drawing.

Figure 3.18 A typical thermal trace of as-spun 10% PCL fibre

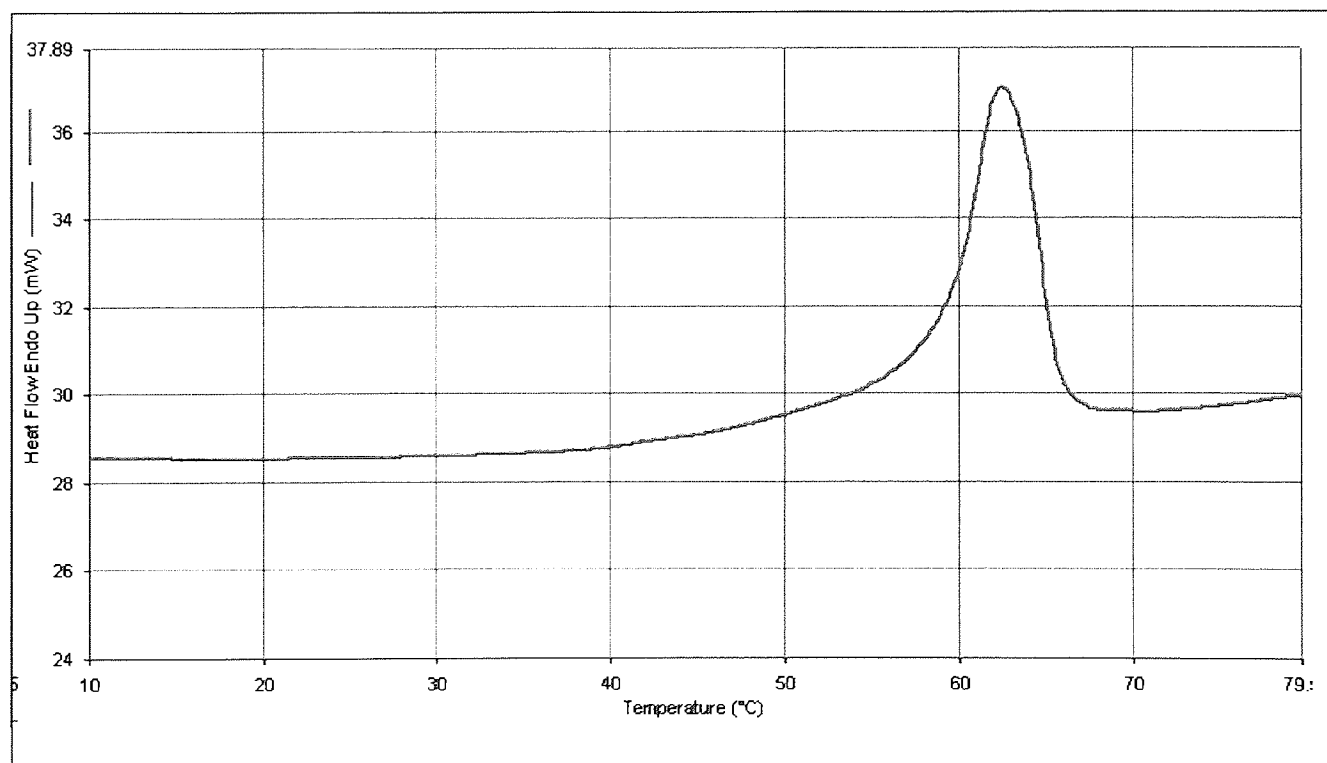


Table 3.17 The thermal properties of PCL fibres 1 – 7 days after production

1 Day after production				
Soln Concentration %	6	10	15	20
T_m °C	56.4±0.82	53.5±0.08	55.1±0.22	55.4±0.77
ΔH_m (J/g⁻¹)	92.9±1.31	89.3±5.03	90.5±14.9	90.2±7.66
% Crystallinity	66.5±0.98	63.9±3.65	64.9±10.7	64.6±5.5

2 Days after production				
T_m °C	54.8±0.77	54.9±0.96	54.5±0.94	54.7±0.49
ΔH_m (J/g⁻¹)	91.8±8.5	97.4±1.3	96±0.25	72.8±2.6
% Crystallinity	65.8±6.1	69.8±0.94	68.7±0.21	52.2±1.9

7 Days after production				
T_m °C	54.7±0.49	55.4±0.57	56.3±1	57.4±0.39
ΔH_m (J/g⁻¹)	72.8±2.6	90.9±6.2	81.9±12.6	92.1±9.1
% Crystallinity	52.2±1.9	65.2±4.4	58.7±9	66±6.5

14 Days after production				
Soln Concentration %	6	10	15	20
T_m °C	56.9±1.2	56.7±0.08	56.8±0.26	57.4±0.27
ΔH_m (J/g⁻¹)	80.6±16	88.3±7.6	106±2.4	104.2±4.9
% Crystallinity	57.8±11.4	63.4±5.4	64.2±3.7	58.6±4.6

28 Days after production				
T_m °C	57±0.51	55.6±0.89	55.9±1.9	57.8±0.7
ΔH_m (J/g⁻¹)	89.2±14.1	92.6±5.3	103.4±1.8	105.1±3.1
% Crystallinity	63.7±10.1	66.2±3.4	54.1±4.7	62.3±4.9

Table 3.18 The thermal properties of as-spun and cold drawn PCL fibres

Conc. of spinning Solution % w/v	Draw ratio	Tg (°C)	Tm (°C)	% Crystallinity
6	As-spun	-66.4	59.4	55.5
10	As-spun	-62.3	62.5	60.4
15	As-spun	-61.3	62.9	56.5
20	As-spun	-60.4	61.8	63.5
10	0.5	-61.6	61.6	61.4
	1	-59.8	62.2	59.9
	2	-59.8	62.2	56.8
	5	-62.4	60.8	58.7

3.16 Discussion

Fibre spinning may be broadly divided into two categories, melt spinning and solution spinning. In melt spinning, the molten polymer is forced through a spinneret and the jet of molten polymer is cooled to form solid threads (Eling et al. 1982, Zein et al. 2002, Hutmacher, 2000). Solution spinning is based upon extrusion under pressure of concentrated polymer solutions (Eling et al. 1982 and Gogolewski et al. 1983). In dry solution spinning, the extruded filaments are dried to remove solvent, whereas in wet solution spinning the filaments are extruded into a non-solvent to precipitate the polymer in the form of a thread. The polymer threads or filaments are usually subjected to a drawing procedure to control chain orientation and fibre tensile properties.

Solution spinning of the poly (α -hydroxy acids) such as PLA normally requires high solution viscosities to enable extrusion of a filament prior to drawing (Eling et al. 1982). In contrast, the technique for PCL fibre formation described here involves free flow of polymer solution through a spinneret under gravity and was found to be dependant on two key factors. Firstly the viscosity of the PCL solution had to be

within a well defined range produced by polymer solution concentrations of 6 - 20% w/v to allow the solution to pass through the spinneret orifice under gravity. The viscosity of a solution with a concentration below 6% w/v was not sufficiently high enough to enable the flow of solution as a cohesive thread to form a fibre. The rate of fibre production as expected, showed an inverse relationship with solution concentration and viscosity. Secondly the choice of solvent/non-solvent system was found to be critical, the higher polymer solution density relative to the non-solvent allowed free-fall of the polymer solution stream, avoiding flotation of the polymer solution on the surface of the non-solvent. In the case of methanol and water combinations (95:5, 96:4 and 90:10) the non-solvent density caused the entering polymer solution to float to the surface of the non-solvent. The PCL fibre gravity spinning technique thus avoids high shear conditions, which can disrupt flow of the solution and produce fibre surface irregularities. This in turn could interfere with cell attachment and growth on the fibre. Extrusion of PLA solutions under pressure for example, has been found to result in a screw or spiral-form structure due to elastic turbulence of the polymer flow above a critical shear rate (Leenslag et al. 1984 and Gogolewski et al. 1983).

The surface of the fibres were modified to produce a textured surface by moulding to the surface of a machined mandrel. The textured fibre is about 400 μm in width, which is over double the normal diameter of as-spun fibres. The fibre exhibited surface cracking and many pores on the surface along with a directional regular groove pattern, which could be beneficial for cell attachment and contact guidance.

The tensile properties of the PCL fibres demonstrated their potential advantage for tissue engineering. The fibres are more compliant than PLA fibres for example (Table 3.19), which could be advantageous for soft tissue repair. The tensile modulus of as-spun PCL fibres was in the range of 0.01 - 0.09 GPa. In comparison PLA fibres exhibit a modulus of 9.5 GPa (Table 3.19) while mould PCL ($M_w = 44,000$) exhibits a modulus of 0.4 GPa (Engelberget al. 1991). The PCL fibres thus exhibit a tensile modulus at least 10 times lower than PLA fibres and so could find wider application than PLA in tissue engineered structures, potentially soft tissue repair. PCL as-spun fibres exhibit a tensile strength of 1.9 - 12 MPa compared with 350 - 1200 MPa for

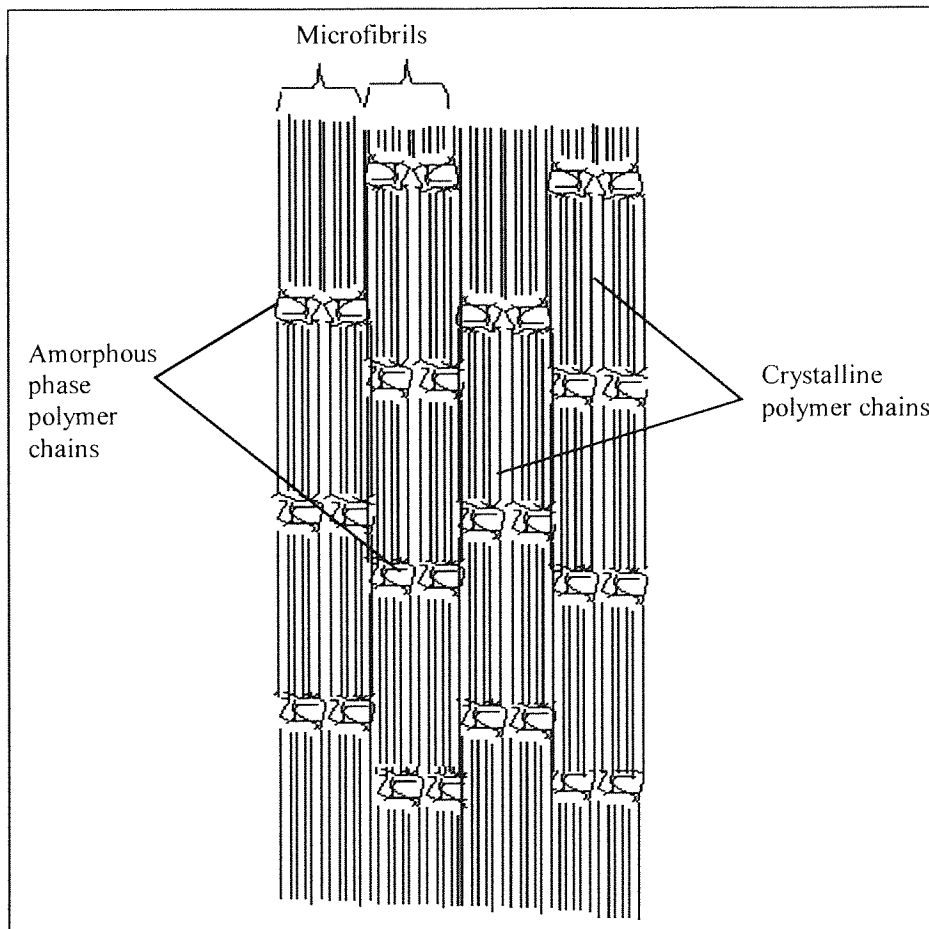
PLA fibres, 1050 MPa for nylon suture, 80 MPa for Dacron monofilament and 9.4 MPa for polypropylene (Table 3.19) and 16 MPa for mould PCL (Engelberget al. 1991). Major differences were observed between the tensile properties of as-spun PCL fibres produced using different solution concentrations. The results showed that the tensile strength and modulus of 10 and 20% PCL fibres was generally increased compared with the 6 and 15% fibres. Fibre tensile properties are strongly dependant on the degree of crystallinity and the crystal defects as fibres are made from several crystalline polymer chains bound by van der Waals bonds with amorphous phase polymer chains (which give elasticity) in between the crystalline chains these create microfibrils and several of these result in a fibre. A decrease in concentration of the spinning solution has been shown to result in a decrease in chain entanglements density and therefore a decrease in tensile strength for PLA fibres (Gogolewski et al. 1983). Similar effects may control the mechanical properties of PCL fibres described here. Those spun from 6% solutions (Table 3.9) exhibited reduced extensibility and strength compared with fibres produced from higher concentration solutions indicating that a population of 'effective' chain entanglements is necessary to allow extension of intervening chain segments. The PCL fibres also exhibit an increased extensibility compared to PLA and other fibres used in tissue engineering and therefore could have advantages in soft tissue repair. The tensile properties of the PCL fibres are similar to those of soft tissue, such as tendons (tensile modulus 0.6 GPa and tensile strength 82 MPa), cartilage (tensile modulus 0.02 GPa and tensile strength 3 MPa) and artery wall (tensile strength 3 MPa).

The fibre retraction experiments demonstrated that as-spun PCL fibre do not exhibit high elasticity or elastic recovery. Following low extensions (50%) the retraction is only 1-3%. Length recovery does increase as the fibre extension increases, but even at 500% extension the retraction is only 9-15%. The reason for the lack of elasticity is that the as-spun PCL fibres deform plastically under load beyond the yield point resulting in structural reorganisation, which does not recover to the original state on removal of the load.

Table 3.19 Tensile properties of synthetic biodegradable fibres

Fibre	Modulus (GPa)	Strength (MPa)	Elongation (%)	Ref.
PGA	8.4	890	30	Chu, 2000
Vicryl	8.6	850	24	Chu, 2000
PLA (solution spun)	9-15	1000-1200	<16	Gogolewski et al. 1983 and Eling et al. 1982
PLA (melt spun)	6	500	25	Eling et al. 1982
PLA (reactive extrusion)	4-6	350	30-150	Schmack et al. 2001
Polypropylene suture	-	9.4	40	Wada et al. 2001
Dacron monofilament	2-4	80	-	Vascutek

Figure 3.19 Schematic of the morphology of a polyester fibre



Drawing of as-spun PCL fibres at room temperature essentially involves a process of breakdown and unfolding of crystalline units and extension of amorphous tie chain segments as described by (Peterlin, 1967). These changes in molecular organisation result in the production of extended chain crystals and give rise to the oriented, fibrillar morphology of drawn PCL fibres (Figure 3.12) Similar morphology was described for solution (dry) spun PLA fibres by Eling et al. 1982. Chain extension in the amorphous phase is facilitated by the low T_g of PCL (-60°C), which ensures high chain mobility at room temperature. The improvement in PCL fibre strength and stiffness with increasing draw ratio (Tables 3.14 and 3.16) can in turn be related to the corresponding increase in molecular extension and alignment within the amorphous and crystalline phases of the fibre. An increase in the tensile strength of dry-spun PLA fibres with draw ratio has also been recorded (Eling et al. 1982, Leenslag et al. 1984 and Fambri et al. 1994). The importance of the concentration of the spinning solution in controlling the tensile strength of hot drawn PLA fibres has also been emphasised in several publications (Eling et al. 1982 and Gogolewski et al. 1983). Optimisation of chain entanglement density in the as-spun fibre is conducive to high draw ratios and the development of high tensile strength.

Hot drawing of as-spun PCL fibres at 37°C produced a dramatic increase but only when fibres were extended to 500%. This increased the tensile strength by 2 fold and increased the tensile modulus by 1.5 fold compared to the cold drawn fibre and was 10 fold higher compared to the as-spun 10% PCL fibres for tensile strength and tensile modulus. The increase in strength and stiffness could result when drawing at 37°C (which is near to the melting point of PCL (approx. 60°C)) as melting of a fraction of the crystalline units at the onset of melting (around 40°C (Figure 3.18)). Drawing at this temperature would cause the poor crystals to melt. The stress applied to the fibre shifts its melting point to higher temperatures and therefore increases supercooling. The molten material reorganises quickly into larger crystals, which decreases the chain mobility and reduces drawability of the fibre (Eling et al. 1982). Hot drawing could be a means of controlling the mechanical properties of the fibres to match the mechanical properties of specific tissues.

The PCL fibres when drawn at increasing speeds of extension show no alteration of mechanical properties, which has also been described using UHMW-PE fibres (Kromm et al. 2003). This shows that the fibres could tolerate rapid deformation *in vivo*. For example, fibres used in soft tissue such as skeletal muscle could be required to perform at high speeds. The fibre when incubated in PBS at 37°C for a month also showed no change in mechanical properties. Under these conditions the fibre could provide a stable substrate over the first month of implantation so that an anchorage dependant cell could lay down optimal extracellular matrix for tissue development.

The melting point of the PCL fibres was found to be around 56°C, which is comparable with moulded PCL pellets (56.3°C). Retained solvent in the fibre above a certain threshold level is undesirable and would raise toxicological concerns. Retained solvent can influence the crystallinity of the polymer. The % crystallinity of the PCL fibres was generally around 66% compared with 67.6% for PCL pellets. These results are similar and indicate that solvent retention does not appear to be a problem in the spinning technique investigated.

The mechanical and thermal properties of the cold drawn fibres are close to the properties of mould PCL, this is probably due to the overriding influence of the amorphous phase which is not having efficiently extended and maintained in the extended form during cold drawing.

CHAPTER 4

CELL INTERACTION WITH PCL FIBRES

4.1 Introduction

Biocompatibility is a term that broadly defines many specific properties of a material used in vivo that include; cell attachment, proliferation and function, immune response to the material and the effects that the breakdown products have on the surrounding tissue. For one example the scaffold could be toxic to the cells and hence inhibit their proliferation. If cells cannot attach, grow and differentiate upon the material correctly the performance of the implant is compromised. There are modifications that could be applied, for example a coating of extracellular matrix molecules. The scaffold also could be toxic to the cells and hence inhibit their proliferation. The cells attach to the scaffold via mechanisms described in the main introduction. The first biocompatibility experiments were performed with immortalised cells. The two cell lines used were Swiss 3T3 mouse fibroblasts exhibiting a dividing time of 24 hrs and they were grown to 90% confluence. C2C12 mouse myoblasts were the second cell line used. These cells differentiate rapidly, forming contractile myotubes upon confluence and therefore were only grown to 80% confluence. The attachment and proliferation characteristics of both cell lines on various PCL fibres were examined via proliferation experiments and by means of S.E.M.

4.2 Cell Proliferation Experiments

The results from the initial cell proliferation experiment are shown in Figure 4.1. This was performed using 3T3 fibroblasts seeded on three lengths of 15mm PCL fibres, held in the base of a 24 well plate by silicon O-rings and TCP was used as a control. The results show that the fibroblasts attach to the fibres at an extremely high rate compared with TCP, which is recognised to be a good substrate for cell proliferation. The cell numbers were counted using a haemocytometer and the lowest number of cells that can be counted accurately with a haemocytometer is $1 \times 10^4/\text{ml}$ and the number of cells counted was probably lower than this concentration.

The cell counting technique was then altered so that the adhered cells were lysed with Zaponin and the nuclei were counted using a Beckman Coulter counter. The rate of proliferation of C2C12 myoblast cells observed on the PCL fibre and TCP substrates is shown in Figure 4.2. The results show that cells attached and proliferated in greater numbers over 2-7 days on the PCL fibres than on TCP but the cell density was equivalent at day 8. The results demonstrate that C2C12 cells do attach to as-spun PCL fibre and proliferate at a high rate, the cell number at day 4 being 3-fold higher on the fibres than on TCP. Over the next 3 days a decrease in myoblast proliferation rate was observed on PCL fibres resulting in a 1.5-fold increase in cell number relative to TCP at day 7. Cell numbers were equivalent on TCP and the PCL fibre at day 8. The experimental findings for proliferation of 3T3 fibroblasts on PCL fibres are shown in Figure 4.3. At day 4 the cell numbers on PCL fibres were higher than on TCP. At this point the cell are probably confluent this is confirmed by a large fall in cell number measured at day 7, which was probably due to contact inhibition. Contact inhibition of cell proliferation results due to cells reaching high density and this causes the cell cycle progression cease (this is clearly due to cell contact, not nutrient depletion). Contact inhibition is presumably a consequence of cell-cell adhesions between fibroblasts, although the cell surface molecules have not been identified (Aplin et al. 1998) this is a characteristic of this cell line. The difference of cell numbers at confluence for the PCL fibres and TCP with fibroblasts is probably due to the surface area of the substrates, where the actual area available to the fibroblasts on the fibre is smaller than calculated.

Figure 4.1 Initial Swiss 3T3 fibroblasts attachment and proliferation rate on 10% as-spun PCL fibres and TCP substrates over 3 days. Seeding density 5×10^4 cells. The values are mean \pm SD for 6 replicates of each substrate type

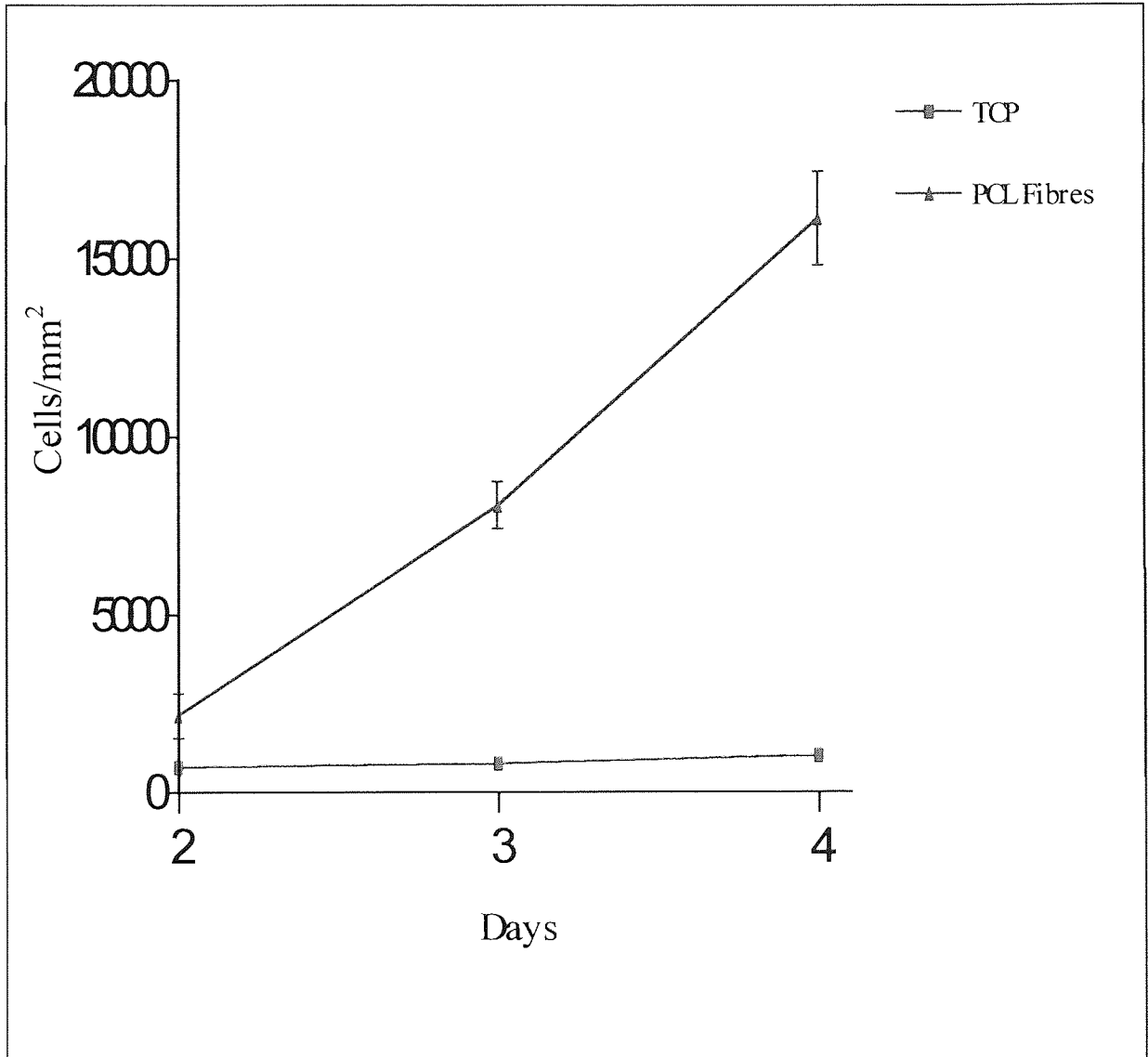


Figure 4.2 C2C12 mouse myoblasts attachment and proliferation rate on 10% as-spun PCL fibres and tissue culture plastic substrates over 8 days. Seeding density 2×10^4 cells. Cell nuclei counted by Coulter counter after zaponin incubation. The values are mean \pm SD for 6 replicates of each substrate type.

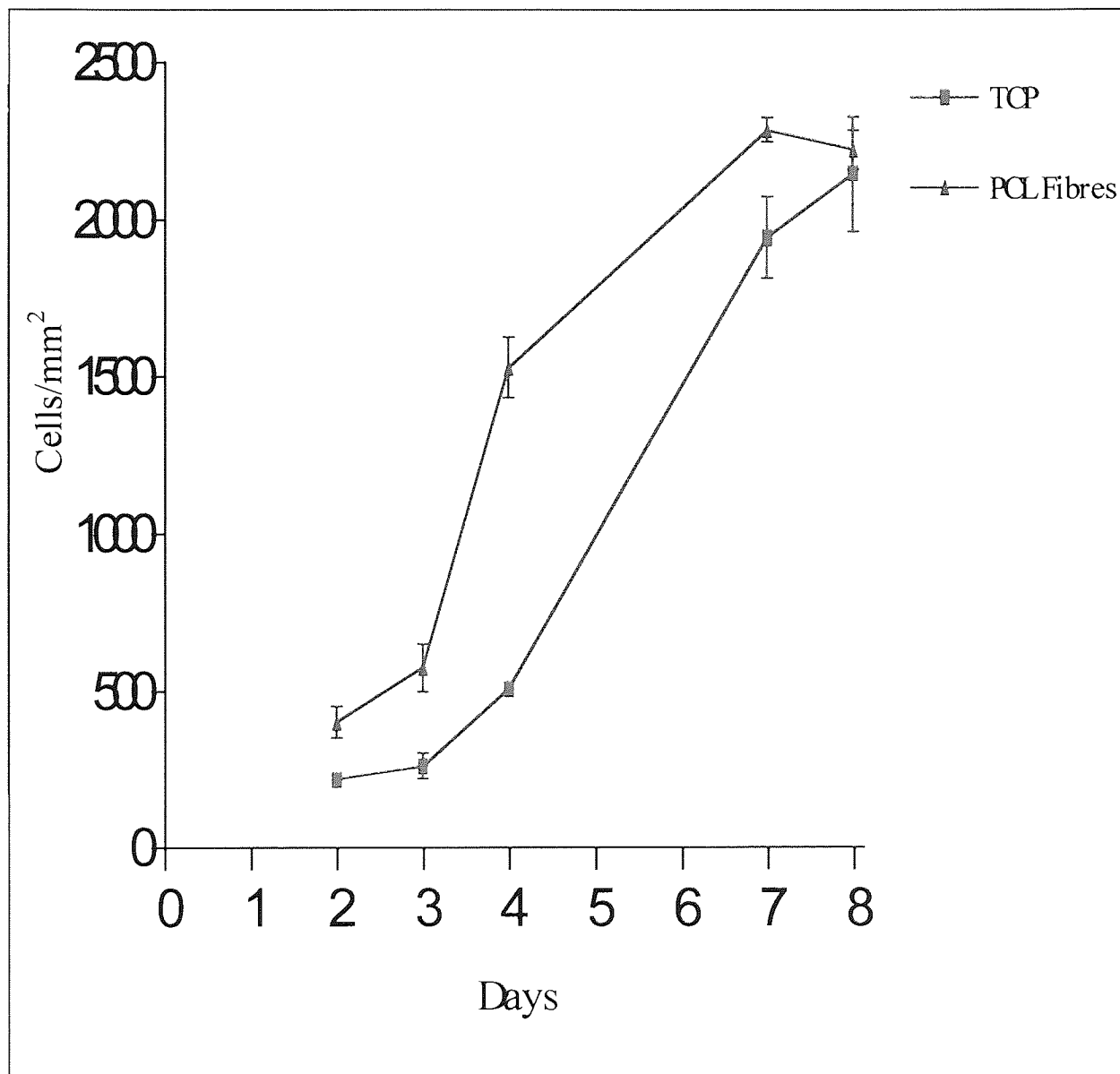
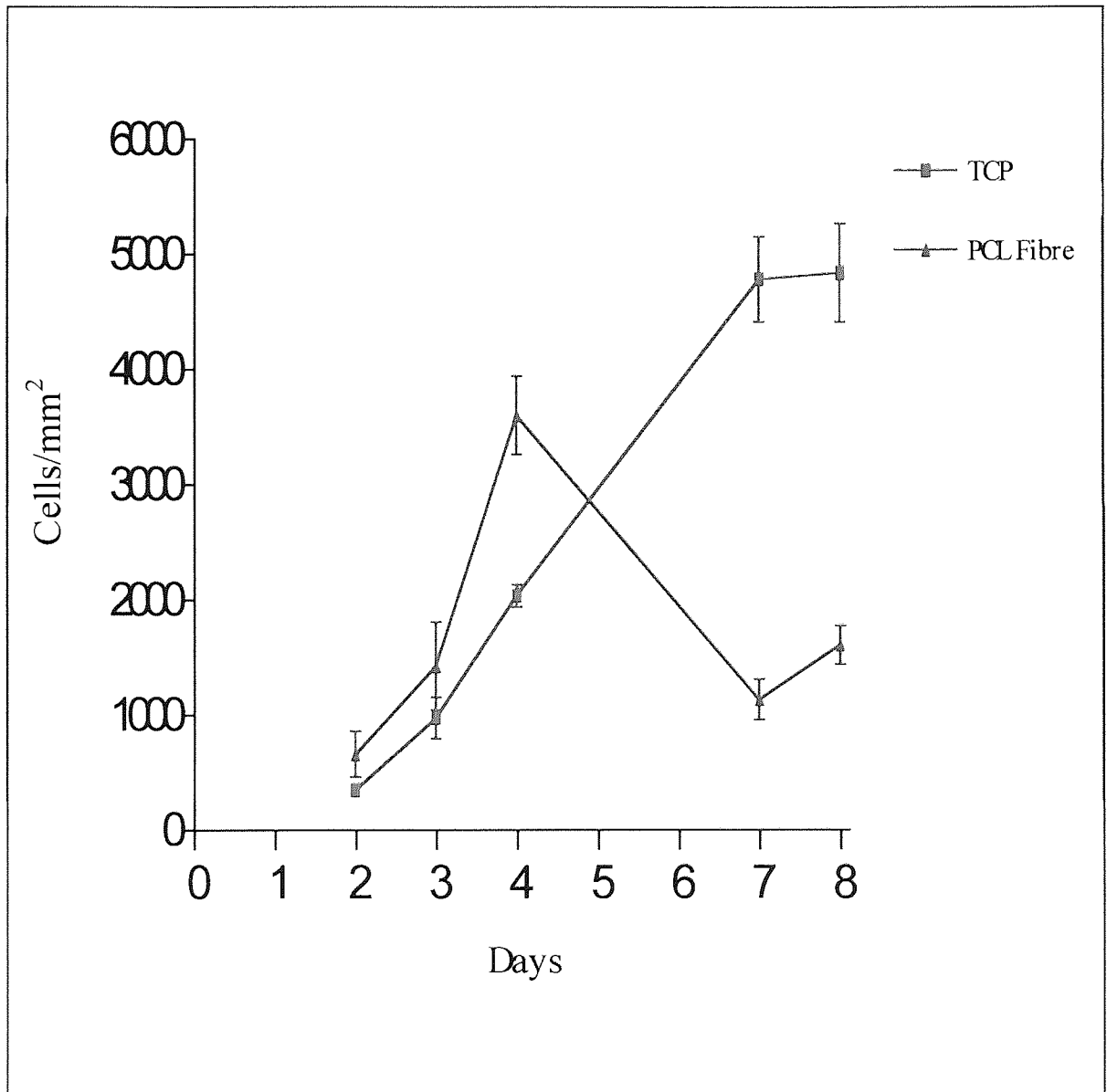


Figure 4.3 Swiss 3T3 fibroblasts attachment and proliferation rate on 10% as-spun PCL fibres and tissue culture plastic substrates over 8 days. Seeding density 2×10^4 cells. Cell nuclei counted by Coulter counter after zaponin incubation. The values are mean \pm SD for 6 replicates of each substrate type.



The cell proliferation study was optimised during the initial experiments described above. The counting procedure was changed. Since the Coulter counter registers particles of a certain size that are pre-specified in the setting up procedure. The problem was that the cells had to be lysed with zaponin so that the cell nuclei could be counted and therefore the Coulter counter could be counting cell debris along with the nuclei of the cell, thereby giving an incorrect result. In the optimised experimental procedure the cells were counted using a haemocytometer. Increasing the area of fibre was achieved by wrapping the fibre around a 22 mm x 22 mm glass coverslip and this increased the cell numbers on the fibre and therefore improved the accuracy of measurements.

The proliferation rate of fibroblasts on the increased surface area of 10% PCL fibres (124 mm²) over 9 days is shown in Figure 4.4. The number of attached fibroblasts on PCL fibres at day 1 was significantly higher (*P<0.05) than on TCP, but the cell number was higher by a factor of 1.5 on TCP at day 5 (**P<0.01) and all subsequent time points. The proliferation curves are similar in trend with a slowing in proliferation rate at day 7. After this point the curves appear to flatten which is a sign of confluence. The two proliferation curves trends are similar over the course of this study are not indicating that as-spun PCL fibre surface is favourable for fibroblast proliferation since TCP is produced to enhance cell proliferation.

Figure 4.5 shows the proliferation curves of myoblasts on 10% as-spun PCL fibre and TCP. The number of attached myoblasts was consistently higher on TCP than PCL fibres at all time points investigated by a factor of approximately 1.5. The two proliferation curves show a similar trend to fibroblast proliferation curves, with a tendency for the proliferation rate to decline at about day 7, again a sign of an approach to confluence. The two curves are significantly different (P<0.05), but the trends of the two curves are similar.

Figure 4.4 Swiss 3T3 fibroblasts attachment and proliferation rate on 10% as-spun PCL fibres and tissue culture plastic substrates over 9 days. PCL fibres were wrapped around a 22 mm x 22 mm glass coverslip (124 mm²). Seeding density 5 x 10⁴ cells. The values are mean \pm SD for 6 replicates of each substrate type. (* = P<0.05,** = P<0.01, NS = not significant)

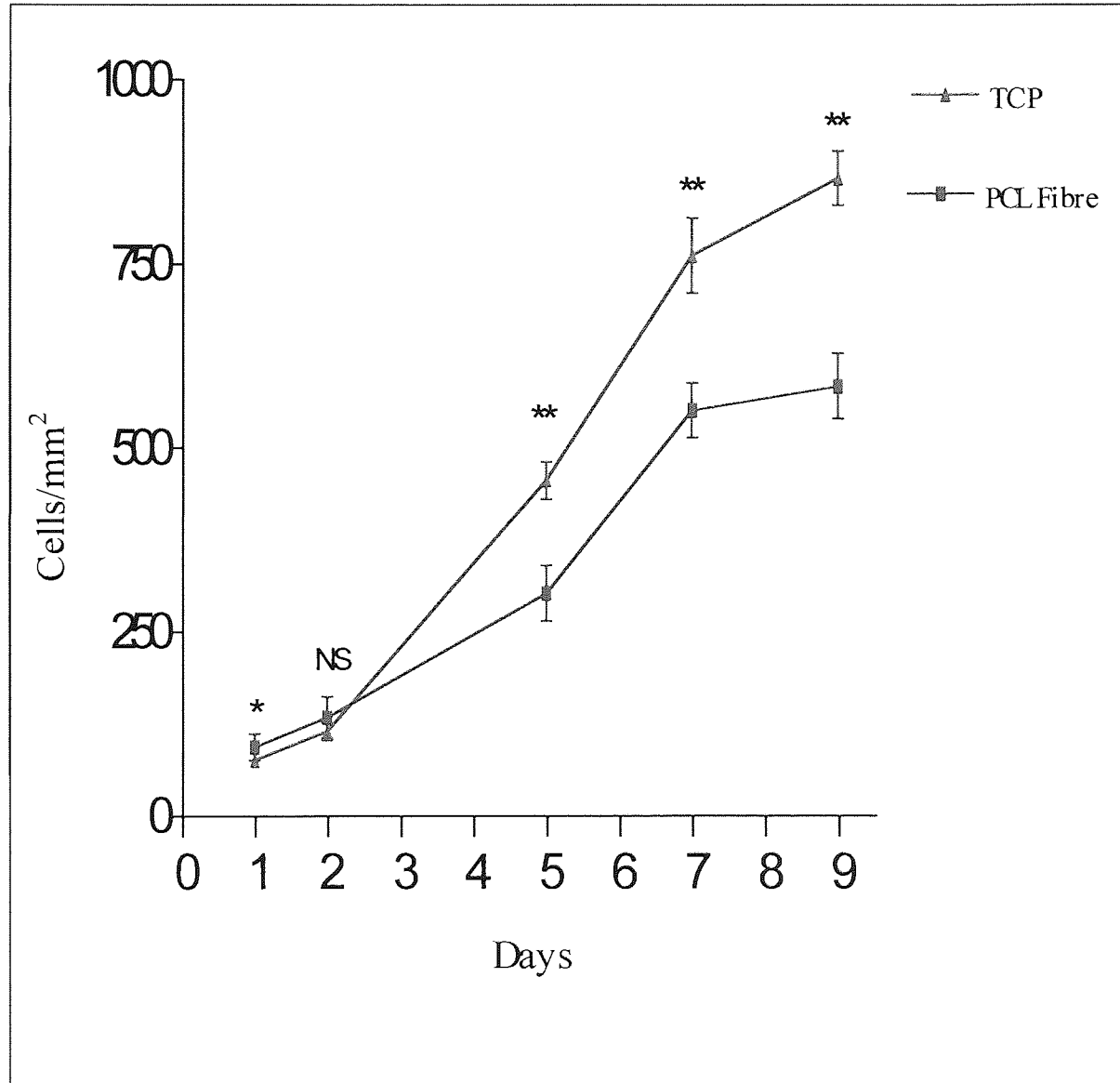
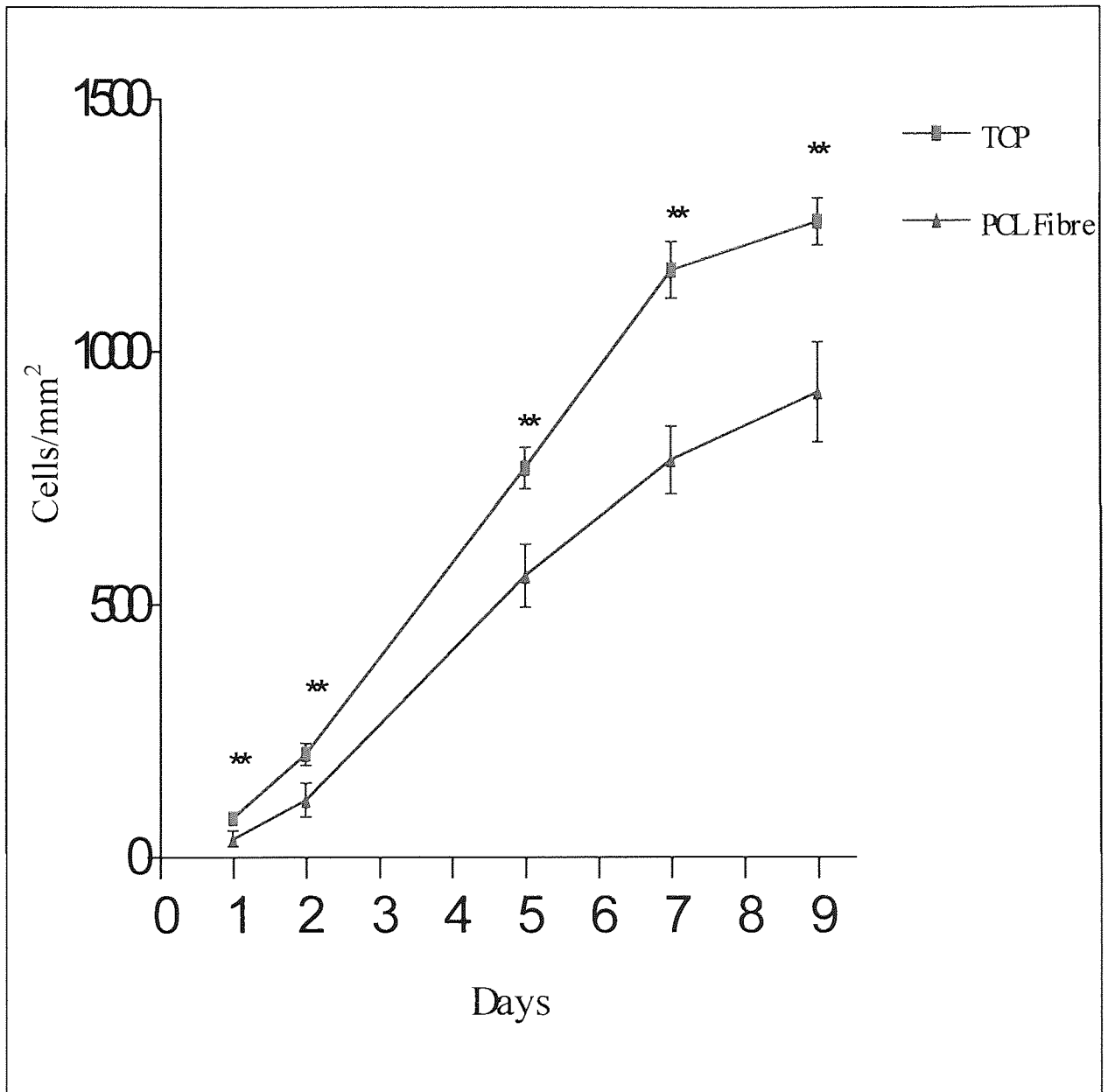


Figure 4.5 C2C12 mouse myoblasts attachment and proliferation rate on 10% as-spun PCL fibres and tissue culture plastic substrates over 9 days. PCL fibres were wrapped around a 22 mm x 22 mm glass coverslip (124 mm²). Seeding density 5 x 10⁴ cells. The values are mean \pm SD for 6 replicates of each substrate type.



4.3 Cell Interactions with 1) As-spun PCL Fibres 2) Gelatin Coated As-spun PCL Fibres and 3) Dacron Monofilament

The experimental findings for proliferation rates of 3T3 fibroblasts on as-spun 10% PCL fibres, 5% gelatin coated as-spun (10%) PCL fibre and Dacron monofilament are shown in Figure 4.6. Over the first 48 hours the number of attached cells on the gelatin coated PCL fibre is double and 3 times that on the uncoated PCL fibre and TCP respectively. The first 48 hours appears to show a lag phase (or slow cell proliferation rate). Up to day 5 for the gelatin coated PCL fibre and day 7 for the other substrates show the log phase of cell proliferation seem to be occurring which is a period of rapid proliferation. The proliferation curves level off for TCP and gelatin coated PCL fibres beyond day 7 and 5 respectively in a sign of confluence and thus a slowing in proliferation. All the substrates cell numbers at all time intervals were significantly greater proliferation rates than Dacron.

The rate of proliferation of C2C12 myoblast cells observed on 10% as-spun PCL fibres, gelatin coated as-spun (10%) PCL fibres, Dacron monofilament and TCP substrates is shown in Figure 4.7. The results show that cells attached and proliferated in significantly greater numbers on all the substrates relative to Dacron. Cells proliferation was highest on TCP over all time points apart from day 1 where the gelatin coated PCL fibre cell number was 1.5 fold higher. Both TCP and gelatin coated PCL fibre exhibited similar shaped proliferation curves, with both systems reaching confluence at day 5. The uncoated fibres may be moving towards confluence beyond day 7.

4.4 Cell Interactions with 1) As-spun PCL Fibres 2) 500% Cold Drawn PCL Fibres and 3) Dacron Monofilament

Cell proliferation experiments involving Swiss 3T3 mouse fibroblasts on as-spun 10% PCL fibres, 10% PCL fibre cold drawn to 500%, Dacron monofilament and TCP are shown in Figure 4.8. The data shows that the cells attach at an increased rate on the cold drawn PCL fibre relative to all the other substrates over 7 days. Dacron monofilament results in relatively poor cell attachment and proliferation with the

other substrates having significantly higher cell numbers at all time intervals. Cell confluence is indicated on the cold drawn as-spun fibres by day 7. The proliferation curve for TCP however does not indicate confluence at 9 days.

Figure 4.6 Swiss 3T3 fibroblasts attachment and proliferation rate on 10% as-spun PCL fibres, 10% PCL fibres coated with a 5% gelatin solution, Dacron monofilament and tissue culture plastic substrates over 9 days. Fibres were wrapped around a 22 mm x 22 mm glass cover slip. Seeding density 5×10^4 cells. The values are mean \pm SD for 6 replicates of each substrate type. (* TCP compared to as-spun PCL fibres, + TCP compared to gelatin coated fibres, # as-spun PCL fibres compared to gelatin coated fibres)

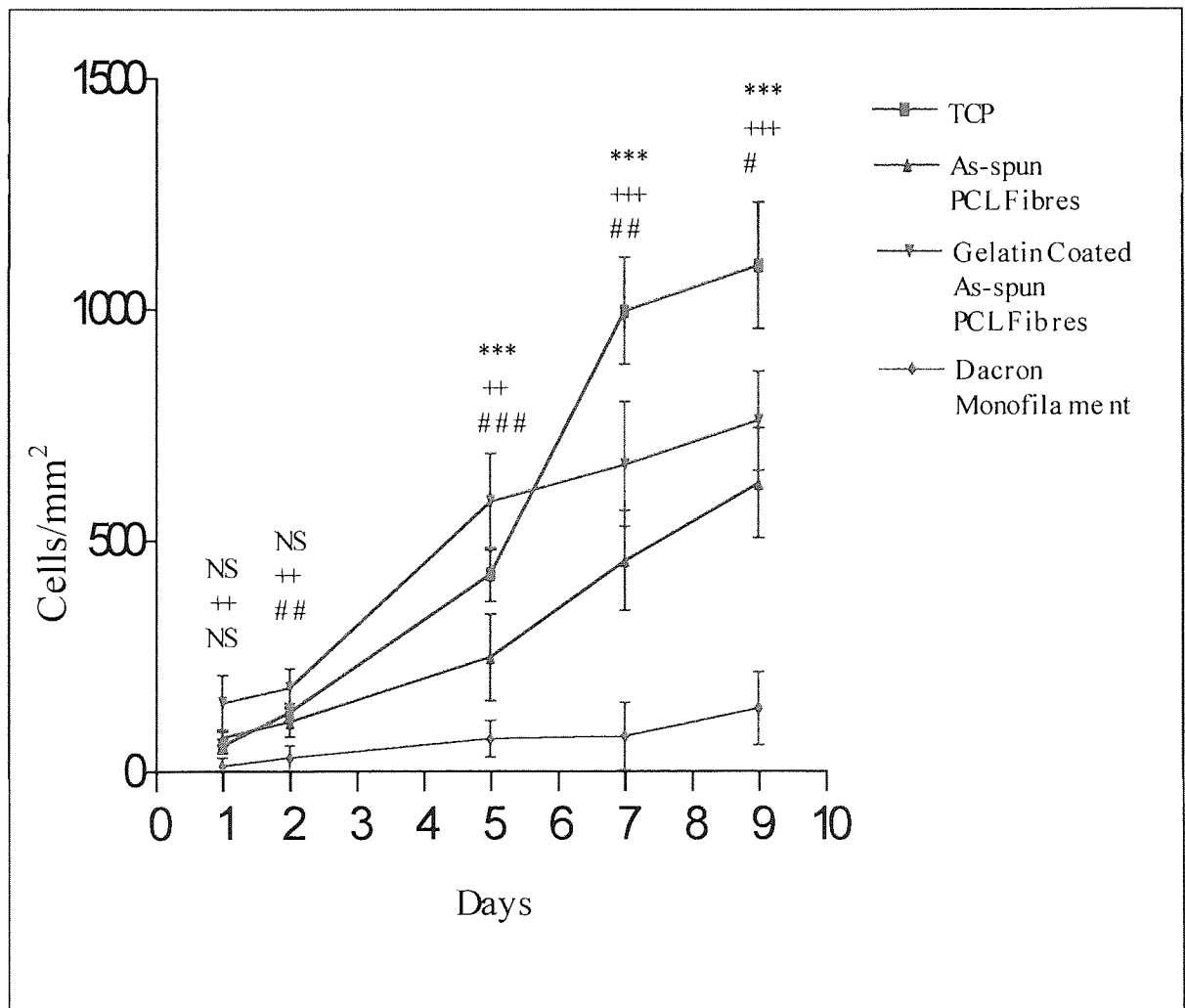


Figure 4.7 C2C12 mouse myoblasts attachment and proliferation rate on 10% as-spun PCL fibres, 10% PCL fibres coated with a 5% gelatin solution, Dacron monofilament and tissue culture plastic substrates over 9 days. Fibres were wrapped around a 22 mm x 22 mm glass cover slip. Seeding density 5×10^4 cells. The values are mean \pm SD for 6 replicates of each substrate type. (* TCP compared to as-spun PCL fibres, + TCP compared to gelatin coated fibres, # as-spun PCL fibres compared to gelatin coated fibres)

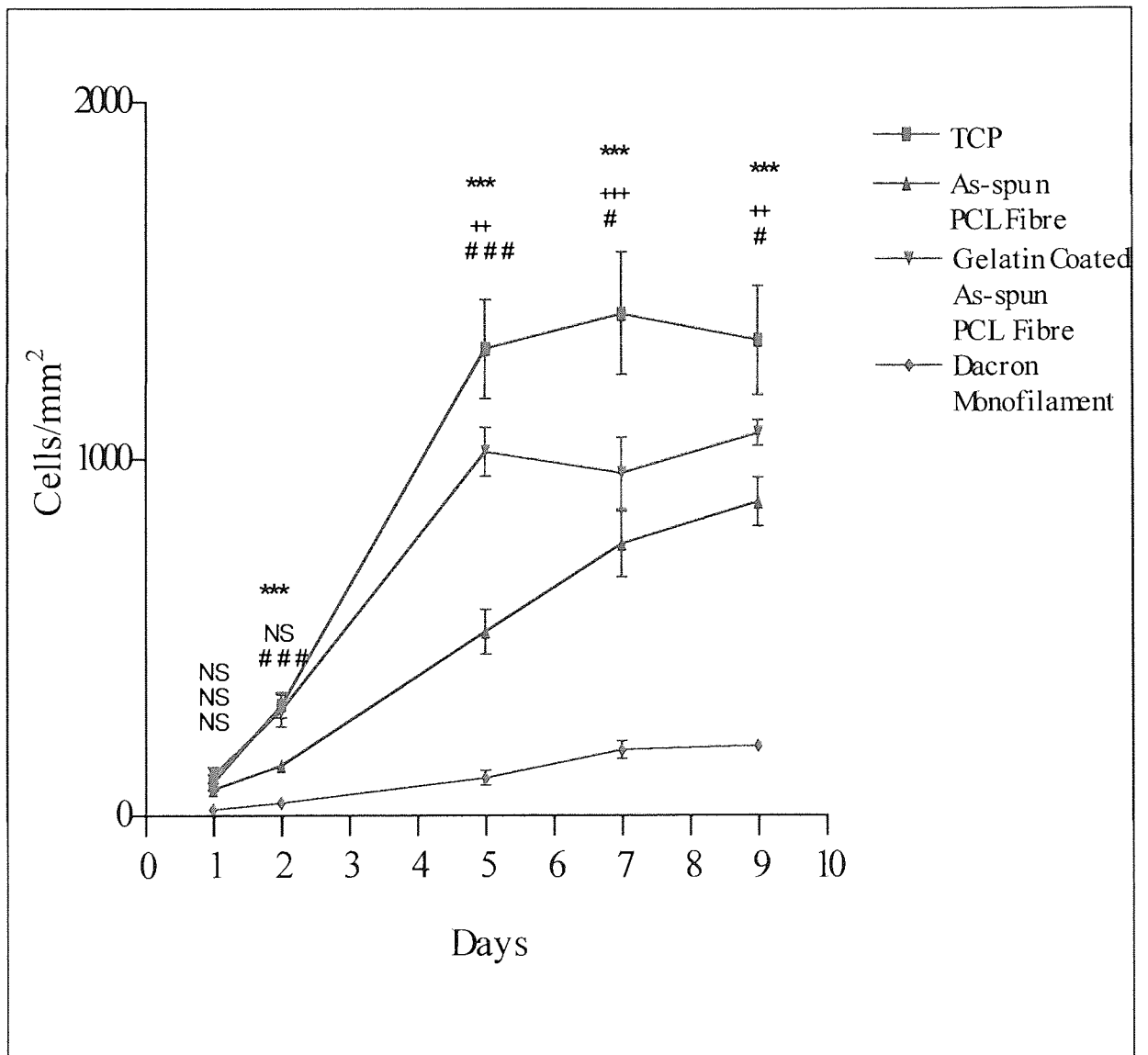
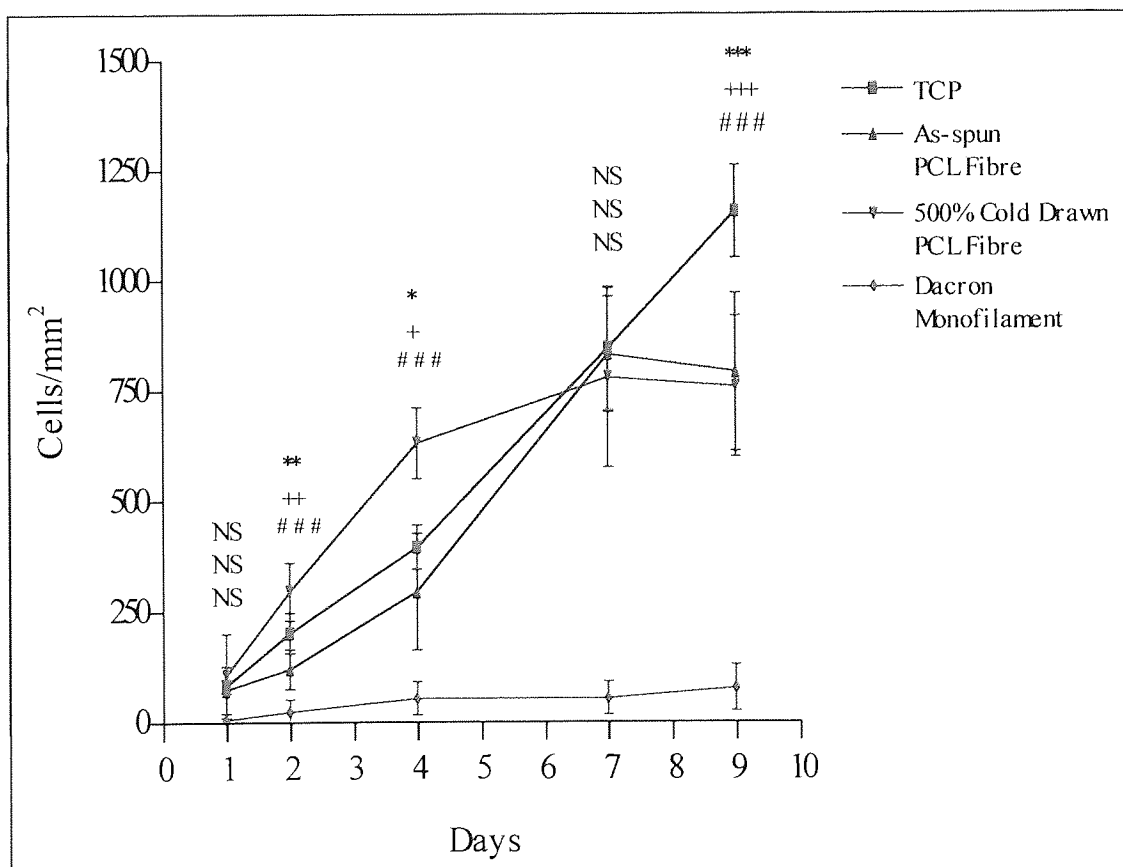


Figure 4.9 show the results of C2C12 mouse myoblast proliferation on as-spun 10% PCL fibres, 10% PCL fibre cold drawn to 500%, Dacron monofilament and TCP. The results suggest that Dacron monofilament is again a poor substrate for myoblasts with the other substrates showing greatly increased ($P < 0.05$) attachment and proliferation. The proliferation curves obtained using cold drawn and as-spun PCL fibres show a very similar trend, with cells appearing to reach confluence on the cold drawn fibres by day 7. Cell attachment and proliferation rate on TCP is lower in this experiment over the first two days relative to as-spun and cold drawn PCL fibres compared to Figure 4.5. However by day 4 cell proliferation is higher in TCP than the fibre substrates by almost 8 fold.

Figure 4.8 Swiss 3T3 fibroblasts attachment and proliferation rate on 10% as-spun PCL fibres, 500% cold drawn (10%) PCL fibres, Dacron monofilament and tissue culture plastic substrates over 9 days. Fibres were wrapped around a 22 mm x 22 mm glass cover slip. Seeding density 5×10^4 cells. The values are mean \pm SD for 6 replicates of each substrate type. (* TCP compared to as-spun PCL fibres, + TCP compared to gelatin coated fibres, # as-spun PCL fibres compared to 500% cold drawn fibres)



4.5 Fibroblast Cell Attachment to As-spun PCL Fibres and 500% Cold Drawn PCL Fibres

Fibroblast attachment to drawn PCL fibres was measured over 8 hours in cell culture and was at a higher rate than to TCP and the as-spun PCL fibre at all time points investigated over 8 hours (Figure 4.10) but was not significantly different. The number of attached cells on all substrates appears to have levelled off by two hours. This trend was particularly strong for the as-spun PCL fibre and TCP substrates. Cells still seemed to be attaching to the 500% drawn fibres but not at the rate as observed during the first two hours.

4.6 Fibroblast Cell Attachment to As-spun PCL Fibres and Gelatin Coated As-spun PCL Fibres

The attachment rate of fibroblasts on gelatin coated as-spun PCL fibres was found to be 3 fold higher (and significantly different) at 1 hour compared to TCP and uncoated PCL fibres (Figure 4.11). This underlines the good cell adhesion qualities of gelatin compared to the cell attachment rates on the uncoated PCL fibre and TCP. The decrease in cell number on the gelatin-coated fibre after 2 hours may be due to gradual loss of the gelatin coating. The loss of the gelatin coating from the PCL fibre over time has been observed in section 6.5 (Figure 6.8), in this experiment the gelatin coated as-spun PCL fibre was washed but not incubated in PBS prior to culture.

Figure 4.10 Swiss 3T3 fibroblasts attachment rate on 10% as-spun PCL fibres and 10% PCL fibre cold drawn to 500% and tissue culture plastic substrates over 8 hours. Fibres were wrapped around a 22 mm x 22 mm glass coverslip. Seeding density 1×10^5 cells. The values are mean \pm SD for 6 replicates of each substrate type. (* TCP compared to as-spun PCL fibres, + TCP compared to gelatin coated fibres, # as-spun PCL fibres compared to 500% cold drawn fibres)

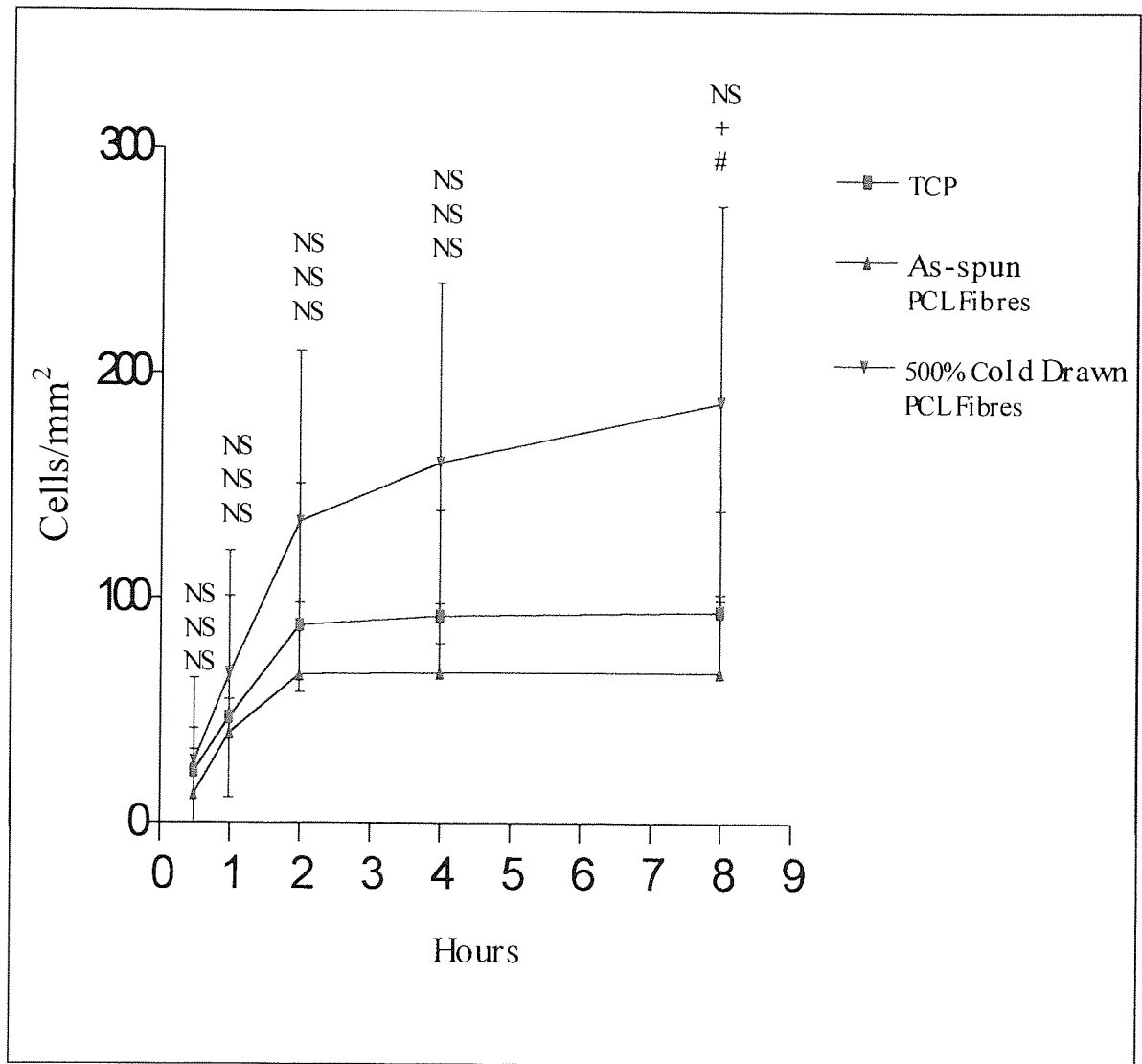
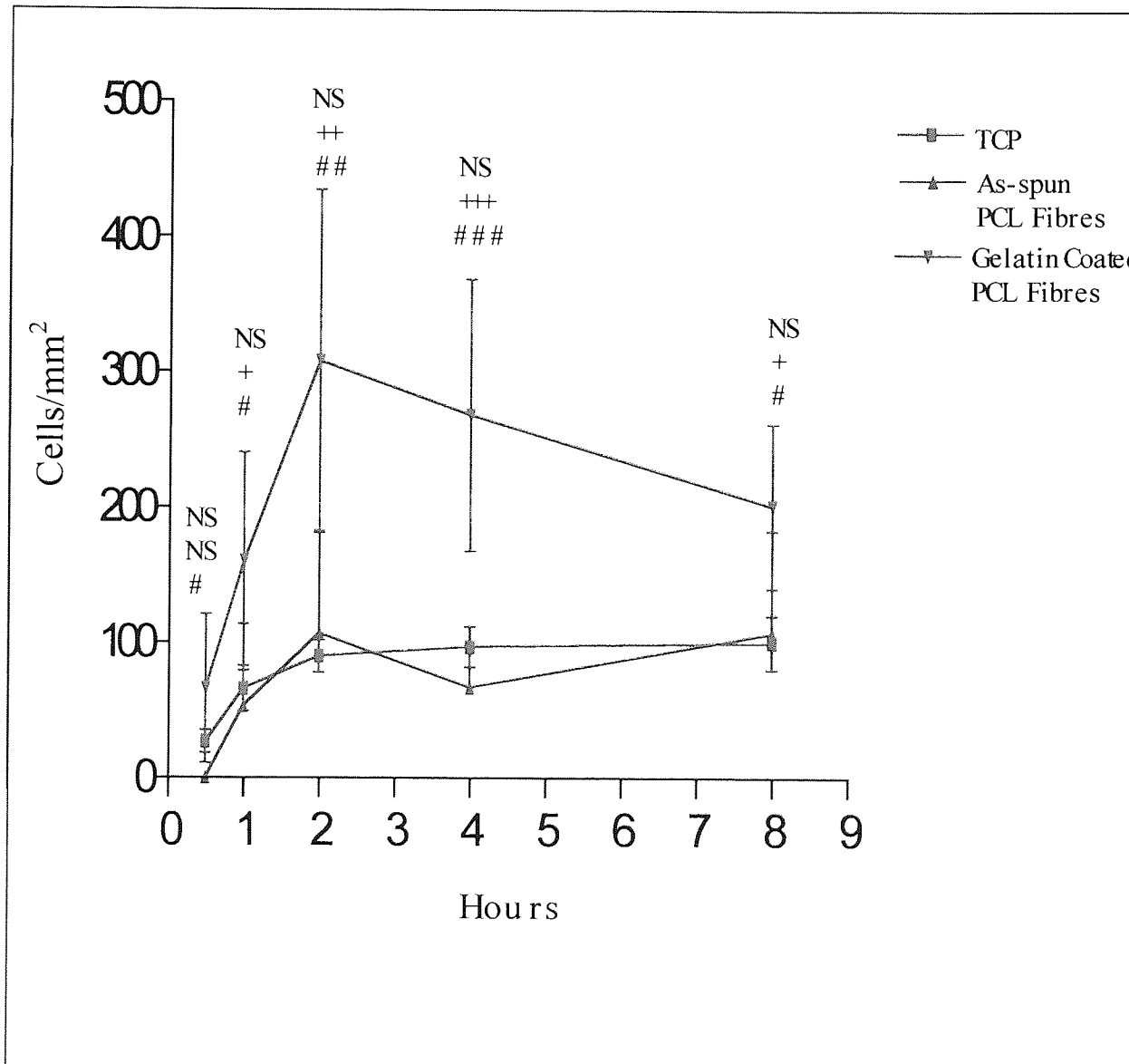


Figure 4.11 Swiss 3T3 fibroblasts attachment rate on 10% as-spun PCL fibres and 10% as-spun PCL fibre coated with a 5% w/v gelatin solution and tissue culture plastic substrates over 8 hours. Fibres were wrapped around a 22 mm x 22 mm glass coverslip. Seeding density 1×10^5 cells. The values are mean \pm SD for 6 replicates of each substrate type. (* TCP compared to as-spun PCL fibres, + TCP compared to gelatin coated fibres, # as-spun PCL fibres compared to gelatin coated fibres)



4.7 SEM Study of Cell-Fibre Interaction and Morphology

The interaction of fibroblasts and myoblasts with as-spun, 500% cold drawn and gelatin coated PCL fibres in cell culture were investigated using scanning electron microscopy. Cells were allowed to attach and grow on the fibre over 8 hours, 1 day and 3 days. The cells were washed, fixed, dehydrated and dried before SEM examination as described in section 2.2.24.

Figure 4.12 shows Swiss 3T3 mouse fibroblasts attached to as-spun, gelatin coated PCL fibre. A group of fibroblasts are observed many of which are still rounded, indicating that strong attachments via focal contacts has not yet occurred. Some of the cells are starting to show the first signs of cell spreading via focal contact formation with the fibre surface.

Spreading of a C2C12 mouse myoblast after 8 hours on an as-spun gelatin coated, as-spun PCL fibre is shown in Figure 4.13. The cell's main body has flattened. This occurs when the integrin cell surface receptors and proteoglycan combines to form a focal contact between the substrate and the base of the cell body and along the bottom of the process. The SEM also shows that the cell has extended two long processes from either end of the cell to contact other cells or nutrients.

Preparation of fibres with attached cell for SEM analysis is problematic. The fibres have to be cut from the cover slips and which results in a considerable amount of movement, that could dislodge weakly attached rounded cells. This factor could account for the sparse population of cells observed after 8 hours cell culture.

Figure 4.12 SEM of Swiss 3T3 mouse fibroblasts on an as-spun PCL fibre coated with a 5% gelatin solution. Fixed 8 hours after seeding with an initial cell density of 1×10^5 cells.

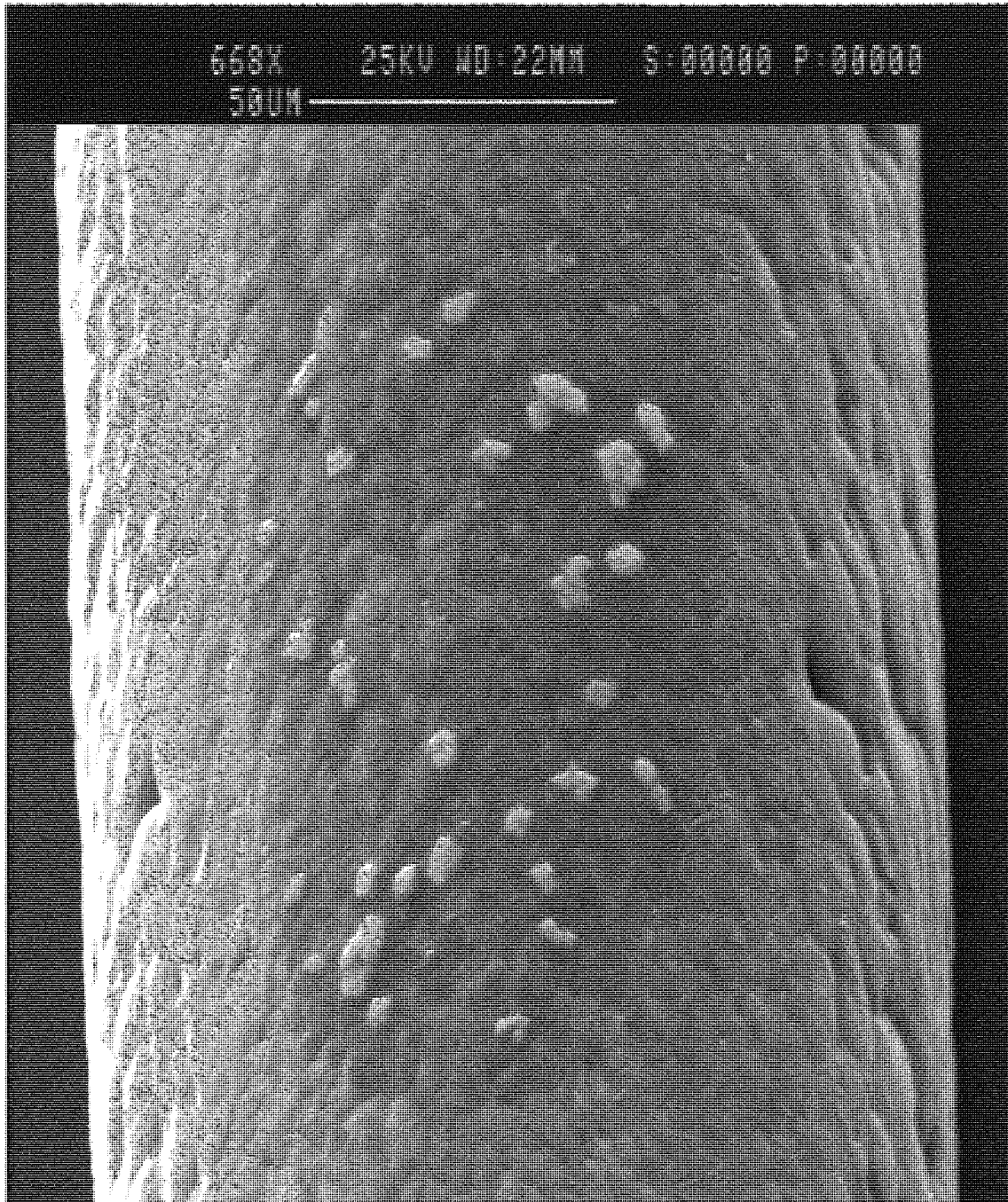
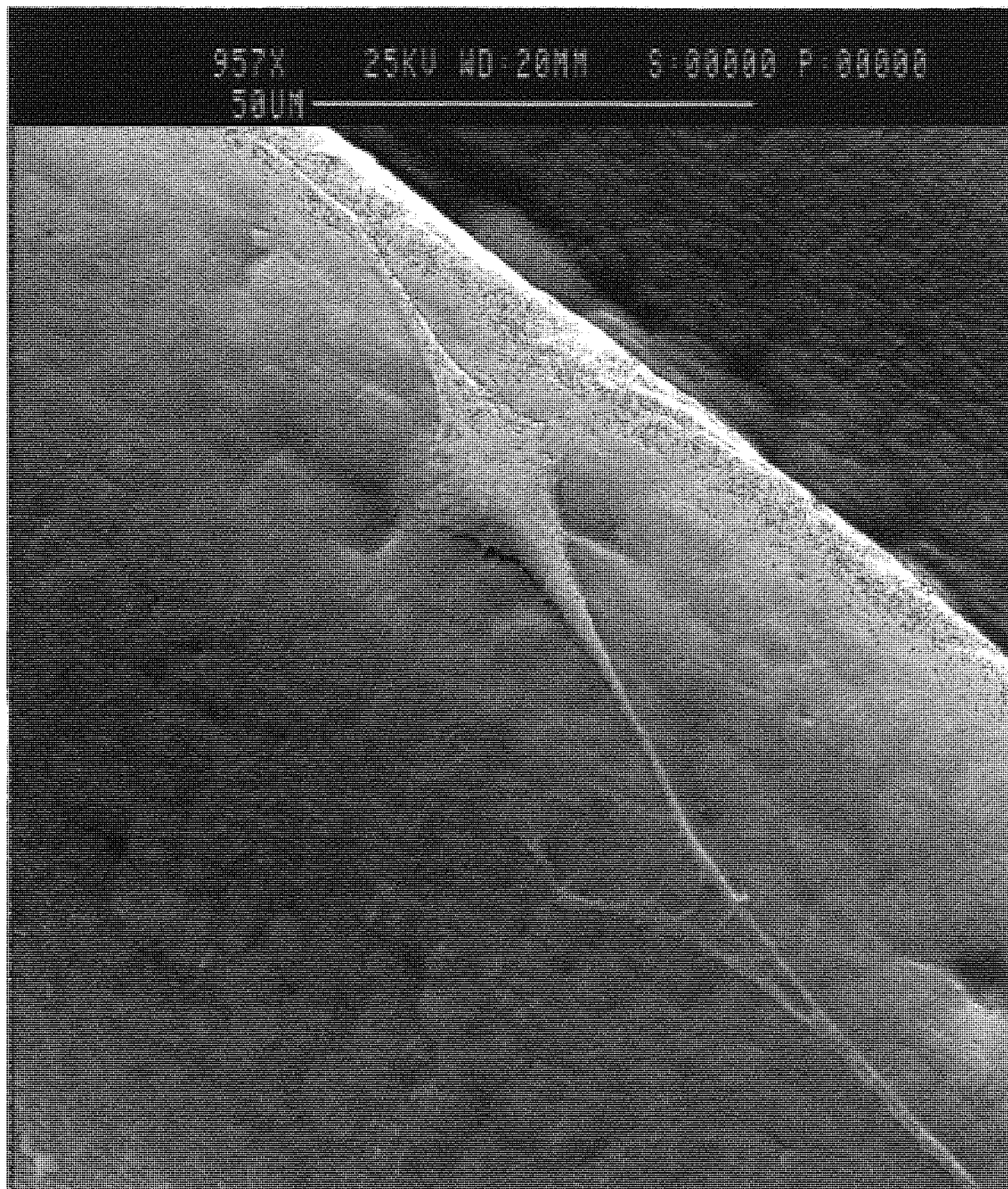


Figure 4.13 SEM of C2C12 mouse myoblasts at on an as-spun PCL fibre coated with a 5% gelatin solution. Fixed 8 hours after seeding with an initial cell density of 1×10^5 cells.



The fibroblast morphology on the various PCL fibres was examined after 1 day after cell seeding. Figures 4.14A and 4.14B shows fibroblasts at an initial density of 1×10^5 attached to, as-spun PCL fibres. The cells appear to cover the fibre surface and mould to the surface topography. The cells attached to the surface are identified by two areas where the cell layer has detached slightly and curled back from the surface upon dehydration and drying [D]. The cell layer is also clearly seen in Figure 4.14B (arrowed), which shows a distinct edge of the cell layer. The depression near the centre of this SEM is formed from a second cell monolayer that is approaching the first monolayer but this area has cracked upon dehydration and drying.

Figures 4.15A and 4.15B show the morphology of myoblasts on as-spun PCL fibres. The myoblasts attached and proliferated over a significant area of the fibre. Figure 4.15A shows that there are distinct areas where the myoblasts spread, flatten and coalesce. Other areas of the fibre have not been colonised. Processes are observed extending between one area of a cells to another. Figure 4.15B shows the same fibre but at a higher magnification. The cells have flattened and spread and again moulded to the surface of the fibre. Figure 4.15B also shows the communication of processes from one cell to another.

The cell interaction with a PCL fibre coated with gelatin after 1 day in cell culture is indicated in Figures 4.16 and 4.17 for fibroblasts and myoblasts respectively. The fibroblasts appear to have formed a monolayer or coating over the surface of the fibre. The morphology of the fibre seems to be slightly smoother in appearance compared to the SEM of a fibre without cells attached (Figures 4.16b and 3.5). This effect is not due to the coating of gelatin, as this does not change the morphology of the fibre (Figures 4.16c and 6.3). Figure 4.17 shows myoblasts on a gelatin-coated, as-spun PCL fibre after 1 day after cell culture. A monolayer has been formed with a few areas of the underlying fibre exposed. The area where the cells have formed a monolayer is smoother than the original surface of the fibre, which confirms that the cells mould to the surface of the fibre upon confluence.

Figure 4.14A (a) SEM of Swiss 3T3 mouse fibroblasts on as-spun PCL fibre. Fixed 1 day in cell culture after seeding with an initial cell density of 1×10^5 cells. (b) As-spun PCL fibre without cells attached

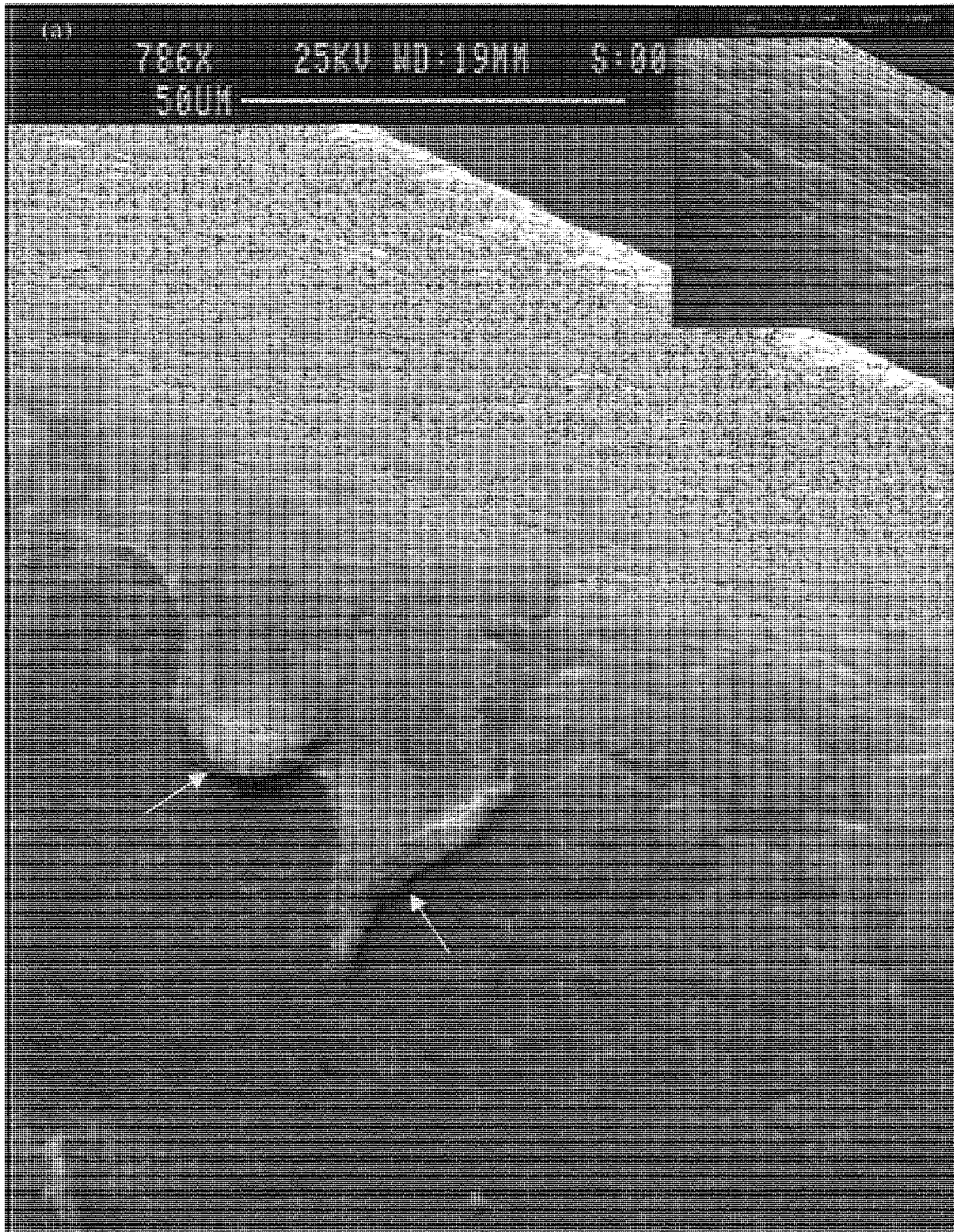


Figure 4.14B (a) SEM of Swiss 3T3 mouse fibroblasts on as-spun PCL fibre. Fixed 1 day in cell culture after seeding with an initial cell density of 1×10^5 cells. (b) As-spun PCL fibre without cells attached

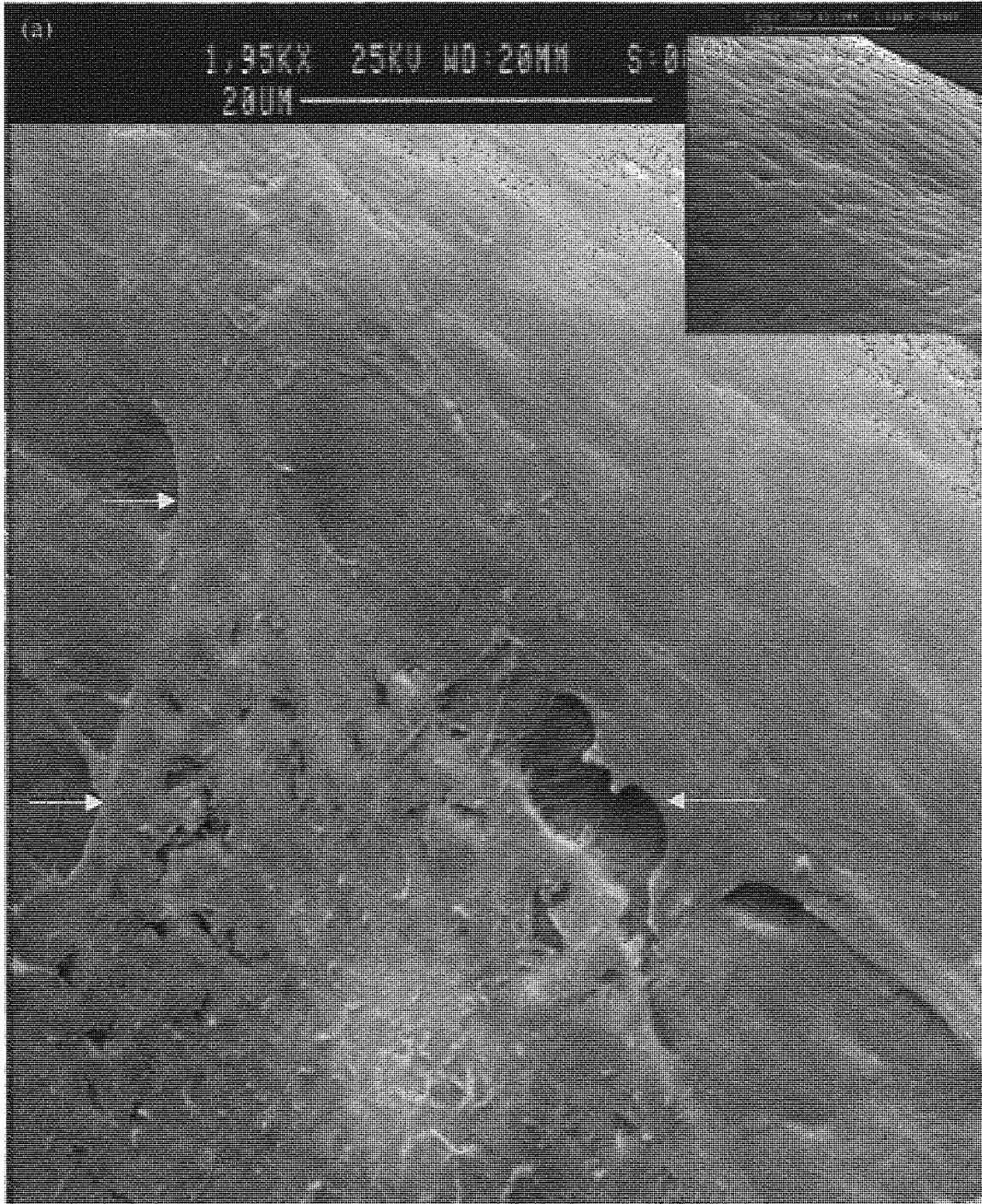


Figure 4.15A (a) SEM of C2C12 mouse myoblasts on as-spun PCL fibre. Fixed 1 day in cell culture after seeding with an initial cell density of 1×10^5 cells. (b) As-spun PCL fibre without cells attached

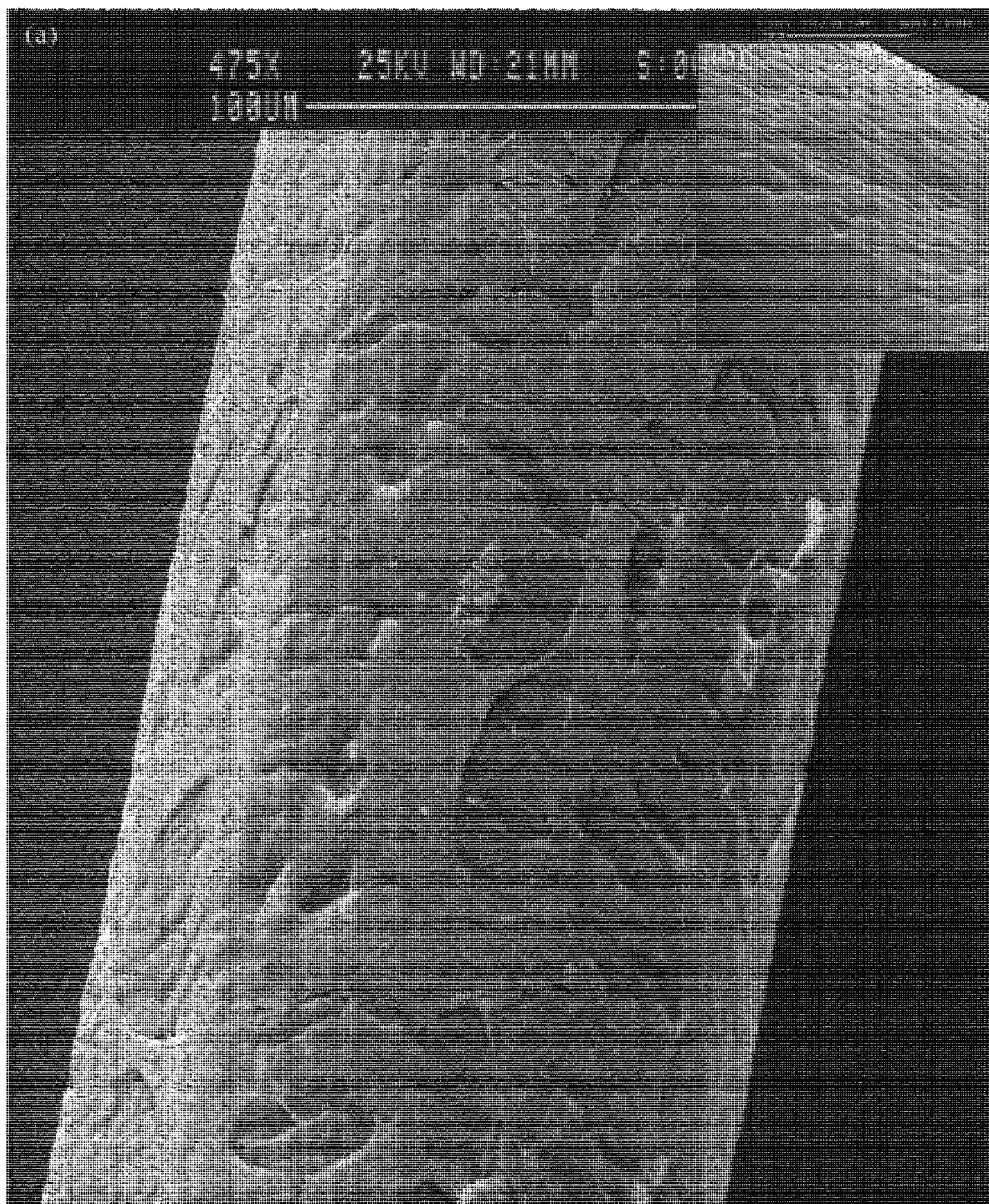
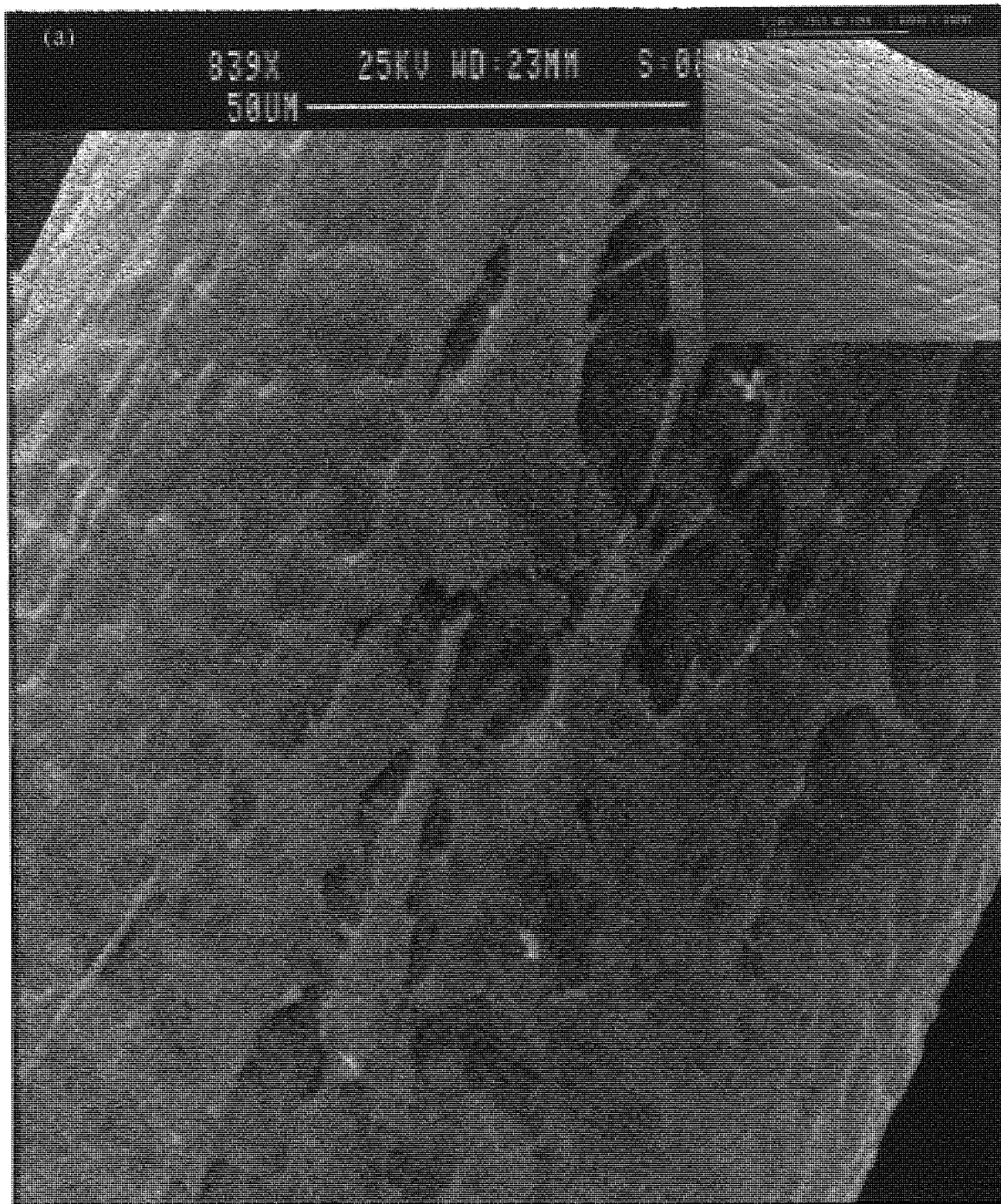


Figure 4.15B (a) SEM of C2C12 mouse myoblasts on as-spun PCL fibre. Fixed 1 day in cell culture after seeding with an initial cell density of 1×10^5 cells. (b) As-spun PCL fibre without cells attached



Figures 14.18A and 14.18B show the morphology of fibroblasts growing upon 500% cold drawn PCL fibres after 1 day in culture. The cells show the same signs of masking or coating the fibres' topography, forming a layer having a similar fibrillar/ridged appearance to the underlying fibre. Several processes are visible which the cell(s) have extended to either move to an uncolonised area or to contact other cells that are not observed. Figure 4.18B shows a higher magnification of the SEM image area where the cells have extended processes. The SEM shows a cell layer growing over the surface of the fibre, which has cracked during the dehydration, and drying process of specimen preparation.

Figure 4.19 shows the interactions of the myoblasts with a 500% cold drawn PCL fibre. The observations are similar to those for the fibroblasts interactions. The cell layer has moulded to the fibres' surface morphology and evidence for the cell layer are processes extending between cells.

Figure 4.16 (a) SEM of Swiss 3T3 mouse fibroblasts on an as-spun PCL fibre coated with gelatin. Fixed 1 day in cell culture after seeding with an initial cell density of 1×10^5 cells. (b) As-spun PCL fibre without attached cells (c) Gelatin coated PCL fibre without cells attached

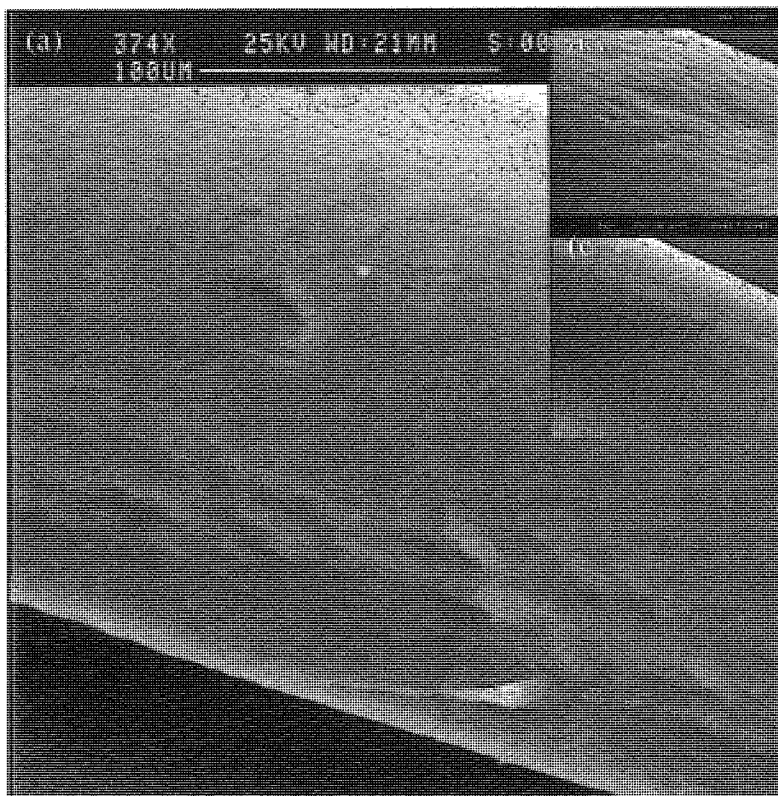


Figure 4.17 (a) SEM of C2C12 mouse myoblasts on an as-spun PCL fibre coated with gelatin. Fixed 1 day in cell culture after seeding with an initial cell density of 1×10^5 cells. (b) As-spun PCL fibre without attached cells (c) Gelatin coated PCL fibre without cells attached

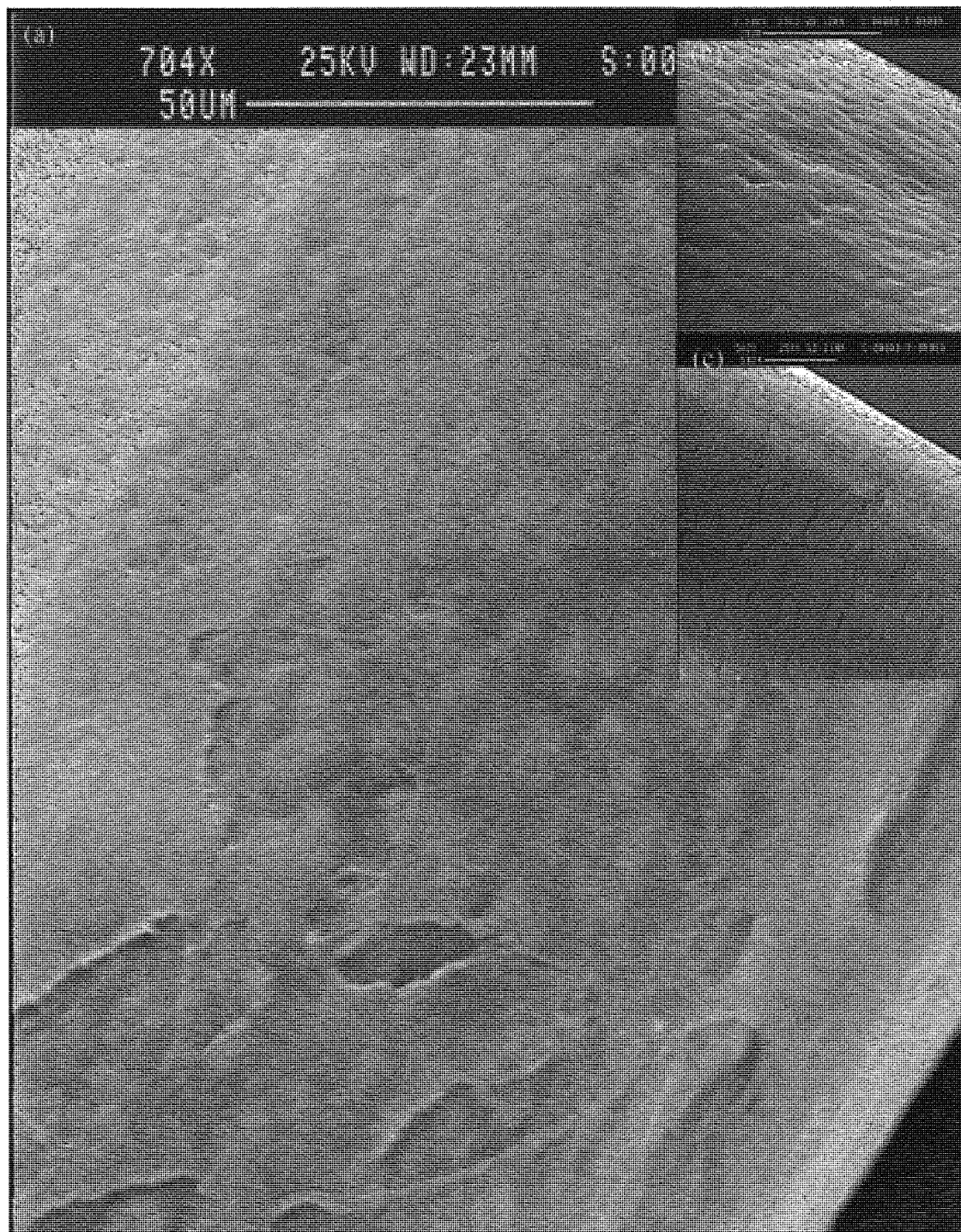


Figure 4.18A (a) SEM of Swiss 3T3 mouse fibroblasts on 500% cold drawn PCL fibre. Fixed 1 day in cell culture after seeding with an initial cell density of 1×10^5 cells. (b) 500% cold drawn PCL fibre without attached cells



Figure 4.18B (a) SEM of Swiss 3T3 mouse fibroblasts on 500% cold drawn PCL fibre. Fixed 1 day in cell culture after seeding with an initial cell density of 1×10^5 cells. (b) 500% cold drawn PCL fibre without attached cells



Figure 4.19 (a) SEM of C2C12 mouse myoblasts on 500% cold drawn PCL fibre. Fixed 1 day in cell culture after seeding with an initial cell density of 1×10^5 cells. (b) 500% cold drawn PCL fibre without attached cells



The myoblast interactions with as-spun, gelatin coated and 500% cold drawn PCL fibres are indicated in Figure 4.23, 4.24 and 4.25 respectively. As with the fibroblasts interaction the myoblasts after achieving a confluent monolayer have created a smoother fibre surface compared to as-spun fibres but still display some of the original surface roughness of the fibres. The monolayer formed over the 500% cold drawn fibre again has a slightly ridged appearance, which has been copied from the original fibres' surface topography. The myoblasts monolayer as with the fibroblasts has slightly disguised the original surface as the fibre, now clearly displays fewer fibillar structures. Figure 4.26 shows a fibre when attached to the carbon tab has exposed the underside of the fibre. This SEM clearly shows the edge of a layer of cells and the original cell free fibre surface.

Figure 4.20 (a) SEM of Swiss 3T3 mouse fibroblasts on an as-spun PCL fibre. Fixed 3 days in cell culture after seeding with an initial cell density of 1×10^5 cells. (b) As-spun PCL fibre without attached cells

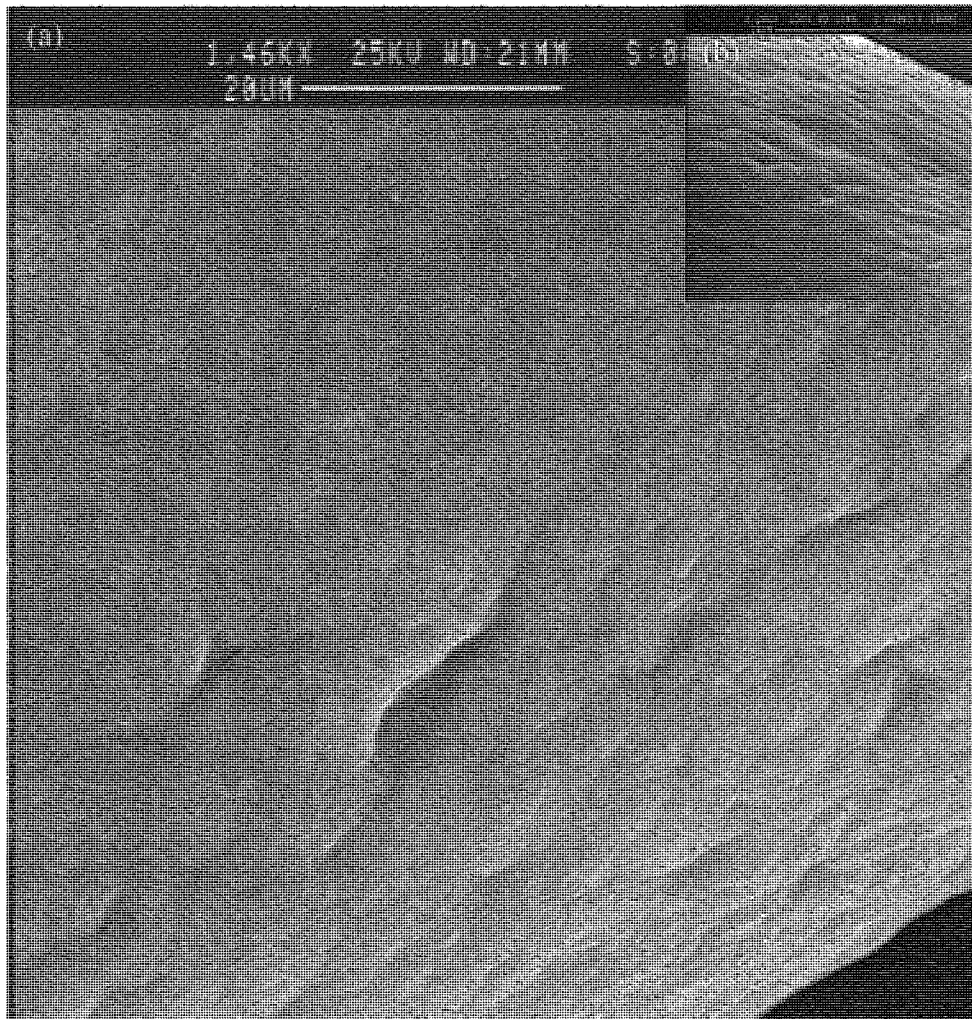


Figure 4.21 (a) SEM of Swiss 3T3 mouse fibroblasts on an as-spun PCL fibre coated with gelatin. Fixed 3 days in cell culture after seeding with an initial cell density of 1×10^5 cells. (b) As-spun PCL fibre without attached cells (c) Gelatin coated PCL fibre without cells attached

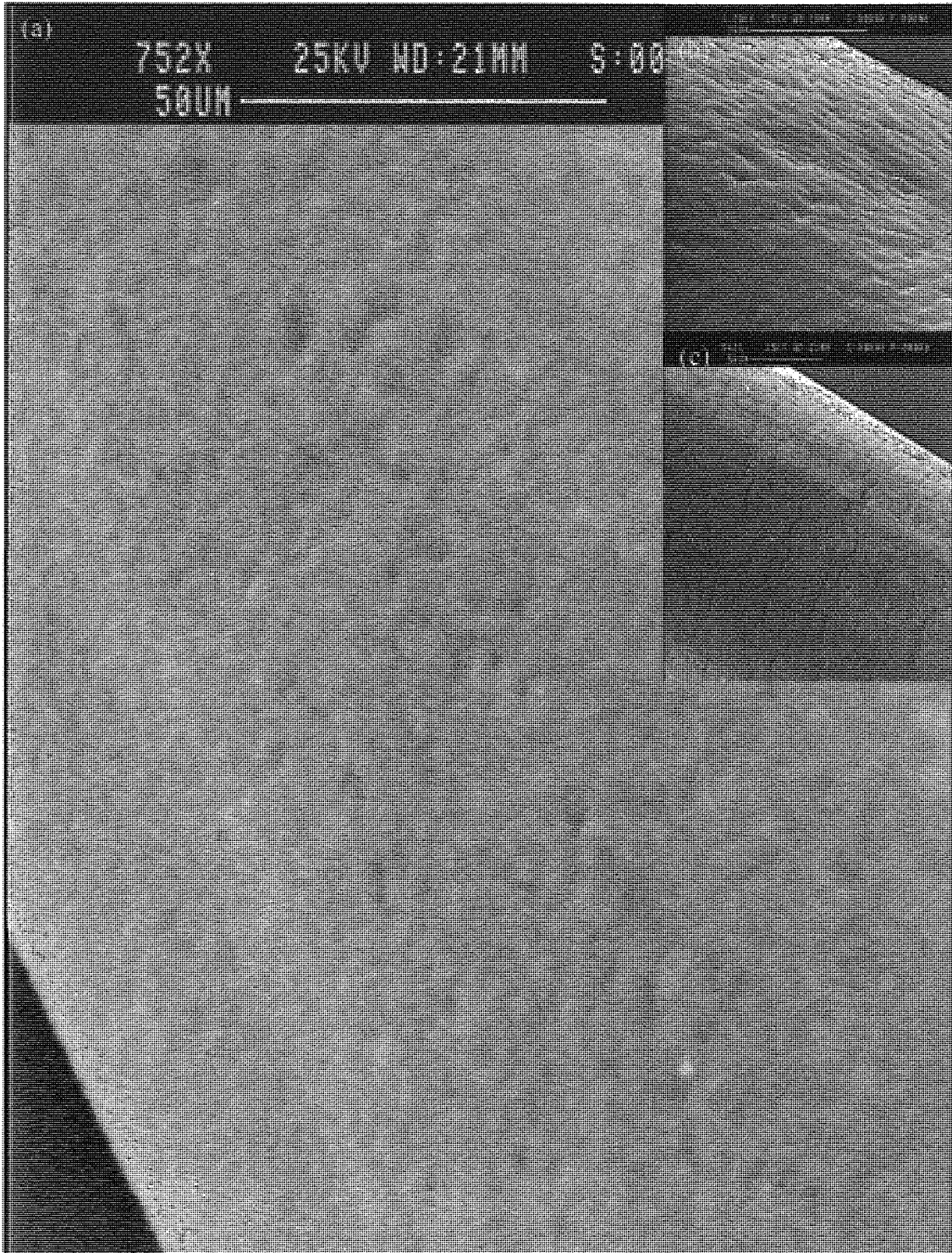


Figure 4.22 (a) SEM of Swiss 3T3 mouse fibroblasts on 500% cold drawn PCL fibre coated with gelatin. Fixed 3 days in cell culture after seeding with an initial cell density of 1×10^5 cells. (b) 500% cold drawn PCL fibre without attached cells

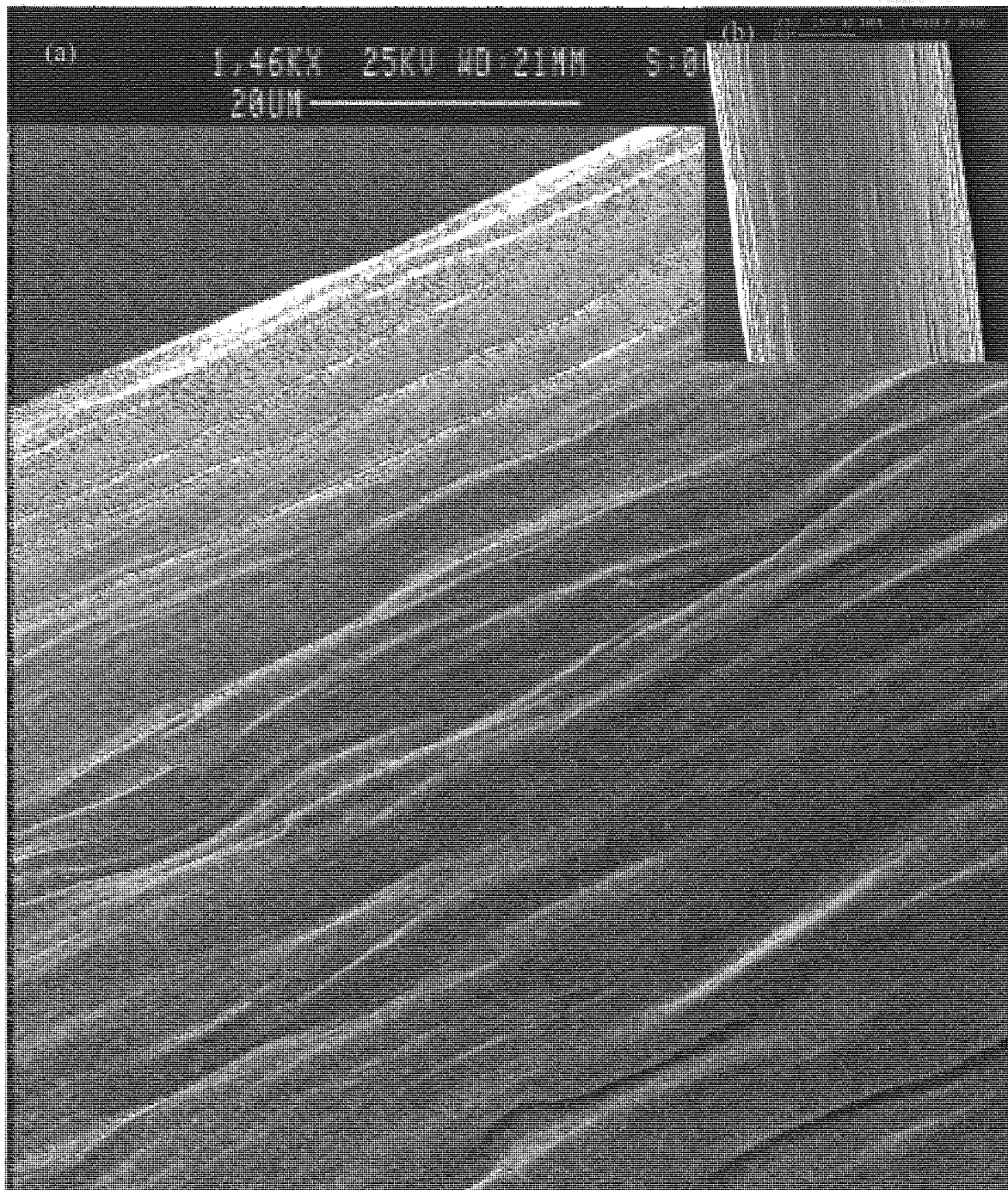


Figure 4.23 (a) SEM of C2C12 mouse myoblasts on an as-spun PCL fibre. Fixed 3 days in cell culture after seeding with an initial cell density of 1×10^5 cells. (b) As-spun PCL fibre without attached cells

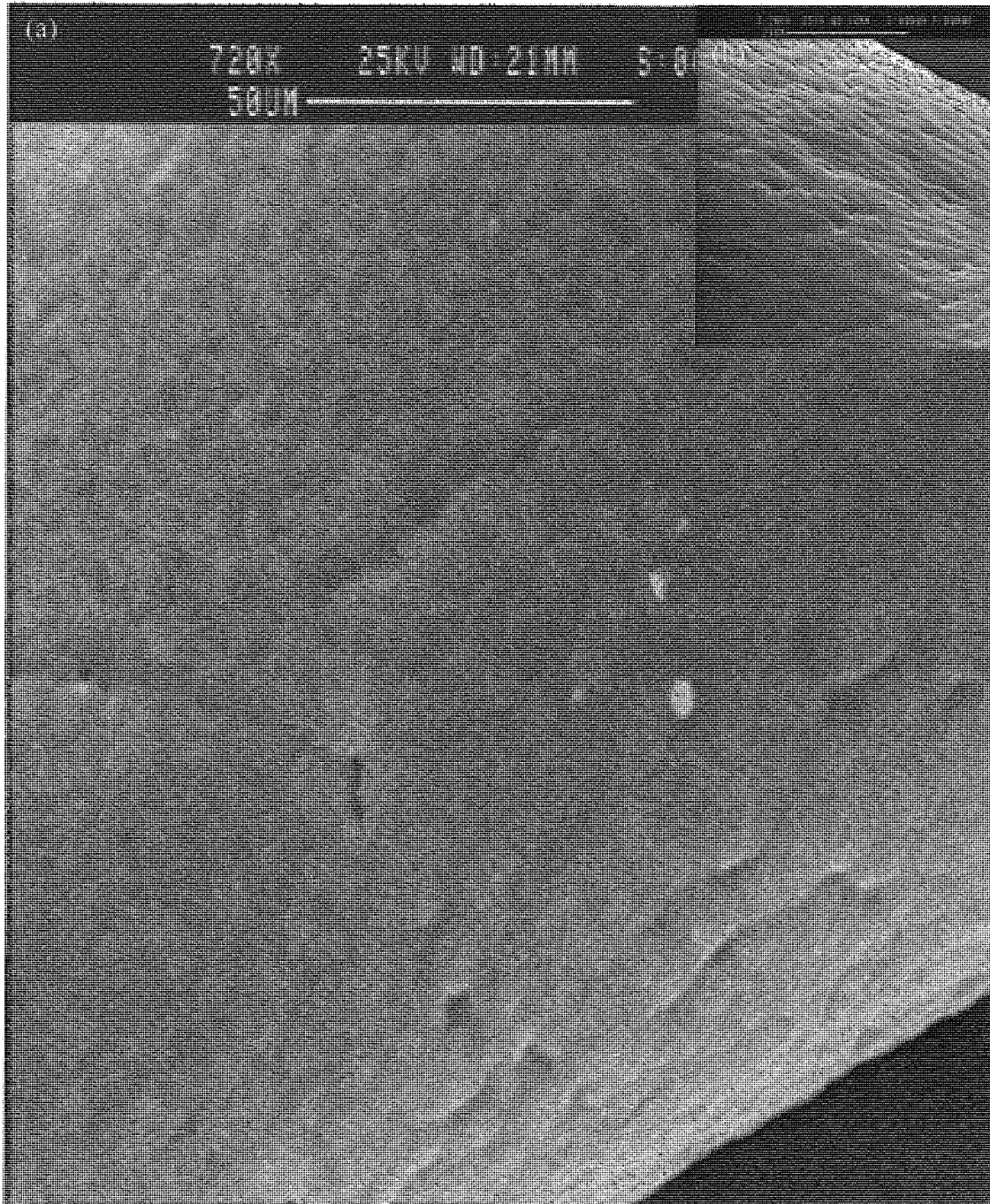


Figure 4.24 (a) SEM of C2C12 mouse myoblasts on an as-spun PCL fibre coated with gelatin. Fixed 3 days in cell culture after seeding with an initial cell density of 1×10^5 cells. (b) As-spun PCL fibre without attached cells (c) Gelatin coated PCL fibre without cells attached

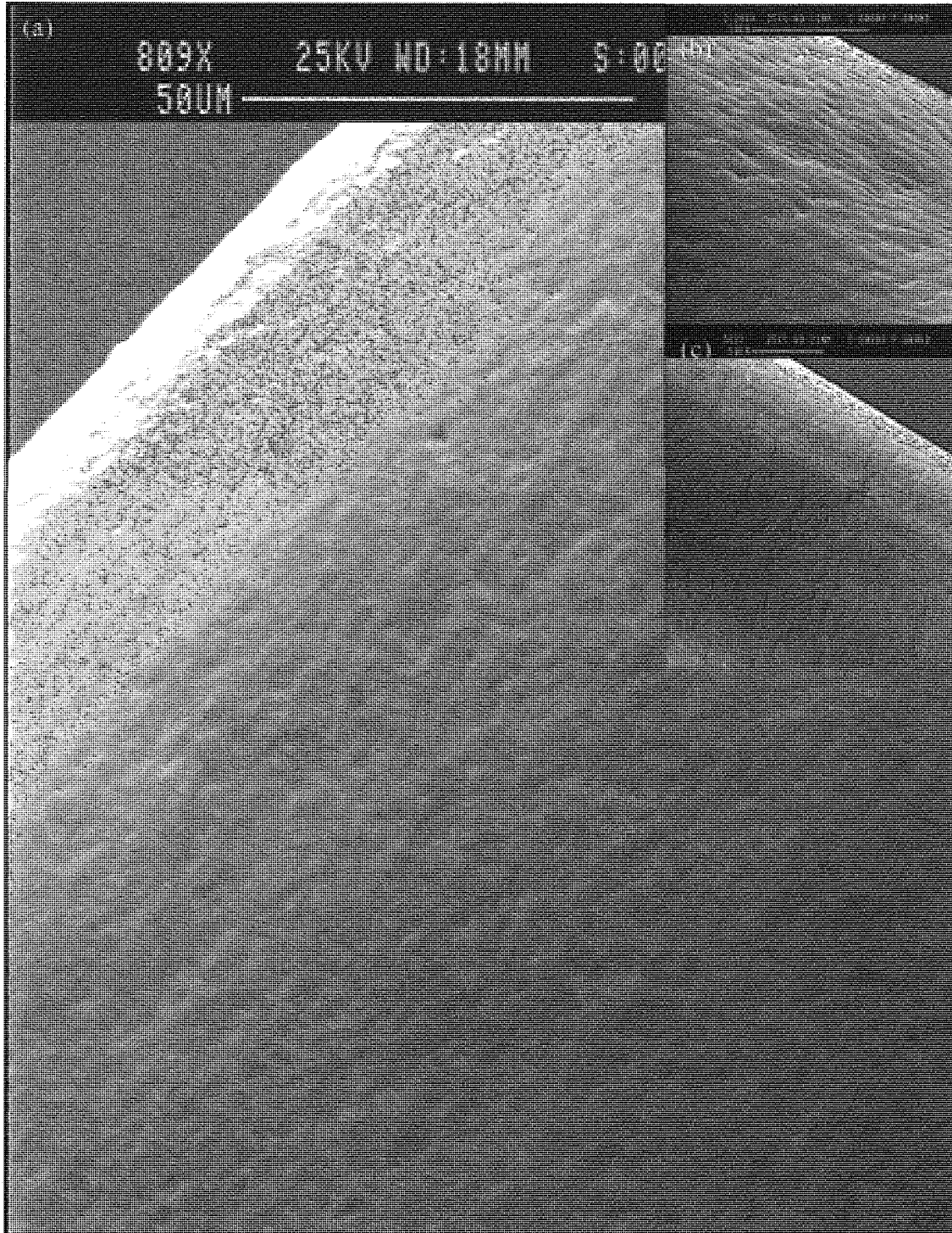


Figure 4.25 (a) SEM of C2C12 mouse myoblasts on 500% cold drawn PCL fibre. Fixed 3 days in cell culture after seeding with an initial cell density of 1×10^5 cells. (b) 500% cold drawn PCL fibre without attached cells

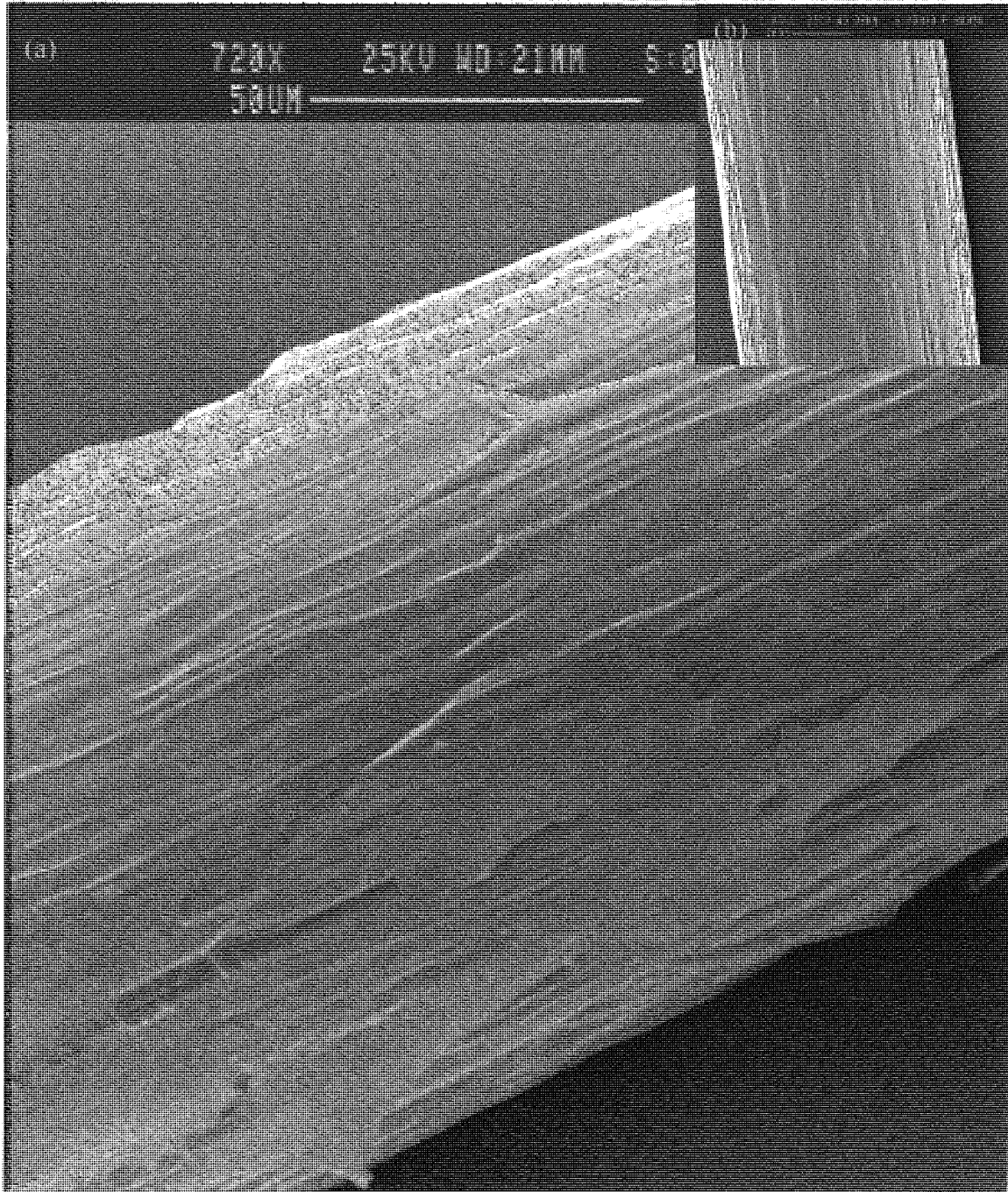
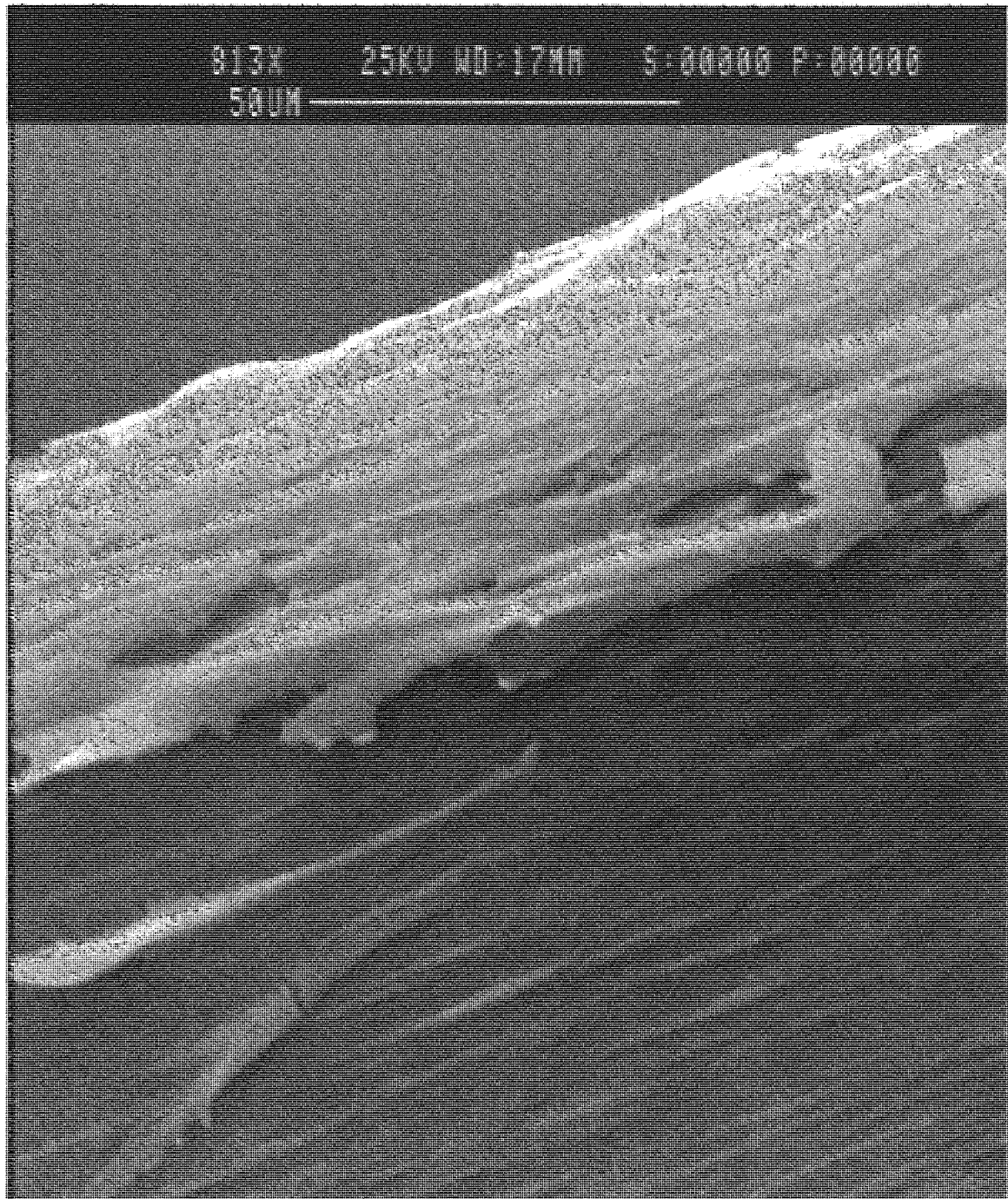


Figure 4.26 SEM of C2C12 mouse myoblasts on 500% cold drawn PCL fibre. Fixed 3 days in cell culture after seeding with an initial cell density of 1×10^5 cells.



4.8 Discussion

PCL fibres are able to promote cell attachment and sustain proliferation in much the same way as TCP. Cell proliferation on TCP was slightly elevated with both cell types but the proliferation curves trends are similar (Tables 4.1 and 4.2). Both types of cell investigated, C2C12 myoblasts and 3T3 fibroblasts, were able to grow on the fibres with doubling times of about 1 day, which is normal for both these cell lines. All of the PCL fibres could support cell attachment and proliferation at significantly higher rates compared with the Dacron monofilament. The ability of the PCL fibre to enhance the initial attachment of the cells was greater than standard tissue culture plastic surfaces but the proliferation rate did not exceed that on TCP. It is also shown that cell proliferation rate on PCL with osteoblasts does not exceed that of TCP (HaeYong Kweon et al. 2003). In this study a PCL scaffold was produced into three-dimensional gels by photopolymerisation and then Human MG-63 osteoblasts used to examine cell proliferation rates compared to TCP over 4 days. The good proliferation rates of cells on the PCL fibres is probably due to the material's favourable surface properties, which influence the initial cellular events at the cell-biomaterial interface.

Table 4.1 Summarised cell proliferation (from Figures 4.4, 4.6 and 4.8) of Swiss 3T3 mouse fibroblasts on various substrates over time.

Days	Substrates (Cells/mm ²)				
	TCP	As-spun PCL Fibre	Gelatin Coated PCL Fibre	500% Cold Drawn PCL Fibre	Dacron Monofilament
1	82	73	113	105	5
2	202	120	295	295	23
4	397	295	1021	632	53
7	847	832	960	780	53
9	1157	792	1072	759	77

Table 4.2 Summarised cell proliferation (from Figures 4.5, 4.7 and 4.9) of C2C12 mouse myoblasts on various substrates over time.

Days	Substrates (Cells/mm ²)				
	TCP	As-spun PCL Fibre	Gelatin Coated PCL Fibre	500% Cold Drawn PCL Fibre	Dacron Monofilament
1	80	73	113	231	47
2	146	140	295	442	94
4	1141	517	1021	716	154
7	1304	761	960	1138	118
9	1456	880	1072	1029	201

The nature and control of cell/biomaterial interactions (cell adhesion, spreading, proliferation and differentiation) have been studied intensively since they provide the key to biocompatibility, the clinical success of an implanted device and wound healing. Cell adhesion and cytoskeletal reorganisation leading to cell spreading usually occur within a few hours of cell culture and cells are normally expected to have started proliferating within 24 hours. This can be observed with the SEMs, in Figure 4.12 which shows cells fixed after 8 hours in cell culture it can be seen that some cells are still rounded and so no cytoskeleton reorganisation has occurred yet. Once focal contacts have been produced between the cell and material the cells would then flatten by stretching out the main cell body via several extended processes, this can be seen after 8 hours in Figure 4.13. Then after 24 hours the cells have attached, flattened and started proliferating as can be seen in Figure 4.14 to 4.15B that show greater areas of the fibres have been covered by the cells and cell layers have formed over the fibres. The exact timing of these events varies with changes in substrate characteristics and cell type (Kirkpatrick et al. 1992). Cell attachment to synthetic polymer implants surfaces in vitro is typically dependent on surface adsorbed cell adhesion glycoproteins such as fibronectin, vitronectin and laminin (Hubbell, 1995, Boyan et al. 1996, Fabrizio-Homan et al. 1991, Grinnell et al. 1982, Nikolovski et al. 2000, Steele et al. 1996 and Underwood et al. 1989).

Figure 4.27 Schematic diagrams of the structures of (A) Fibronectin, (B) Laminin (Addison Wesley Longman Inc.) and (C) Vitronectin. (www.haemtech.com)

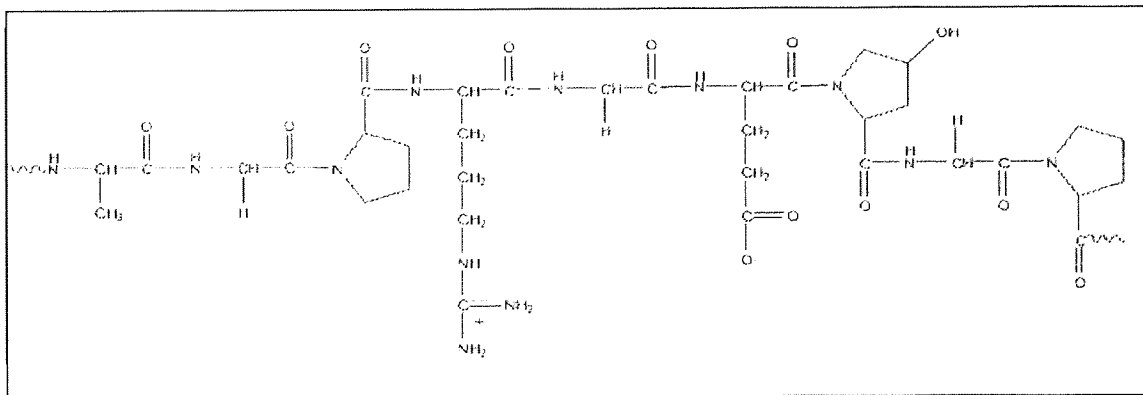


The structure of these proteins have been well document to show that they have several amino acid sequences that allow the various receptors (integrins) to bind to the proteins (Hubbell, 1995). The sequences shown to influence cell attachment are RGDS, LDEV and REDV for fibronectin, RGDV for vitronectin and YIGSR and PDSGR for laminin. There are many cells that are influenced by these proteins via their integrin receptors, most cells have integrins that recognise the sequences in fibronectin these include fibroblasts, endothelial cells, epithelial cells, muscle cells and immune response cells. Vitronectin is also shown to have several integrins that will bind and are on the same cells that are mentioned above and laminin also has many integrins that recognise its binding sites and these are on a diverse number of cells (The Integrin Page @ www.geocities.com). Previous studies have shown that cell adhesive activity onto biomaterial surfaces in the presence of serum-containing medium is accounted for by vitronectin (Yamada, 1983). Thus cell/biomaterial interactions are sensitive to several factors of the substrate surface. Cells are sensitive surface chemistry, with differences in the functional groups on the surface of the material affecting attachment and proliferation but this mechanism is unclear (Boyan et al. 1996). Charge is another factor that can affect the response of cells, a biomaterial is defined by its general charge density and the net polarity of the charge.

This then can affect whether the material is hydrophilic (positive or negative) or hydrophobic (neutral) (Boyan et al. 1996) as this will influence cell attachment as cells have negative charges on their surface and so will interact better with materials with a positive charge (Lee et al.). The charge of a material cannot only affect cells' attachment onto the surface but it can also affect what proteins are absorbed on to the surface from the biological fluid (Boyan et al. 1996). The slightly lower fibroblast and myoblast proliferation rate recorded on PCL fibres relative to TCP in the present study may be partly explained in terms of competitive and/or selective adsorption of adhesion molecules which produce a more favourable packing density and conformation-controlled presentation of cell adhesion sequences on TCP. The concentration of cell adhesion molecules has an affect of cell spreading and morphology, where proteins have absorbed onto cell culture surfaces and showed that a surface density of 1200 ligands/ μm^2 was needed to support cell spreading, receptor clustering and cytoskeletal organisation (Hubbell, 1995) but in another parallel study with the binding amino acid sequence of the protein only 60 ligands/ μm^2 was needed for the same biological response (Hubbell, 1995). Therefore TCP may change the proteins conformation postabsorption due to its surface chemistry, this could induce a higher exposure of the active binding sites of the proteins and thus allowing cell spreading and proliferation to occur at a slightly higher rate. In addition, the numbers of adhered cells, cell shape and attachment forces have been shown by many investigators (Hubbell, 1995, Grinnell et al. 1982) to be affected by the substrate microstructure (eg porosity) and surface topography. It has been well documented that most cells attach at a higher percentage to a rougher surface and this is probably the cause of the PCL fibres' favourable environment for cell attachment. This effect has been seen in several studies. Deligianni et al. (2001) showed that human bone marrow stromal cells attached at greater rates to rougher surfaces of titanium over 2 hours and also proliferated at higher rates as well over 16 days, the study also showed that fibronectin also attached to rougher surface at a 10 fold increase compared with the smooth surface. Scheven et al. (2002) showed that human osteosarcoma cell lines and primary human osteoblast-like cells also attached and spread more quickly over 2 hours on rougher surfaces.

Surface modification of PCL fibres obtained by coating with gelatin increases the attachment of cells. Myoblasts and fibroblasts attached and proliferated at an increased rate over 5 days on the gelatin-coated fibres (Figures 4.6 and 4.7). Gelatin is a denatured type of collagen (Figure 4.28), which does not show any antigenicity (Lee et al.) and results in similar cell proliferation properties to fibrin (Kumar et al. 2001). Kumar et al. studied coating TCP with 2% gelatin and fibrin. Then looking at the attachment on proliferation of human umbilical vein endothelial cells. Fibrin increased cell attachment over 2 hours compared to gelatin, but the proliferation rate of the cells over 3 days showed that the gelatin substrate achieved that same cell number. Gelatin improved cell attachment and proliferation because of the presence of acidic residues, such as lysine and arginine, that have a positive charge and the specific cell adhesion sites such as RGD groups (Lee et al.). Cells adhere more effectively to substrates with basic or neutral groups, due to the electrostatic interaction with the cells negative charges on their surface. In addition, the RGD group actively induces cellular adhesion by binding to integrin receptors, and this interaction has been shown to play an important role in cell proliferation, differentiation and overall regulation of cells (Quirk et al. 2001).

Figure 4.28 A diagram of the chemical structure gelatin



The cold drawn PCL fibres enhanced attachment and proliferation of fibroblasts and myoblasts relative to as-spun fibres. Cells use the morphology of the substrate for orientation and migration. Fibroblasts are known to align along specifically machined or replicated grooves inscribed on culture surfaces (Chehroudi et al. 1991). In the study by Chehroudi et al. fibroblasts and epithelial cells were examined using SEM

and light microscopy on silicon substrates with grooves of 3 μm deep and 4 μm in width, 10 μm deep and 18 μm in width and 22 μm in depth and 15 μm in width. The results showed that cells aligned with the grooves of 3 μm depth but not with the larger grooves. This is comparable with the results shown in Figures 4.18A, 4.19, 4.22 and 4.25 as the width of the grooves are from 0.5 – 3 μm and the cells appear to align with the fibres grooved surface.

CHAPTER 5

PRIMARY CELL INTERACTIONS WITH PCL FIBRES

5.1 Introduction

Once the characteristics of cell-biomaterial interaction have been established using immortalised cell lines subsequent investigation (eg biocompatibility) generally proceeds using a primary cell line. This chapter characterises the cell:biomaterial interaction, cell proliferation and the response of cells to normal stimulus. The primary cell line selected was human umbilical vein endothelial cells (HUVEC). These cells are of interest as the PCL fibres with their low compliance could have application in vascular graft construction. Atherosclerotic vascular disease, in the form of coronary artery and peripheral vascular disease, is the largest cause of mortality in the USA (Niklason et al. 1999). Surgical procedures for treatment of affected vessels less than 6 mm in diameter include bypass grafting with autologous veins or arteries; but, adequate tissue for bypass conduits is lacking in many patients. Artificial materials used for bypass vascular grafts with small diameters are highly thrombogenic and therefore limited in clinical application (Chan et al. 1999, Kumar et al. 2001). Endothelial cells are frequently seeded onto the lumen of vascular grafts in attempts to improve their patency (Seifalian et al. 2002, Tiwari et al. 2001, Tiwari et al. 2003, Williams, 1994, Bhat et al. 1998) and nonthrombogenic behaviour (Chan et al. 1999). Novel approaches for producing small-calibre arterial grafts have developed problems with mechanical properties (Niklason et al. 1999). Another problem is that cells seeded onto vascular grafts must be able to resist the forces exerted by the blood flow (Chan et al. 1999) and so need strong and rapid adhesion. Biomaterials coated with adhesive molecules and extracellular matrix proteins however face a problem in that they are also good substrates for platelet adhesion and thrombus formation (Schneider et al. 1997, Vohra et al. 1990 and 1991). The problems of cell-graft adhesion need to be overcome and attached cells are required to demonstrate normal cell function if tissue engineered vascular grafts are to lead to improvements over existing designs.

5.2 Initial HUVECs Proliferation Experiment

In this study an alternative system of cell counting was examined using 3 strands of fibre held in a 24 well plate by a silicone O-ring. The cells were allowed to proliferate and were counted at various time points by staining with BCECF/AM, which is a fluorescent dye taken up by the cells and then this can be measured using a spectrofluorimeter. The results from this experiment proved to be unreliable. The calibration curve had an R-value far from 1 and the equation of the line did not permit estimation of small numbers of attached cells. Also a comparison of the cell number from day 0 to day 6 indicated that the cells had not proliferated. A cell number of 4×10^4 was counted using the BCECF/AM assay, the cell number at the same time point was then counted using a haemocytometer and the actual cell number was 12×10^4 . The observations led to an optimised method for the cell proliferation experiments that were also applied the immortalised cell proliferation experiments in Chapter 4.

5.3 HUVECs Proliferation Experiments

The proliferation rate of HUVECs on 10% as-spun PCL fibres over 10 days is shown in Figure 5.1. The number of attached HUVECs was similar on TCP and PCL fibres at day 1 but then the proliferation rate on the PCL fibres exceeded that on TCP until day 6 by a factor of 1.2. After day 6 cells proliferating on TCP rate increased and HUVECs on the PCL fibre appeared to reach confluent by day 8. The proliferation curves shown in Figure 5.1 are similar in trend, exhibiting a slowing down in proliferation at day 8 which may be a sign of confluence. The two proliferation curves are not significantly different over all time intervals.

The rate of proliferation of HUVECs observed on 10% as-spun PCL fibres, 5% gelatin coated 10% PCL fibres, Dacron monofilament and TCP substrates are shown in Figure 5.2. The results show that cells attached and proliferated in significantly ($P < 0.05$) greater numbers on all the substrates at all time intervals compared with Dacron. Initially the cells attached and proliferated at a slightly higher rate on the gelatin coated PCL fibre over the first 5 days. At day 1 there was a 1.7 fold increase

and by day 5 this was a 1.2 fold increase relative to TCP. After day 5 the proliferation rate on the gelatin coated PCL fibres slowed due the cells achieving confluence, whereas the number of cells proliferating on TCP continued to increase up to day 9. The trends of the proliferation curves over the time period do appear to be similar between the PCL fibre and TCP. The results demonstrate that HUVECs do proliferate at a high rate on gelatin coated PCL fibre compared to the other substrates.

Proliferation experiment of HUVECs on as-spun 10% PCL fibres, 500% cold drawn PCL fibres, Dacron monofilament and TCP are shown in Figure 5.3. The data shows that the cells attach at an increased rate (4 fold increase at day 1) on the cold drawn PCL fibres over TCP and as-spun PCL fibres. All the substrates investigated appear to be able to sustain significantly higher attachment and proliferation of HUVECs compared with the Dacron monofilament. The HUVEC proliferation curves obtained using the cold drawn and as-spun PCL fibres are quite different. The cold drawn PCL fibres show higher cell attachment and thus the cells seem to achieve confluence by day 4 whereas cell numbers continue to increase up to day 9 for the as-spun fibres. The proliferation curves for TCP and the as-spun PCL fibre do not appear to reach confluence within the time period of this experiment. In previous experiments the cells appeared to be reaching confluence on the as-spun PCL fibres at day 8 in Figure 5.1. The results from this experiment show that as-spun PCL fibres are only slightly inferior to TCP as a substrate for proliferation of HUVECs but cell proliferation is enhanced on 500% cold drawn PCL fibres compared with TCP.

Figure 5.1 HUVECs attachment and proliferation rate on 10% as-spun PCL fibres and tissue culture plastic substrates over 9 days. PCL fibres were wrapped around a 22 mm x 22 mm glass coverslip (124 mm²). Seeding density 5 x 10⁴ cells. The values are mean ± SD for 6 replicates of each substrate type.

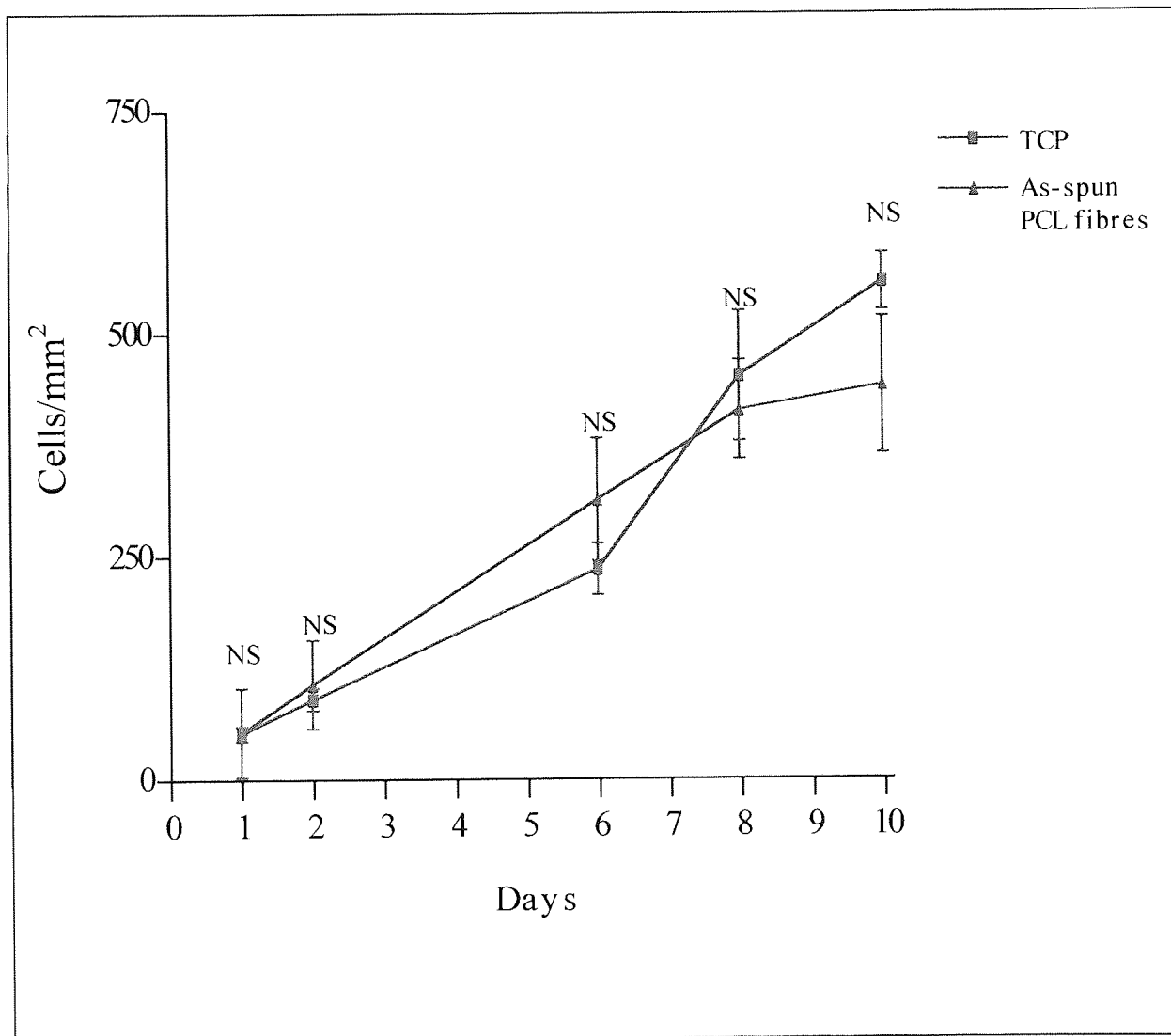


Figure 5.2 HUVECs attachment and proliferation rate on 10% as-spun PCL fibres, 10% PCL fibres coated with a 5% gelatin solution, Dacron monofilament and tissue culture plastic substrates over 9 days. Fibres were wrapped around a 22 mm x 22 mm glass cover slip. Seeding density 5×10^4 cells. The values are mean \pm SD for 6 replicates of each substrate type. (* TCP compared to as-spun PCL fibres, + TCP compared to gelatin coated fibres, # as-spun PCL fibres compared to gelatin coated fibres)

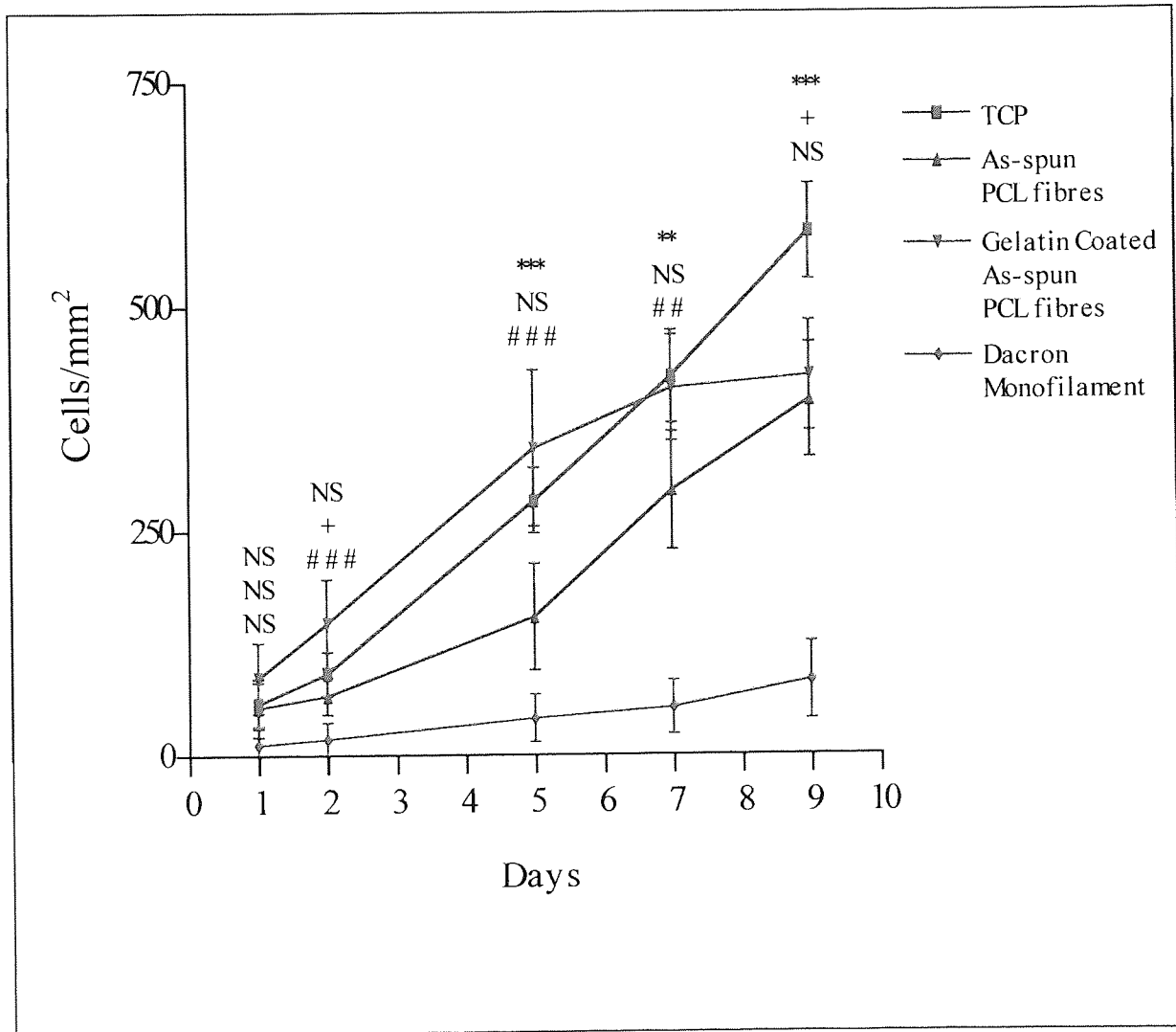
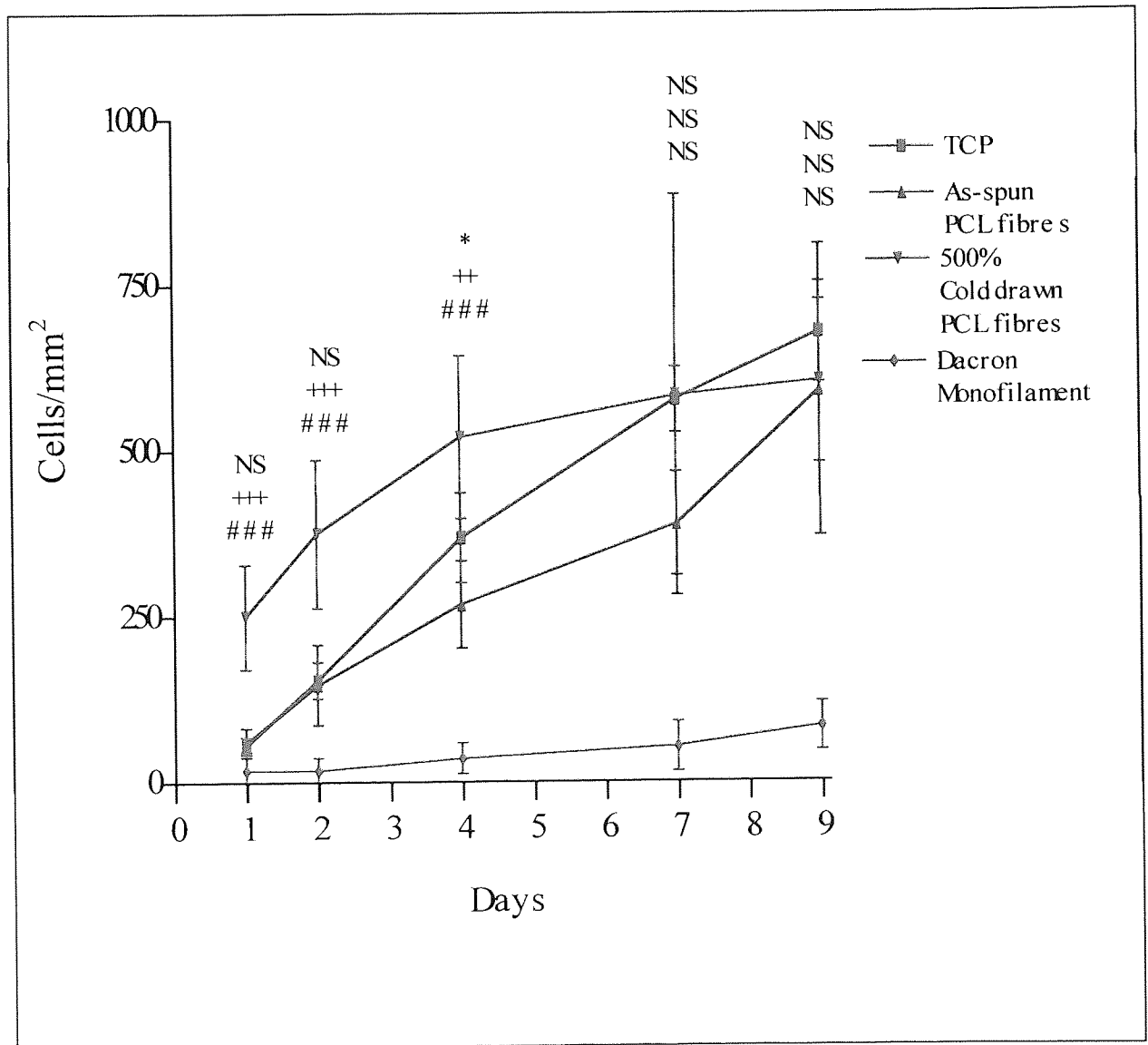


Figure 5.3 HUVECs attachment and proliferation rate on 10% as-spun PCL fibres, 500% cold drawn (10%) PCL fibres, Dacron monofilament and tissue culture plastic substrates over 9 days. Fibres were wrapped around a 22 mm x 22 mm glass cover slip. Seeding density 5×10^4 cells. The values are mean \pm SD for 6 replicates of each substrate type. (* TCP compared to as-spun PCL fibres, + TCP compared to gelatin coated fibres, # as-spun PCL fibres compared to 500% cold drawn fibres)



5.4 Cell-Fibre Morphology

The morphology of HUVECs on as-spun PCL fibres, 500% cold drawn PCL fibres and gelatin coated PCL fibres were investigated using scanning electron microscopy after 8 hours, 1 day and 3 days in cell culture.

Figure 5.4 shows a HUVEC on an as-spun PCL fibre 8 hours after seeding. The cell has not yet spread which indicates an initial state of cell attachment to a substrate before formation of effective focal contacts, which enable the transfer of forces to the cytoskeleton to cause the cell to flatten.

A group of three cells attached to a gelatin-coated PCL fibre can be seen in Figure 5.5. The cells are still quite rounded but less so than in Figure 5.4. The cells have extended processes out towards each other and appear to be spreading and flattening. This behaviour is a vital part of cell proliferation since cells need to establish contact with neighbouring cells to stimulate proliferation, differentiation or migration.

A HUVEC that has attached to a 500% cold drawn PCL fibre is shown in Figure 5.6. The cell has started to spread and flatten on to the fibre, but there is still a rounded slightly. The cell would have put out processes to attach to the fibre and form focal contacts. Extension of other processes in different directions would allow cytoskeleton rearrangement and cause an area to flatten.

The cell morphology of HUVECs 1 day after seeding on an as-spun PCL fibre is shown in Figure 5.7. The cell has clearly flattened against the fibre compared to the cell shown in Figure 5.4, which was seeded for 8 hours. The HUVEC also appears to have replicated the surface morphology of the fibre by following the contours of the fibre surface. This effect may be achieved by the focal contacts allowing the main body of the cell to be pressed strongly against the underlying substrate.

Figure 5.4 SEM of HUVECs on an as-spun 10% PCL fibre. Fixed 8 hours after seeding with an initial cell density of 1×10^5 cells.

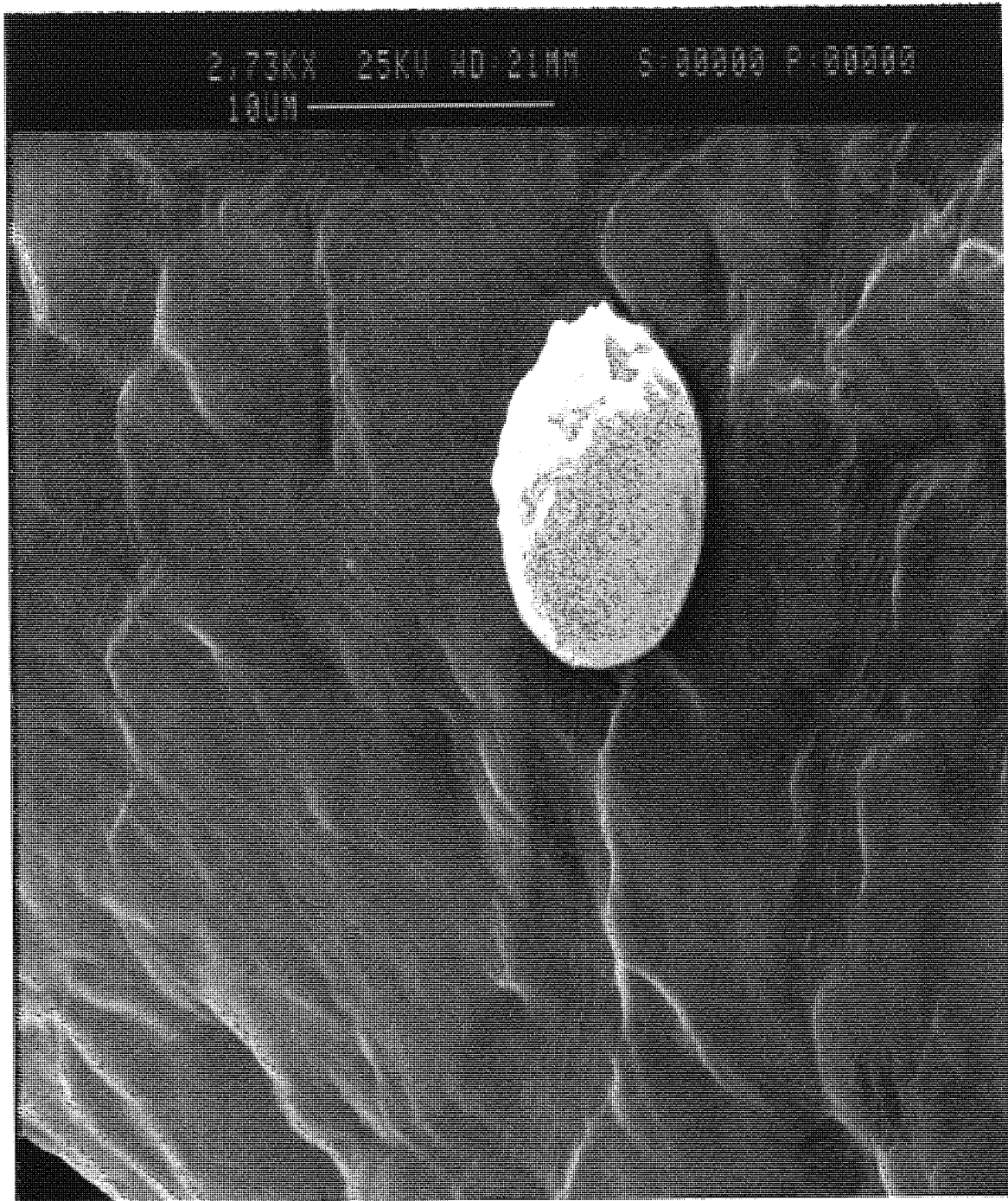


Figure 5.5 SEM of HUVECs on an as-spun PCL fibre coated with a 5% gelatin solution. Fixed 8 hours after seeding with an initial cell density of 1×10^5 cells.

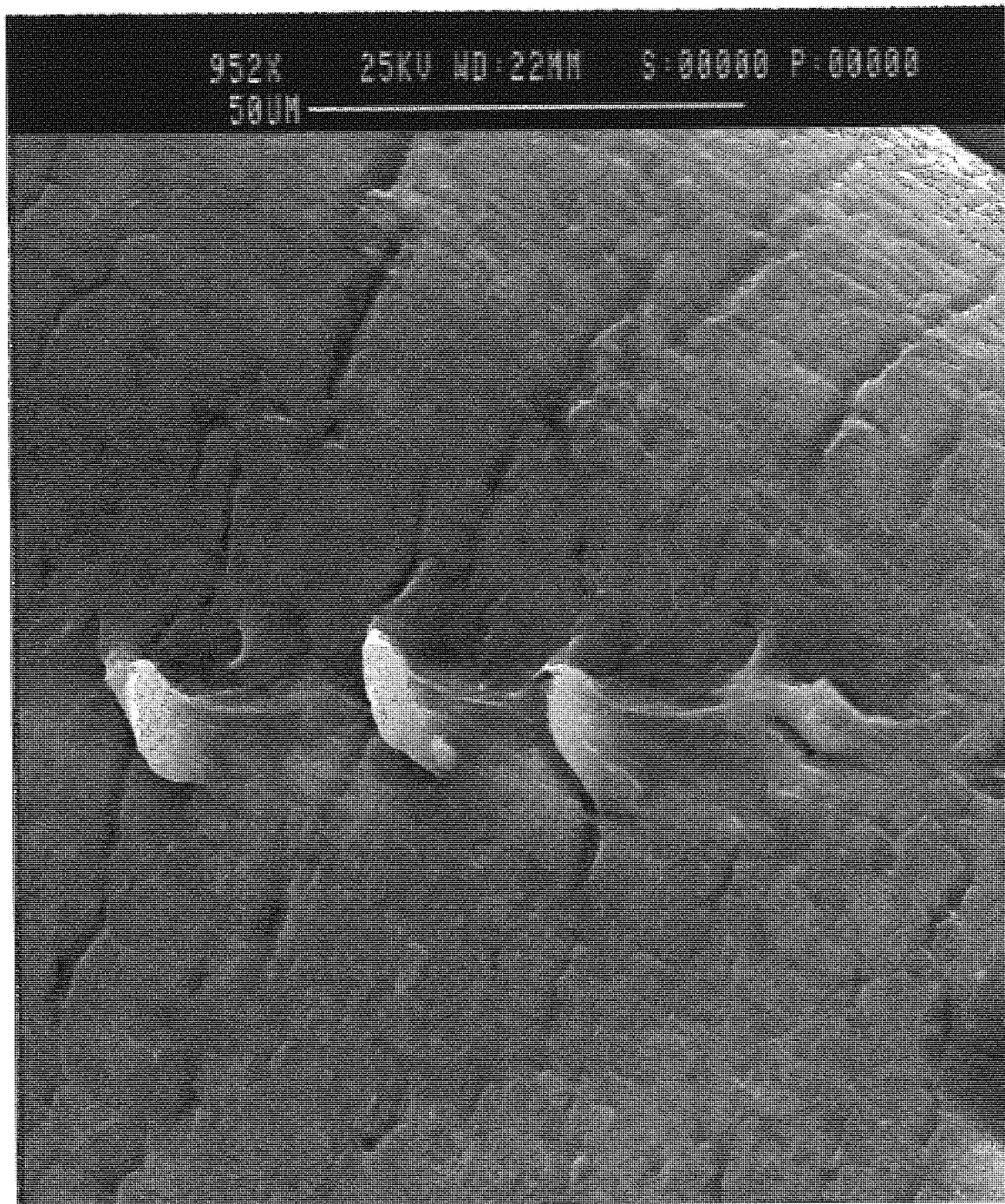


Figure 5.6 SEM of HUVECs on 500% cold drawn PCL fibre. Fixed 8 hours after seeding with an initial cell density of 1×10^5 cells.

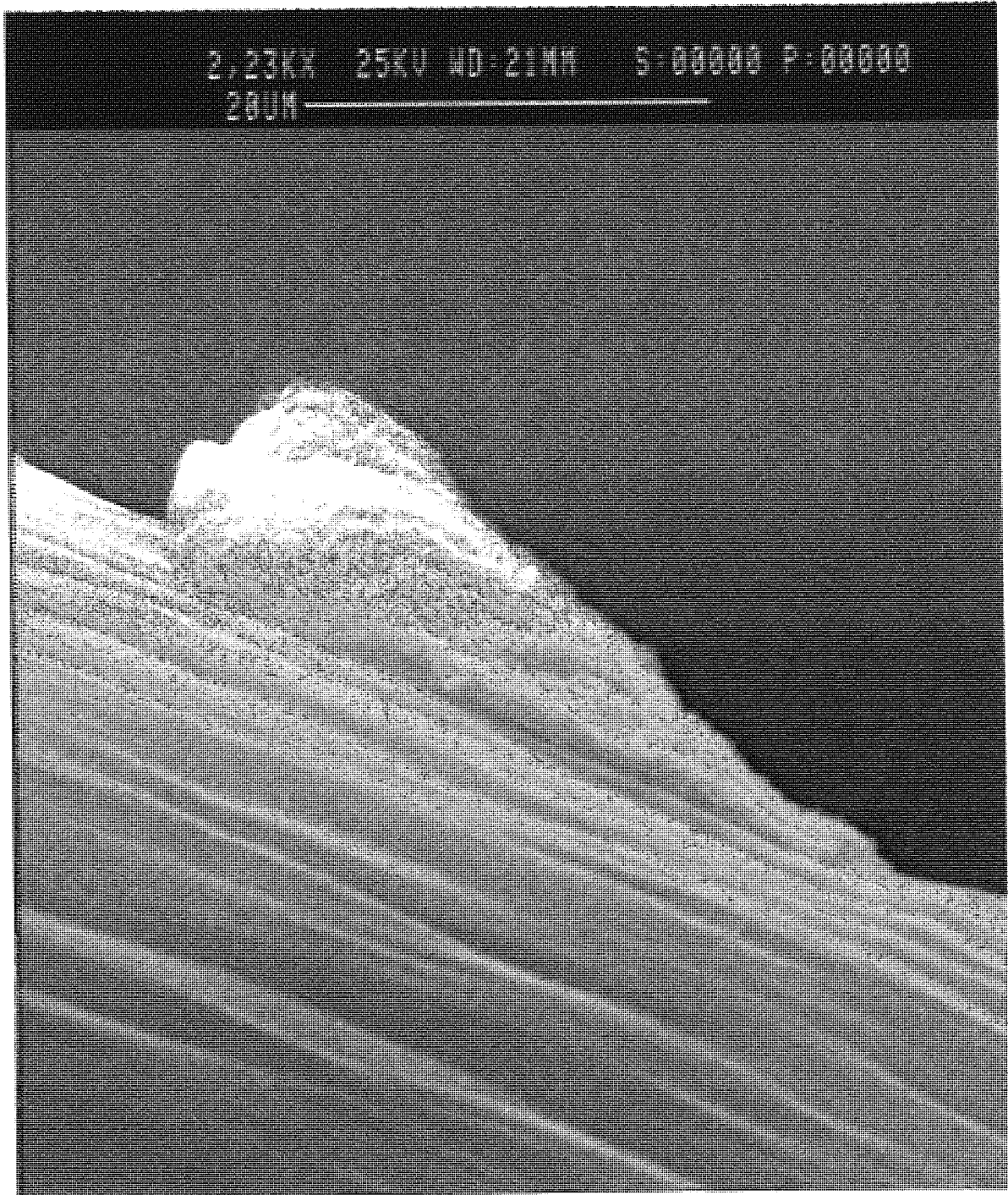


Figure 5.8A shows cells that have attached and proliferated on a gelatin-coated fibre for 1 day. Figure 5.8A shows that the cells have covered a significant area of the fibre, if not the whole area that was exposed to them (aside: when attaching the fibre to an SEM stub there is no way of assuring that the fibre is attached with the same orientation in cell culture). Two distinct areas having slightly different morphologies can be more clearly observed in Figure 5.8B. The right-hand side of the fibre shows the typical fibre morphology while the left-hand side clearly shows a raised level of the fibre that is not found on an as-spun fibres or a gelatin coated fibres (compare Figures. 3.5 and 6.3) and is probably the edge of a cell layer covering the fibre.

The morphology of a HUVEC on a cold drawn PCL fibre is shown in Figure 5.9 1 day after seeding. The cell has spread to a large degree over the area of fibre that it has attached to. This SEM provides a very good example of cells adapting or conforming closely to the surface contours of the substrate to which that they attach. The distinct fibrillar oriented surface morphology of the fibre can clearly be seen around the cell. The cell has flattened and moulded to the fibres' surface so effectively that the ridges though the cells surface match the ridges on the fibres' surface.

The morphology of HUVECs 3 days after seeding on as-spun PCL fibres, gelatin coated fibres and 500% cold drawn PCL fibres are shown in Figures 5.10, 5.11 and 5.12 respectively. The cells on the as-spun fibre appear to have formed a confluent monolayer over the fibre. The morphology of the fibre seems to have become slightly smoother in appearance compared to the SEM of a fibre without any cells (Figure 3.5). The fibre was scanned extensively but showed no obvious signs of cell cracking on lift from the fibre, indicating that the cells have formed strong contacts with the fibre surface.

Figure 5.7 SEM of HUVECs on an as-spun 10% PCL fibre. Fixed 1 day after seeding with an initial cell density of 1×10^5 cells.

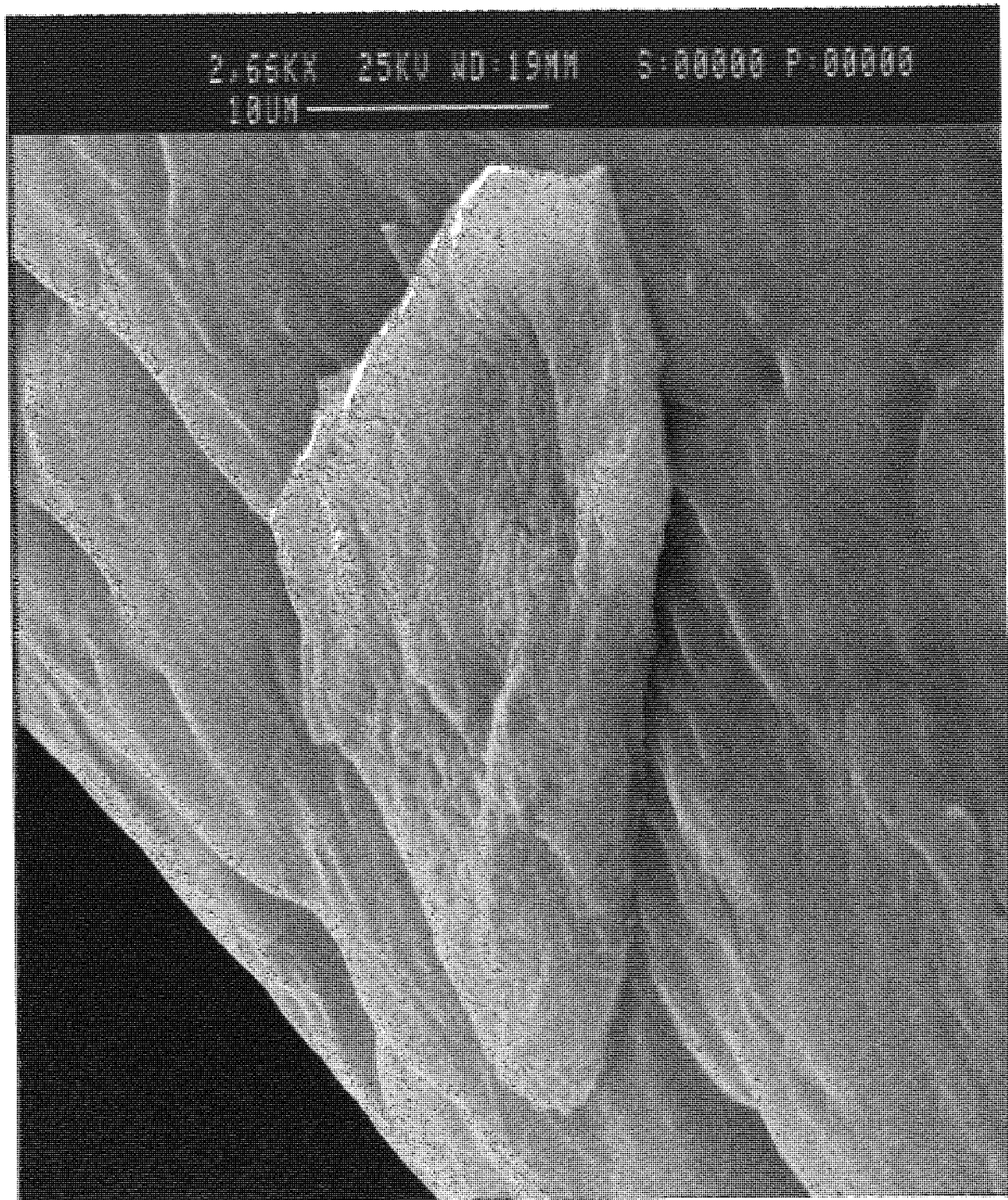


Figure 5.8A (a) SEM of HUVECs on an as-spun PCL fibre coated with gelatin. Fixed 1 day in cell culture after seeding with an initial cell density of 1×10^5 cells. (b) As-spun PCL fibre without attached cells (c) Gelatin coated PCL fibre without cells attached

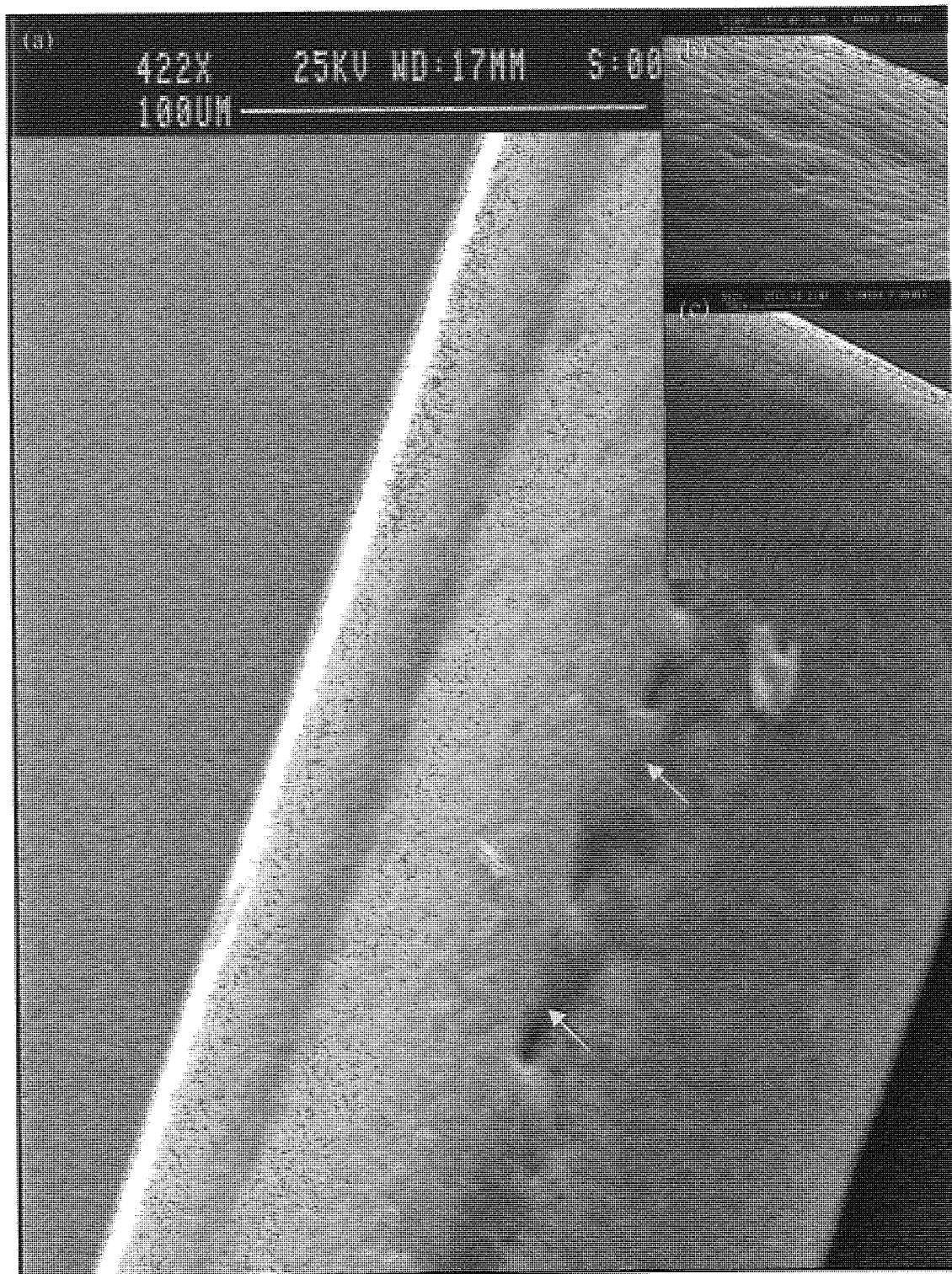


Figure 5.8B (a) SEM of HUVECs on an as-spun PCL fibre coated with gelatin. Fixed 1 day in cell culture after seeding with an initial cell density of 1×10^5 cells. (b) As-spun PCL fibre without attached cells (c) Gelatin coated PCL fibre without cells attached

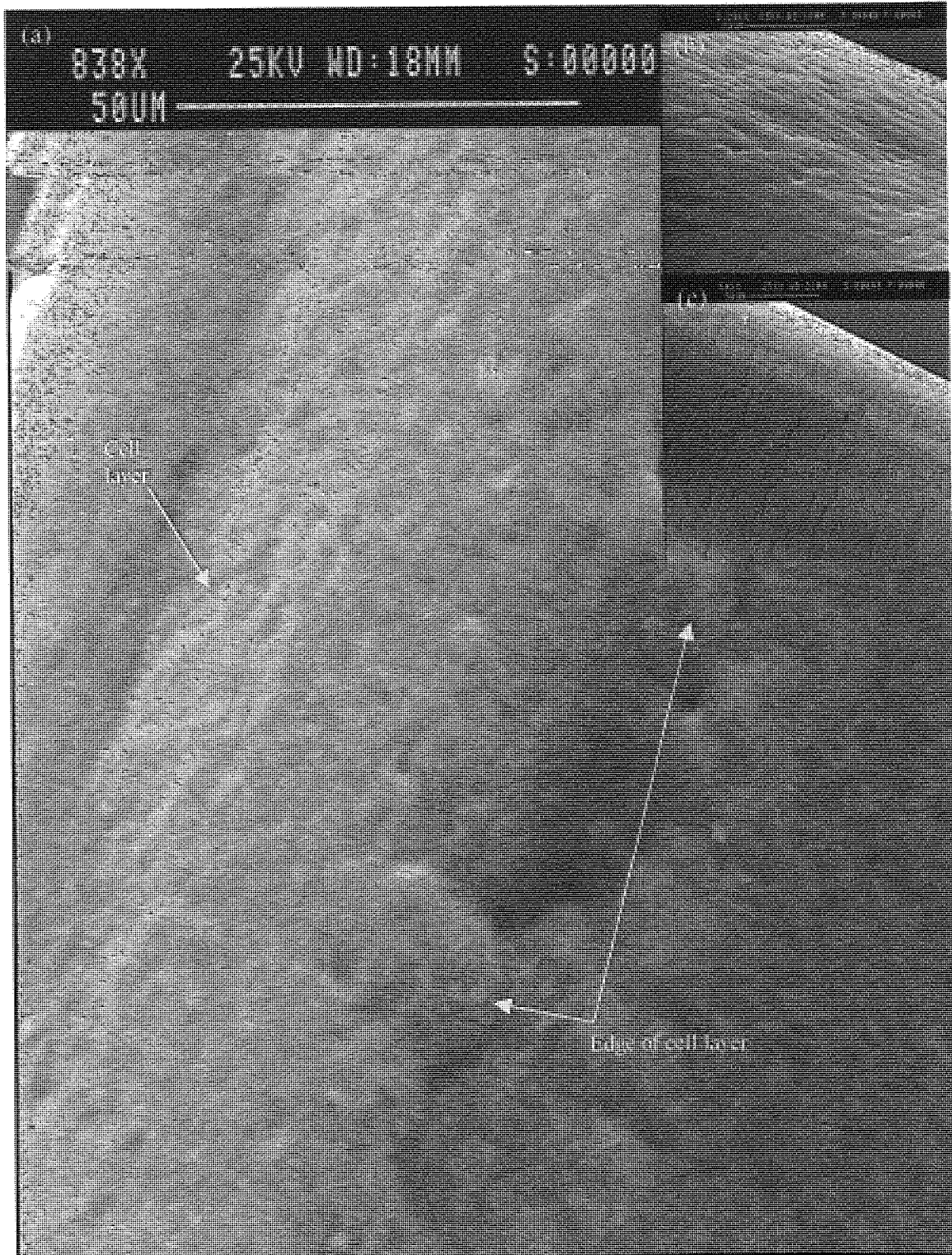


Figure 5.9 SEM of HUVECs on an as-spun 10% PCL fibre. Fixed 1 day after seeding with an initial cell density of 1×10^5 cells.

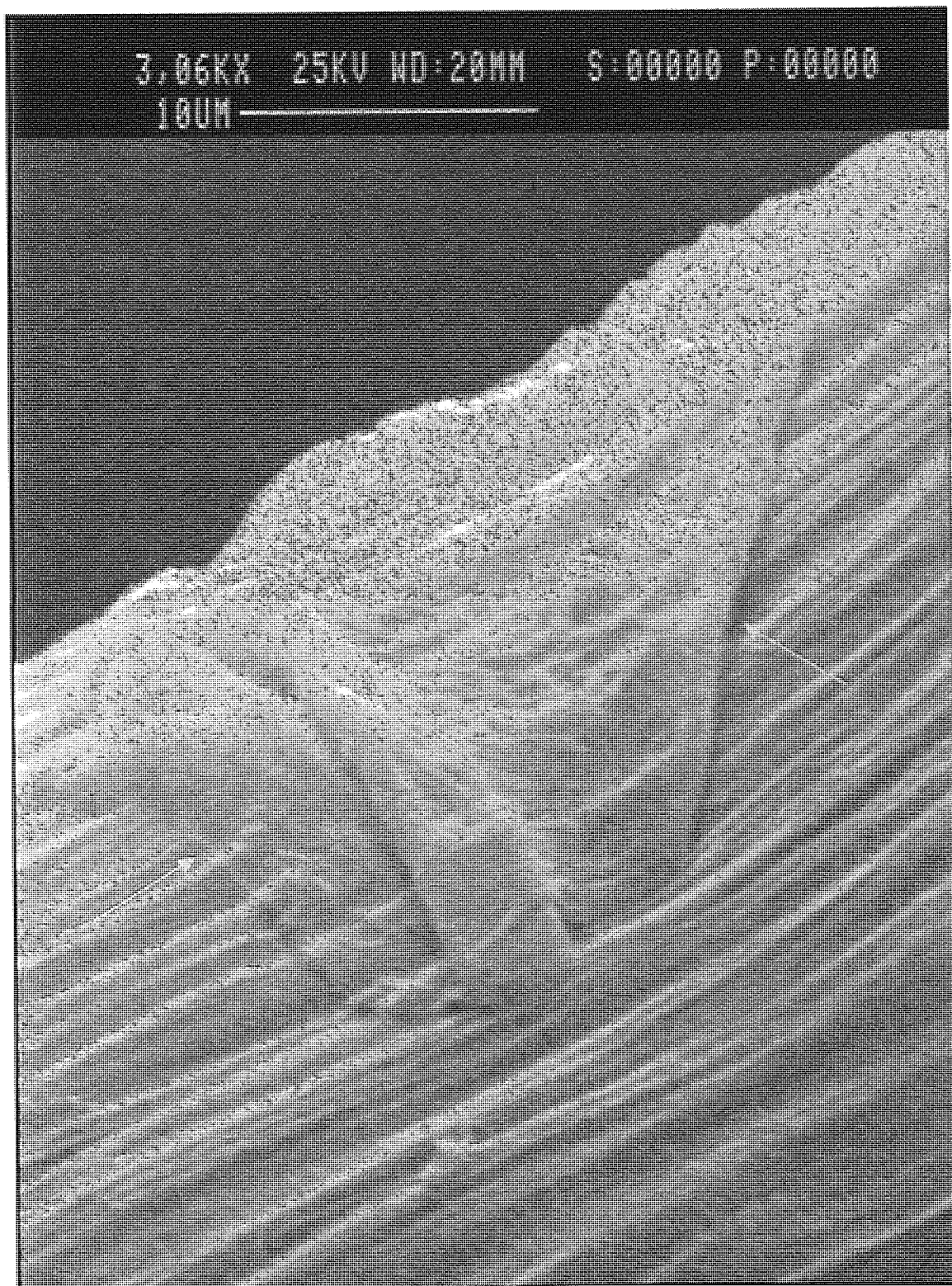


Figure 5.11 shows that HUVECs have formed a confluent monolayer over the whole surface of a gelatin coated PCL (compare the cell-free fibre morphology in Figure 5.9 and the cell-gelatin coated fibre in Figure 6.3). As observed with the cells grown on the as-spun PCL fibre after 3 days, there were no signs of cracking of the cell layer, indicating strong adhesion with the fibre surface.

HUVEC forming a confluent monolayer attached to a cold drawn PCL fibre is shown in Figure 5.12. The surface morphology typical of the cold drawn fibre has been altered completely if compared to the drawn fibre without cells attached (compare Figure 3.12). The cells forming the monolayer still have masked the oriented fibre surface to an extent as the ridged fibre structure can still be discerned.

Figure 5.10 (a) SEM of HUVECs on an as-spun PCL fibre. Fixed 3 days in cell culture after seeding with an initial cell density of 1×10^5 cells. (b) As-spun PCL fibre without attached cells

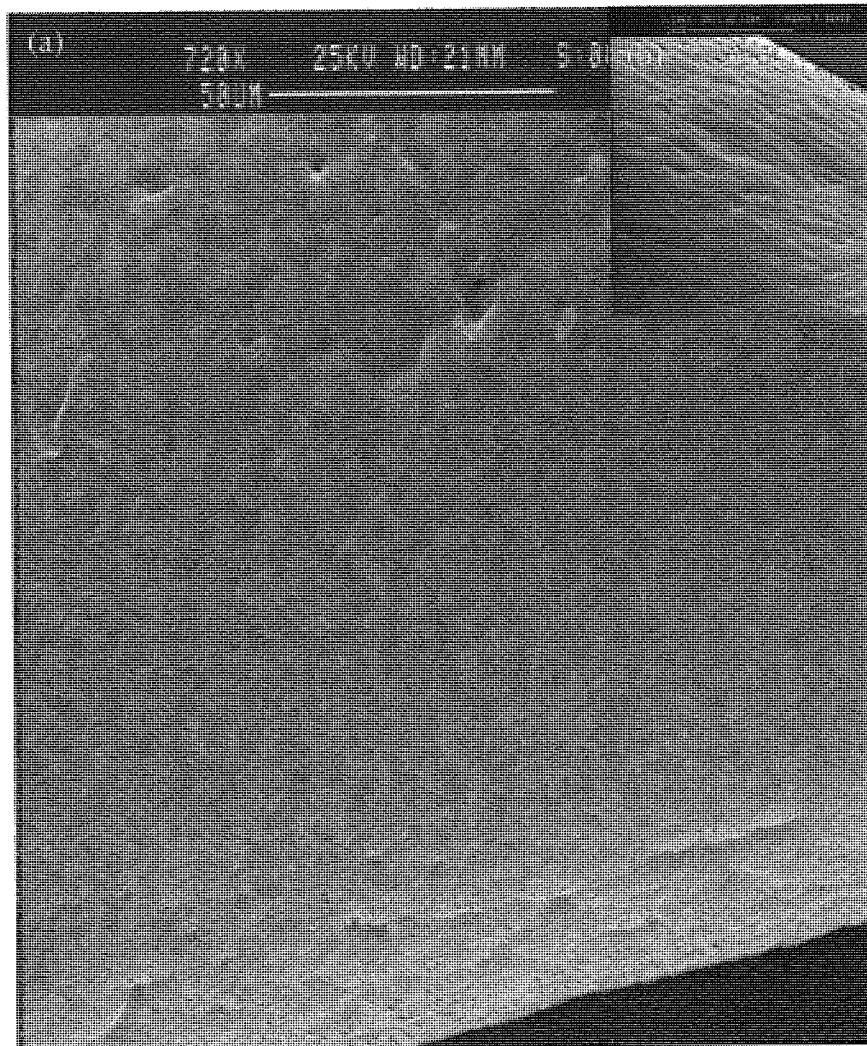


Figure 5.11 (a) SEM of HUVECs on an as-spun PCL fibre coated with gelatin. Fixed 3 days in cell culture after seeding with an initial cell density of 1×10^5 cells. (b) As-spun PCL fibre without attached cells (c) Gelatin coated PCL fibre without cells attached

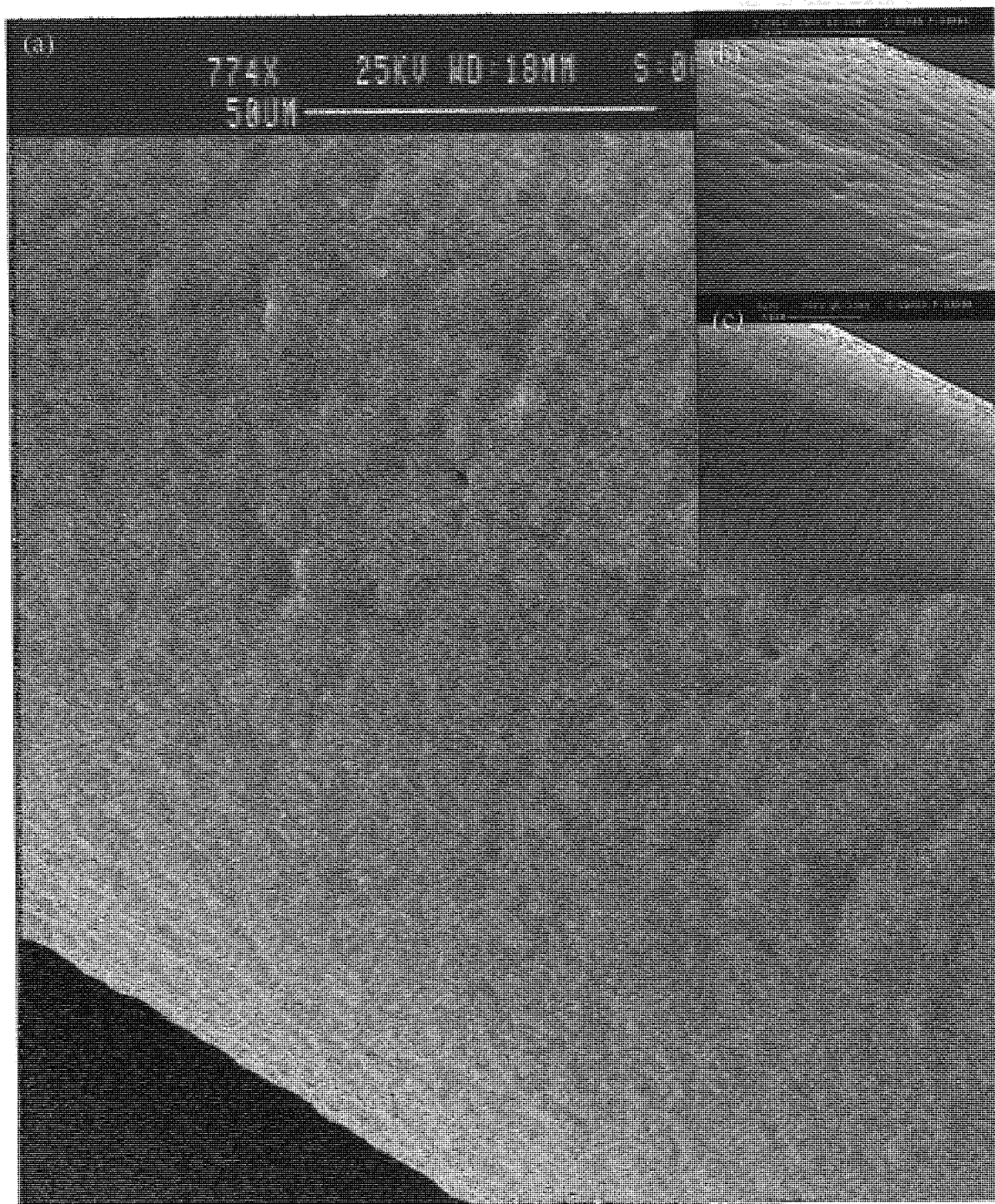
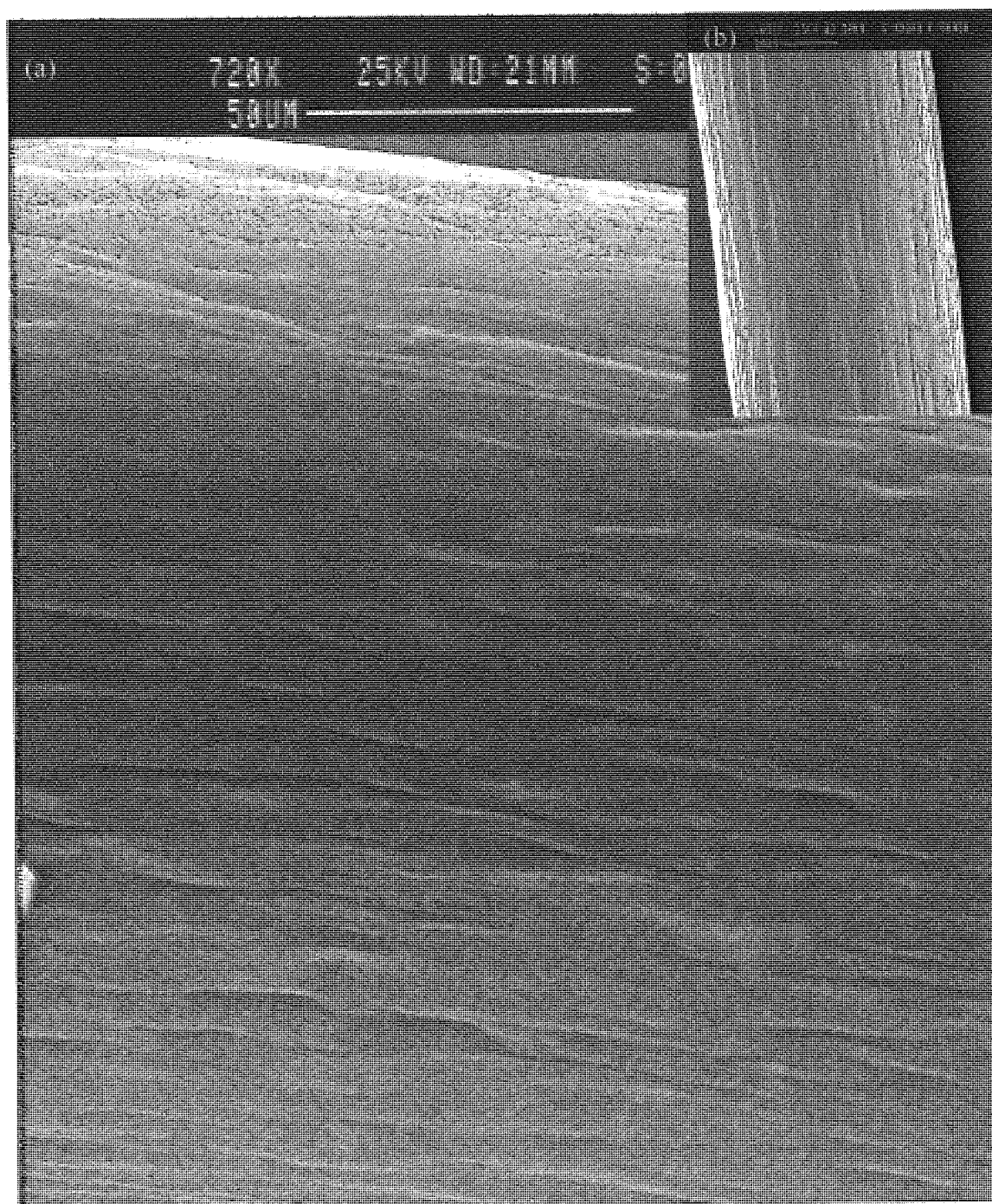


Figure 5.12 (a) SEM of HUVECs on a 500% cold drawn PCL fibre. Fixed 3 days in cell culture after seeding with an initial cell density of 1×10^5 cells. (b) 500% cold drawn PCL fibre without attached cells



5.5 Retention of HUVECs Function

Figure 5.13 HUVECs expressing ICAM-1
before and after LPS for 24 hours (red)

Experiments were carried out to determine whether HUVECs as confluent monolayer could maintain function on the PCL fibres as they would on TCP, which is a recognised as a control good surface for achieving normal cell function *in vitro*. Once the cells were at confluence lipopolysaccharide (LPS) was added to the culture incubated for 24 hours. Then the number of cell surface receptors (ICAM-1) and were compared to cells that were not stimulated with LPS to observe if the response was the same size for HUVECs cultured on PCL fibres compared with TCP (described in section 2.2.23.4). The levels of ICAM-1 mRNA were also examined to back up the surface expression of ICAM-1. HUVECs were stimulated with LPS and then the levels of ICAM-1 mRNA was measured using RT-PCR, as described in sections 2.2.23.1 to 2.2.23.3.

The results for this experiment (Figure 5.13) shows the change in percentage positive cells (cells that express ICAM-1) once LPS had been added to the cells. HUVECs number of ICAM-1 receptors were counted using flow cytometry and then counted again after stimulation with LPS. The result of percentage positive cells without stimulation of LPS was very similar for TCP and the PCL fibre being 0.7 and 0.9 respectively, showing that the cells cultured on both materials are both expressing low levels of ICAM-1. This shows that the HUVECs were not activated into an immune response when seeded and proliferating on the PCL fibre compared to TCP. When the cells produce an immune response to LPS and therefore should express higher levels of ICAM-1 receptors on their surface membranes. The change in percentage positive cells is very similar for both substrates as shown in Figure 5.13 both have increased by approximately by 11% and this indicates that the cells retain their function on PCL fibres compared to TCP. Figure 5.14 shows the histograms of ICAM-1 expression on HUVECs with and without stimulation with LPS on TCP and PCL fibres. The red histogram shows the ICAM-1 expression before stimulation and the black histogram shows the ICAM-1 expression after stimulation. The results show a shift left of the histogram after stimulation, this is an increase in ICAM-1 expression.

Figure 5.13 The change in percentage positive HUVECs expressing ICAM-1. Attached to TCP and as-spun PCL fibres after stimulation with LPS for 24 hours and compared with HUVECs without stimulation with LPS. ICAM-1 expression was measured by antibody staining and flow cytometry.

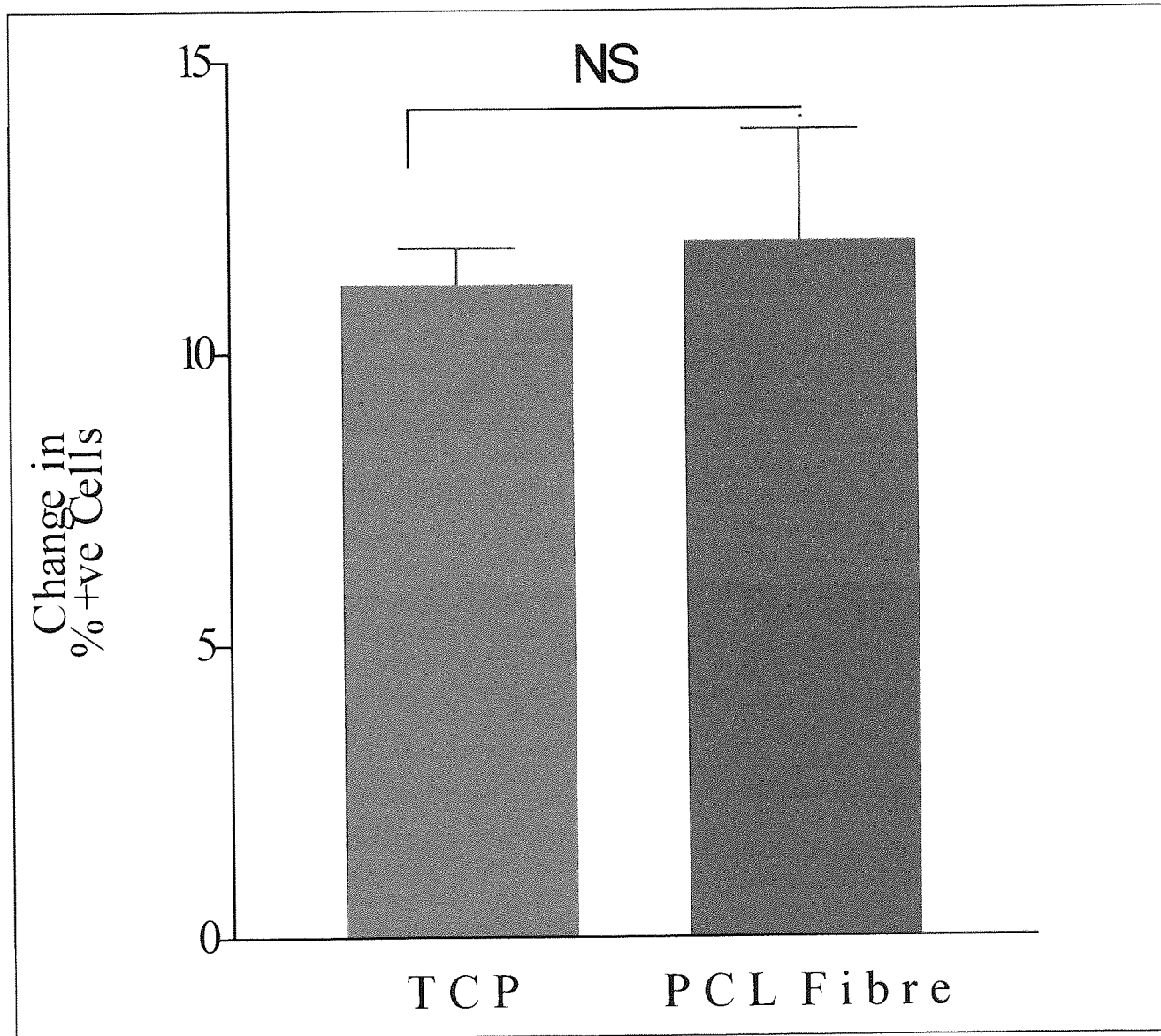
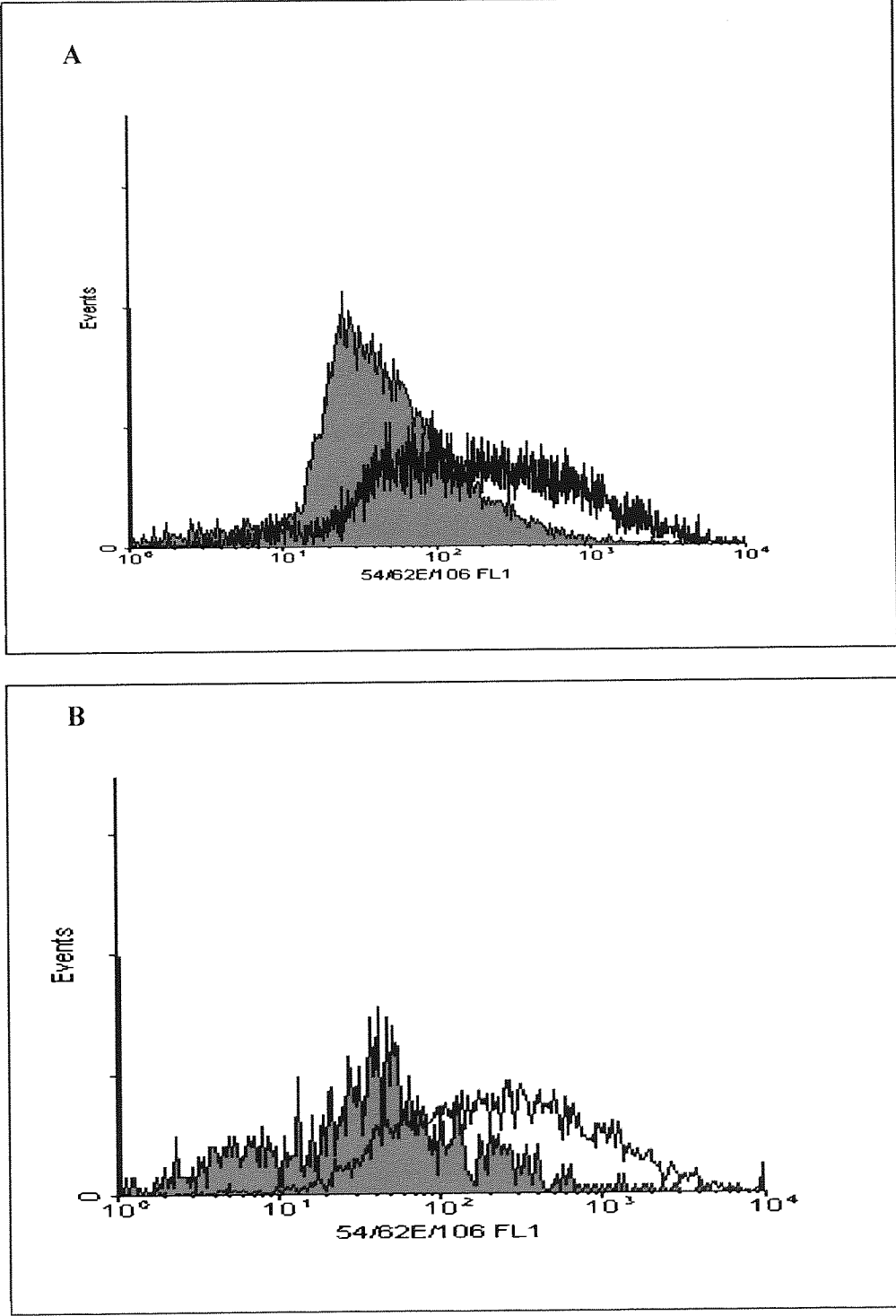


Figure 5.14 Histograms of FL-1 fluorescence labelled ICAM-1 on HUVECS attached to (A) TCP, control and (B) as-spun PCL fibres



Protein data from the study described above demonstrated the impact of LPS on the surface expression of ICAM-1. To confirm the role of LPS in the upregulation of ICAM-1 expression, mRNA was isolated from HUVECs pretreated with LPS. The total RNA was reversed transcribed to cDNA and submitted to PCR using forward and reverse oligonucleotides primers. The PCR products using GADPH and ICAM-1 primers were visualised by agarose gel electrophoresis (Figure 5.15). The density of the PCR products was measured using Scion Image Beta 3b software. The ICAM-1 products were then normalised to GADPH expression levels (dividing the value for the density of the ICAM-1 product bands by the density value of the GADPH product bands) so that the expression can be quantified, as cell numbers could not be counted. Figure 5.16 shows the levels of ICAM-1 mRNA after LPS treatment of HUVECs attached to TCP and as-spun PCL fibres. The levels of ICAM-1 mRNA were similar for both substrates, which indicates that the cells function is retain when the cell are attached to PCL fibres compared with TCP and this confirms the results shown in Figure 5.13.

Figure 5.15 Photograph of UV-illuminated gel electrophoresis of (1) GADPH specific mRNA and (2) ICAM-1 specific mRNA. (A) Fibre – RT (B) Fibre + RT (C) Fibre + LPS + RT (D) Fibre + LPS – RT (E) TCP – RT (F) TCP + RT (G) TCP + LPS + RT (H) TCP + LPS – RT (I) ICAM-1 Positive Control

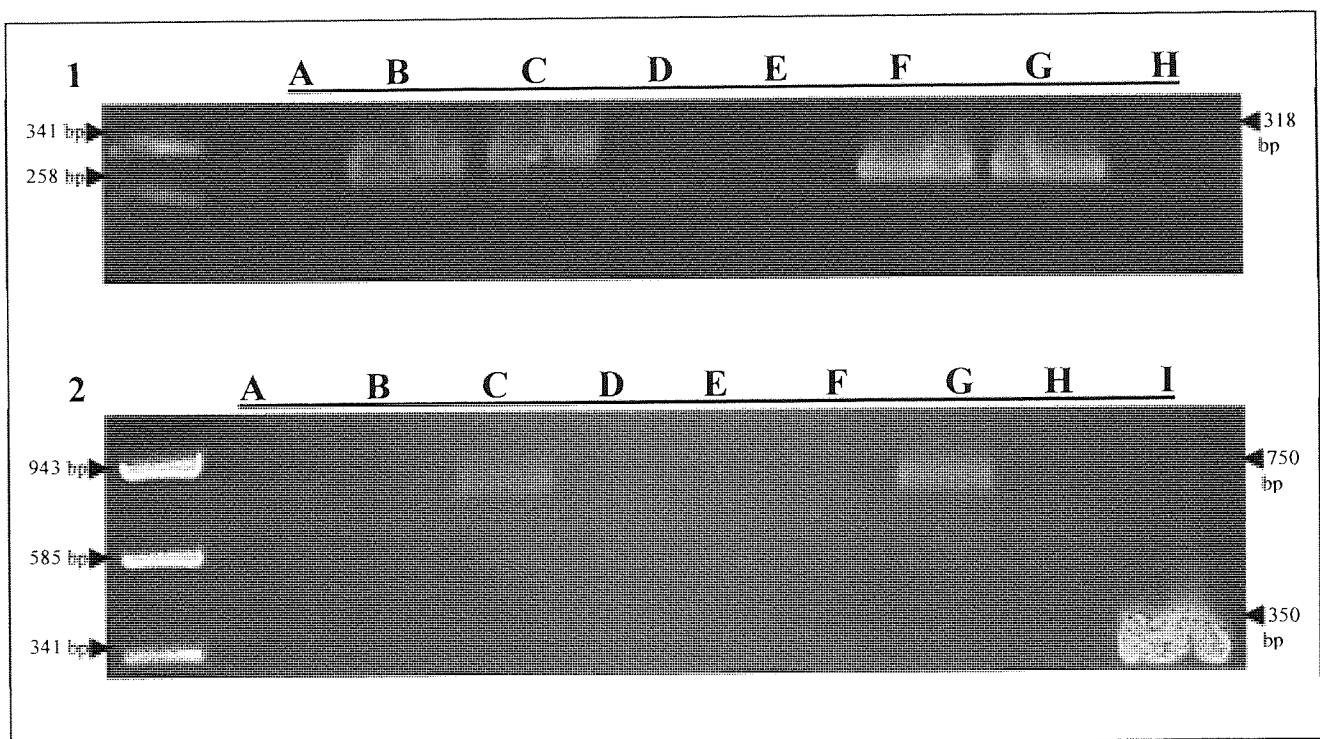
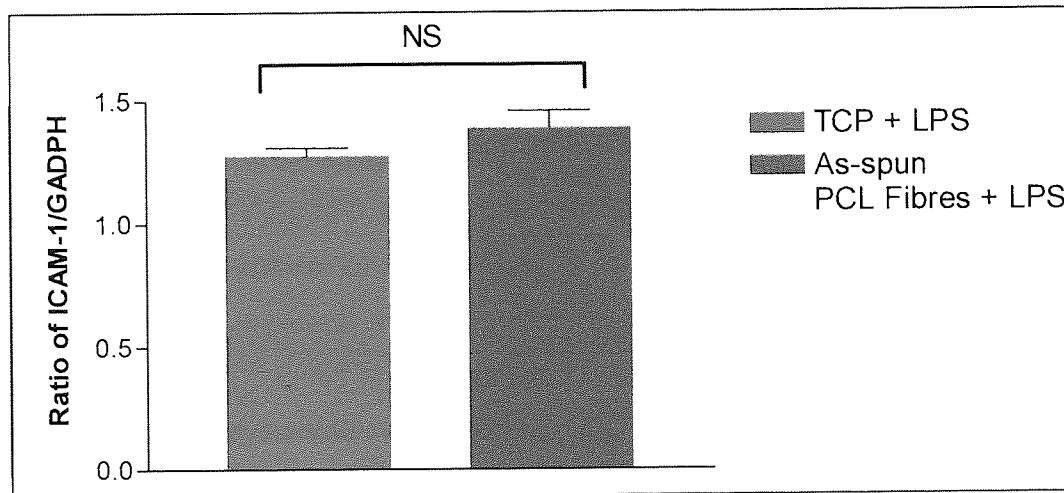


Figure 5.16 Optical density levels of ICAM-1 after normalisation to GADPH as internal standard. Data is expressed as a ratio of ICAM-1 divide by GADPH



5.6 Discussion

PCL fibres are able to promote cell attachment and sustain proliferation in a similar way as TCP. The as-spun PCL fibres were able to match initial attachment of the HUVECs to standard tissue culture plastic surfaces but the proliferation rate did not exceeded that on TCP. This effect was confirmed in the study by HaeYong Kweon et al. (2003) where a PCL scaffold was produced into three-dimensional gels by photopolymerisation and then Human MG-63 osteoblasts used to examine cell proliferation rates compared to TCP over 4 days. The fibres coated with the gelatin solution and cold drawn to 500% showed an increased rate of attachment and therefore an increased proliferation rate compared with the as-spun PCL fibres.

As discussed in Chapter 4 the nature and control of cell/biomaterial interactions (cell adhesion, spreading, proliferation and differentiation) are critically dependent on surface absorbed cell adhesion glycoproteins such as fibronectin, vitronectin and laminin (Hubbell, 1995, Boyan et al. 1996, Fabrizio-Homan et al. 1991, Grinnell et al. 1982, Nikolovski et al. 2000, Steele et al. 1996 and Underwood et al. 1989). These proteins are absorbed onto the surface from the serum in the media used (Yamada, 1983, Hubbell, 1999) or from the biological fluids that the implant would be *in vivo*.

Many investigators have studied Endothelial cells intensively. They have been used to improve the biocompatibility of vascular grafts before implantation to create an endothelium so that the surface of the graft is covered (Tiwari et al. 2003). Many of synthetic vascular graft designs exhibit poor biocompatibility with endothelial cells. This is shown in Cenni et al. (1997) investigated knitted Dacron as a substrate for endothelial cells. The study showed that endothelial cells contacting the knitted Dacron graft demonstrated scarce cells, with respect to the negative control (TCP). Cells contacting knitted Dacron did not form a monolayer after 24 hrs incubation, while the negative control always formed a monolayer and the cells on the Dacron graft were often observed to be round and non-adherent. Chu et al. (1999) examined biodegradable polymers for vascular grafts and reported that PLLA served as a poor substrate for HUVEC proliferation over 7 days. Imegwu et al. (2001) showed that endothelial cells proliferated, but not at their normal doubling rate on a porous polyethylene tetraphthalate membrane. In contrast the as-spun PCL fibres, demonstrated good cell adhesion and proliferation of HUVECs over a period of 9 days (Figures 5.2, 5.3 and 5.8A). The PCL fibres gave rise to a similar proliferation rate to TCP but the PCL fibres present a more favourable surface than other substrates, Dacron monofilament for example (Figures 5.2 and 5.3). The as-spun PCL fibres favourable surface properties for HUVECs adhesion and proliferation is reflected by the confluent monolayer of cells which were generally observed during SEM analysis that can be seen in the SEM picture (Figure 5.10).

The surface chemistry of the material has been modified by several groups of investigators to improve the biocompatibility of various scaffolds for support of cells other than endothelial cells. Much of this in research has involved the coating of TCP and glass with various adhesive factors, for example collagen, fibronectin, laminin, thrombospondin-1 glycoprotein, fibrin glue, biotin, gelatin and cell adhesion peptides such as RGD, REDV, RGDS, YIGSR. The aim was to control cell-material interactions and increase cell adhesion (Badylak et al. 1999, Outerio-Bernstein et al. 2002, Mann et al. 1999, Chan et al. 1999, Bhat et al. 1998). Attempts have also been made to modify the surface of polymers used specifically for vascular graft production. Tiwari et al. (2003) investigated chemical bonding of RGD via a FEPP polymer that incorporates multiple copies of the RGD sequence ligand from human

fibronectin and FAPP which is a sequence found in the carboxy-terminal heparin-binding domain of fibronectin to the lumen of vascular grafts made from poly(carbonate-urea)urethane (MyoLink). This approach resulted in improved cell adhesion and retention compared to native MyoLink graft. Chu et al. (1999) investigated solvent cast PLLA for vascular grafts. PLLA was left native, coated with fibronectin, modified with ammonia plasma (by placing in a plasma reactor) or coating the modified PLLA with fibronectin. The results showed that native PLLA is a poor substrate for HUVEC proliferation with a lower cell number than the seeding density after 7 day in culture. The other substrates showed a dramatic increase in cell number after 7 days in culture compared to the native PLLA. Zund et al. (1998) attempted to improve endothelial cell adhesion on the PLG fibre mesh for vascular grafts by firstly seeding fibroblasts. Non-woven PGA fibres were seeded first with human fibroblasts and cultured for 21 days, followed by seeding of endothelial cells and were examined by microscopy. The results showed that the endothelial cell did attach to the polymer-fibroblast construct. In the investigation described here, as-spun fibres were modified by gelatin coating to investigate the effect on cell proliferation. Endothelial cells attached and proliferated at a higher rate and reached confluence by day 7 on gelatin modified PCL fibres relative to unmodified fibres (Figure 5.2). This behaviour could be due to more cell-to-cell contacts, which are needed for stimuli to turn on downstream signals that progress the cell through the stages of the cell cycle (Osdoby et al. 1980, Tachetti et al. 1992, Freed et al. 1998). This is also observed in Figure 5.8A where a monolayer formed on the gelatin coated PCL fibre but not on the as-spun or cold drawn PCL fibres. Gelatin has been used to modify substrates to (TCP) examine its potential to increase cells for vascular grafts and skin grafts (Kumar et al. 2001, Daniels et al. 1997). Gelatin has shown to result in lower adhesive properties than fibronectin but cells (HUVECs and keratinocytes) appear to have increased proliferation rates. Gelatin improves cell attachment and proliferation because it contains acidic residues, such as lysine and arginine, which are positively charged. Specific cell adhesion sites such as RGD groups are also exposed along the gelatin molecule (Lee et al.).

HUVECs also showed dramatic increase in attachment and proliferation rate on the cold drawn fibres compared to TCP and as-spun PCL fibres. The reason for this

appears to be due to the oriented fibrillar structure of the drawn fibres. It has been reported previously that increases in cell adhesion relative to flat surfaces can be achieved by varying the surface topography (Dalby et al. 2002). In this study endothelial cells were seeded on a polymer demixing of polystyrene and poly(4-bromostyrene) that produced nanometrically high islands. The results showed an increase in spreading of the cells over the manufactured surfaces compared to the flat surfaces. Cold drawing of PCL fibres causes groove formation along the surface of the fibre that range from 1-3 μm . Grooves of this size on titanium and silicon with seeded fibroblasts upon them have been shown to influence cell spreading and alignment over 24 hours (Oakley et al. 1997, Walboomers et al. 1998). Cells attach via focal adhesions along the ridges and therefore produce alignment of the entire cell. Cells also appear to proliferate at a faster rate on a modified topography compared to a smooth surface. It has been suggested (Curtis, 1994) that alignment of cells by stresses on the cytoskeleton can rearrange the centromeres (which are points that join chromosomes together within the nucleus) through deformation stress experienced by the nucleus and this may in turn affect gene expression (Curtis et al. 1978, Curtis. 1994). Cells seeded on to surfaces with modified topography would align and exert stress upon the cell body at a higher rate than smooth surfaces, which may induce the S (or DNA replication) phase of the cell cycle (Alberts et al. 1994). Increased numbers of cells entering the S phase would result in higher proliferation rates. It has also been shown that human fibroblasts activities, such signalling, transcription, translation, production of ECM and cytoskeleton alteration are initially increased over 24 hours in culture in response to grooves 12.5 μm width on a quartz slide surface (Dalby et al. 2003).

Maintenance of cell function in tissue engineering is an important aspect that is often not investigated in sufficient detail. The retention of HUVECs function attached to PCL fibres was investigated by monitoring the capability of HUVECs to bind circulating leucocytes via the intracellular adhesion molecule-1 (ICAM-1), a molecule implicated in the inflammatory process. ICAMs are structurally related to members of the immunoglobulin supergene family and are ligands for the $\beta 2$ integrin molecules present on leukocytes (Hubbard et al. 2000). ICAM-1 (CD54) appears to interact with the cytoskeleton protein α actinin via a short cytoplasmic tail (Springer, 1990).

ICAM-1 is expressed constitutively only at low levels on vascular endothelial cells (Rothlein et al. 1986) and stimulation by a variety of inflammatory cytokines or with lipopolysaccharide (LPS) (Pober et al. 1986) has been documented to increase ICAM-1 expression on cells. ICAM-1 appears to participate in leukocyte-endothelial cell interactions and transendothelial migration (Smith et al. 1989). Interaction of ICAM-1 with its ligand (β 2 integrin) causes tyrosine phosphorylation and activation of tyrosine kinases that lead to downstream activation of mitogen-activated protein kinase (MAPK) pathways. Following activation of MAPK, a transcription factor is activated resulting in production of cytokines by the cell, increased membrane protein expression and an altered pattern of cell proliferation. The physiological outcome of ICAM-1 mediated signal transduction can be changes in inflammatory or immune response (Hubbard et al. 2000).

LPS was used to stimulate the endothelial cells to increase the expression of ICAM-1 on the surface membrane. LPS is a constituent of Gram-negative bacteria cell wall and is a mediator of septic shock (Ishii et al. 1995). That activates the endothelial cells by binding to CD14 but this is found on the membrane of macrophages and granulocytes (Pugin et al. 1993). Endothelial cells do not have CD14 bound to their membrane and so much investigation of how LPS stimulates them has been carried out. It is suggested that LBP binds to LPS and then carries it to soluble CD14 (sCD14) (Chakravorty et al. 1999, Frey et al. 1992, Furst-Ladani et al. 2000, Hailman et al. 1996, Ishii et al. 1995, Pugin et al. 1993, Read et al. 1993). sCD14 is released from the cell surface of mononuclear cells through a proteolytic mechanism and the glycerophosphatidylinositol anchor is lacking but this is not necessary for it perform its role (Frey et al. 1992). The mechanism that the LPS-sCD14 interacts with the cell is then unclear. It has been suggested that the complex binds to an additional component on the membrane to bring about association with the cell and signalling of a response (Frey et al. 1992, Ishii et al. 1995).

The response described above is seen in the examination of HUVECs function. The HUVECs attached to as-spun PCL fibres responded in the same way as they did on TCP after stimulating with LPS. Cells on both substrates demonstrated a similar increase in expression of surface ICAM-1 that was measured by flow cytometry.

This was confirmed by examining the levels of ICAM-1 mRNA using RT-PCR. The results showed that the levels of ICAM-1 mRNA increase after stimulation with LPS. This would suggest that there is an up-regulation in gene expression for the ICAM-1 cell surface receptor. The results shown here demonstrate that HUVECs attached on as-spun PCL fibres does not alter the cells function compared with TCP (a substrate that should not alter cell response) with respect to ICAM-1.

The cells on the PCL fibres showed no sign of an inflammatory response before stimulation with LPS compared with TCP (less than 1% of the population of tested cells were positive for ICAM-1). This result is confirmed by the investigation by Jackson et al. (2000) assessed PLA, PMMA, PLA:EVA and PCL microspheres activation of neutrophils and therefore an immune response. The results showed that PCL induced low levels of activation. Similar behaviour was also reported by Lowry et al. (1997) and Wu et al. (2000). The latter workers showed that PCL showed a mild inflammatory response in the early days of implantation, which disappeared after 3 months. In contrast PLA in a study by Solheim et al. (2000) was shown to provoke a chronic inflammation with multinuclear giant cells, macrophages engulfing material. This in turn inhibited bone formation. The results presented here show that the PCL fibres are not pro-inflammatory to HUVECs, in comparison with TCP control, (which is a substrate that should not cause a response) and therefore constitutes an advantageous property of as-spun PCL fibres for scaffold production (Kao, 1999, Kirkpatrick et al. 2002).

CHAPTER 6 *Controlled delivery of the OVA particles*

BIOACTIVE FIBRES *180*

6.1 Introduction

Controlled delivery systems are widely used to improve therapeutic efficacy and safety of drugs by delivering them to the site of action at a defined rate (dictated by the need of physiological environment) over a defined time period of treatment (Kenawy et al. 2002). A variety of polymeric materials, either synthetic or natural biodegradable or non-biodegradable but biocompatible, have been used to formulate delivery matrices, and the choice of polymer is dictated by the requirements of the specific application (Kenawy et al. 2002). Controlled delivery of bioactive agents such as growth factors has been applied to aid regeneration of skin, bone, cartilage, nerves and blood vessels (Whitaker et al. 2001). However, there is a need to control the time, extent and sequence of growth factor delivery to responsive cells to mimic physiological processes as to maximise the therapeutic potential of these agents. The controlled delivery and presentation of polypeptide growth factors, cell adhesion molecules or sequences, or DNA, which encodes for these factors, would be advantageous for production of tissue engineered constructs. This chapter investigates the potential of PCL fibres for presentation and delivery of proteins and controlled release of steroidal drugs to create bioactive fibres and fibre-based matrices.

6.2 Protein Loading of PCL Fibres

Different loadings of the PCL fibre were investigated as shown in Table 6.1. OVA powder was crushed with a pestle and mortar and added to a 10% PCL solution in acetone for fibre spinning (section 2.2.25). Fibres formed at all concentrations but encapsulation of the protein powder did not occur in every case. Concentrations of OVA above 0.1% resulted in increased amounts of powder aggregates, which caused the spinneret to become partially blocked, but still allowed the polymer solution to flow. At 0.1% w/v of OVA the amount of large particles was low enough to allow flow of the polymer solution and encapsulation of OVA powder. Homogenising the

suspension before spinning the fibre further reduced the size of the OVA particles. This approach however did not result in an increase of OVA loading.

The fibre production rate and diameter are shown in Table 6.2. The diameters of the fibres loaded with OVA are slightly increased compared to as-spun fibres. The production rates of the fibres are very similar to those recorded for as-spun fibre.

Table 6.1 Observations on spinning of PCL fibres from 10% w/v solution in acetone containing OVA powder.

Concentration of OVA %	Observations
0.1	Powder dispersed and formed uniform fibre
0.5 - 5	Powder dispersed in PCL solution but the powder blocked spinneret. Fibre could form but with minimal amounts of OVA powder encapsulated

Table 6.2 Spinning rate and diameters of PCL fibres produced from different concentration of PCL solutions containing 0.1% w/v OVA powder.

PCL Concentration %	Production Rate m/min		Diameter of Fibre (μm)	
	OVA loaded	OVA-free	OVA loaded	OVA-free
6	2.3 \pm 1.0	2.5 \pm 1.0	210.0 \pm 10.2	190.0 \pm 8.2
10	1.9 \pm 0.8	2.1 \pm 0.6	185.3 \pm 8.7	153.3 \pm 4.7
15	1.7 \pm 0.7	1.9 \pm 0.6	165.0 \pm 5.2	150.0 \pm 8.2
20	1.0 \pm 0	0.9 \pm 0	160.3 \pm 10.1	150.3 \pm 7.1

OVA-loaded PCL fibres were produced using OVA nanoparticles (section 2.2.26). PVP was used as a resuspending agent in some freeze dried formulations and without. The nanoparticles size was measured (Brookhaven ZetaPlus Particle Sizer) at 784.9 nm with and without PVP added. The incorporating of a resuspending agent to the suspension in the freeze dried nanoparticle preparation did not improve suspension of

the nanoparticle powder in the PCL solution. Homogenisation of the suspension did however result in a higher loading of the nanoparticles in the PCL solution compared with the OVA powder (Table 6.3), this was due to the smaller particle size allowing a more homogenous suspension.

The diameter and production rate of the PCL fibres incorporating OVA nanoparticles are shown in Table 6.3. The fibre production rate is similar to the as-spun fibre made from the 10% PCL solution, but the diameter of the OVA-loaded fibres has increased by about 40 μm compared with unloaded fibres.

Table 6.3 Spinning rate and diameter of PCL fibre produced from a 10% PCL solution containing different concentrations of OVA nanoparticles.

OVA Nanoparticle concentration (w/v%) in spinning solution	Fibre Production Rate m/min		Diameter of Fibre (μm)	
	Nanoparticle loaded	OVA-free	Nanoparticle loaded	OVA-free
0.1	2.3 \pm 1.0	2.1 \pm 0.6	201.0 \pm 6.2	153.3 \pm 4.7
0.5	1.9 \pm 0.8		206.6 \pm 6.2	
1	-		-	

6.3 Mechanical Properties

The mechanical properties of the 10% PCL fibres produced from suspensions containing 0.1% w/v OVA powder, 0.1% w/v and 0.5% w/v nanoparticles are shown in Table 6.4. The properties of both the 0.1% w/v OVA powder and 0.1% w/v nanoparticle-loaded fibres are similar to the mechanical properties of the as-spun 10% PCL fibre. The 0.5% w/v OVA nanoparticle-loaded fibre shows some similarities (Yield stress and % extension at yield) but the fibre failure stress is reduced by around 50% and the failure extension is decreased by 3 fold. This behaviour compared to the unloaded fibres is due to the particle presence in the fibre, effectively reducing the polymer load-bearing component.

Table 6.4 The tensile properties of 10% PCL fibres spun from solutions containing 0.1% w/v OVA powder, 0.1% w/v and 0.5% w/v nanoparticles

Bioactive PCL Fibre	0.1 % w/v OVA powder	0.1% w/v OVA Nanoparticles	0.5% w/v OVA Nanoparticles	As-spun unloaded fibres
Tensile modulus GPa	0.05±0.0018	0.04±0.03	0.02±0.006	0.08±0.01
Failure stress MPa	6.9±0.16	6.9±0.09	3.7±0.47	7.9±2.0
% Failure extension	353.7±71.3	439±67.9	153±26.7	514.9±257.3
Yield stress MPa	2.8±0.59	4.3±0.22	2.0±0.41	3.8±0.51
% Extension at yield	10.8±3.6	16.4±2.9	8.6±1.3	10.8±6

6.4 Thermal Properties

Table 6.5 presents the thermal properties of as-spun 10% PCL fibres loaded with 0.1% w/v OVA powder, 0.1% w/v and 0.5% w/v nanoparticles. The melting point of the fibres does not vary significantly with the different loadings used to prepare the fibres. The melting point (T_m) of the fibres is consistently around 60°C. The % crystallinity of PCL fibres did not vary between the different fibres (average 54%) and so the loading concentration and the loading product did not appear to have much of an effect upon the thermal properties of the fibres compared with the as-spun fibres.

Table 6.5 The thermal properties 10% PCL fibres spun from solutions containing 0.1% w/v OVA powder, 0.1% w/v and 0.5% w/v nanoparticles

Bioactive Fibre	0.1 % OVA powder	0.1% OVA Nanoparticles	0.5% OVA Nanoparticles	As-spun unloaded fibres
T_m °C	62.5±2.5	58.6±0.89	63.5±1.9	62.5±0.89
ΔH_m (J/g-1)	75.0±5.1	78.2±5.3	72.5±11.8	84.3±5.3
% Crystallinity	53.9±10.1	56.2±3.4	54.7±7.7	60.4±3.4

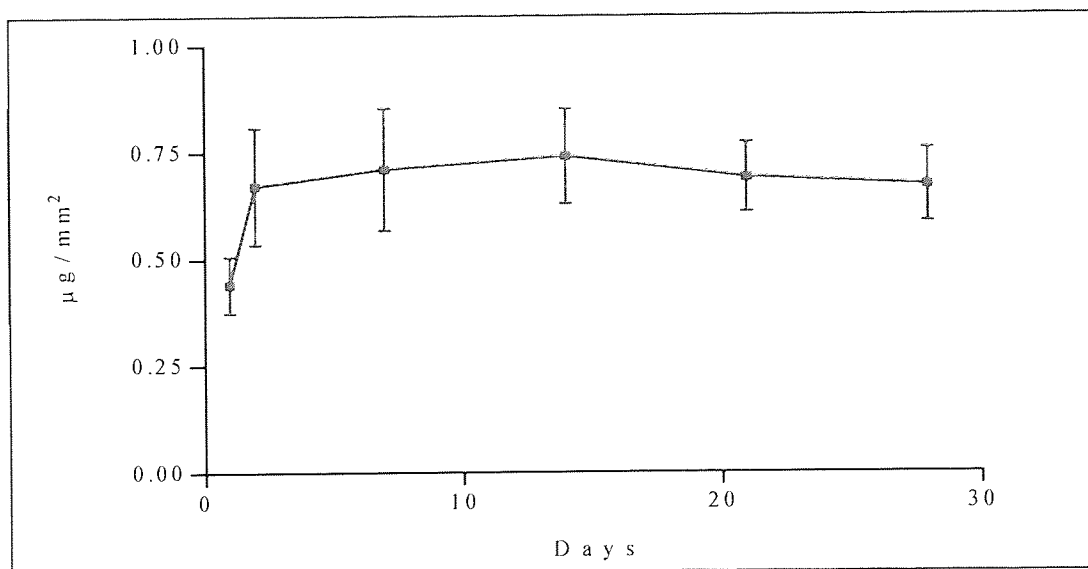
6.5 Fibre Surface Modification by Incorporated Protein

The amount of OVA exposed at the fibre surface increased with incubation time in PBS at 37°C as measured using BCA total protein assay (Table 6.6). At Day 1 the amount of protein measured at the fibre surface was 97 µg on an area of 177mm² (0.55 µg/mm²). This then increased by 1.3 fold by Day 2 (0.74 µg/mm²) and by almost 1.1 fold at Day 7 (0.79 µg/mm²). Re-absorbance of OVA on to the fibres surface after OVA release is indicated since the release medium was not changed over the duration of the experiment.

Table 6.6 The amount of OVA measured on the surface of a 10% PCL fibre after incubation in PBS at 37°C.

Day	Surface Protein (µg)	OVA/ fibre surface area (µg/mm ²)
1	97.3±74.0	0.55
2	130.7±43.8	0.74
7	139.0±57.9	0.79

Figure 6.1 OVA expression on the surface of 10% as-spun PCL fibres spun from a 0.1% OVA powder suspension. Incubated for 28 days in PBS at 37°C. Release medium was not changed



6.6 Fibre Surface Modification by Gelatin Coating

As-spun PCL fibres were surface modified by adsorption of gelatin from solution to improve cell adhesion. The results in Table 6.7 showed that the different concentrations of gelatin coating solutions had a major effect on the amount of gelatin coating the fibre surface. The lower the concentration of the coating solution the higher the amount of gelatin adsorbed on the fibre. As the concentration doubled the protein absorbed on the surface decreased by almost 50%. Use of 5% gelatin coating solution resulted in adsorption of 688 μg of gelatin on 177 mm^2 of fibre ($3.9 \mu\text{g}/\text{mm}^2$) compared with use of a 20% gelatin coating solution which resulted in 125 μg on 177 mm^2 of fibre ($0.7 \mu\text{g}/\text{mm}^2$), a decrease of about 5 fold.

Table 6.7 The amount of gelatin measured on the surface of a 10% as-spun PCL fibre coated using various concentrations of gelatin solution

Solution concentration of gelatin coating (% w/v)	Gelatin/ fibre surface area ($\mu\text{g}/\text{mm}^2$)
5	3.9
10	1.8
20	0.7

Figure 6.2 shows the amount surface protein associated with PCL fibres was measured using the BCA total protein assay after culture in PBS for 28 days. The results show that there is a decrease of approximately 2.7 times from the initial concentration to the concentration associated with the fibre after 28 days, the largest decrease was observed after day 1 with a decrease of 1.3 times. The results in Figure 6.3 shows the release of the gelatin coating from the PCL fibre into a release medium. This results demonstrates that the amount of gelatin release from the coating almost increase by 50% from day 1 to day 28 and shows the most largest release after at day 1. Both these results show that the gelatin coating has an initial burst of release over the first 24 hours and then show a steady release profile.

Figure 6.2 The amount of gelatin measured on the surface of a 10% as-spun PCL fibre coated using a 5% w/v gelatin solution. Incubation period 28 days in PBS at 37°C

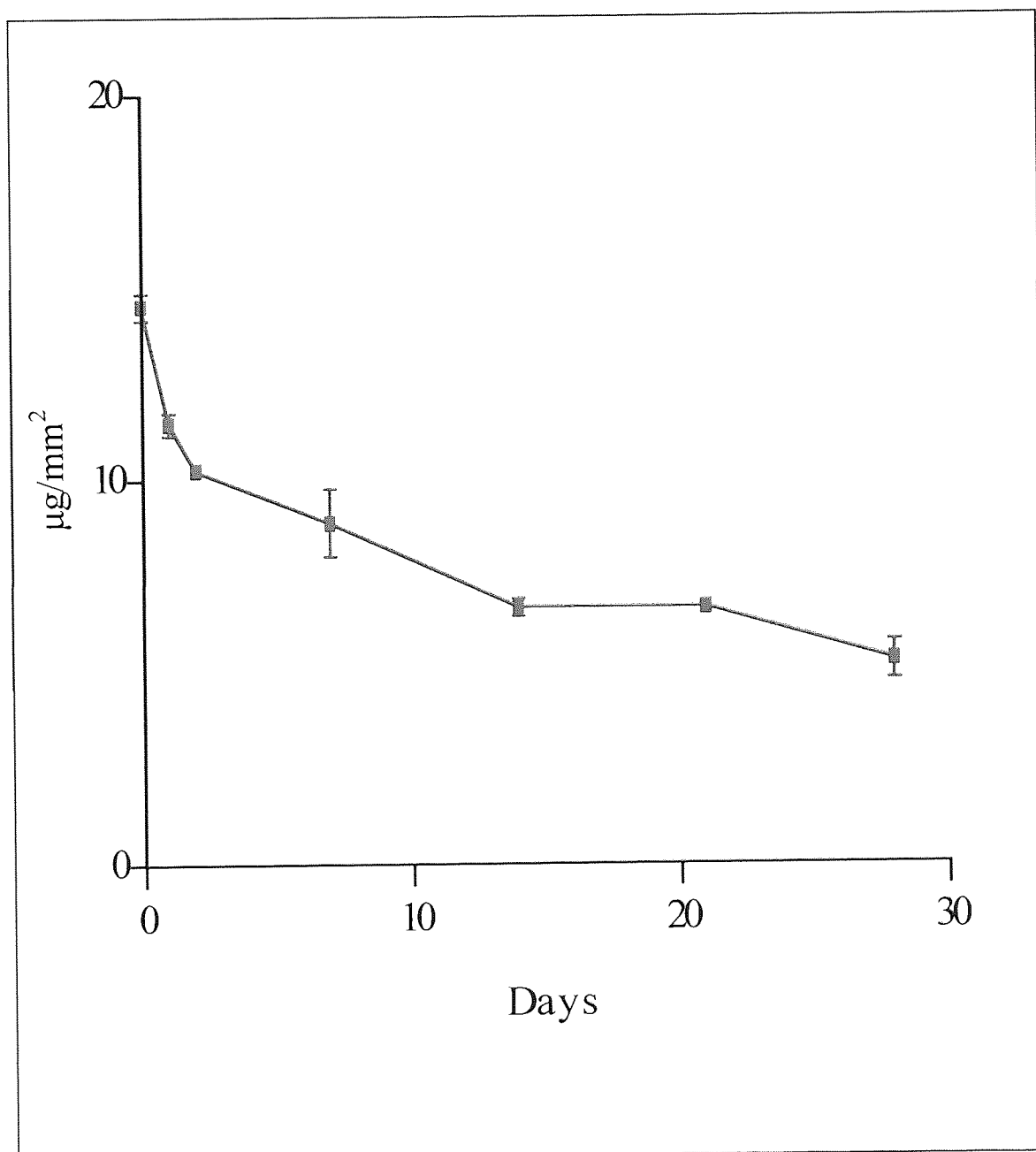
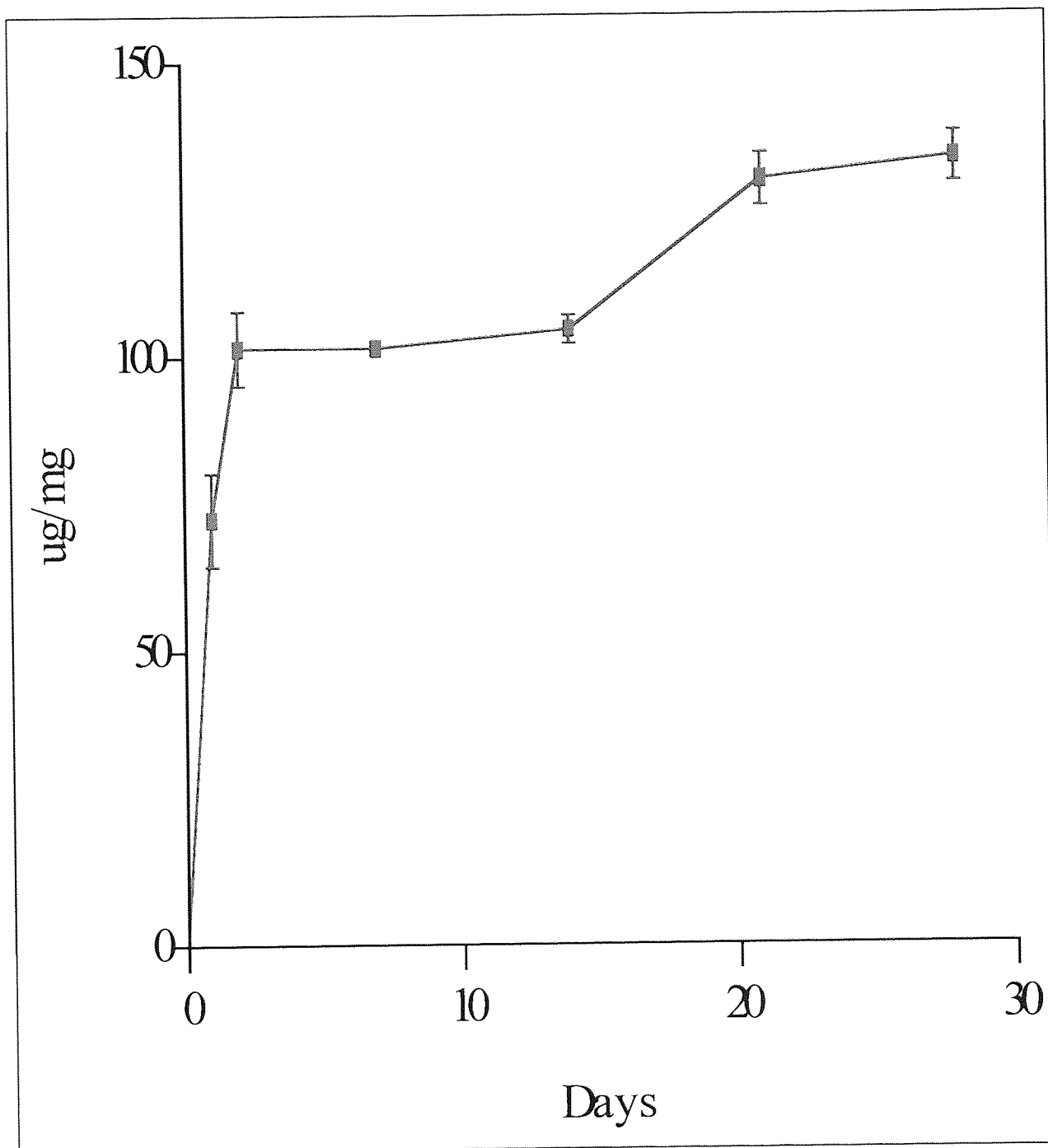


Figure 6.3 Release of gelatin from an as-spun PCL fibre coated with a 5% w/v gelatin solution. Release period 28 days. PBS release medium was not removed during this study



6.7 SEM Examination of Modified PCL Fibres Surface Topography

Figures 6.4 and 6.5 show scanning electron micrographs of as-spun fibres with a 1% loading of OVA powder and 5% loading of OVA nanoparticles respectively. The fibre with loaded with OVA powder showed distinct difference in surface morphology compared to an as spun PCL fibre (Figure 3.5). The OVA powder (flake-like in appearance) has tended to protrude from the fibre, giving rise to a more porous nodule-like appearance.

The as-spun PCL fibre spun from a 0.5% w/v OVA nanoparticle loaded fibre surface is shown in Figure 6.5. The surface morphology of this fibre does not appear to have been significantly altered compared with that of the as-spun fibre (Figure 3.6). The fibre exhibits a rough surface texture and there are no signs of the nanoparticles (784.9 nm) protruding through the surface.

Figure 6.6 show the surface morphology of an as-spun PCL fibre coated with a 5% gelatin solution. The fibre morphology appears not to have been altered significantly by the gelatin coating. The characteristic rough surface is clearly visible and is comparable to the surface of the uncoated as-spun fibre (Figure 3.5).

Figure 6.4 SEM of the surface topography of (a) as-spun PCL fibre spun from a 0.1% OVA powder suspension. (b) An unloaded as-spun PCL fibre

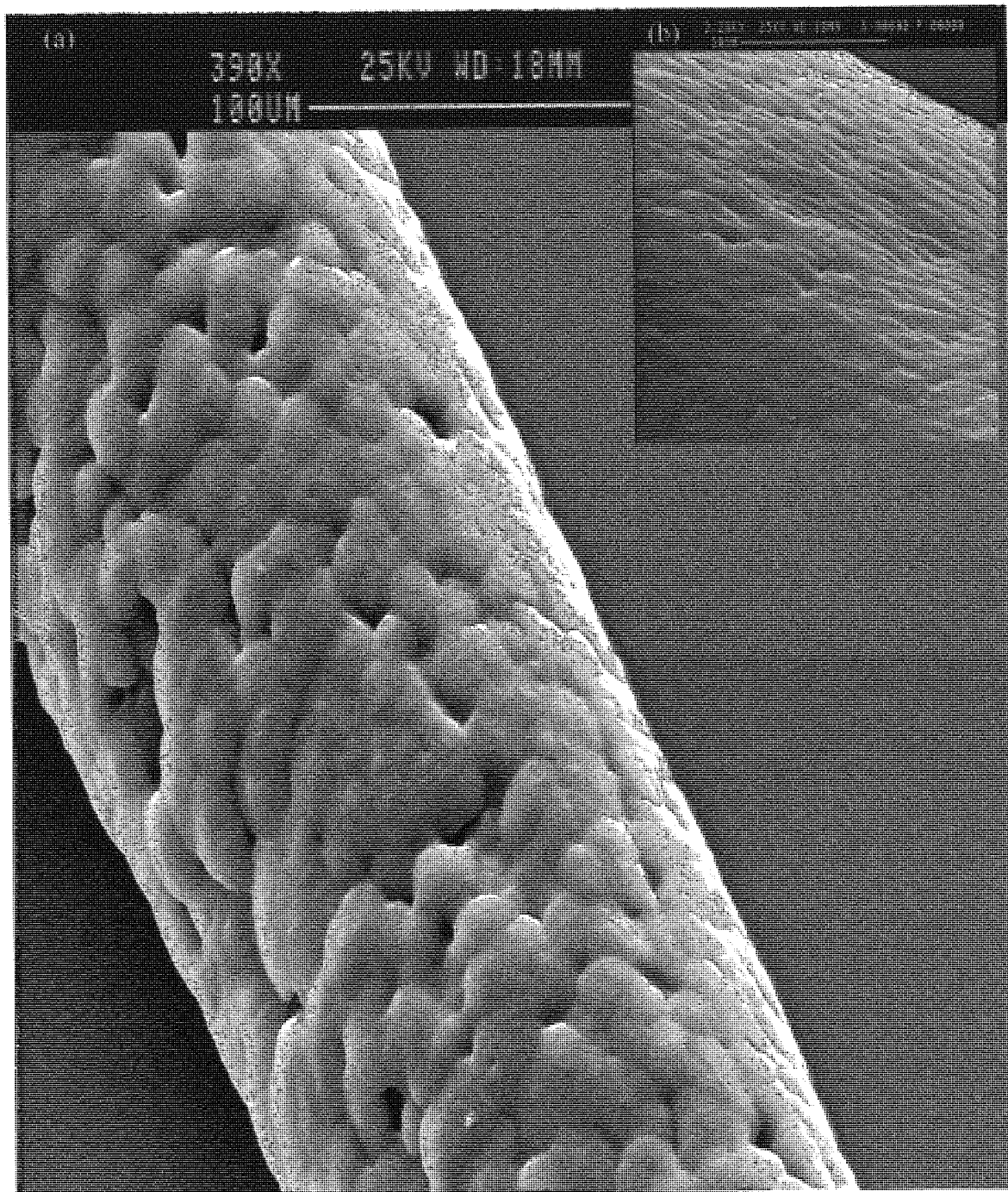


Figure 6.5 SEM of the surface topography of (a) as-spun PCL fibre spun from a 0.5% w/v OVA nanoparticles suspension. (b) An unloaded as-spun PCL fibre

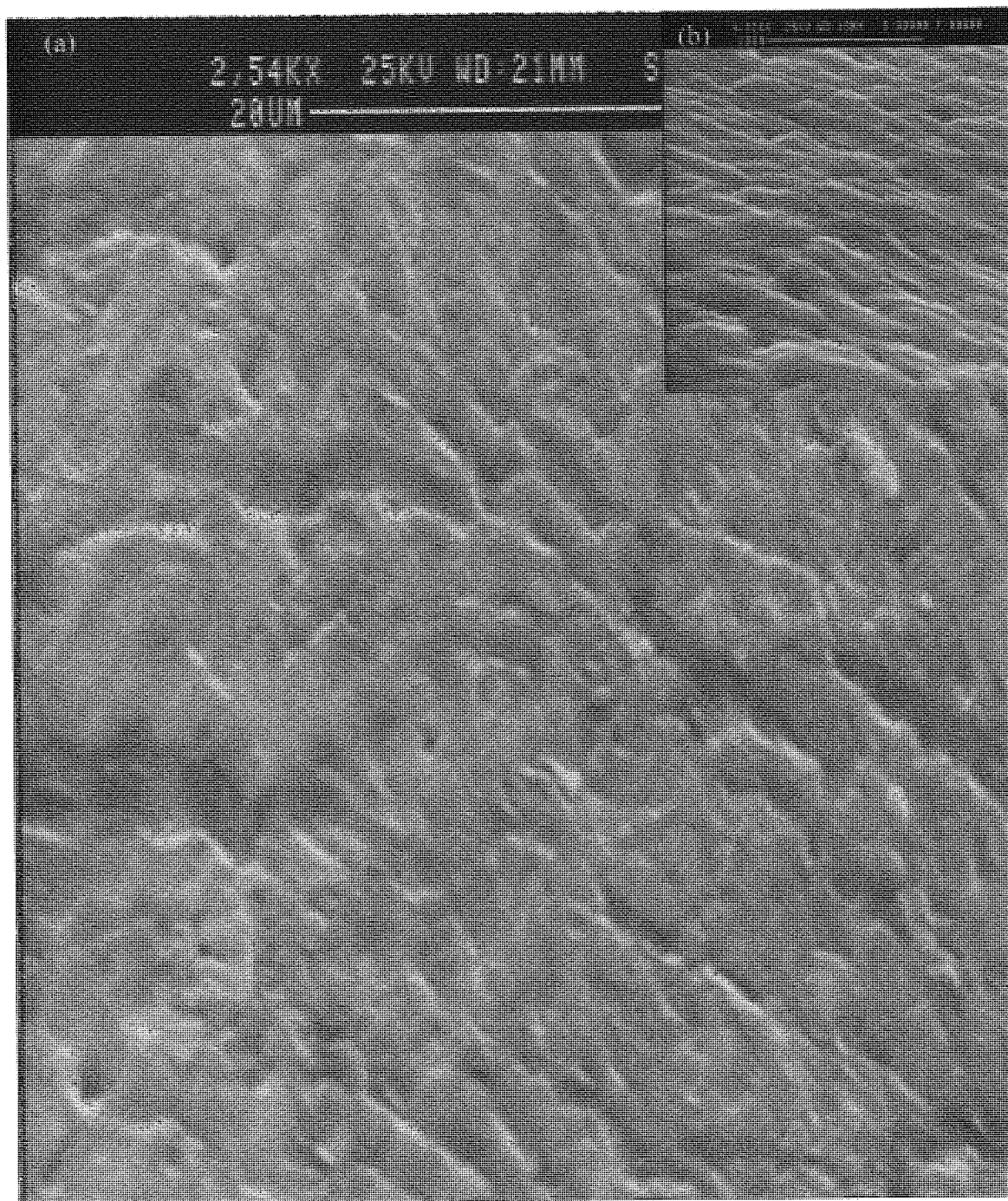
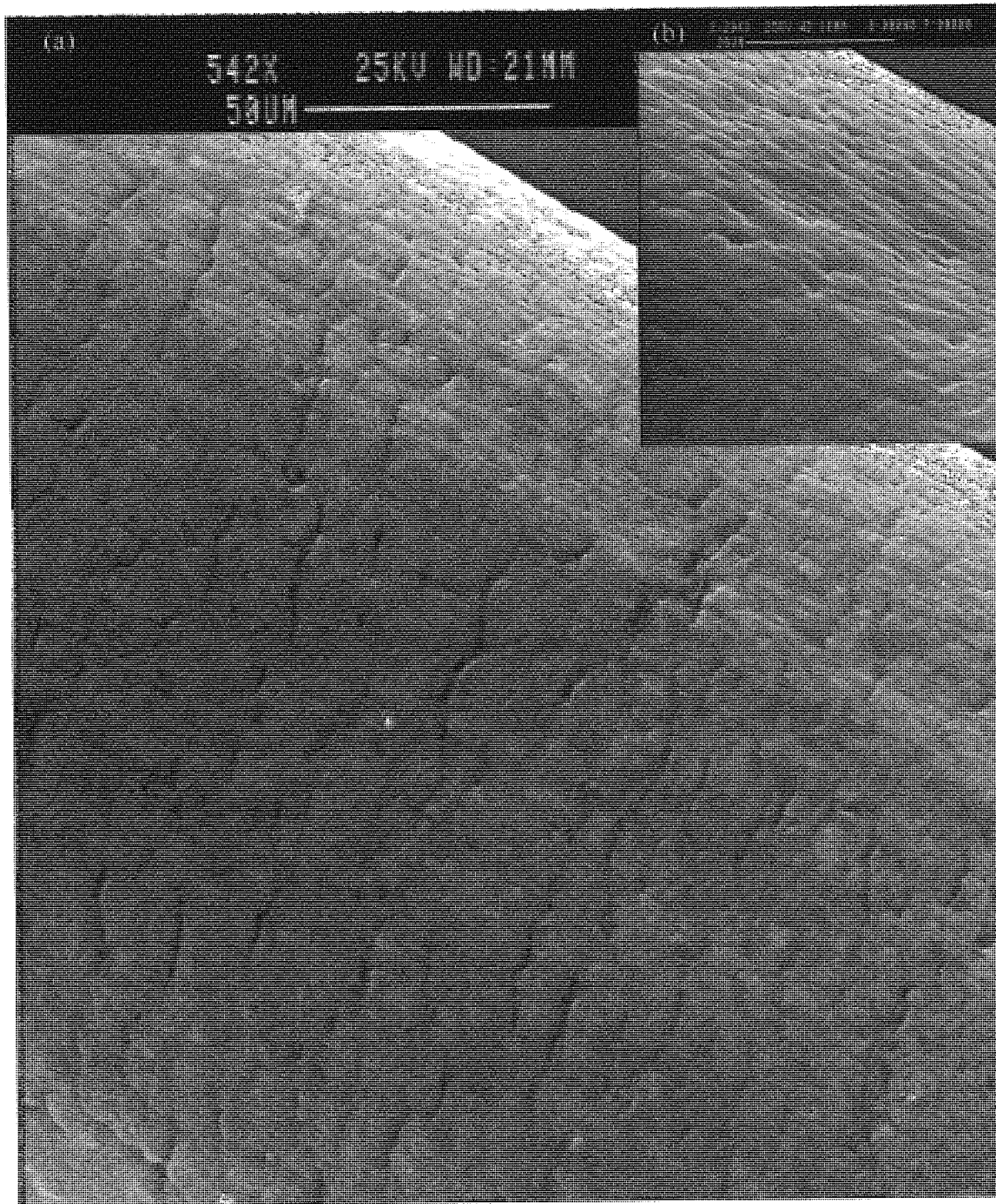


Figure 6.6 SEM of the surface topography of (a) as-spun PCL fibre coated with a 5% w/v gelatin solution. (b) An uncoated as-spun PCL fibre.



6.8 Release of Protein from OVA-Loaded PCL Fibres

The amount of OVA released from PCL fibres spun using a 0.1% w/v OVA suspension into PBS at 37°C, was measured using the BCA assay. The results in Table 6.8 show that the weight of OVA measured in the PBS release medium at day 1 was approximately 103.2 µg. Gradual protein release occurred over 7 days.

Table 6.8 The amount of protein released from the OVA-loaded PCL modified fibre into 2ml of PBS.

Day	Protein (µg)	Protein release/ mg of fibre (µg/mg)
1	103.2±26.8	3.4
2	147.6±14.4	4.9
7	216.2±23.6	7.2

Fibres with a 1% OVA loading (produced using a PCL solution containing 0.1% w/v OVA powder) were incubated in PBS for 28 days to investigate the release. In this experiment the release media was not removed completely at each sampling interval, which could lead to readsorption of OVA onto the fibre, thereby giving incorrect release amounts. The fibre still showed protein release revealed in Figure 6.7 and the release % is shown in Figure 6.8. A gradual increase in OVA release occurred over 28 days, the release amount increasing by 2 fold from day 1 to day 28.

Figure 6.7 Release of OVA from a 1% OVA loaded PCL fibre. Release period 28 days. PBS release medium at 37°C was not removed during this study.

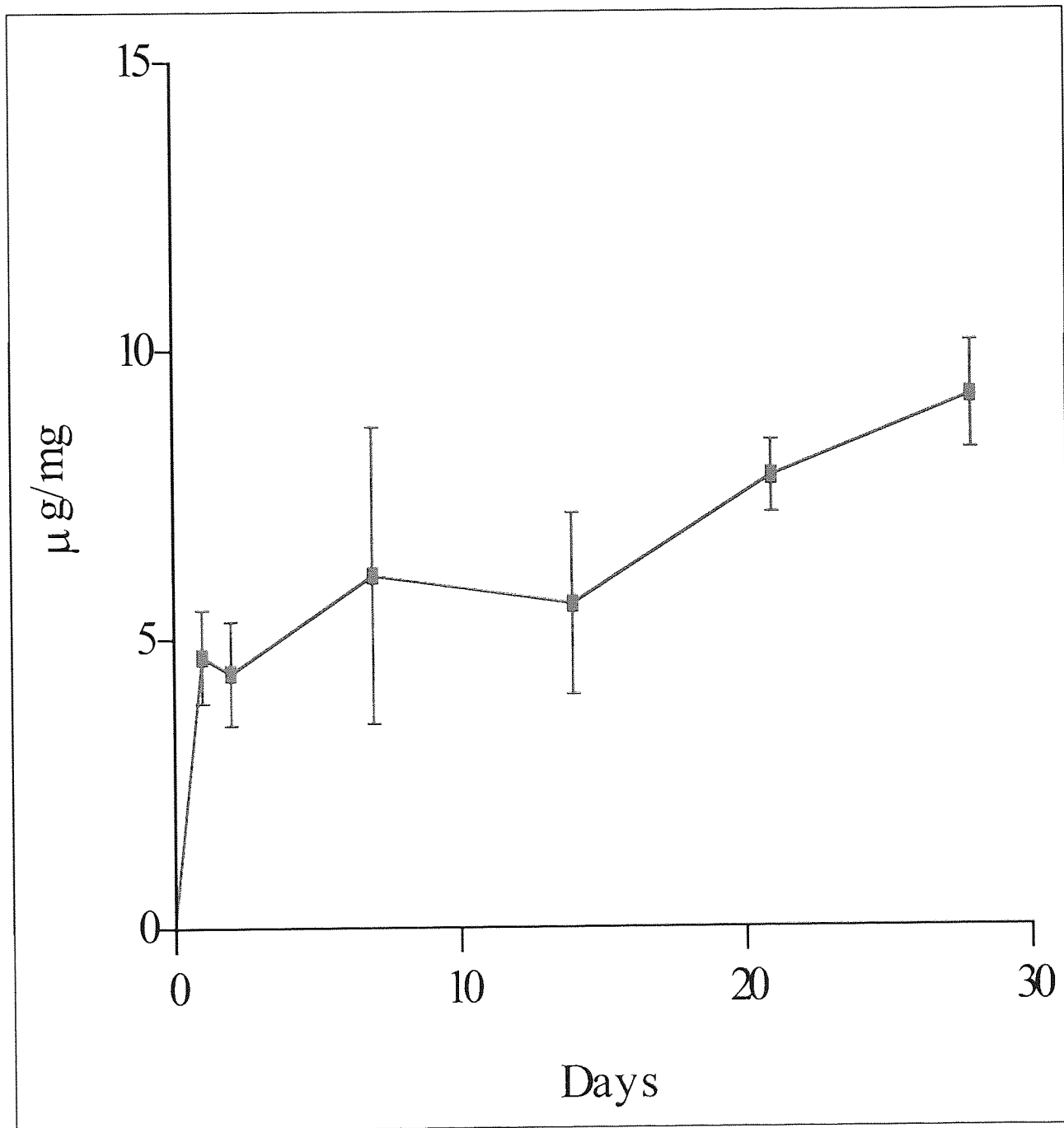


Figure 6.8 Release % of OVA from a 1% OVA loaded PCL fibre. Release period 28 days. Release medium PBS at 37°C was not removed during this study.

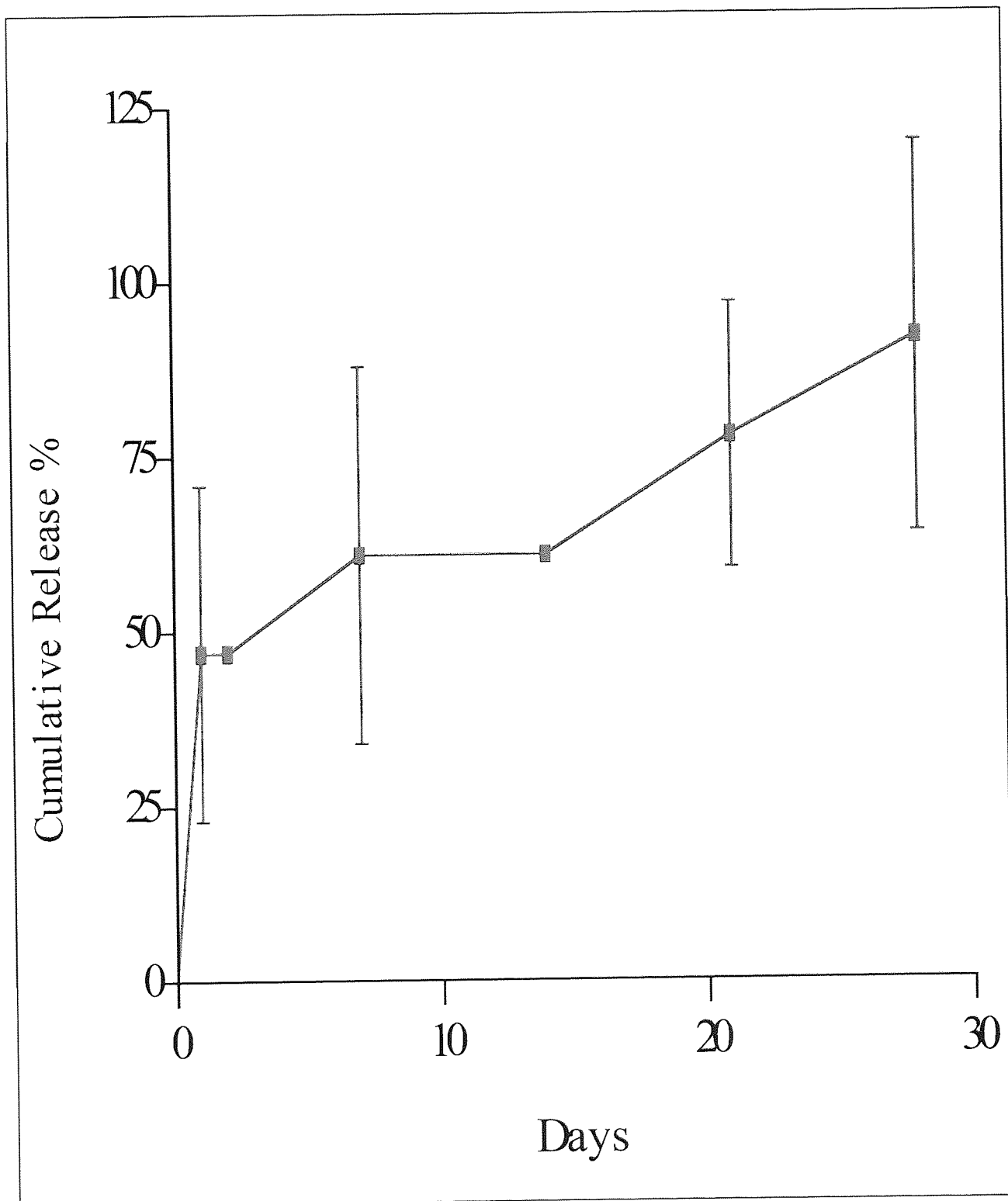


Figure 6.9 shows the cumulative release of protein ($\mu\text{g}/\text{mg}$) from PCL fibres with a 1% OVA powder loading, 1% OVA nanoparticles loading and 5% OVA nanoparticles loading respectively over 28 days. PVP was added to the OVA nanoparticles in this experiment before freeze drying to aid powder resuspension in the spinning solution. The release media in this experiment was also removed every 3 or 4 days to avoid large scale readsorption of OVA to the fibre. The 1% OVA powder loaded fibres gave rise to the largest rate of release over 14 days, with a pronounced burst effect over the first two days. The release curve then flattened before a gradual release from day 14 to day 28 where there is an increase of 1.2 fold. The OVA release rates obtained for both concentrations of nanoparticles (1% and 5%) are greatly reduced compared to that of the OVA powder containing fibres over the first 14 days. The curves appear to have the same trend. There is a slight increase in OVA release from day 1 to day 2 and then a plateau region over the next 12 days until day 14 when larger amounts of protein are released. From day 14 to day 21 the 5% nanoparticle loaded fibres result in a 3.7 fold increase in OVA release compared to the 1% nanoparticle loaded fibres that increased 3.9 fold. The cumulative release % for PCL fibres with a 1% OVA powder loading, 1% OVA nanoparticles loading and 5% OVA nanoparticles loading (PVP incorporated) is shown in Figure 6.10.

The release curves for PCL fibres loaded with 1% OVA powder, 1% OVA nanoparticles and 5% OVA nanoparticles with over 28 days are shown in Figure 6.11. Fibres spinning used nanoparticles that did not have PVP added to aid suspension in the spinning solution to examine the effect on OVA release. The 1% OVA powder loaded fibre released the most protein over the first 7 days. Following the initial burst release phase the release curve flattens and there was gradual increase of 1.3 fold from day 2 to day 28. The nanoparticle-base PCL fibres release profiles were not similar. An initial burst from day 1 to 2 followed with a lag phase. After this initial burst, a slight increase in release of protein to day 7.

Figure 6.9 Cumulative release of OVA from PCL fibres with a 1% OVA powder, 1% OVA nanoparticles and 5% OVA nanoparticles loadings. PVP incorporated in nanoparticle powder to aid suspension in PCL solution. Release period 28 days. Release medium PBS at 37°C

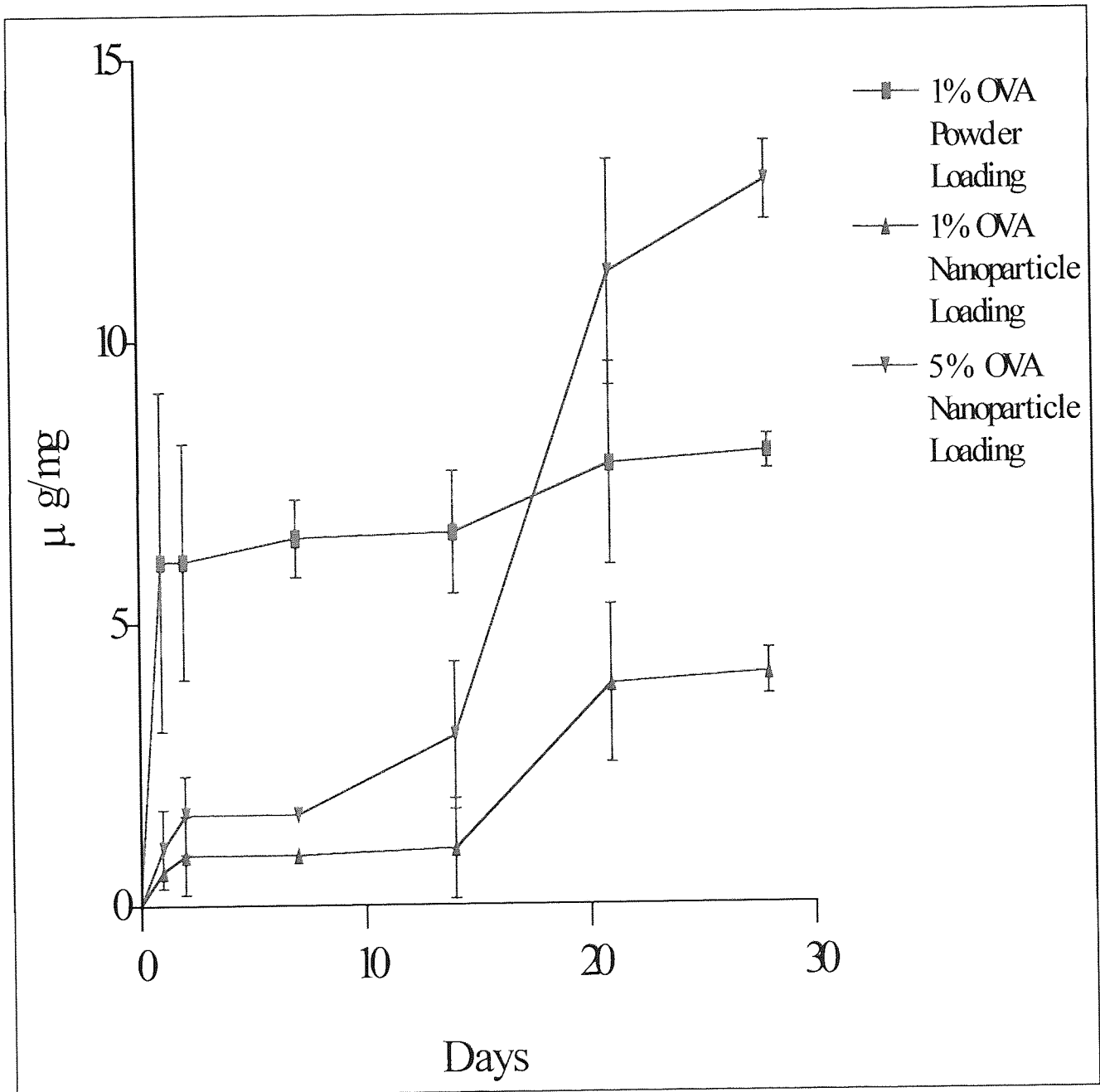
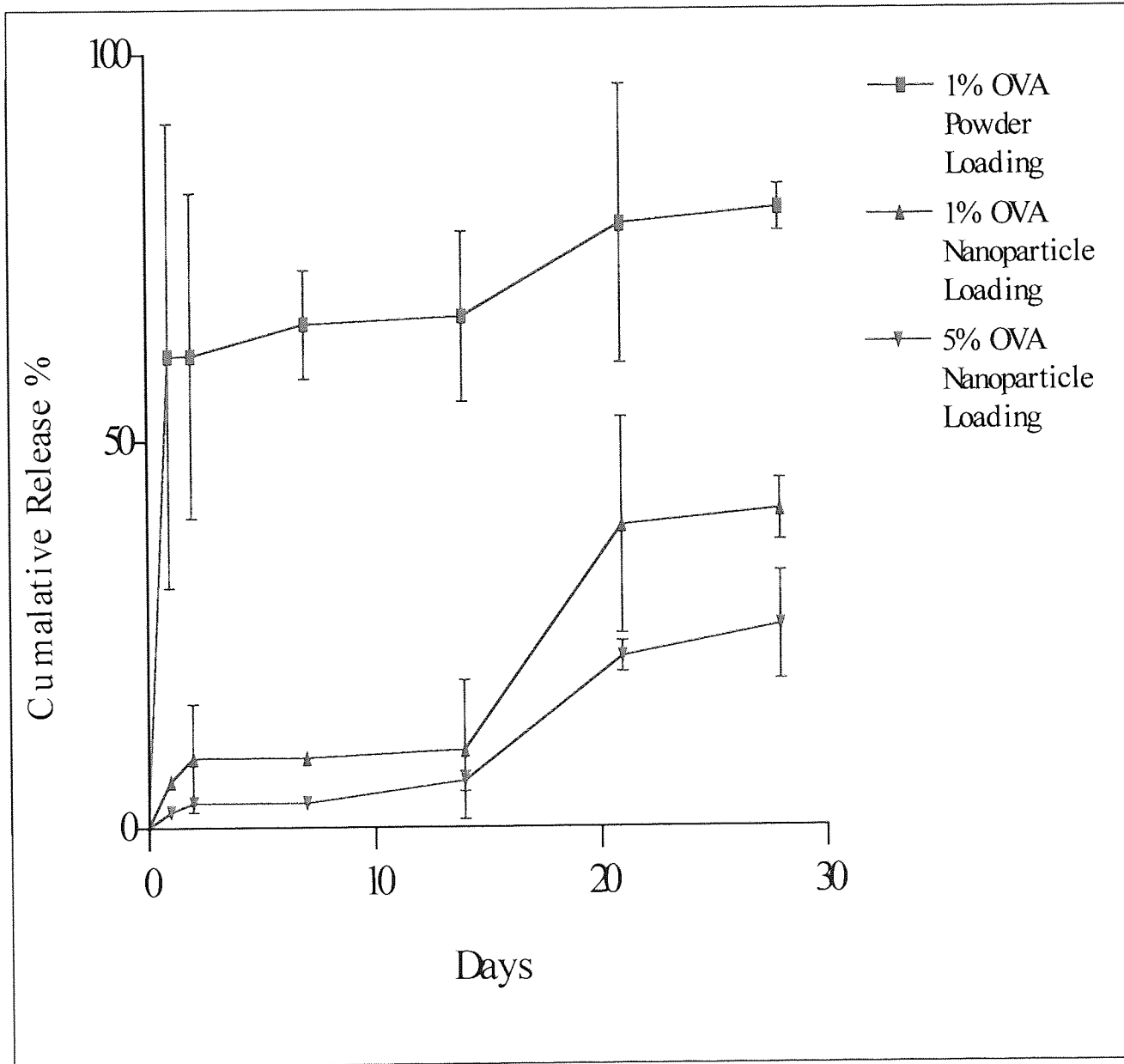


Figure 6.10 Cumulative release % of OVA from PCL fibres with a 1 % OVA powder, 1% OVA nanoparticles and 5% OVA nanoparticles loadings. PVP incorporated in nanoparticle powder to aid suspension in PCL solution. Release period 28 days. Release medium PBS at 37°C



Following the steady release phase there was an increase in release rate for both nanoparticle-base PCL fibres. The 5% nanoparticles loaded fibre increases by 2.8 fold from day 7 to day 28 and the 1% nanoparticle loaded fibre increase by 2.9 fold. The release profile obtained using PVP-modified nanoparticle powders in the PCL fibres (Figure 6.9) are similar to that obtained when OVA nanoparticle powder does not incorporate PVP (Figure 6.11). The release profiles observed in the former case show an increase in release at day 14 and burst release is much reduced compared to the fibres loaded with nanoparticles without PVP that show a larger initial burst and an increase in release rate at day 7. The cumulative release % for PCL fibres with a 1% OVA powder loading, 1% OVA nanoparticles loading and 5% OVA nanoparticles loading is shown in Figure 6.13.

Figure 6.11 Cumulative release of OVA from PCL fibres with a 1 % OVA powder, 1% OVA nanoparticles and 5% OVA nanoparticles loadings. Release period 28 days. Release medium PBS at 37°C

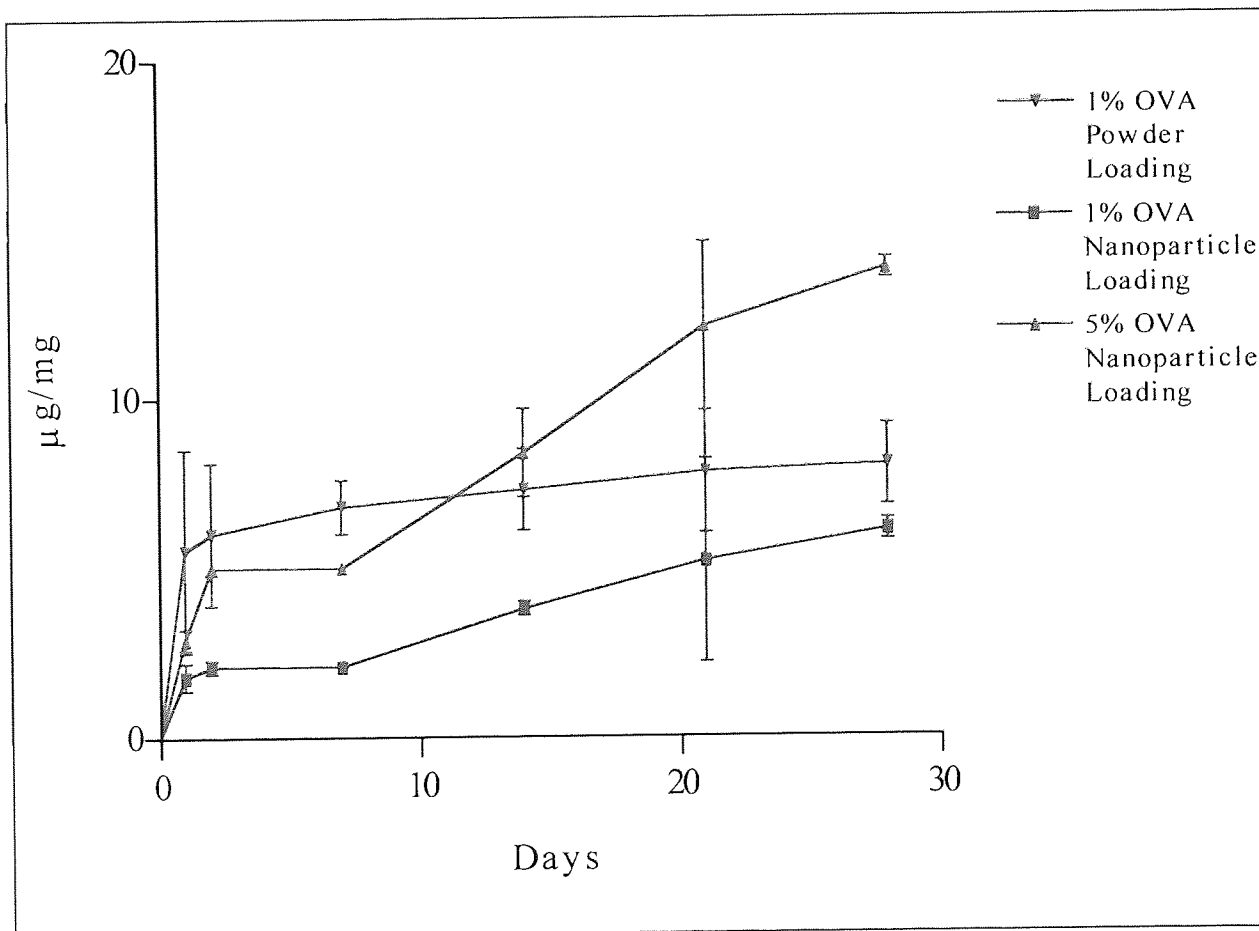
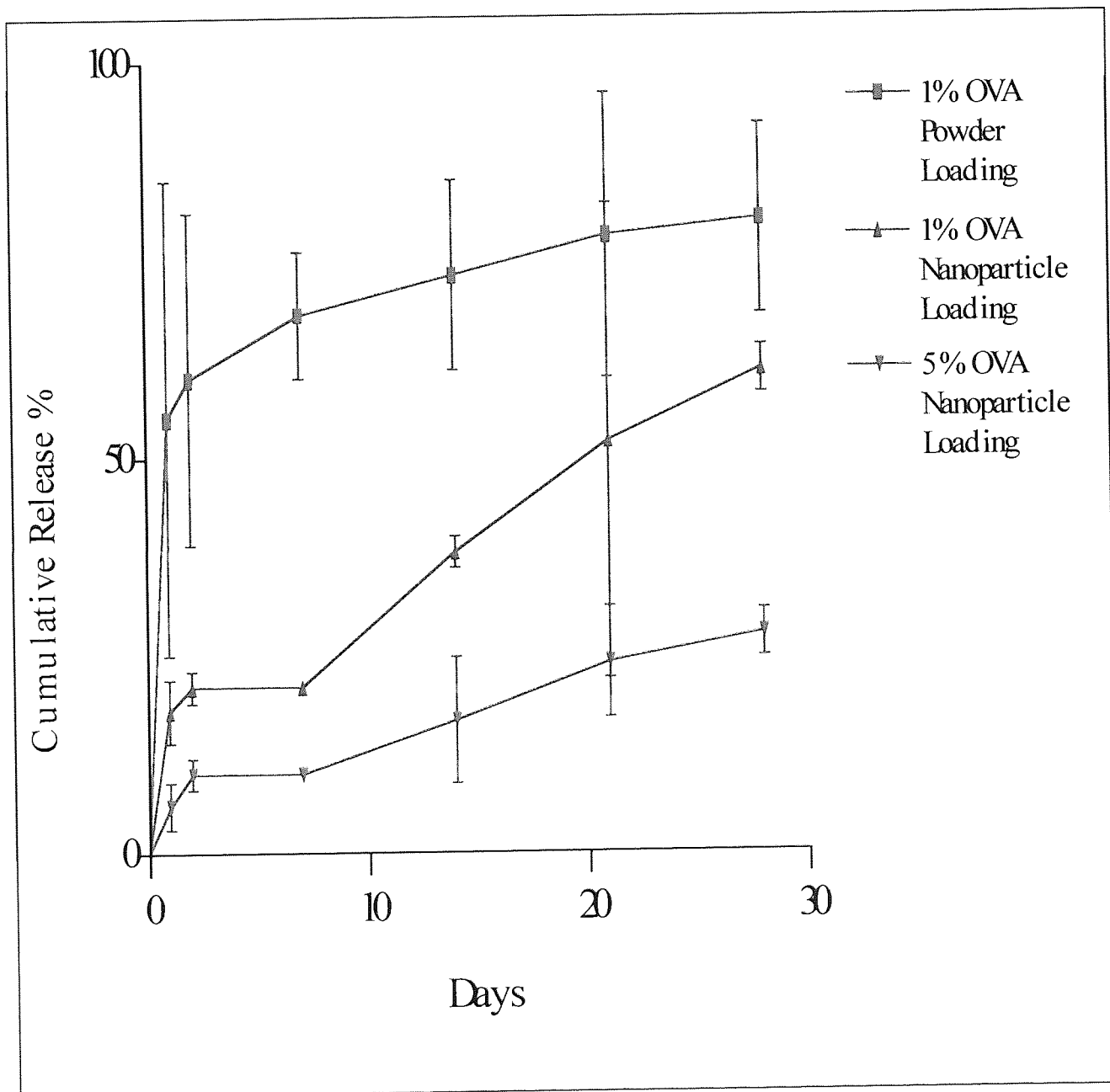


Figure 6.12 Cumulative release % of OVA from PCL fibres with a 1 % OVA powder, 1% OVA nanoparticles and 5% OVA nanoparticles loadings. Release period 28 days. Release medium PBS at 37°C



6.9 The Effect of Lipase in the PBS Release Medium on Protein Release from OVA-Loaded PCL Fibres

The release of OVA from PCL fibres with 1% OVA powder, 1% OVA nanoparticle and 5% OVA nanoparticle loadings respectively is shown in Figure 6.13. Nanoparticles were prepared with and without PVP and lipase was added to the PBS release medium. The fibres with 5% OVA nanoparticle loading (with and without PVP incorporation) released the most protein (11.3 $\mu\text{g}/\text{mg}$) this is a slight decrease compared to previous studies (Figure 6.9 and 6.11). The fibre with 1% OVA powder loading released a slightly decreased amount (8.1 $\mu\text{g}/\text{mg}$) of protein to the 5% OVA nanoparticle loaded fibres. The 1% nanoparticle loaded fibre without PVP released (6.7 $\mu\text{g}/\text{mg}$) in 28 days, which was an increase of 1.1 times (Figure 6.11). The 1% nanoparticles loaded fibres with PVP released the least amount of protein but a slight increase on previous studies (Figure 6.9). All the fibres showed an initial burst release over the first 2 days with the fibres containing PVP modified nanoparticles giving rise to the lowest burst release. Following the initial burst phase the protein release decrease in all systems apart from the 5% nanoparticle loaded fibres with and without PVP, which exhibit an almost linear rate of release over 28 days. All the systems appear to release protein at an increased rate compared to the previous studies (Figure 6.9 and Figure 6.11), in the release profiles in this study there are no plateaus and therefore show continuous release compared to the studies without the presence of lipase. This provides evidence that lipase has some affect upon the release rate of protein from PCL fibres.

Figure 6.13 (A) Cumulative release of OVA from PCL fibres with a 1 % OVA powder, 1% OVA nanoparticles and 5% OVA nanoparticles loadings. PVP incorporated in nanoparticle powder to aid suspension in PCL solution. (B) without PVP incorporated in nanoparticle powder. Release period 28 days. Release medium PBS at 37°C with a 1000 units/ml of lipase.

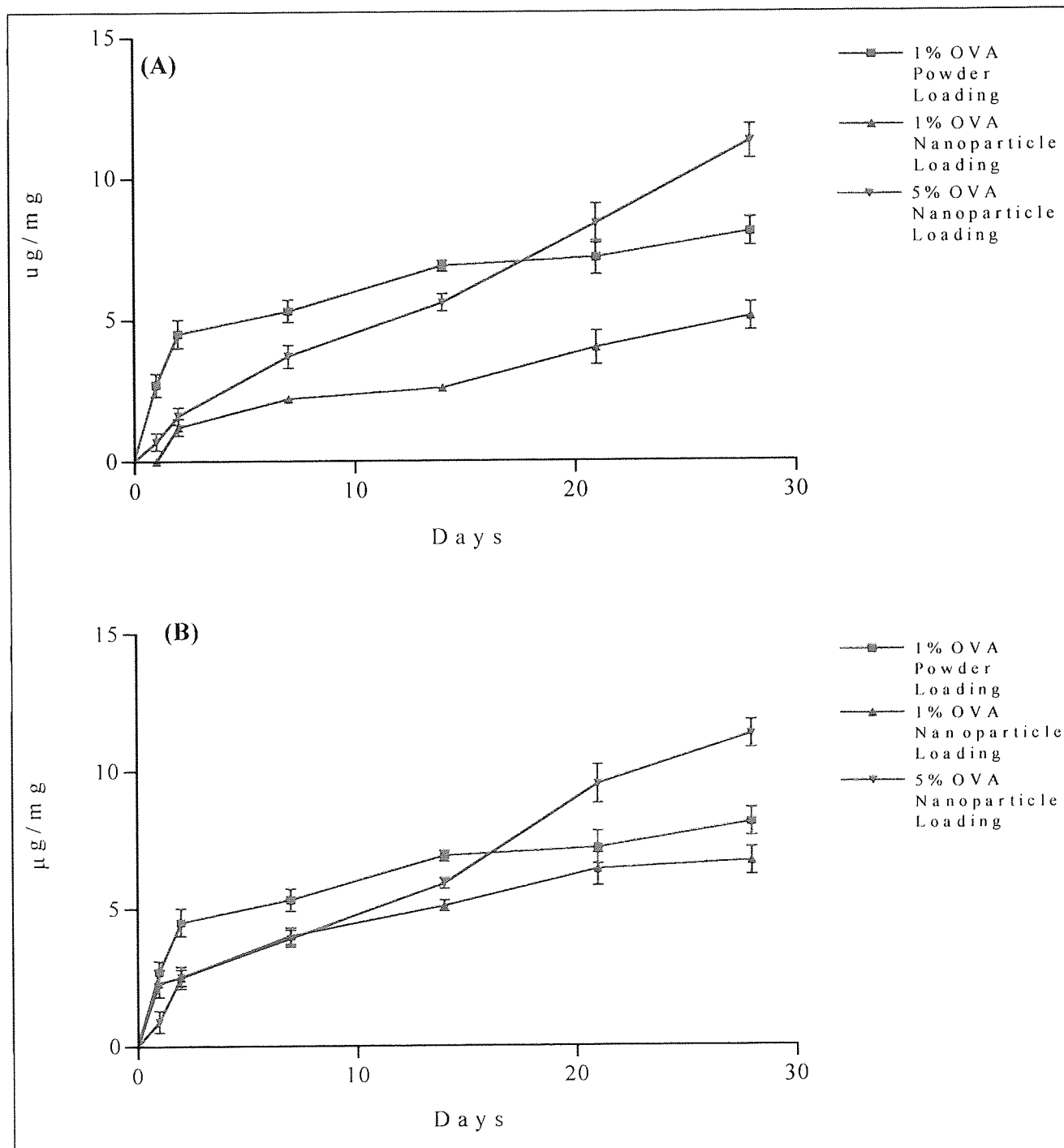
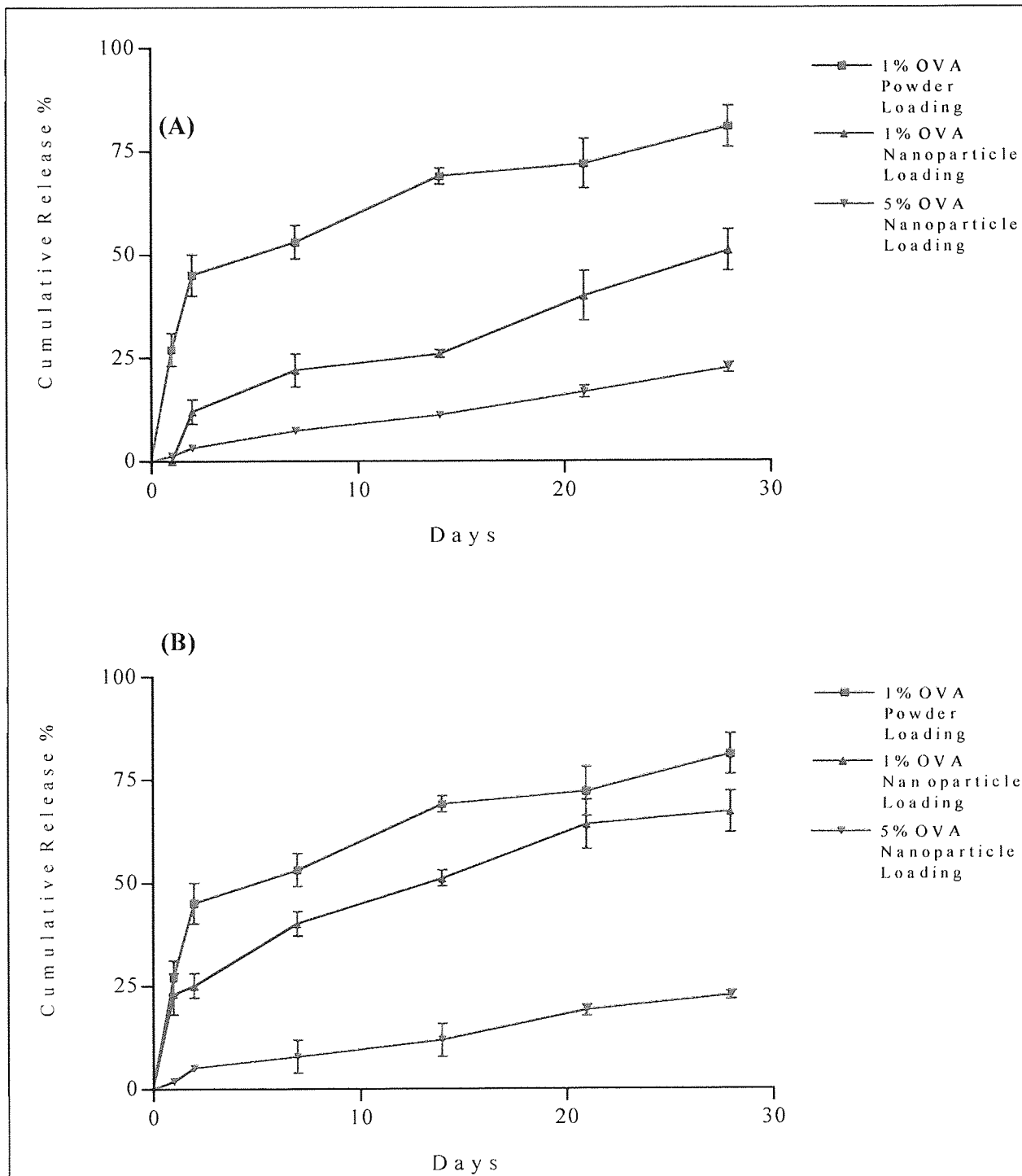


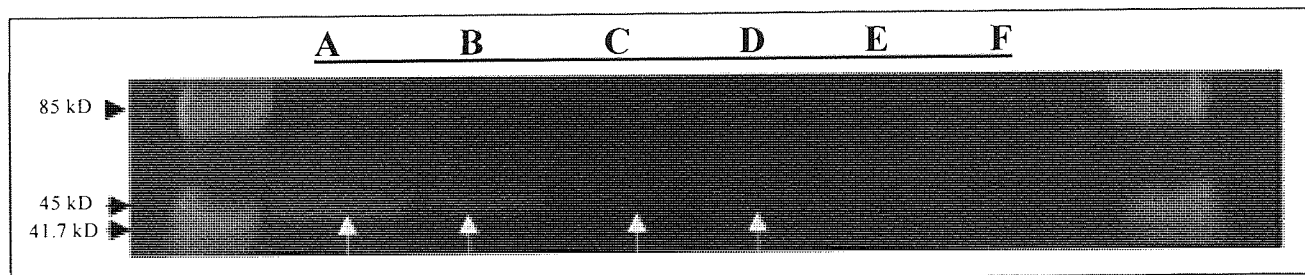
Figure 6.14 (A) Cumulative release % of OVA from PCL fibres with a 1 % OVA powder, 1% OVA nanoparticles and 5% OVA nanoparticles loadings. PVP incorporated in nanoparticle powder to aid suspension in PCL solution. (B) without PVP incorporated in nanoparticle powder. Release period 28 days. Release medium PBS at 37°C with a 1000 units/ml of lipase.



6.10 SDS-PAGE Analysis of Protein Release from PCL Fibres

PCL fibres with a 1% OVA powder or 5% OVA nanoparticles loading were incubated at 37°C in PBS for time periods of 2 and 7 days. The release medium was removed and protein molecular weight was analysed using SDS page to examine if the gravity spinning affects protein structure. Figure 6.15 shows a photograph of the SDS gel. In lanes A and B was OVA solution that had been incubated at 37°C for 2 and 7 days respectively and here clear bands can be seen at 45 kD which is the molecular size of OVA. Lanes C and D show OVA release samples from a 1% OVA powder loaded as-spun PCL fibre incubated for 2 and 7 days respectively, bands can be seen at 45 kD. In lanes E and F are OVA release samples taken at day 2 and day 7 from a 5% OVA nanoparticle loaded fibre. Bands cannot be seen in this photograph as the light intensity could not be adjusted to observe the faint bands which could be seen at 45 kD after staining. This result shows that the incorporation of proteins into the spinning solution and subsequently spinning the fibre does not alter the molecular weight of the protein.

Figure 6.15 Photograph of the a SDS-PAGE gel to analyse protein release from as-spun PCL fibres with a 1% OVA powder or 5% OVA nanoparticles loading and incubated at 37°C for 2 and 7 days. (A) OVA solution (2 days) (B) OVA solution (7 days) (C) 1% OVA powder loading (2 days) (D) 1% OVA powder loading (7 days) (E) 5% OVA nanoparticles loading (2 days) (F) 5% OVA nanoparticles loading (7 days)

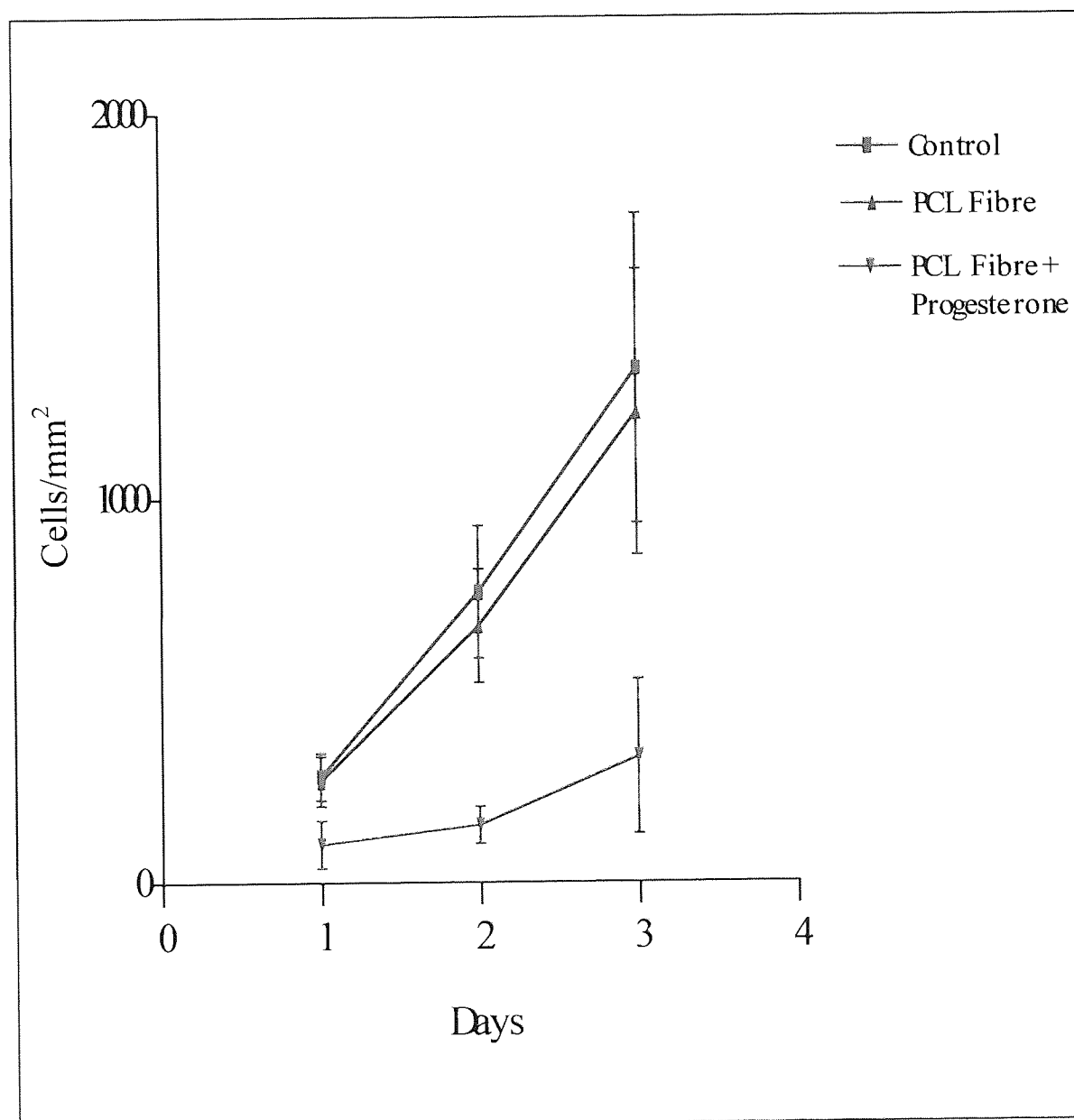


6.11 Release of Progesterone from PCL Fibres

Progesterone was loaded into PCL fibre by gravity spinning using a PCL solution in acetone containing 5% w/v of progesterone. Xhin-I Chang performed the formulation work of this experiment provided the fibre spinning conditions and progesterone loading. The aim of this experiment was to prove that the drugs could be loaded into PCL fibres and released in an active form after gravity spinning.

Figure 6.16 shows the proliferation profiles of MCF-7 breast epithelial cells attached to TCP in the presence of medium that had been incubated for 4 days with an as-spun PCL fibre and a PCL fibre that had been loaded with progesterone respectively. The proliferation curve for the control (medium only) and for the medium that was incubated with an as-spun PCL fibres are very similar and shows that the cells are proliferating. Furthermore the PCL fibre does not release any products that affect cell proliferation. The curve for the cells proliferating in the medium that were incubated with progesterone-loaded PCL fibre demonstrates that the cells are proliferating at a very much-reduced rate. At day 1 the number of cells was decreased by 2.5 fold in comparison to the control and drug-free PCL fibre and by day 2 the cell proliferation was decrease by 5 fold and 4.5 fold respectively compared to the control and drug-free PCL fibre incubated medium respectively. Day 3 showed an increase in cell number for the MCF-7 cells incubated with the progesterone-loaded fibre but the cell number was still 4 and 3.7 fold lower than that of the control and PCL fibre incubated medium respectively.

Figure 6.16 Activity of progesterone released from a PCL fibre over 4 days. Release medium (0.5 ml) was added to MCF-7 breast epithelial cells that were seeded at 2×10^4 and cultured for 3 days following incubation



6.12 Discussion

Bioactive macromolecules have been incorporated into biomaterials for controlled release by several investigators, eg angiogenic growth factors in vascular repair (Zarge et al. 1997), neuronal survival and differentiating factors in neurodegenerative diseases (Haller et al. 1998), growth factor transforming growth factor β for bone repair and plasmid DNA presented to be taken up by smooth and cardiac muscle cells and several others have been reviewed in Whitaker et al. (2001) and Hubbell (1999). Tetracycline hydrochloride (Kenaway et al. 2002) was examined for conventional drug delivery from polymer fibres. The many investigations have examined the use of polymers for controlling drug delivery and growth factor release from tissue engineered constructs. Drug delivery devices (scaffolds, fibres microparticles and nanoparticles) have been loaded or coated with a variety of bioactive agents as mentioned above.

Protein-loaded PCL fibres were produced by spinning from solutions containing protein particulates to investigate the potential for loading and controlled release of biopharmaceuticals such as growth factors. An increase of OVA on the surface of OVA-loaded fibres over time was measured when the fibres were incubated in PBS. Fibre surface may crack and pores expose the protein that was initially covered by the polymer, or alternatively protein particles within the fibre may be increasingly exposed by gradual protein release. The most likely explanation is that the protein that was released from the PCL fibre could have been reabsorbed onto the surface of the fibre (Yamada, 1983 and Hubbell, 1999), as the release media was not removed during the study. Modification of the surface of PCL fibres by adsorption of gelatin from solution demonstrated the potential for attachment of cell adhesion molecules (shown in Chapters 4 and 5) or biopharmaceuticals for modulation of cell/fibre interaction. The attachment of adhesion factors to materials to improve cell attachment, proliferation and differentiation has been investigated extensively. The methods generally involve either direct covalent attachment or physico-chemically incorporating adhesion-promoting oligopeptides and oligosaccharides, which could be used to link different cell types or to initiate different cell functions. For example galactose could be immobilised to promote hepatocyte adhesion (Hubbell, 1999) or

binding short bioactive peptides so that various cell types can be selected, this a common goal in drug targeting (Langer, 1998). In the other situations adhesion ligands could be incorporated in the pores of vascular grafts to promote capillary in growth. The present investigations show that as the concentration of the gelatin coating solution increased the amount of protein bound to the surface decreased. This suggests that the conformation and association of the gelatin molecules in the coating solution affects fibre protein binding.

The release of protein from the PCL fibres could be varied by loading with OVA powder or OVA nanoparticles made with and without PVP (Figures 6.9 and 6.11) therefore demonstrating the potential for controlled delivery of biopharmaceuticals. The initial experiments might not have given an accurate indication of the amount of protein released because the release media was not changed during the experiment and this could have allowed protein to reabsorb onto the fibres surface (Yamada, 1983 and Hubbell, 1999). The experimental model was altered so that the release media was changed to give an improved result. In subsequent experiments the PCL fibres loaded with the various concentrations and types of OVA showed a burst of release from day 0 to day 2. The largest burst effect was observed from PCL fibres loaded with OVA powder, probably due to the powder particles protruding through the fibre surface (Figure 6.4). The PCL fibres loaded with the OVA nanoparticles (784.9 nm) exhibited a smaller burst effect probably due the nanoparticles being more effectively covered by the PCL in the fibre formation. The burst effect seen with the release of proteins from the PCL fibres could have application within the initial stages of wound repair. The fibres could be loaded with chemotaxins to recruit the specific cell types required over the first 24 hours and/or with growth factors like VEGF to initiate angiogenesis and other growth factors to enhance cell proliferation and therefore decreasing the time taken for wound repair.

The PCL fibres showed gradual OVA release over time after a burst phase but 100% release was not achieved. This behaviour may be compared to results obtain by Sohier et al. (2002) who investigated lysozyme release from polymer films that then coated porous scaffolds for repair of tissue. The results showed that 100% protein release varied form 1 day to 50 days. Murphy et al. (2000) looked at VEGF from PLG

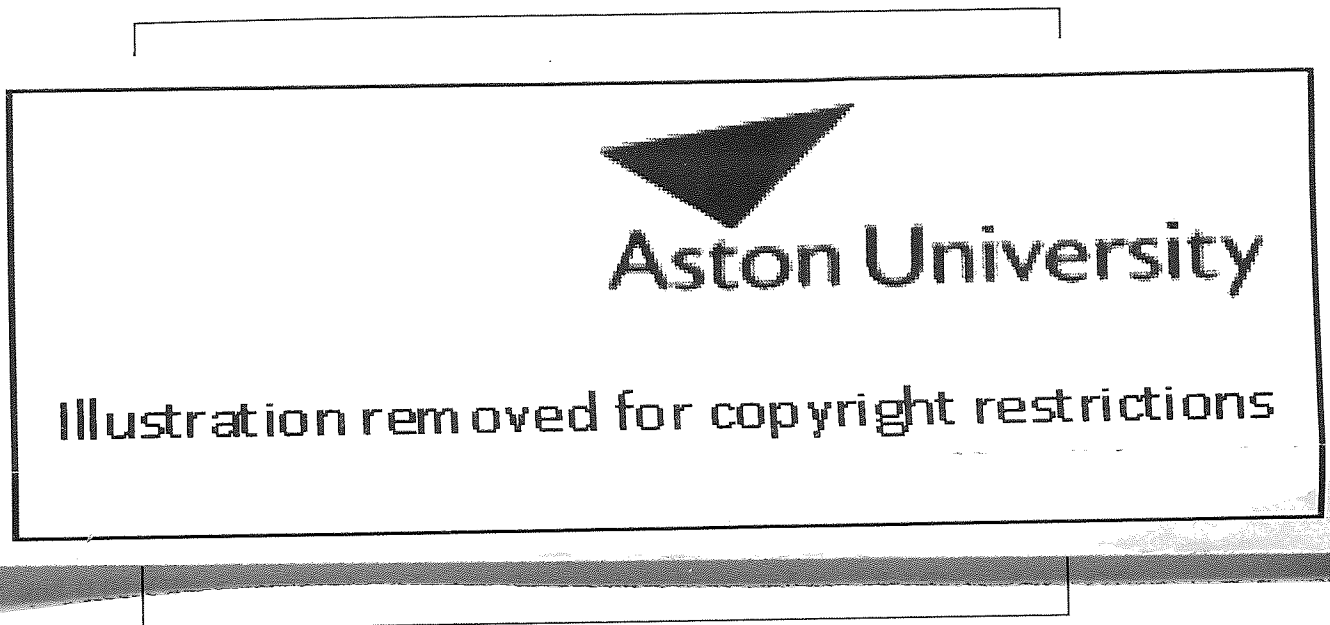
scaffolds for increasing bone repair. This study observed protein release over 15 days and achieved 85% release in this time. Kenaway et al. (2002) showed 100% tetracycline release from electrospun PEVA and PLA blend fibres over 5 days. The release profiles of the PCL fibres loaded with the OVA nanoparticles made with and without PVP were very similar. The PCL fibres with 5% OVA nanoparticles loading (with and without PVP) both release approximately 13 $\mu\text{g}/\text{mg}$, which about 25% release over 28 days. The 1% nanoparticle loadings (with and without PVP) both released approximately 5 $\mu\text{g}/\text{mg}$ that equated to 50% release. The 1% OVA powder loaded fibre the release of OVA was approximately 8 $\mu\text{g}/\text{mg}$, this was slightly a higher release rate with almost 80% of protein released. This is probably due to powder particles protruding through the fibre surface causing a more porous fibre allowing fluid to dissolve the protein incorporated within the fibre. Compared to PCL fibres loaded with the OVA nanoparticles, which exhibited a less porous surface probably due to the fact that the nanoparticles were covered more effectively by the PCL in the fibre formation.

The release of OVA from the PCL fibres in the presence of lipase to investigate enzymatic control of protein delivery. Lipase has been widely investigated to degrade PCL (Chen et al. 2000, Gan et al. 1999, Hirotsu et al. 2000, Tsuji et al. 2001). Lipase primarily involves the hydrolysis of the ester bonds in the polymer chain backbone. There are two proposed mechanisms of how this is achieved. The first is that the enzyme binds to the polymer substrate and then catalyses the hydrolytic scission of the polymer chains (Gan et al. 1999). The second process involves enzymatic biodegradation mainly on the polymer surface because it is difficult for a hydrophilic enzyme to diffuse into a hydrophobic polymer (Huang et al. 1994). Lipase was added to the release media to investigate the potential for enzymatic enhanced biodegradation of the PCL fibre resulting in increased protein release. The results showed that the amount of protein released did not increase in the presence of lipase but there was a change in release profile for fibres with 1% OVA nanoparticle and 5% OVA nanoparticle loading. An initial burst was present and an increased release rate compared with the experiment without lipase that appears to flatten after the initial burst before a second burst (Figures 6.9 and 6.11).

SDS-PAGE was then used to analyse the molecular weight to investigate if OVA had been denatured during gravity fibre spinning. The results from this study (Figure 6.15) showed that the protein's molecular weight had not altered after being spun into fibres. This shows that the PCL fibres have potential for incorporation of other proteins, such as growth factors without damage to their structure and therefore their function.

Progesterone was incorporated into gravity spun PCL fibres to investigate the potential for drug loading and retaining the activity of drug molecules during fibre spinning. Progesterone is a lipophilic steroid that produces its effect in target cells by enhancing the synthesis of new enzymatic or structural proteins. Progesterone diffuses through the plasma membrane (Figure 6.17) of the cell and binds with its receptor located in the nucleus. The receptor-steroid complex then binds with a specific region on DNA known as the hormone response element (HRE). The binding of the receptor-steroid complex "turns on" specific genes within the cell and the activated genes direct the synthesis of a new cell protein, which has a physiological effect (Sherwood, 1997). One physiological effects of progesterone is to inhibit cell growth of human breast epithelial cells (Dereux et al. 2000, Malet et al. 2000, Sager et al. 2003). The result in Figure 6.16 show that the progesterone released from the PCL fibres does have a pronounced affect upon the MCF-7 cells and does inhibit their proliferation, demonstrating activity retention after fibre spinning. The grow curves show a slight increase in proliferation at day 3, this is due to the rapid metabolism of progesterone in cultured breast epithelial cells (Matel et al. 2000) and if continued suppression of growth was required then additional treatment with the release media would be needed. The progesterone activity results show that steroids can be incorporated into PCL fibres produced by gravity spinning for subsequent release to control cell response. Similar drugs have been incorporated into fibres which have shown release, Kenawy et al. (2002) investigated release of tetracycline hydrochloride from electrospun PEVA and PLA blend fibres for a drug delivery model and Denkbas et al. (2000) examined 5-fluorouracil from wet spun chitosan fibres for enhancing tissue repair but neither of these studies showed activity of the molecule after release.

Figure 6.17 Schematic diagram of steroid receptor and how it acts to bring about a physiological change to its target cells. (www.members.aol.com)



The low shear conditions used to produce PCL fibres would avoid shear-induced degradation of biopharmaceuticals. In addition PCL's desirable characteristics of high permeability to low molecular weight drugs (<400 Da) means that it can be used in diffusion-controlled delivery of hormones and antibiotics (Pitt et al. 1979). The lack of toxicity of PCL also makes it of interest as a matrix for controlled-release (Lin et al. 1994).

CHAPTER 7

SUMMARY AND GENERAL DISCUSSION

The PCL fibre spinning technique described in Chapter 3 involves free flow of polymer solution through a spinneret under gravity and was found to be dependant on two key factors. Firstly the viscosity of the PCL solution over the concentration range investigated (6-20% w/v) was sufficiently low to allow the solution to pass through the spinneret orifice under gravity. Secondly the choice of solvent/non-solvent system was found to be critical, the higher polymer solution density relative to the non-solvent allowed free-fall of the polymer solution stream, avoiding flotation of the polymer solution on the surface of the non-solvent. The tensile strength and stiffness of as-spun fibres were highly dependent on the concentration of the spinning solution. Use of a 6% w/v solution resulted in fibres having strength and stiffness of 1.8 MPa and 0.01 GPa respectively, whereas these values increased to 9.9 MPa and 0.1 GPa when fibres were produced from 20% w/v solutions. Cold drawing to an extension of 500% resulted in further increases in fibre strength (up to 50 MPa) and stiffness (0.3 GPa). Hot drawing to 500% further increased the fibre strength (up to 81 MPa) and stiffness (0.5 GPa). The surface morphology of as-spun fibres was modified, to yield a directional grooved pattern by drying in contact with a mandrel having a machined topography characterised by a peak-peak separation of 91 μm and a peak height of 30 μm . DSC analysis of as-spun fibres revealed the characteristic melting point of PCL at around 58°C and a % crystallinity of approximately 60%.

PCL fibres are able to promote fibroblast and myoblast attachment in cell culture and sustain proliferation similar to TCP (Chapter 3). All of the PCL fibres (as-spun, 500% cold drawn and gelatin coated as-spun) could support cell attachment and growth at significantly higher rates than Dacron monofilament. The PCL fibre's ability to enhance initial cell attachment was greater than TCP surfaces but the proliferation rate did not exceed that on TCP. The good proliferation rates of cells on the PCL fibres are brought about by the material's favourable surface properties, which positively influence cellular events at the cell-biomaterial interface. Surface modification of PCL fibres by coating with gelatin increases cell attachment. Myoblasts and fibroblasts attached and proliferated at an increased rate over 5 days on the gelatin-

coated fibres compared with TCP. The cold drawn PCL fibres enhanced attachment and proliferation of fibroblasts and myoblasts relative to as-spun fibres suggest that cells use the oriented, fibillar morphology of the substrate for orientation and migration.

As with the fibroblasts and myoblasts, as-spun PCL fibres could promote attachment and sustain proliferation of HUVECs similar to TCP (Chapter 5). The fibres coated with gelatin and cold drawn to 500% showed an increased rate of attachment and proliferation rate compared with the as-spun PCL fibres. The favourable surface properties of as-spun PCL fibres for HUVEC adhesion and growth are reflected by the confluent monolayer of cells, which was generally observed during SEM analysis.

Maintenance of cell function in tissue engineering is an important aspect that is often not investigated in detail. The retention of HUVECs function when attached to PCL fibres was investigated by monitoring the capability of HUVECs to increase the amount of intracellular adhesion molecule-1 (ICAM-1) following an inflammatory stimulus (Chapter 5). The HUVECs grown on as-spun PCL fibres responded in the same way they did on TCP after stimulating with LPS. Cells on both substrates demonstrated a similar increase in expression of surface ICAM-1 that was measured by flow cytometry. This was confirmed by examining the levels of ICAM-1 mRNA using RT-PCR. The levels of ICAM-1 mRNA increased after stimulation with LPS indicating an up-regulation in gene expression for the ICAM-1 cell surface receptor. The results demonstrate that HUVECs attached to as-spun PCL fibres display comparable function comparable with TCP (a substrate that should not alter cell response) with respect to ICAM-1.

Protein-loaded PCL fibres (Chapter 6) were produced by spinning from solutions containing protein particulates to investigate the potential for loading and controlled release of biopharmaceuticals such as growth factors. PCL fibres loaded with various concentrations and types of OVA showed a burst of release from day 0 to day 2. The largest burst effect was observed from PCL fibres loaded with OVA powder, probably due to the powder particles protruding through the fibre surface. The PCL fibres loaded with the OVA nanoparticles exhibited a smaller burst effect probably due the

nanoparticles being more effectively covered by the PCL in the fibre formation. The observed burst release of proteins from the PCL fibres could have application for growth factor delivery in the initial stages of wound repair. The PCL fibres incorporating 5% w/w OVA nanoparticles loading released approximately 13 $\mu\text{g}/\text{mg}$ in total, which about 25% release over 28 days. The 1% nanoparticle loaded released approximately 5 $\mu\text{g}/\text{mg}$ that equated to 50% release. The 1% OVA powder loaded fibres the released 8 $\mu\text{g}/\text{mg}$ in total, with almost 80% of protein released over 28 days. This behaviour is probably due to powder particles protruding through the fibre surface causing a more porous fibre and allowing fluid to dissolve the protein incorporated within the fibre.

Lipase was added to the release media to investigate the potential for enzymatic enhanced biodegradation of the PCL fibre resulting in increased protein release. The amount of protein released did not increase in the presence of lipase but there was an increase in release profile for fibres loaded with 1% w/w OVA nanoparticle and 5% OVA nanoparticle loading. An initial burst was present and an increased release rate compared with the experiment without lipase that appeared to flatten after the initial burst before a second burst. SDS-PAGE was used to analyse the structural integrity of OVA from PCL fibres. The results showed that the molecular weight of the protein compared after being incorporated into fibres. These experiments indicated that the PCL fibres have potential for incorporation of proteins, such as growth factors, without damaging their structure and therefore their function.

Progesterone was incorporated into gravity spun PCL fibres to investigate the potential for drug loading and retaining the activity of drug molecules during fibre spinning. The result showed that the progesterone released from the PCL fibres does have a pronounced affect upon the MCF-7 breast epithelial cells inhibiting their proliferation and thus demonstrating activity retention after fibre spinning.

Gravity spun PCL fibres display high fibre compliance, the potential for controlling the fibre surface architecture to promote contact guidance effects, a favourable proliferation rate of fibroblasts, myoblasts and HUVECs and the ability to release pharmaceuticals. The PCL fibres can therefore be recommended for use in 3-D

scaffold production in soft tissue engineering and could be exploited for controlled presentation and release of biopharmaceuticals such as growth factors.

REFERENCES

- Abatangelo G, O'Regan M. Hyaluronan: biological role and function in articular joints. *European Journal of Rheumatology and Inflammation* 1995;15:9-16
- Alberts B, Bray D, Lewis J, Raff M, Watson J. *Molecular Biology of the Cell*. New York: Garland Publishing Inc. 1994:357
- Ali SA, Zhong SP, Doherty PJ, Willimas DF. Mechanisms of polymer degradation in implantable devices I. PCL. *Biomaterials* 1993;14:648-656
- Anderson JM. Inflammatory response to implants. *Transactions American Society of Artificial Internal Organs* 1988;34:101-107.
- Anderson JM, Langone JJ. Issues and perspectives on the biocompatibility and immunotoxicity evaluation of implanted controlled release systems. *Journal of Controlled Release* 1999;57:107-113.
- Aplin AE, Howe A, Alahari SK, Juliano RL. Signal transduction and signal modulation by cell adhesion receptors: The role of integrins, cadherins, immunoglobulin-cell adhesion molecules, and selectins. *Pharmacological Reviews* 1998;50:2:197-263
- Assoian RK, Zhu X. Cell anchorage and the cytoskeleton as partners in growth factor dependent cell cycle progression. *Current Opinion in Cell Biology* 1997;9:93-98
- Babensee JE, Anderson JM, McIntire LV, Mikos AG. Host response to tissue engineered devices. *Advanced Drug Delivery Reviews* 1998;33:111-139.
- Badylak S, Liang, Record R, Tullius R, Hodde J. Endothelial cell adherence to small intestinal submucosa: an acellular bioscaffold. *Biomaterials* 1999;20:2257-63

Bass MD, Humphries MJ. Cytoplasmic interactions of syndecan-4 orchestrate adhesion receptor and growth factor receptor signalling. *Journal of Biochemistry* 2002;368:1-15

Bhat VD, Truskey GA, Reichert WM. Improving endothelial cell adhesion on vascular graft surfaces: clinical need and strategies. *Journal of Biomaterial Science Polymer Edition* 1998;9:1117-35

Bonasser TJ, Vacanti CA. Tissue engineering: The first decade and beyond. *Journal of Cellular Biochemistry* 1998;30:297-303.

Boyan BD, Hummert TW, Dean DD, Schwartz Z. Role of material surfaces in regulating bone and cartilage cell response. *Biomaterials* 1996;17:137-146

Burg KJL, Porter S, Kellam JF. Biomaterial developments for bone tissue engineering. *Biomaterials* 2000;21:2347-2359

Campoccia D, Doherty P, Radice M, Brun P, Abatangelo G, Williams DF. Semisynthetic resorbable materials from hyaluronan esterification. *Biomaterials* 1998;19:2101-2127

Cenni E, Granchi G, Verri E, Cavedagna D, Gamberini S, Cervellati M, Di Leo A, Pizzoferrato A. Expression of adhesion molecules on endothelial cells after contact with knitted Dacron. *Biomaterials* 1997;18:489-94

Chakravorty D, Kato Y, Koide N, Sugiyama T, Kawai M, Fukada, Yoshida, Yokochi T. Production of tissue factor in CD14-expressing human umbilical vein endothelial cells by lipopolysaccharide. *FEMS Microbiology Letters* 1999;178:235-39

Chan BP, Bhat VD, Yegnasubramanian S, Reichert WM, Truskey. An equilibrium model of endothelial cell adhesion via integrin-dependent and integrin-independent ligands. *Biomaterials* 1999;20:2395-2403

- Chehroudi B, Gould TR, Bunette DM. A light and electron microscopic study of the effects of surface topography on the behaviour of cells attached to titanium-coated precutaneous implants. *Journal of Biomedical Material Research* 1991;25:387-405
- Chen DR, Bei JZ, Wang SG. Polycaprolactone microparticles and their biodegradation. *Polymer degradation and stability* 2000;67:455-59
- Chen G, Lin W, Coombes A, Davis SS, Illum L. Preparation of human serum albumin microspheres by a novel acetone-heat denaturation method. *Journal of Microencapsulation* 1994;11:395-407
- Chu CC. Biodegradable polymeric biomaterials: an updated overview. In: Bronzino JD editor. *The biomedical engineering handbook*. CRC Press;2000. p41-2
- Chu CFL, Lu A, Liszkowski M, Sipehia R. Enhanced growth of animal and human endothelial cells on biodegradable polymers. *Biochimica et Biophysica Acta* 1999;1472:479-85
- Coombes AGA, Meikle AMC. Resorbable synthetic polymers as replacements for bone graft. *Clinical Materials* 1994;17:35-67
- Costantino HR, Schwendeman SP, Langer R, Klibanov AM. Deterioration of lyophilized pharmaceutical proteins. *Biochemistry* 1998;63:357-63
- Couchman JR, Woods A. Syndecan-4 and Integrins: combinatorial signalling in cell adhesion. *Journal of Cell Science* 1999;112:3415-20
- Curtis ASG, Seehar GM. The control of cell division by tension or diffusion. *Nature* 1978;274:52-3
- Curtis ASG. Mechanical tensing of cells and chromosome arrangement. In Lyall F, El Haj AJ editors. *Biomechanics and Cells*. Cambridge University Press. Cambridge 1994:121-130

Dalby MJ, Riehle MO, Johnstone H, Affrossman S, Curtis ASG. In vitro reaction of endothelial cells to polymer demixed nanotopography. *Biomaterials* 2002;23:2945-54

Dalby MJ, Riehle MO, Yarwood SJ, Wilkinson CDW, Curtis ASG. Nucleus alignment and cell signalling in fibroblasts: response to a micro-grooved topography. *Experimental Cell Research* 2003;284:274-82

Daniels JT, Kearney JN, Ingham E. An investigation into the potential of extracellular matrix factors for attachment and proliferation of human keratinocytes on skin substitutes. *Burns* 1997;23:1:26-31

Deligianni DD, Katsala N, Ladas S, Sotiropoulou D, Amedee J, Missirlis YF. Effect of surface roughness of the titanium alloy Ti-6Al-4V on human bone marrow cell response and on protein adsorption. *Biomaterial* 2001;22:1241-1251

Denkbas EB, Seyyal M, Piskin E. Implantable 5-fluorouracil loaded chitosan scaffolds prepared by wet spinning. *Journal of Membrane Science* 2000;172:33-38

Desreux J, Kebers F, Noel A, Francart D, van Cauwenberge H, Heinen V, Thomas JL, Bernard AM, Paris J, Delansorne R, Foidart JM. Progesterone receptor activation: an alternative to SERMs in breast cancer. *European Journal of Cancer* 200;36:81-91

Eiselt P, Yeh J, Latvala RK, Shea LD, Mooney DJ. Porous carriers for biomedical applications based on alginate hydrogels. *Biomaterials* 2000;21:1921-7

Eling B, Gogolewski S, Pennings AJ. Biodegradable materials of poly (L-lactic acid) 1. *Polymer* 1982;23: 1587-93

Engelberg I, Kohn J. Physicomechanical properties of degradable polymers used in medical applications - a comparative study. *Biomaterials* 1991;12(3):292-304

Fambri L, Pegoretti A, Fenner R, Incardona SD, Migliaresi C. Biodegradable fibres. Poly-L-lactic acid fibres produced by solution spinning. *Journal of Material Science in Medicine* 1994;5:679-683

Fabrizius-Homan DJ, Cooper SL. A comparison of the adsorption of the three adhesive proteins to biomaterial surfaces. *Journal of Biomaterial Science Polymer Edition* 1991;3:27-47

Freed LE, Vunjak-Novakovic G, Biron RJ, Eagles DB, Lesnoy DC, Barlow SK, Langer R. Biodegradable polymer scaffolds for tissue engineering. *Biotechnology* 1994;12:689-93.

Freed LE, Vunjak-Novakovic G. Culture of organised cell communities. *Advanced Drug Delivery Reviews* 1998;33:15-30

Frey EA, Miller DS, Jahr TG, Sundan A, Bazil V, Espevik, Finlay BB, Wright SD. Soluble CD14 participates in the response of cells to lipopolysaccharide. *Journal of Experimental Medicine* 1992;92:1665-71

Freyman TM, Yannas IV, Gibson LJ. Cellular materials as porous scaffolds for tissue engineering. *Progress in Materials Science* 2001;46:273-82

Fu K, Griebenow K, Hsieh L, Klibanov AM, Langer R. FTIR characterization of the secondary structure of proteins encapsulated within PLGA microspheres. *Journal of Controlled Release* 1999;58:357-66

Furst-Ladani S, Redl H, Haslberger A, Lubitz W, Messner P, Sleytr UB, Schlag G. Bacterial cell envelopes (ghosts but not S-layers activate human endothelial cells (HUVECs) through sCD14 and LBP mechanism. *Vaccine* 2000;18:440-48

Galassi G, Brun P, Radice M, Cortivo R, Zanon GF, Genovese P, Abatangelo G. In vitro reconstructed dermis implanted in human wounds: degradation studies of the HA-based supporting scaffold. *Biomaterials* 2000;21:2183-91

Galletti PM, Hellman KB, Nerem RM. Tissue engineering: From basic science to products: A preface. *Tissue Engineering* 1995;1:147-149.

Gan Z, Fung JT, Jing X, Wu C, Kuliche WK. A novel laser light-scattering study of enzymatic biodegradation of poly(ϵ -caprolactone) nanoparticles. *Polymer* 1999;40:1961-67

Gogolewski S, Pennings A.J. Resorbable materials of poly(L-lactide) 2. *Journal of Applied Polymer Science* 1983;28:1045-1061

Grinnell F, Feld MK. Fibronectin absorption on hydrophilic and hydrophobic surfaces detected by antibody binding and analysed during cell adhesion in serum-containing medium. *Journal of Biological Chemistry* 1982;257:488-93

Griffith LG. *Polymeric Biomaterials*. *Acta Materialia* 2000;48:263-277.

Griffith LG. *Biomaterials*. WTEC Tissue Engineering Research Report 2000:7-15

HaeYong Kweon, Mi Kyong Yoo, In Kyu Park, Tae Hee Kim, Hyun Chul Lee, Hyun-Sook Lee, Jong-Suk Oh, Toshihiro Akaike and Chong-Su Cho. A novel degradable polycaprolactone networks for tissue engineering. *Biomaterials* 2003;24;5:801-8

Hailman E, Vasselon T, Kelley M, Busse LA, Hu MCT, Lichenstien HS, Detmers PA, Wright SD. Stimulation of macrophages and neutrophils by complexes of lipopolysaccharide and soluble CD14. *Journal of Immunology* 1996;170:4384-90

Hall LL, Bicknell GR, Primrose L, Pringle JH, Shaw JA, Furness PN. Reproducibility in the quantification of mRNA levels by RT-PCR-ELISA and RT competitive-PCR-ELISA. *Biotechniques* 1998;24:652-664

Hansen LK, Mooney DJ, Vacanti JP, Ingber DE: Integrin binding and cell spreading on extracellular matrix act at different points in the cell cycle to promote hepatocyte growth. *Molecular Biology of the Cell* 1994;5:967-975.

- Hanson SJ. Mechanical evaluation of resorbable copolymers for end use as vascular grafts. *ASAIO Transactions* 1998;34:789-93
- Hellman KB, Knight E, Durfor CN. Tissue engineering: Product applications and regulatory issues. In W.C. Patrick, A.G. Mikos, and L.V. McIntire, editors. *Frontiers in tissue engineering* 1998;Amsterdam: Elsevier Science:341-366.
- Hellman KB, Solomon RR, Gaffey C, Durfor CN, Bishop JG. Tissue engineering: Regulatory considerations. In Lanza R, Langer R, Vacanti JP, editors. *Principles of tissue engineering*, 2nd edition 2000; San Diego, CA: Academic Press:915-928.
- Hench LL, Wilson J. Surface-active biomaterials. *Science* 1984;226: 630- 6.
- Hench LL, Polak JM. Third-generation biomedical materials. *Science* 2002;295:1014- 7.
- Hirotsu T, Ketelaars AAJ, Nakayama K. Biodegradation of poly(ϵ -caprolactone)-polycarbonate blend sheets. *Polymer Degradation and Stability* 2000;68:311-16
- Huang SJ, Ho LH, Huang MT, Koeing MF, Cameron JA. In: Doi Y, Fukuda K, editors. *Biodegradable plastics and polymers*. Amsterdam: Elsevier, 1994:3-7
- Hubbard AK, Rothlein R. Intercellular adhesion molecule-1 (ICAM-1) expression and cell signalling cascades. *Free Radical Biology & Medicine* 200;28;9:1379-86
- Hubbell JA. Biomaterials in tissue engineering. *Biotechnology* 1995;13:565-576
- Hubbell JA. Bioactive biomaterials. *Current opinion in biotechnology* 1999;10:123-29
- Hutmacher DW. Polymer scaffolds in tissue engineering bone and cartilage. *Biomaterials* 2000;21:2529-2543

Hynes RO. Integrins: Versatility, modulation, and signalling in cell adhesion. *Cell* 1992;69:11-25

Ingber DE, Prustry D, Sun Z, Betensky H, Wang N. Cell shape, cytoskeletal mechanics, and cell cycle control in angiogenesis. *Journal of Biomechanics* 1995;28:1471-84

Ingber DE. Mechanochemical switching between growth and differentiation by extracellular matrix. In Lanza RP, Langer R, Chicks W. Editors. *Principles of Tissue Engineering*. Academic Press and RG Landes, Texas USA. 1997;89-100

Imegu OJ, Entersz I, Graham AM, Nackman GB. Heterotypic smooth muscle cell/endothelial cell interactions differ between species. *Journal of Surgical Research* 2001;98:85-88

Ishii Y, Shuyi W, Kitamura S. Soluble CD14 in serum mediates LPS-induced increase in permeability of bovine pulmonary arterial endothelial cell monolayers in vitro. *Life Sciences* 1995;56:2263-72

Ito Y. Surface micropatterning to regulate cell functions. *Biomaterials* 1999;20:2333-2342

Jackson JK, Springate CM, Hunter WL, Burt HM. Neutrophil activation by plasma opsonized polymeric microspheres: inhibitory effect of Pluronic F127. *Biomaterials* 2000;21:1483-91

Kao WJ. Evaluation of protein-modulated macrophage behaviour on biomaterials: designing biomimetic materials for cellular engineering. *Biomaterials* 1999;20:2213-21

Kast CE, Frick W, Losert U, Bernkop-Schnürch A. Chitosan-thioglycolic acid conjugate: a new scaffold material for tissue engineering? *International Journal of Pharmaceutics* 2003. In Press

Kenawy E, Bowlin GL, Mansfield K, Layman J, Simpson DG, Sanders EH, Wnek GE. Release of tetracycline hydrochloride from electrospun poly(ethylene-co-vinylacetate), poly(lactic acid), and a blend. *Journal of Controlled Release* 2002;81:57-64

Kenawy E, Layman JM, Watkins JR, Bowlin, Matthews JA, Simpson DG, Wnek GE. Electrospinning of poly(ethylene-co-vinyl alcohol) fibres. *Biomaterials* 2003;24:907-13

Kirkpatrick CJ, Dekker A. Quantitative evaluation of cell interaction with biomaterials in vitro. *Advances in Biomaterials* 1992;10:31-41

Kirkpatrick CJ, Krump-Konvalinkova V, Unger RE, Bittinger UF, Otto M, Peters K. Tissue response and biomaterial integration: the efficacy of in vitro methods. *Biomolecular Engineering* 2002;19:211-17

Kromm FX, Lorroit T, Coutand B, Harry R, Quenisset JM. Tensile and creep properties of ultra high molecular weight PE fibres. *Polymer Testing* 2003;22:463-470

Kumar TRS, Krishnan LK. Endothelial cell growth factor (ECGF) enmeshed with fibrin matrix enhances proliferation of EC in vitro. *Biomaterials* 2001;22:2769-76

Langer R, Vacanti JP. Tissue engineering. *Science* 1993; 260; 920-924

Langer R. Drug delivery and targeting. *Nature* 1998;392:5-10

Langer R. Selected advances in drug delivery and tissue engineering. *Journal of Control Release* 1999;62:7-11.

LaVan DA, Lynn DM, Langer R. Moving smaller in drug discovery and delivery. *Nature Reviews Drug Discovery* 2002;1:77-84

Lee SB, Jeon HW, Lee YW, Lee YM, Song KW, Park MH, Nam YS, Ahn HC. Bio-artificial skin composed of gelatin and (1-3, (1-6)- β -glucan. *Biomaterials* (In press)

Leenslag JW, Gogolewski S, Pennings AJ. Resorbable materials of poly (L-lactide) V Influence of secondary structure on the mechanical properties and hydrostability of poly(L-lactide) fibres produced by a dry spinning method. *Journal of Applied Polymer Science* 1984;29: 2829-2842

Leor J, Aboulafia-Etzion S, Dar A, Shapiro L, Barbash IM, Battler A, Granot Y, Cohen. Bioengineered cardiac grafts: A new approach to repair the infarcted myocardium? *Circulation* 2000;102:56-61

Lin WJ, Flanagan DR, Linhardt RJ. Accelerated degradation of poly(ϵ -caprolactone) by organic amines. *Pharmaceutical Research* 1994;11;7:1030-34

Lisignoli G, Zini N, Remiddi G, Piacentini A, Puggioli A, Trimarchi C, Fini M, Maraldi NM, Facchini A. Basic fibroblast growth factor enhances in vitro mineralization of rat bone marrow stromal cells grown on non-woven hyaluronic acid based polymer scaffold. *Biomaterials* 2001;22:2095-105

Lloyd LL, Kennedy JF, Methacanon P, Paterson M, Knill CJ. Carbohydrate polymers as wound management aids. *Carbohydrate Polymers* 1998;37:315-22

Lowry KJ, Hamson KR, Bear L, Peng YB, Calaluce R, Evans ML, Anglen JO, Allen WC. Polycaprolactone/glass bioabsorbable implant in a rabbit humerus fracture model. *Journal of Biomedical Materials Research* 1997;36:536-41

Lysaght MJ, O'Loughlin JA. Demographic scope and economic magnitude of contemporary organ therapies. *ASAIO Journal* 2000;46:515-521.

Lysaght MJ, Reyes J. The growth of tissue engineering. *Tissue Engineering* 2001;7;5:485-488

Ma J, Wang H, He B, Chen J. A preliminary in vitro study on the fabrication and tissue engineering applications of a novel chitosan bilayer material as a scaffold of human neonatal dermal fibroblasts. *Biomaterials* 2001;22:331-6

Madhally SV, Matthew HW. Porous chitosan scaffolds for tissue engineering. *Biomaterials* 1999;20:1133-42

Malet C, Spritzer P, Guillaumin, Kuttenn F. Progesterone effect on cell growth, ultrastructural aspect and estradiol receptors of normal human breast epithelial (HBE) cells in culture. *Journal of Steroid Biochemistry and Molecular Biology* 2000;73:171-181

Mann BK, Tsai AT, Scott-Burden T, West JL. Modification of surfaces with cell adhesion peptides alters extracellular matrix deposition. *Biomaterials* 199;21:2281-86

Marijnissen WJ, van Osch GJ, Aigner J, van der Veen SW, Hollander AP, Verwoerd-Verhoef HL, Verhaar JA. Alginate as a chondrocyte-delivery substance in combination with a non-woven scaffold for cartilage tissue engineering. *Biomaterials* 2002;23:1511-7

Marler JJ, Upton J, Langer R, Vacanti JP. Transplantation of cells in matrices for tissue engineering. *Advanced Drug Delivery Reviews* 1998;33:165-182

Marra KG, Szem JW, Kumta PN, DiMilla PA, Weiss LE. In vitro analysis of biodegradable polymer/hydroxyapatite composites for bone tissue engineering. *Journal of Biomedical Material Research* 1999;47:324-35

Matsui M. Biodegradable fibres made of poly-lactic acid. *Chemistry of Fibres International* 1996;46:318-319

Mikos AG. Preparation of PGA bonded fibre structure for cell attachment and transplantation. *Journal of Biomedical Material Research* 1993;27:183-91

Mooney DJ, Baldwin DF, Suh NP, Vacanti JP, Langer R. Novel approach to fabricated porous sponges of poly(D,L-lactic-co-glycolic acid) without the use of organic solvents. *Biomaterials* 1996;17:1417-22

Mooney DJ, Mikos AG. The promise of tissue engineering; Growing new organs. *Scientific American* 1999;2:37-43

Murphy WL, Peters MC, Kohn DH, Mooney DJ. Sustained release of vascular endothelial growth factor from mineralised poly(lactide-co-glycolide) scaffolds for tissue engineering. *Biomaterials* 2000;21:2521-7

Nerem RM. Tissue Engineering. *Annuals Biomedical Engineering* 1991;19:529-537

Niklason LE, Gao J, Abbott WM, Hirschi KK, Houser S, Marini R, Langer R. Functional arteries grown in vitro. *Science* 1999;16:489-493

Nikolovski J, Mooney DJ. Smooth muscle cell adhesion to tissue engineering scaffolds. *Biomaterials* 2000;21;20;2025-32

Oakley C, Jaeger NAF, Brunette DM. Sensitivity of fibroblasts and their cytoskeletons to substratum topographies: Topographic guidance and topographic compensation by micromachined grooves of different dimensions. *Experimental Cell Research* 1997;234:413-24

Outerio-Bernstein MAF, Nunes SS, Andrade ACM, Alves TR, Legrand C, Morandi V. A recombinant NH₂ – terminal heparin-binding domain of the adhesive glycoprotein, thrombospondin-1, promotes endothelial tube formation and cell survival: a possible role for syndecan-4 proteoglycan. *Matrix Biology* 2002;21:311-24

Osdoby P, Caplan AI. Scanning electron microscopic investigation of vitro osteogenesis. *Calcification Tissue International* 1980;30:45-50

Pachence JM, Kohn J. Biodegradable polymers. In: Lanza RP, Langer R., Vacanti J. *Principles of Tissue Engineering*. Academic Press 2000:263-277

Peterlin A. Man made fibres: Science and technology. In: Mark HF et al editors. *Textile Book Service*. Wiley New York;1967. p283

Pitt CG, Chasalow FI, Hibionada YM, Kilmas DM, Schindler A. Aliphatic polyesters. 1, The degradation of poly(ϵ -caprolactone) in vivo. *Journal of Applied Polymer Science* 1981;26:3779-3787

Pitt CG, Jeffcoat AR, Zweidinger RA, Schindler A. Sustained drug delivery systems I. The permeability of poly(ϵ -caprolactone), poly(DL-lactic acid) and their copolymers. *Journal of Biomedical Material Research* 1979;13:497-507

Pitt CG, Gratzl MM, Jeffcoat AR, Zweidinger RA, Schindler A. Sustained drug delivery systems II: Factors affecting release rates from poly(ϵ -caprolactone) and related biodegradable polyesters. *Journal of Pharmaceutical Science* 1979;68:1534-38

Presti D, Scott J. Hyaluronon-mediated protective effect against cell damage caused by enzymatically produced hydroxyl radicals is dependant on hyaluronan molecules mass. *Cell Biochemical Function* 1994;12:281-8

Prober JS, Gimbrone MA, Lapierre LA, Mendrick DL, Fiers W, Rothlein RT, Springer TA. Overlapping patterns of activation of human endothelial cells by interleukin 1, tumour necrosis factor and interferon. *Journal of Immunology* 1986;137:1893-96

Pugin J, Schurer-Maly CC, Leturco D, Moriarty, Ulevitch RJ, Tobias PS. Lipopolysaccharide activation of human endothelial and epithelial cells is mediated by lipopolysaccharide-binding protein and soluble CD14. *Proceedings of the National Academy of Science USA* 1993;90:2744-48

Quirk RA, Chen WC, Davies MC, Tendler SJB, Shakesheff KM. Poly(L-lysine)-GRGDS as biomimetic surface modifier for poly(lactic acid). *Biomaterials* 2001;22:865-72

Read MA, Cordle SA, Veach RA, Carlisle CD, Hawiger J. Cell-free pool of CD14 mediates activation of transcription factor NF- κ B by lipopolysaccharide in human endothelial cells. *Proceedings of the National Academy of Science USA* 1993;90:9887-91

Rothlein R, Dustin ML, Marlin SD, Springer TA. A human intracellular adhesion molecule-1 distinct from LFA-1. *Journal of Immunology* 1986;137:1270-74

Sachlos E, Reis N, Ainsley C, Derby B, Czernuszka JT. Novel collagen scaffolds with predefined internal morphology made by solid freeform fabrication. *Biomaterial* 2003;24:1487-97

Sagar G, Orbo A, Jaeger R, Engstrom C. Non-genomic effects of progestins-inhibition of cell growth and increased intracellular levels of cyclic nucleotides. *Journal of Steroid Biochemistry and Molecular Biology* 2003;84:1-8

Scheven BAA, Marshall D, Aspden RM. In vitro behaviour of human osteoblasts in dentin and bone. *Cell Biology International* 2002;26:337-346

Schneider A, Chandra M, Lazarovici G, Vlodaysky I, Merin G, Uretzty G, Borman JB, Schwalb H. Naturally produced extracellular matrix is an excellent substrate for canine endothelial cell proliferation and resistance to shear stress on PTFE vascular grafts. *Thromb Haemost*;78:1392-8

Seifalian AM, Tiwari A, Hamilton G, Salacinski HJ. Improving the clinical patency of prosthetic vascular and coronary bypass grafts: the role of seeding and tissue engineering. *Artificial Organs* 2002;26:307-320

Skalak, R, Fox CF. Editors. *Tissue engineering*. California 1988. New York: Alan Liss.

Sherwood L. Principles of Endocrinology; The central endocrine glands. In: *Human Physiology from cells to systems* 3rd edition. Wadsworth Publishing Company, Belmont:629-30

Shmack G. Jehnichen D. Vogel R. Tandler B. Beyreuther R. Jacobsen S. Fritz H-G. Biodegradable fibres spun from poly(lactide) generated by reactive extrusion. *Journal of Biotechnology* 2001;86:151-160

Smith CW, Marlin SD, Rothlien R, Toman C, Anderson DC. Cooperative interactions of LFA-1 and MAC-1 with intercellular adhesion molecule-1 in facilitating adherence and transendothelial migration of human neutrophils in vitro. *Journal of Clinical Investigations* 1989;83:2008-17

Sohier J, Haan RE, de Groot K, Bezemer JM. A novel method to obtain protein release from porous polymer scaffolds: emulsion coating. *Journal of Controlled Release* 2002. In press.

Solheim E, Sudmann B, Bang G, Sudmann E. Biocompatibility and effect on osteogenesis of poly(orthoester) compared to poly(DL-lactic acid). *Journal of Biomedical Materials Research* 2000;49:257-63

Springer TA. Adhesion receptors of the immune system. *Nature* 1990;346:425-34

Steele JG, Johnson G, Underwood PA. Role of serum vitronectin and fibronectin in adhesion of fibroblasts following seeding on to tissue culture polystyrene. *Journal of Biomedical Material Research* 1992;26:861-84

Tachetti C, Tavella S, Dozin B, Quarto R, Robino G, Cancedda R. Cell condensation in chondrogenic differentiation. *Experimental Cell Research* 1992;200:22-33

Tiwari A, Salacinski HJ, Hamilton G, Sefalian AM. Tissue engineering of vascular bypass grafts: role of endothelial cell extraction. *European Journal of Vascular Surgery* 2001;21:193-201

Tiwari A, Kidane A, Salacinski HJ, Punshon G, Hamilton G, Sefalian AM. Improving endothelial cell retention for single stage seeding of prosthetic grafts: Use of polymer sequences of arginine-glycine-aspartate. *European Journal of Vascular Surgery* 2003;25:325-329

Tsuji H, Ishizaka T. Blends of aliphatic polyesters. VI. Lipase-catalysed hydrolysis and visualized phase structure of biodegradable blends from poly(ϵ -caprolactone) and poly(L-lactide). *International Journal of Biological Macromolecules* 2001;29:83-89

Underwood PA, Bennett FA. A comparison of the biological activities of the cell-adhesive proteins vitronectin and fibronectin. *Journal of Cell Science*. 1989;93:641-9

Vohra RK, Thompson GL, Carr HMH, Sharma H, Walker MG. Fibronectin coating of expanded polytetrafluoroethylene grafts and its role in endothelial cell seeding. *Artificial Organs* 1990;14:41-5

Vohra RK, Thompson GL, Carr HMH, Sharma H, Walker MG. Comparison of different vascular prostheses and matrices in relation to endothelial cell seeding. *British Journal of Surgery* 1991;78:417-20

Wada A, Kubota H, Hatanaka H, Miura H, Iwamoto Y. Comparison of mechanical properties of polyvinylidene fluoride and polypropylene monofilament sutures used for flexor tendon repair. *Journal of Hand Surgery* 2001;26:212-216

Walboomers XF, Croes HJE, Ginsel LA, Jansen JA. Growth behaviour of fibroblasts on microgrooved polystyrene. *Biomaterials* 1998;19:1861-68

Whitaker MJ, Quirk RA, Howdle SM, Shakesheff KM. Growth factor release from tissue engineering scaffolds. *Journal of Pharmacy and Pharmacology* 2001;53:1427-37

Williams D. Collagen: Ubiquitous in nature, multifunctional in devices. *Material Matters* 1998;5:11-13

Williams S. Endothelial cell transplantation. *Cell Transplantation* 1994;4:401-10

Wintermantel, E. Tissue engineering scaffolds using superstructures, *Biomaterials* 1996;17:83-91

Wojciak B, Crossan J, Curtis A, Wilkinson C. Grooved substrata facilitate in vitro healing of completely divided flexor tendons. *Journal of Material Science* 1995;6:266-271

Woods A, Longley RL, Turnova S, Couchman JR. Syndecan-4 binding to the high affinity heparin-binding domain of fibronectin drives focal adhesion formation in fibroblasts. *Archives of Biochemical Biophysics* 2000;374:66-72

Woods A, Crouchman JR. Syndecan-4 and focal adhesion functions. *Current Opinion in Cell Biology* 2001;13:578-83

Wu S, Cheng YXG, Zhi XZ. Study on the biocompatibility and toxicology of biomaterials – polycaprolacton. *Journal of Biomedical Engineering (Chinese)* 2000;17:380-382

Yamada KM. Cell surface interactions with extracellular materials. *Annual Review of Biochemistry* 1983;52:761-99

Yoshimoto H, Shin YM, Terai H, Vacanti JP. A biodegradable nanofibre scaffold by electrospinning and its potential for bone tissue engineering. *Biomaterials*. In press

Zhang Y, Zhang M. Microstructural and mechanical characterization of chitosan scaffolds reinforced by calcium phosphates. *Journal of Non-Crystalline Solids* 2001; 282:159-164

Zein I, Hutmacher DW, Cheng Tan K, Teoh SH. Fused deposition modelling of novel scaffold architectures for tissue engineering applications. *Biomaterial* 2002;23:1169-1185

Zun G, Hoerstrup SP, Schoeberlein A, Lachat M, Uhlsxhmind G, Vogt PR, Turina M. Tissue engineering: A new approach in cardiovascular surgery; Seeding of human fibroblasts followed by human endothelial cells on resorbable mesh. *European Journal of Cardio-Thoracic Surgery* 1998;13:160-64

ABBREVIATIONS

- AMV** - avian myeloblastosis virus
- CAMs** - cell adhesion molecules
- ECM** - extracellular matrix
- EGF** - epidermal growth factor
- DSC** - differential scanning calorimetry
- FAK** - focal adhesion kinase
- GADPH** - glyceraldehyde-3-phosphate dehydrogenase
- GDP** - guanosine 5'-diphosphate
- GTP** - guanosine 5'-triphosphate
- GRB2** - growth factor receptor binding protein 2
- HA** - hyaluronic acid
- HRE** - hormone response element
- HUVECs** - human umbilical vein endothelial cells
- ICAM-1** - intracellular cell adhesion molecules 1
- LDEV** – aspartic acid-glutamic acid-valine
- LPS** - lipopolysaccharide
- MAPK** - mitogen-activated protein kinase
- MEK** - MAPK-ERK kinase
- NGF** - nerve growth factor
- OVA** - ovalbumin
- PCL** - polycaprolactone
- PCR** - polymerase chain reaction
- PE** - polyethylene
- PDSGR** – proline-aspartic acid-serine-glycine-arginine
- PKC α** - protein kinase C α
- PGA** – poly (glycolide)
- PLA** – poly (lactide)
- PLG** - poly (lactide-co-glycolide)
- POE** - poly(orthoesters)
- REDV** – arginine-glutamic acid-aspartic acid-valine
- RGD** - arginine-glycine-aspartic acid
- RGDS** - arginine-glycine-aspartic acid-serine

RGDV - arginine-glycine-aspartic acid-valine
RT - reverse transcription
SEM - scanning electron microscope
SH2 - Src homology region 2 domain
TCP – tissue culture plastic
Tg - glass to rubber transition
Tm - melting point
VEGF - vascular endothelial growth factor
YIGSR – tyrosine-isoleucine-glycine-serine-arginine

PUBLICATIONS

Emanating from this thesis

Coombes AGA, Williamson MR. British patent application number: 0208418.4. PCL fibres.

Williamson MR, Coombes AGA. Gravity spinning of poly- ϵ -caprolactone fibres for applications in tissue engineering. *Biomaterials*. (in proof)

Williamson MR, Adams E, Coombes AGA. Cell interactions with gravity spun polycaprolactone fibres with application in soft tissue engineering. (in preparation)

Williamson MR, Woollard KJ, Griffiths H, Coombes AGA. Endothelial cell interaction and function with gravity spun polycaprolactone fibres for application in soft tissue engineering. (in preparation)

Williamson MR, Coombes AGA. Controlled drug release from gravity spun polycaprolactone fibres. (in preparation)

Williamson MR, Adams EF, Coombes AGA. Cell attachment and proliferation on polymer films and novel fibres having application in soft tissue engineering. ICMAT (2001) Singapore

Williamson MR, Adams EF, Coombes AGA. Cell attachment and proliferation novel fibres having application in soft tissue engineering. ESB (2002) Barcelona, Spain.

Williamson MR, Adams EF, Coombes AGA. The characterisation of PCL fibres thermal, mechanical properties and biocompatibility. TCES (2002) Glasgow, UK.

Williamson MR, Adams EF, Griffiths HR, Coombes AGA. Attachment and proliferation of Swiss 3T3 fibroblasts on novel solution spun PCL fibres. Third Smith & Nephew Int. Symposium (2002) Atlanta, USA.

Other work

Coombes AGA, Rizzi S, Williamson MR, Barralet JE, Downes S, Wallace WA. Precipitation casting of polycaprolactone for applications in tissue engineering and drug delivery. *Biomaterials*. (in proof)

Dai N-T, Williamson MR, Adams EF, Coombes AGA. Biocomposite cell support membranes based on collagen and polycaprolactone for tissue engineering of skin. *Biomaterials*. (accepted)

Chang X, Perry Y, Williamson MR, Coombes AGA. Micro-porous polymer matrices for controlled drug delivery. (in preparation)

Patel P, Cook M, Williamson MR, Coombes AGA. Biocomposites of gelatin and polycaprolactone for applications in tissue engineering and drug delivery. (in preparation)